

# **Exploration of new drug delivery pathways:**

- I. Mechanism of folate uptake in cultured human cells**
- II. Role of nuclear localization signal peptides in the delivery of  
oligonucleotide into reconstituted nuclei**

Thesis by  
**Kyoung Joon Oh**

In Partial Fulfillment of the Requirements for  
the Degree of Doctor of Philosophy

Department of Chemistry  
California Institute of Technology  
Pasadena, California

1994  
(Submitted August 2, 1993)

© 1994

Kyoung Joon Oh  
All Rights Reserved



## Acknowledgments

This work could not have been possible without the help and support of many people. I would like to thank my advisor, John Baldeschwieler, for his continuous guidance, support and encouragement during the course of my graduate studies. I would also like to thank the rest of my thesis committee, Sunney Chan, Peter Dervan and James Strauss, for their time and encouragement. I am truly grateful to Dr. Wilton Vannier for his helpful discussions and trouble in reading and correcting the manuscripts of my thesis. I also would like to thank Professor William Dunphy and his wife Akiko Kumagai for helping me carry out part of my research in their laboratory. I thank Professors Sunney Chan, Peter Dervan, Carl Parker, Judy Campbell and Henry Lester for allowing me to use the equipments in their laboratory for my thesis research. I give special thanks to John Evans for his help in peptide modifications. I also give special thanks to Hogyu Han and Changmoon Park for their help and discussions in this research.

I am grateful to all the past and present JDB group members; Tracey Handel, John Kramar, Raymond Goodrich, Steven Novick, Christopher Di Simone; Michael Youngquist, Robert Driscoll, Shenda Baker, Tery Coley, Mitsuko Fujiwara, Roxanne Male, David Baselt, Steve O'Connor, Kim Mislick, Thomas Theriault and Solomon Ting for their helpful discussions and friendship. Steven Novick and Christopher Di Simone helped me greatly in starting and continuing my research in the group during the first two years. Mitsuko Fujiwara, David Baselt and Roxanne Male who had been in the same classes were very helpful, friendly and inspiring. Solomon Ting, Thomas Theriault and David Baselt helped me learn useful computer programs and made it easy to write this thesis. Kim Mislick read the manuscripts of this thesis and made helpful

suggestions to me. The happy moments that I shared with them in the laboratory, during group lunches, and during outdoor activities will not be forgotten.

I would like to thank my family for all the help and encouragement. I do not know how to thank my parents-in law. They supported and encouraged me all the time. I also thank my brothers and sisters for their continuous support and prayers. Without them, I could not have continued my education. I also thank my uncle and aunt for their encouragement. I miss and thank my parents who have passed away years ago from the bottom of my heart. I am sorry that I cannot show them how I have grown up. However, I can turn myself away from regret to joy because of my wonderful, beautiful, patient, understanding and beloved wife Kyoung Eun. She has supported me and raised Johnny throughout the hard times here without a word of complaint. If praises were given to this work, it is not I, but she who deserves them. Oh, I praise the Lord! He who lives in me and whom I want to live in forever made all this possible!

## Abstract

The roles of the folate receptor and an anion carrier in the uptake of 5-methyltetrahydrofolate (5-MeH<sub>4</sub>folate) were studied in cultured human (KB) cells using radioactive 5-MeH<sub>4</sub>folate. Binding of the 5-MeH<sub>4</sub>folate was inhibited by folic acid, but not by probenecid, an anion carrier inhibitor. The internalization of 5-MeH<sub>4</sub>folate was inhibited by low temperature, folic acid, probenecid and methotrexate. Prolonged incubation of cells in the presence of high concentrations of probenecid appeared to inhibit endocytosis of folate-receptors as well as the anion carrier. The  $V_{\max}$  and  $K_M$  values for the carrier were  $8.65 \pm 0.55$  pmol/min/mg cell protein and  $3.74 \pm 0.54$   $\mu$ M, respectively. The transport of 5-MeH<sub>4</sub>folate was competitively inhibited by folic acid, probenecid and methotrexate. The carrier dissociation constants for folic acid, probenecid and methotrexate were 641  $\mu$ M, 2.23 mM and 13.8  $\mu$ M, respectively. Kinetic analysis suggests that 5-MeH<sub>4</sub>folate at physiological concentration is transported through an anion carrier with the characteristics of the reduced-folate carrier after 5-MeH<sub>4</sub>folate is endocytosed by folate receptors in KB cells. Our data with KB cells suggest that folate receptors and probenecid-sensitive carriers work in tandem to transport 5-MeH<sub>4</sub>folate to the cytoplasm of cells, based upon the assumption that 1 mM probenecid does not interfere with the acidification of the vesicle where the folate receptors are endocytosed.

Oligodeoxynucleotides designed to hybridize to specific mRNA sequences (antisense oligonucleotides) or double stranded DNA sequences have been used to inhibit the synthesis of a number of cellular and viral proteins (Crooke, S. T. (1993) *FASEB J.* **7**, 533-539; Carter, G. and Lemoine, N. R. (1993) *Br. J. Cancer* **67**, 869-876; Stein, C. A. and Cohen, J. S. (1988) *Cancer Res.* **48**, 2659-2668). However, the distribution of the delivered oligonucleotides in the cell, i.e., in the

cytoplasm or in the nucleus has not been clearly defined. We studied the kinetics of oligonucleotide transport into the cell nucleus using reconstituted cell nuclei as a model system. We present evidences here that oligonucleotides can freely diffuse into reconstituted nuclei. Our results are consistent with the reports by Leonetti et al. (*Proc. Natl. Acad. Sci. USA*, Vol. 88, pp. 2702-2706, April 1991), which were published while we were carrying this research independently. We also investigated whether a synthetic nuclear localization signal (NLS) peptide of SV40 T antigen could be used for the nuclear targeting of oligonucleotides. We synthesized a nuclear localization signal peptide-conjugated oligonucleotide to see if a nuclear localization signal peptide can enhance the uptake of oligonucleotides into reconstituted nuclei of *Xenopus*. Uptake of the NLS peptide-conjugated oligonucleotide was comparable to the control oligonucleotide at similar concentrations, suggesting that the NLS signal peptide does not significantly enhance the nuclear accumulation of oligonucleotides. This result is probably due to the small size of the oligonucleotide.

## Table of Contents

Acknowledgments .....	iii
Abstract.....	v
Table of Contents.....	vii
List of Figures .....	xii
<b>Chapter 1: Introduction .....</b>	<b>1</b>
Objectives.....	2
Thesis organization .....	6
References.....	8
Figures.....	10
<b>Chapter 2: The roles of folate receptor and an anion carrier</b>	
<b>in the intracellular transport of 5-methyltetrahydrofolate.....</b>	<b>18</b>
Summary .....	19
Introduction .....	20
Folate compounds .....	20
Transport systems for folate and methotrexate influx.....	20
High affinity/low capacity transport system (the	
reduced-folate carrier) in L1210 cells .....	20
Low affinity/high capacity transport system in L1210	
cells.....	21
A secondary low capacity system in L1210 cells .....	23
High affinity folate binding proteins (folate receptors)	
in KB cells and L1210 cells .....	24
Folate receptor and an anion carrier in MA104 cells.....	25
Membrane carriers involved in methotrexate efflux .....	26
Purpose of this study .....	28

Materials and methods.....	30
Materials .....	30
Preparation of cell culture media.....	30
Cell culture .....	31
Modification of proteins.....	32
Binding and uptake assay .....	34
Results .....	36
Cooperative binding of 5-methyltetrahydrofolate to the folate receptor in KB cells .....	36
Inhibition of 5-methyltetrahydrofolate uptake by probenecid, folic acid and low temperature in KB cells.....	37
Folate receptor-dependent uptake of folate-BSA conjugates.....	39
Inhibition of uptake of 5-methyltetrahydrofolate-BSA conjugate by prolonged incubation of KB cells in the presence of high concentrations of probenecid .....	41
Effect of short-term incubation of KB cells in varying concentrations of probenecid on the uptake of 5- methyltetrahydrofolate-BSA conjugate by KB cells.....	44
Effect of probenecid on the kinetics of 5- methyltetrahydrofolate binding to folate receptor .....	44
Time-dependent uptake of 5-methyltetrahydrofolate at micromolar concentrations by KB cells .....	44
Competitive inhibition of 5-methyltetrahydrofolate uptake by probenecid, folic acid and methotrexate .....	46
Approximate rate of folate-receptor endocytosis .....	47

The interrelationship between the folate receptor and the reduced-folate carrier in intracellular 5- methyltetrahydrofolate uptake .....	48
Discussion.....	53
Implications and future research .....	60
5-Methyltetrahydrofolate uptake mechanism .....	60
Folate receptor-mediated endocytosis as a potential drug delivery route .....	61
Cellular entry and cytotoxicity of bacterial toxins .....	63
Differential cytotoxicity of liposome-encapsulated gelonin and diphtheria toxin fragment A.....	66
A test for the possible use of folate conjugation for drug delivery of macromolecules .....	67
References.....	69
Acknowledgments .....	78
Footnotes.....	78
Tables .....	79
Figures.....	82
<b>Chapter 3: Transport kinetics of oligonucleotides into reconstituted     cellular nuclei.....</b>	<b>156</b>
Summary .....	157
Introduction .....	158
Methods for delivery of oligonucleotides into cells .....	158
Transport of proteins into cell nucleus.....	158
Nuclear localization sequences in nuclear proteins .....	159
Purpose of this study .....	161

Materials and methods .....	162
Materials .....	162
Synthesis of an oligonucleotide containing an aminohexyl linker .....	162
Solid-phase synthesis of nuclear localization signal peptides.....	162
Conjugation of peptides to bovine serum albumin.....	163
Conjugation of oligonucleotide to FITC-labeled peptide (F- peptide2).....	164
Labeling of peptide1, BSA and peptide1-conjugated BSA with fluorescein isothiocyanate (FITC) or tetramethylrhodamine isothiocyanate (TRITC) .....	165
Labeling of oligonucleotide with FITC or TRITC .....	166
Reconstitution of nuclei using <i>Xenopus laevis</i> egg extracts .....	167
Nuclear transport of proteins and oligonucleotides .....	167
Results .....	168
Synthesis of peptides, BSA-peptide conjugates, oligonucleotide-peptide conjugate and fluorescent labeling of peptide 1, BSA, BSA-peptide conjugate and oligonucleotides .....	168
Reconstitution of the functional nuclear envelope and transport of the nuclear localization signal peptide- conjugated BSA into reconstituted nuclei .....	168
Accumulation of oligonucleotides in the reconstituted nuclei by free diffusion .....	169
Effect of the nuclear localization signal peptide on the nuclear accumulation of oligonucleotides .....	171



Summary of results .....	173
Discussion.....	174
Implications and future research .....	176
Acknowledgments .....	178
References.....	179
Tables .....	182
Figures.....	184
<b>Appendices .....</b>	<b>216</b>
Appendix. A. Cell culture media .....	217
1. Formulation of folate-deficient Dulbecco's Modified Eagle Media (fdDMEM).....	217
2. A recipe for folate-deficient DMEM .....	219
Appendix. B. Procedures for radioiodination.....	221
Radioiodination using Iodo-beads.....	221
Appendix. C. Peterson's modified Lowry assay.....	222
1. Stock solutions for Peterson's modified Lowry protein assay .....	222
2. Procedures for protein determination.....	222
Appendix. D. Reconstitution of cellular nuclei using Xenopus egg extracts and sperm nuclei.....	223
1. Solutions and buffers .....	223
2. Preparation of Xenopus sperm DNA .....	226
3. Frog priming and inducing ovulation.....	227
4. Preparation of cytotstatic factor (CSF) arrested extracts .....	227

## List of Figures

Chapter 1 .....	1
Fig. 1. Absorption of drugs into target cells .....	10
Fig. 2. Fluid mosaic model of biological membranes.....	11
Fig. 3. Schematic diagram of passive transport down an electrochemical gradient and active transport against an electrochemical gradient .....	12
Fig. 4. Schematic diagram of a cell showing endocytosis, the fusion of endocytic vesicles with primary lysosomes to form secondary lysosomes and membrane recycling. ....	13
Fig. 5. Schematic diagram of liposome uptake by the clathrin- coated pit endocytic pathway.....	15
Fig. 6. Drug delivery via folate receptor-mediated endocytosis .....	16
Fig. 7. Possible mechanisms of delivery of oligonucleotides into the cell nucleus .....	17
Chapter 2 .....	18
Fig. 1. Structures of pteronic acid, folate derivatives, probenecid and a glycosylphosphatidylinositol linker .....	82
Fig. 2. Models for folate uptake.....	86
Fig. 3. Binding of 5-MeH <sub>4</sub> folate to KB cells .....	88
(A) Concentration dependent binding of 5-MeH <sub>4</sub> folate to folate receptors .....	90
(B) Scatchard plot .....	90
(C) 1/[L] vs. [m]/[AD] plot .....	91
(D) Extrapolation of Fig. 3 C.....	92
Fig. 4. Effect of probenecid on the uptake of [ <sup>3</sup> H]-5-MeH <sub>4</sub> folate.....	93

(A) Effect of probenecid on the uptake of [ $^3\text{H}$ ]-5-MeH <sub>4</sub> folate in the presence of 100 fold excess DL-5- methyltetrahydrofolate .....	94
(B) Effect of probenecid on the binding of [ $^3\text{H}$ ]-5-MeH <sub>4</sub> folate to KB cells .....	95
(C) Effect of probenecid on the uptake of [ $^3\text{H}$ ]-5-MeH <sub>4</sub> folate in the absence of 100 fold excess DL-5-MeH <sub>4</sub> folate.....	96
Fig. 5. Effect of temperature and probenecid on the uptake of 5- MeH <sub>4</sub> folate .....	97
(A) Effect of temperature and probenecid on the uptake of 5- MeH <sub>4</sub> folate by KB cells .....	98
(B) Effect of temperature and probenecid on the binding of 5-MeH <sub>4</sub> folate to KB cells .....	99
Fig. 6. Effects of folic acid and probenecid on the uptake of physiological concentrations of [ $^3\text{H}$ ]-5-MeH <sub>4</sub> folate.....	100
(A) Effects of folic acid and probenecid on the binding of physiological concentrations of [ $^3\text{H}$ ]-5-MeH <sub>4</sub> folate to KB cells.....	101
(B) Effects of folic acid and probenecid on the uptake of physiological concentrations of [ $^3\text{H}$ ]-5-MeH <sub>4</sub> folate by KB cells.....	102
Fig. 7. Endocytosis of folate-BSA conjugates by folate receptors .....	103
(A) Uptake of [ $^{125}\text{I}$ ]-BSA and [ $^{125}\text{I}$ ]-DL-5-MeH <sub>4</sub> folate- conjugated BSA ([ $^{125}\text{I}$ ]-mfBSA).....	105
(B) Effect of free DL-5-MeH <sub>4</sub> folate on the uptake of [ $^{125}\text{I}$ ]- mfBSA .....	106

(C) Effect of folate-BSA conjugate on the uptake of [ $^3\text{H}$ ]-folic acid by KB cells .....	107
(D) Effect of probenecid, BSA and folate-conjugated BSA on the uptake of [ $^3\text{H}$ ]-5-MeH <sub>4</sub> folate by KB cells .....	108
Fig. 8. Effect of probenecid on the uptake of [ $^{125}\text{I}$ ]-5-MeH <sub>4</sub> folate-BSA by KB cells.....	109
(A) Effect of probenecid on the uptake of [ $^{125}\text{I}$ ]-5-MeH <sub>4</sub> folate-BSA by KB cells .....	110
(B) Effect of varying concentrations of probenecid on the uptake of [ $^{125}\text{I}$ ]-5-MeH <sub>4</sub> folate-BSA conjugate by KB cells .....	111
Fig. 9. Time-dependent uptake of 5 $\mu\text{g}/\text{ml}$ 5-MeH <sub>4</sub> folate-BSA conjugate and BSA by KB cells at 37 $^{\circ}\text{C}$ .....	112
(A) Time-dependent uptake of 5 $\mu\text{g}/\text{ml}$ 5-MeH <sub>4</sub> folate-BSA conjugate and BSA by KB cells at 37 $^{\circ}\text{C}$ .....	113
(B) Expanded region of 0-60 min period in Fig 9 (A).....	114
Fig. 10. Effect of short-term incubation of KB cells in varying concentrations of probenecid on the uptake of 5-MeH <sub>4</sub> folate-BSA conjugate by KB cells.....	115
Fig. 11. Effect of probenecid on the time-dependent binding of 5-MeH <sub>4</sub> folate to folate receptors.....	117
Fig. 12. Time-dependent uptake of 5-MeH <sub>4</sub> folate in the presence of 0.5 mM folic acid.....	119
Fig. 13. Initial rates of 5-MeH <sub>4</sub> folate uptake at varying concentrations of 5-MeH <sub>4</sub> folate.....	121
Fig. 14. Effect of folic acid on the uptake of 5-MeH <sub>4</sub> folate at a fixed concentration ratio .....	123

(A) Effect of folic acid on the uptake of 5-MeH <sub>4</sub> folate at a fixed concentration ratio .....	124
(B) Lineweaver-Burk plot of Fig. 14 A.....	125
Fig. 15. Competitive inhibition of 5-MeH <sub>4</sub> folate uptake by	
probenecid, folic acid and methotrexate.....	126
(A) Uptake of 5-MeH <sub>4</sub> folate by KB cells in the presence or absence of 1 mM probenecid.....	127
(B) Uptake of 5-MeH <sub>4</sub> folate by KB cells in the presence or absence of 500 $\mu$ M folic acid .....	128
(C) Uptake of 5-MeH <sub>4</sub> folate by KB cells in the presence or absence of 30 $\mu$ M methotrexate.....	129
(D) Lineweaver-Burk plot of Fig. 15 (A) .....	130
(E) Lineweaver-Burk plot of Fig. 15 (B).....	131
(F) Lineweaver-Burk plot of Fig. 15 (C) .....	132
Fig. 16. The rate of uptake of [ <sup>3</sup> H]-folic acid by KB cells .....	
(A) % Change of acid-resistant and acid-dissociable fractions as a function of time .....	134
(B) % Change of [ <sup>3</sup> H]-folic acid in the media as a function of time.....	135
(C) Uptake of [ <sup>3</sup> H]-folic acid by KB cells as a function of time.....	136
(D) Rate of endocytosis for the initial 15 min.....	137
Fig. 17. Experimental scheme to define the interrelationship between the folate receptor and a probenecid-sensitive anion carrier in the transport of [ <sup>3</sup> H]-5-MeH <sub>4</sub> folate .....	
	138

(A) If the folate receptor and the probenecid-sensitive anion carrier work independently and if probenecid does not interfere with the acidification of the lumen of caveola, $\{AR(a) - AR(b)\} - \{AR(c) - AR(d)\} \approx 0$ .....	141
(B) If the folate receptor and the probenecid-sensitive anion carrier work in tandem and if probenecid does not interfere with the acidification of the lumen of caveola, $\{AR(a) - AR(b)\} - \{AR(c) - AR(d)\} > 0$ .....	142
(C) If the folate receptor and the probenecid-sensitive anion carrier work independently and if probenecid interferes with the acidification of the lumen of caveola, $\{AR(a) - AR(b)\} - \{AR(c) - AR(d)\} > 0$ .....	143
(D) If the folate receptor and the probenecid-sensitive anion carrier work in tandem and if probenecid interferes with the acidification of the lumen of caveola, $\{AR(a) - AR(b)\} - \{AR(c) - AR(d)\} > 0$ .....	144
Fig. 18. Effect of probenecid and folic acid on uptake of 5-MeH <sub>4</sub> folate at 50 nM.....	145
(A).....	146
(B).....	147
Fig. 19. Transport systems regulating intracellular pH.....	148
Fig. 20. Schematic diagram of Diphtheria toxin and <i>Pseudomonas</i> exotoxin action.....	150
Fig. 21. Schematic representation of the subunit composition of diphtheria toxin and <i>Pseudomonas</i> exotoxin A .....	152

Fig. 22. Schematic diagram of drug delivery using folate receptor-mediated endocytosis of folate-conjugated liposomes .....	154
Chapter 3 .....	156
Fig. 1 .....	184
(A) Schematic diagram of potential sites of antisense oligonucleotide action .....	184
(B) Nuclear import and export .....	185
(C) Models for protein import into the nucleus .....	186
Fig. 2. Synthesis of aminohexyl containing oligonucleotide.....	187
Fig. 3. Schematic diagram of the synthesis of FITC-labeled peptides.....	188
Fig. 4. Conjugation of nuclear localization signal peptide to BSA or oligonucleotide using a bifunctional cross-linking reagent, MBS.....	190
Fig. 5. Coupling of FITC to amine group .....	191
Fig. 6. Coupling of TRITC to amine group .....	192
Fig. 7 Mass spectrum of FITC-labeled peptide 2 .....	193
Fig. 8. Amino acid analysis of peptide 1-conjugated BSA.....	195
(A) Amino acid analysis .....	196
(B) Average number of peptides per BSA .....	197
Fig. 9. Reconstitution of nuclear membranes .....	198
Fig. 10. Transport assay with FITC-labeled peptide 1, BSA and peptide1-conjugated BSA.....	200
(A) Transport assay with FITC-labeled peptide1-conjugated BSA .....	201
(B) Transport assay with FITC-labeled peptide 1 and BSA .....	202

Fig. 11. Accumulation of oligonucleotides in reconstituted nuclei.....	203
(A) Accumulation of FITC-labeled oligonucleotides in reconstituted nuclei .....	204
(B) Accumulation of TRITC-labeled oligonucleotides in reconstituted nuclei .....	205
Fig. 12. Accumulation of TRITC-labeled oligonucleotides in the reconstituted nuclei.....	206
Fig. 13. Simultaneous uptake of FITC labeled BSA-signal peptide conjugates and TRITC-labeled oligonucleotide.....	208
Fig. 14. Time-differential Dual label Experiment .....	210
Fig. 15. Effect of nuclear localization signal peptide.....	212
Fig. 16. Nuclear localization activity of peptide 1 and FITC-labeled peptide 2 .....	214



## Chapter 1: Introduction

## OBJECTIVES

Most drugs administered by oral or parenteral routes such as intravascular administration, intramuscular administration, subcutaneous administration, adsorption through the skin, or by inhalation reach the organs and tissues of the body through the blood circulation (1). Selectively acting drugs release their biological effects by reaction with specific receptor sites associated with nucleic acids, enzymes, or other proteins or biomacromolecules (2). Since many of the drug receptors are located inside cells, the administered drugs must cross cellular and intracellular membranes to reach the sites of action after reaching the target tissue (2). If drugs are designed to act in the cell nucleus, methods need to be developed to deliver the drugs into the cell cytoplasm and into the nucleus sequentially (Fig. 1).

Cellular membranes are two-dimensional bilayers of oriented lipids containing globular proteins according to the fluid mosaic model proposed by Singer and Nicolson (Fig. 2, ref. 3). Cellular membranes are highly selective permeability barriers. Transport of substances across cellular membranes can occur via several different mechanisms (Figs. 3 and 4, refs. 4 a, 4b). Small lipophilic substances or gas molecules can freely diffuse into the cell across the cellular membrane (4a). Transport of small ions and molecules such as sodium ion, potassium ion, calcium ion and amino acids occurs through membrane carriers (4a). In most animal cells, clathrin-coated pits and membrane vesicles provide a specialized pathway for taking up specific macromolecules from the extracellular fluid, a process called receptor-mediated endocytosis (Fig. 4, ref. 4b). Extracellular fluid containing many solutes can be trapped in the vesicles and is ingested as well (pinocytosis, ref. 6). In most cells, the great majority of endocytic vesicles ultimately fuse with small vesicles called primary lysosomes

to form secondary lysosomes, which are specialized sites of intracellular digestion (see Fig. 4, ref. 4b). Liposomes, artificial membrane vesicles, have been introduced as drug carriers since liposome encapsulation of drugs reduces nonspecific interactions of the drugs with undesired tissues and thereby reduces the toxicity of the drugs (review 5). Drug-loaded liposomes can be taken up by cells via the clathrin-coated pit endocytic pathway (Fig. 5, ref. 6). If drug-loaded liposomes are taken up by the clathrin-coated pit endocytic pathway, the liposomes are eventually delivered to lysosomes in the cell, where the liposomal membranes are disassembled by enzymes and the liposome contents are released in the lumen of the lysosomes. Since lysosomes contain various digestive enzymes, therapeutic reagents could be susceptible to the enzymes and could lose their therapeutic activity before they reach the desired intracellular locations such as the cytoplasm or the cell nucleus (Fig. 5).

Cells need vitamins for survival. Folic acid, a vitamin, and its derivatives such as 5-methyltetrahydrofolate (see Fig. 1 in Chapter 2.) are involved in the synthesis of purines and pyrimidines and therefore the genetic material of the cell. Therefore, cells have a special need for folic acid or its derivatives for proliferation (7). Studies have shown that folates are taken up by cells by folate receptor-mediated endocytosis (8). Recent reports have also suggested that the folate receptor-mediated endocytosis pathway might be useful as a new delivery route for large molecule such as bacterial or plant toxins, oligonucleotides, or liposome-encapsulated drugs (Fig. 6, refs. 9, 10). Leamon et al. (9) reported that proteins covalently conjugated to folic acid were taken up by folate receptor-mediated endocytosis and were stable for a prolonged period of time inside the cell. Leamon et al. (10) recently reported that folate-conjugated plant toxin (momordin) could be delivered to the cell cytoplasm from outside of the cell.

Although the intracellular location of proteins other than toxins were not clearly defined in their works, these results suggest that the folate receptor endocytic pathway might be distinct from the clathrin-coated vesicle endocytic pathway. If the folate receptor pathway is distinct from the clathrin-coated vesicle pathway, and the endocytosed vesicles containing folate receptors do not fuse with lysosomes, this would be very promising for the delivery of drugs susceptible to lysosomal enzymes. In addition, some cancer cells have a great need for folates for cell division and express a large number of folate receptors on the cell surface, which could be available for drug delivery and targeting.

Recent studies have shown that there are several distinct mechanisms for folate uptake (review 11). These studies have shown that cells have transmembrane carriers as well as folate receptors for folate uptake (11). Chemotherapeutic agents such as methotrexate and other antifolate reagents are known to be taken up by either one of the two folate uptake pathways (11). However, the interrelationship of the two systems in the uptake of folate or antifolate compounds has not been clearly defined (8, 11). It has not been clearly established whether the folate receptor and the transmembrane membrane carrier work independently or together. In order to develop improved chemotherapeutic reagents and delivery strategies, it is essential to understand the folate uptake mechanisms in greater detail.

Short oligonucleotides which are designed to bind RNA or DNA (antisense oligonucleotides) as well as to inhibit specific enzymes or receptors have been developed for therapeutic applications (reviews 12a-c). Oligonucleotides are relatively large negatively charged molecules and their delivery into a cell is limited by the presence of the cell plasma membrane. Many methods have been developed for the delivery of oligonucleotides into the cell cytoplasm (review

12b, see Introduction section in Chapter 3) and there are some reports which have demonstrated the effects of oligonucleotides or large DNA molecules in the cell nucleus (13). However, it remains to be determined how oligonucleotides can reach a cellular nucleus from the cellular cytoplasm if the oligonucleotides designed to interact with DNA, nuclear RNA, or nuclear proteins are delivered into the cellular cytoplasm by currently available delivery methods. The cell nucleus has a nuclear pore complex through which large nuclear proteins are recognized and transported into nucleus (reviews 14a-g). It is not clear whether oligonucleotides can enter a cellular nucleus through the nuclear pore complex or gain access to genomic DNA during mitosis when the nuclear membranes disappear temporarily (Fig. 7, ref. 4c). Nuclear proteins have nuclear localization signal peptides (14f) which are recognized by the nuclear pore complex. It is not clear whether these signal peptides could be used to enhance the uptake of oligonucleotides or to other therapeutic agents when the peptides are covalently conjugated to them.

In this thesis the roles of folate receptors and transmembrane carriers were examined in cultured human epidermoid carcinoma (KB) cells in order to determine how the folate receptors and membrane carriers work in the folate uptake into cells, focusing on the uptake of 5-methyltetrahydrofolate. Based upon our results, the possible mechanism of entry of folate-toxin (momordin) conjugates into the cellular cytoplasm by folate receptor-mediated endocytosis and the possibility of using the folate uptake pathway for drug delivery into the cell cytoplasm are discussed. In order to determine whether therapeutic agents such as oligonucleoties could reach the cellular nucleus from the cellular cytoplasm, the transport of oligonucleotides into cellular nuclei through the nuclear pore complex was examined in reconstituted cellular nuclei without

plasma membranes (15). The effect of nuclear localization signal peptides on the delivery of oligonucleotides into the cellular nuclei was also examined in order to see if conjugation of nuclear localization signal peptides could enhance the uptake of oligonucleotides by reconstituted nuclei. (see Chapter 3).

## THESIS ORGANIZATION

### Chapter 2.

Current models of folate uptake pathways are examined in the Introduction section. The roles of the folate receptor and the membrane anion carrier in the uptake of 5-methyltetrahydrofolate were studied to determine which model is correct by measuring the effects of temperature and inhibitors such as folic acid, methotrexate and probenecid on the uptake of 5-methyltetrahydrofolate. The effects of folic acid and probenecid on the folate receptor-mediated endocytosis of 5-methyltetrahydrofolate and on the membrane carrier-mediated transport of 5-methyltetrahydrofolate are examined in the Results section. Models compatible with the experimental results from this research are discussed in the Results and Discussion sections. The possibility of using the folate uptake pathway for the intracellular delivery of macromolecules are discussed in the Implications and Future research section.

### Chapter 3.

A general background for antisense oligonucleotide therapeutics is discussed in the Introduction section. Methods for reconstitution of nuclei with functional nuclear membranes and for study of the kinetics of oligonucleotide transport into cell nuclei are discussed in the Materials and Methods section.

Data on the movement of 20-mer oligonucleotides into cellular nuclei are presented in the Results section. The effect of nuclear localization signal peptides on the transport of oligonucleotides into the cellular nuclei is also presented in the Results section. Possible applications of signal peptides are discussed in the Discussion section and also in the Implications and Future Research section.

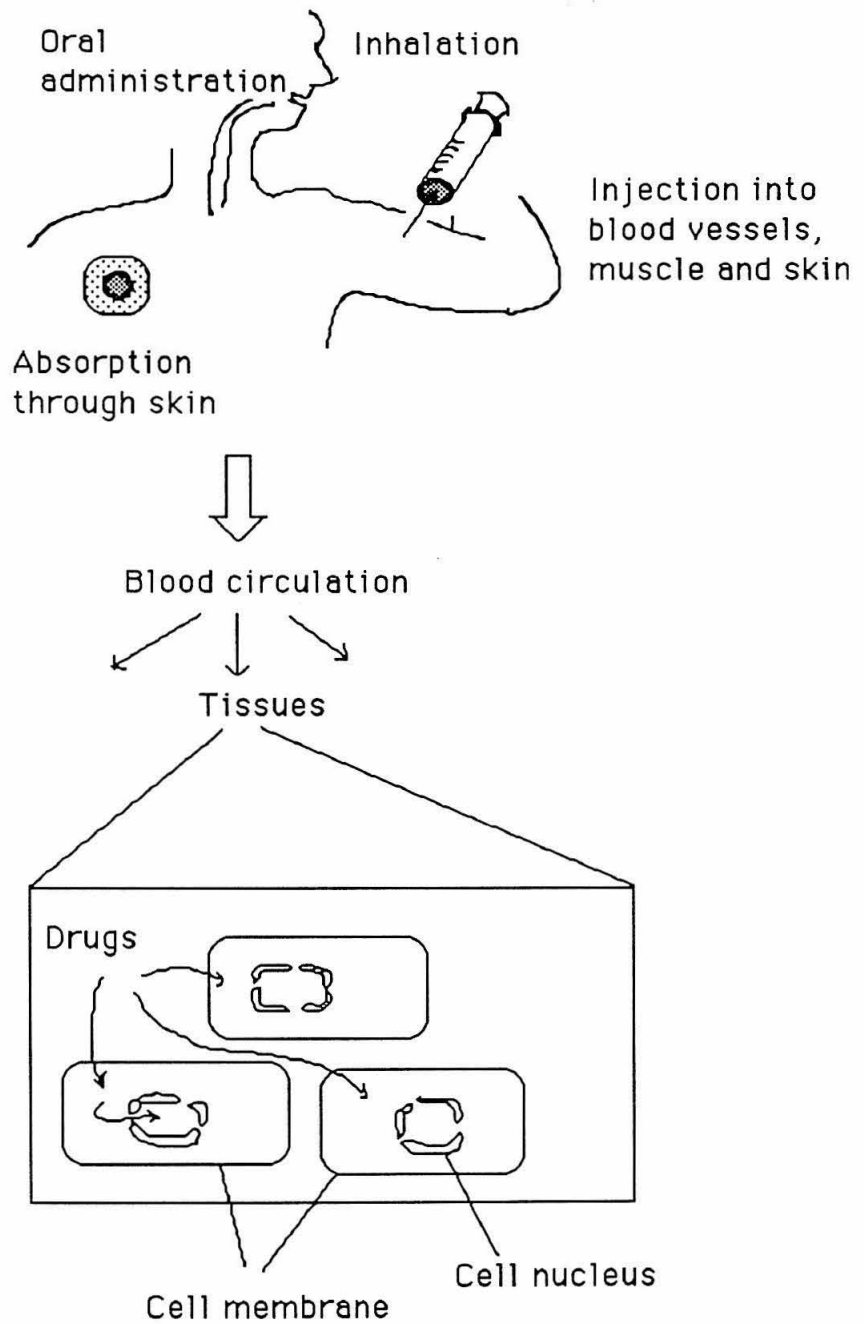
## REFERENCES

1. Goldstein, A., Aronow, L. and Kalman, S. M. (1968) in *Principles of drug action: The basis of pharmacology* pp. 106-205, Harper & Row, Publishers, New York, Evanston, and London
2. Scheler, W. and Blank, J. (1977) "Physicochemical fundamentals and thermodynamics of the membrane transport of drugs," in *Kinetics of Drug Action* (van Rossum, J. M., ed) pp. 3-62, Springer-Verlag Berlin Heidelberg New York
3. Singer, S. J. and Nicolson, G. L. (1972) *Science* **175**, 720-731
4. (a) Alberts, B., Bray, D., Lewis, J., Raff, M., Roberts, K. and Watson, J. D. (1983) in *Molecular biology of the cell* pp. 286-302, Garland Publishing, Inc., New York & London (b) *ibid*, pp. 302-314 (c) *ibid*, pp. 611-671
5. Roerdink, J., Daemen, T/. Bakker-Woudenberg, I., Storm, G., Crommelin, D. and Scherphof, G. "Therapeutic utility of liposomes," in *Drug Delivery Systems*, Vol. 1, (Johnson, P. and Lloyd, G. ed) pp. 1-30, Ellis Horwood Ltd.
6. Straubinger, R., Hong, K., Friend, D. and Papahadjopoulos, D. (1983) *Cell* **32**, 1069-1079
7. Blakley, R. L. (1969) "The biochemistry of folic acid and related pteridines," in *Frontiers of biology*, Vol. 13 (Neuberger, A. and Tatum, E. L. ed), North-Holland Publishing Company, Amsterdam and London
8. Anderson, R. G. W., Kamen, B. A., Rothberg, K. G. and Lacey, S. W. (1992) *Science* **255**, 410-411
9. Leamon, C. P. and Low, P. S. (1991) *Proc. Natl. Acad. Sci. USA* **88**, 5572-5576
10. Leamon, C. and Low, P. S. (1999) *J. Biol. Chem.* **267**, 24966-24971
11. Antony, A. C. (1992) *Blood* **79** (11), 2807-2820

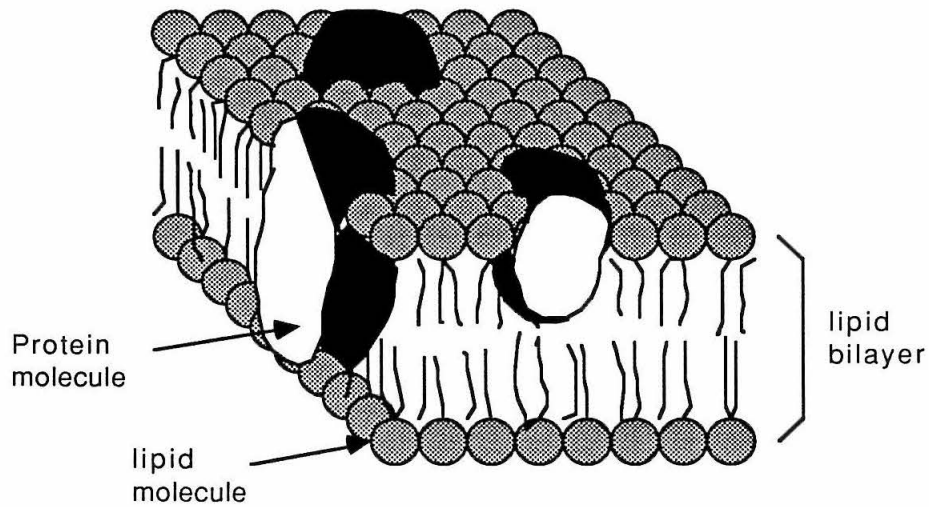


12. (a) Crooke, S. T. (1993) *FASEB J.* **7**, 533-539 (b) Carter, G. and Lemoine, N. R. (1993) *Br. J. Cancer* **67**, 869-876 (c) Stein, C. A. and Cohen, J. S. (1988) *Cancer Res.* **48**, 2659-2668
13. Orson, F. M., Thomas, D. W., McShan, W. M., Kessler, D.J. and Hogan, M. E. (1991) *Nuc. Acid. Res.* **19**, 3435-3441
14. (a) Dingwall, C. and Laskey, R. A. (1986) *Ann. Rev. Cell Biol.* **2**, 367-390 (b) Newport, J. W. and Forbes, D. J. (1987) *Ann. Rev. Biochem.* **56**, 535-565 (c) Gerace, L. and Burke, B. (1988) *Ann. Rev. Cell Biol.* **4**, 335-374 (d) Nigg, E. A., Baeuerle, P. A. and Lührmann, R. (1991) *Cell* **66**, 15-22 (e) Silver, P. A. (1991) *Cell* **64**, 489-497 (f) Garcia-Bustos, J., Heitman, J. and Hall, M. N. (1991) *Biochim. Biophys. Acta* **1071**, 83-101 (g) Stochaj, U. and Silver, P. (1992) *Eur. J. Cell Biol.* **59**, 1-11
15. (a) Murray, A. W., Solomon, M. J. and Kirschner, M. W. (1989) *Nature* **339**, 280-286 (b) Gourdon, J. B. (1976) *J. Embryol. exp. Morph.* **36**, 523-540

**Fig. 1. Absorption of drugs into target cells**



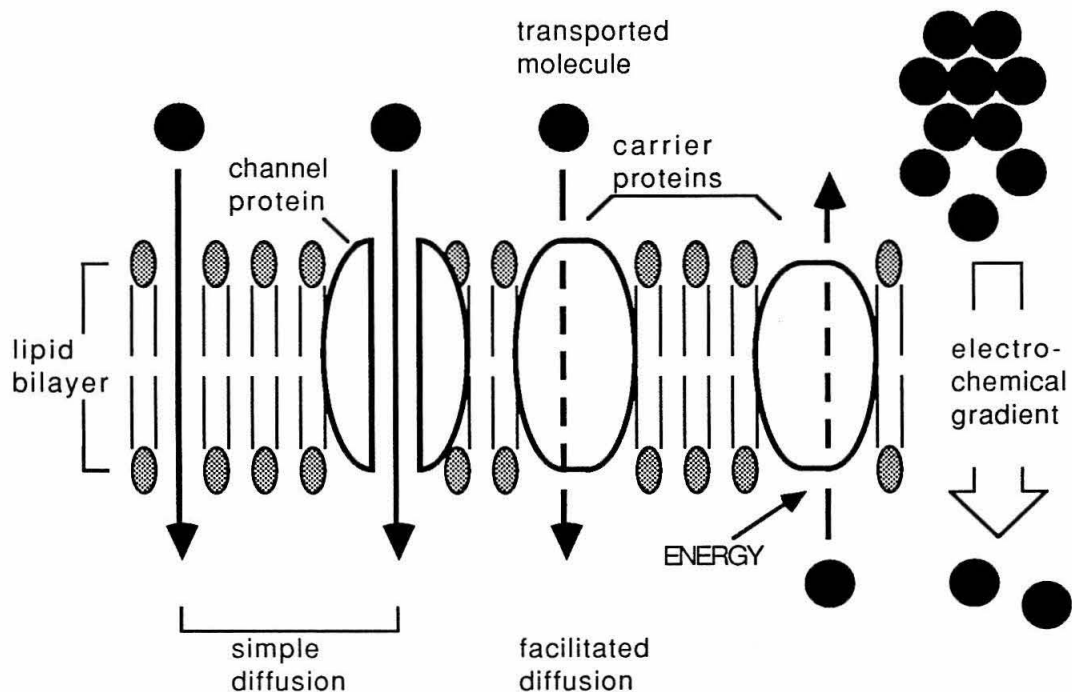
**Fig. 2. Fluid mosaic model of biological membranes\***



\*This was adapted from Singer, S. J. and Nicolson, G. L. (1972) *Science* **175**, 723.

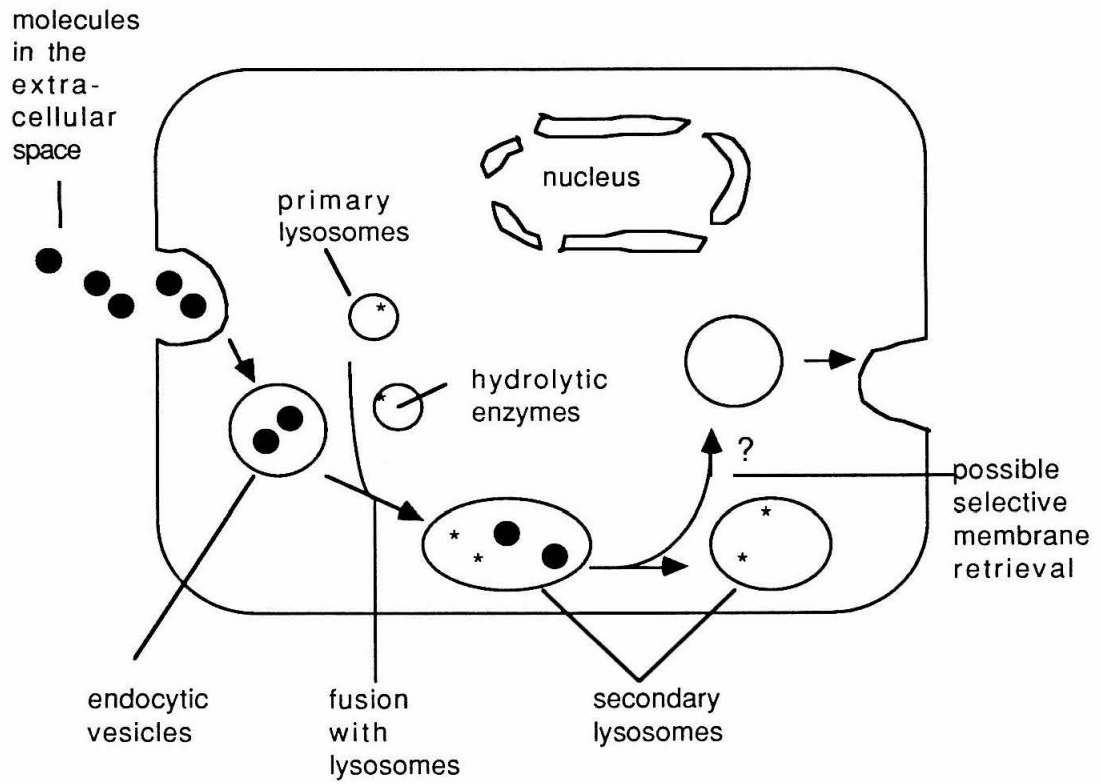
**Fig. 3. Schematic diagram of passive transport down an electrochemical gradient and active transport against an electrochemical gradient**

Small uncharged molecules can directly cross the lipid bilayer (free diffusion). Charged molecules including small ions are transferred through protein channels or carrier proteins (facilitated diffusion). Passive diffusion or facilitated diffusion occurs spontaneously without spending energy. Active transport occurs against an electrochemical or concentration gradient and requires energy. Adapted from Alberts et al. (Molecular biology of the cell, Garland Publishing, Inc. New York & London)

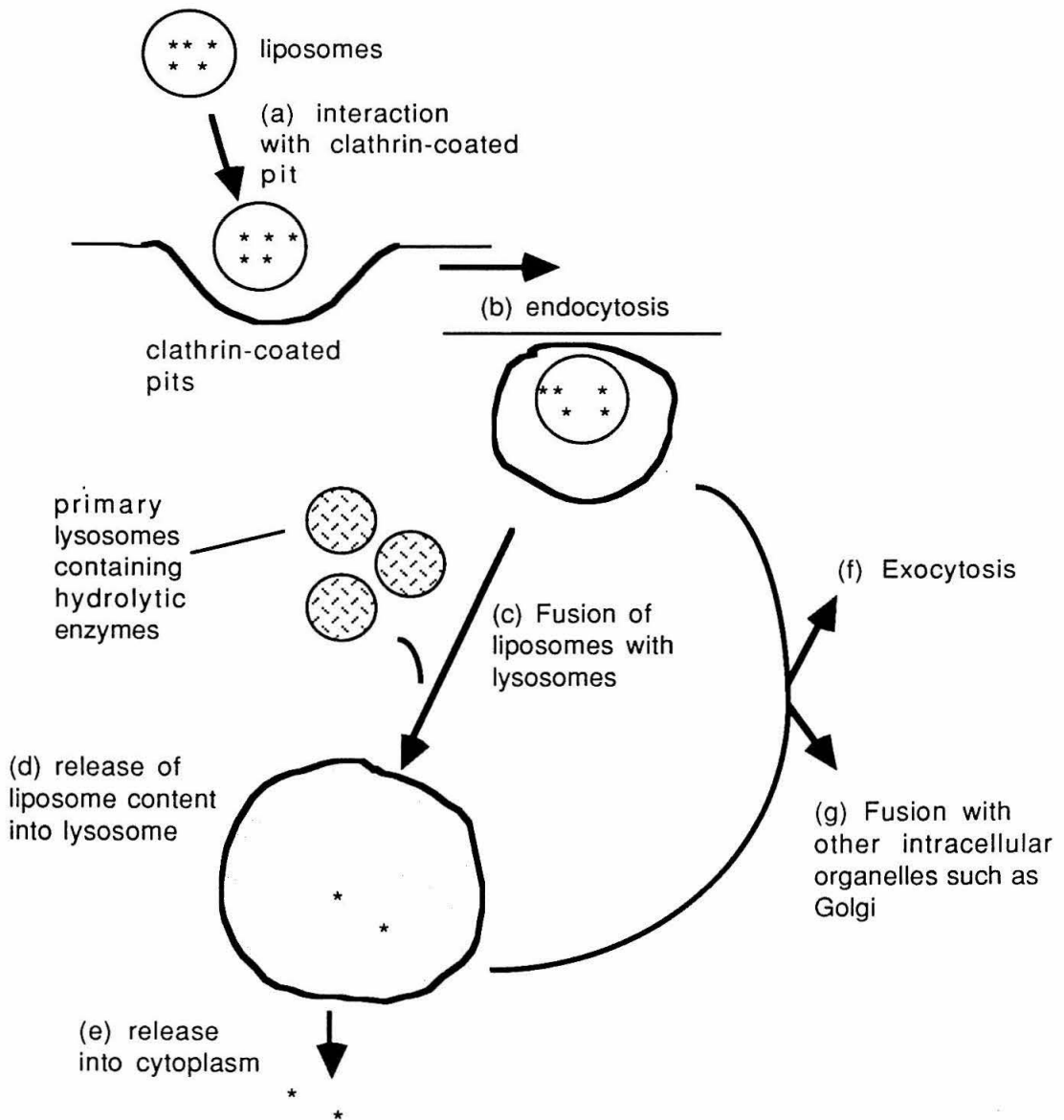


**Fig. 4. Schematic diagram of a cell showing endocytosis, the fusion of endocytic vesicles with primary lysosomes to form secondary lysosomes and membrane recycling.** Most vesicles are thought to fuse with other vesicles in the cytoplasm before fusing with lysosomes (not shown in this figure). The right-hand side of the figure, shows the selective retrieval of the endocytic membrane from the secondary lysosome and its direct return to the plasma membrane. This is only one possible pathway of retrieval. Alternatively, selectively retrieved endocytic membrane can fuse with other intracellular organelles such as Golgi apparatus. Adapted from Alberts et al. (Molecular biology of the cell, Garland Publishing, Inc. New York & London).

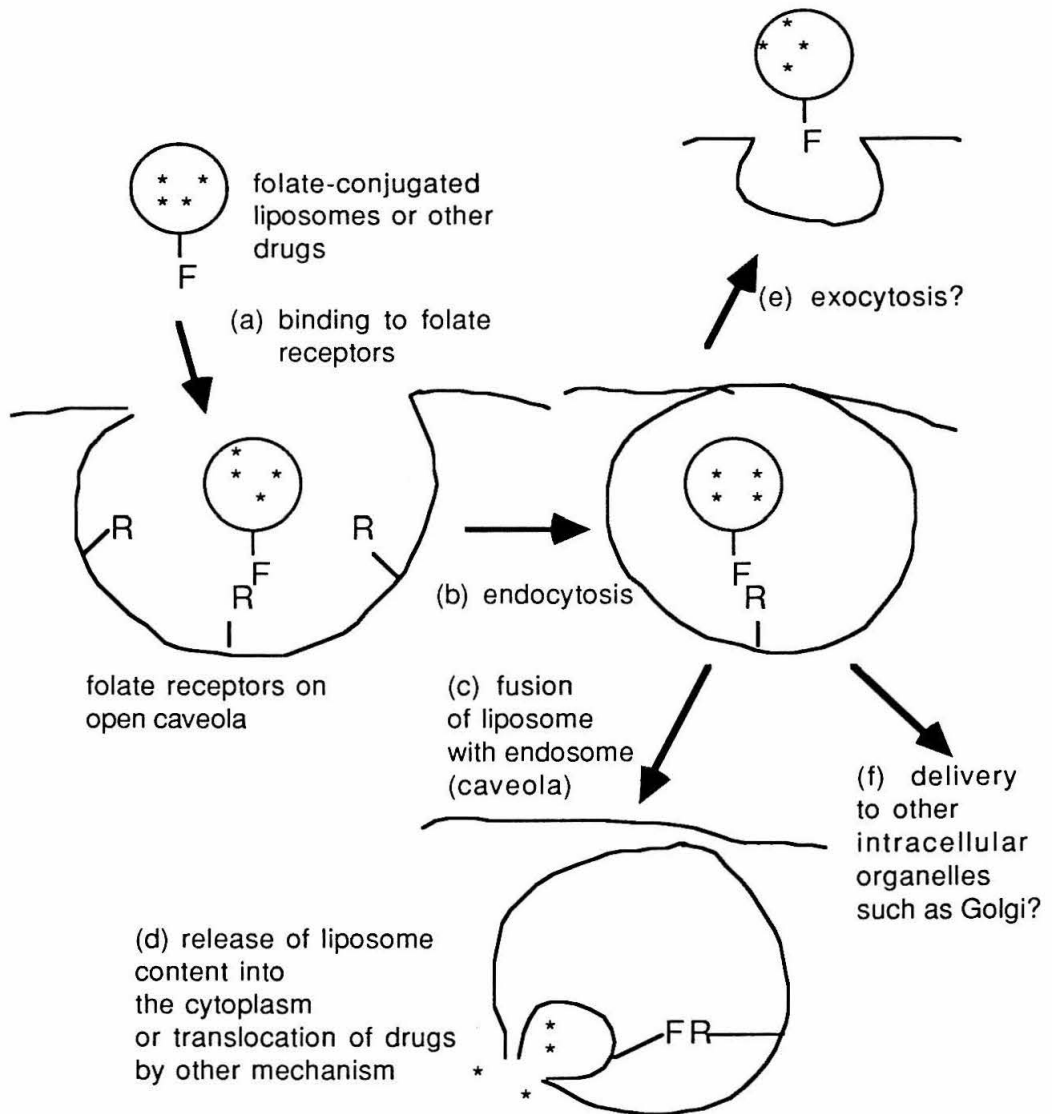
Fig. 4



**Fig. 5. Schematic diagram of liposome uptake by the clathrin-coated pit endocytic pathway**



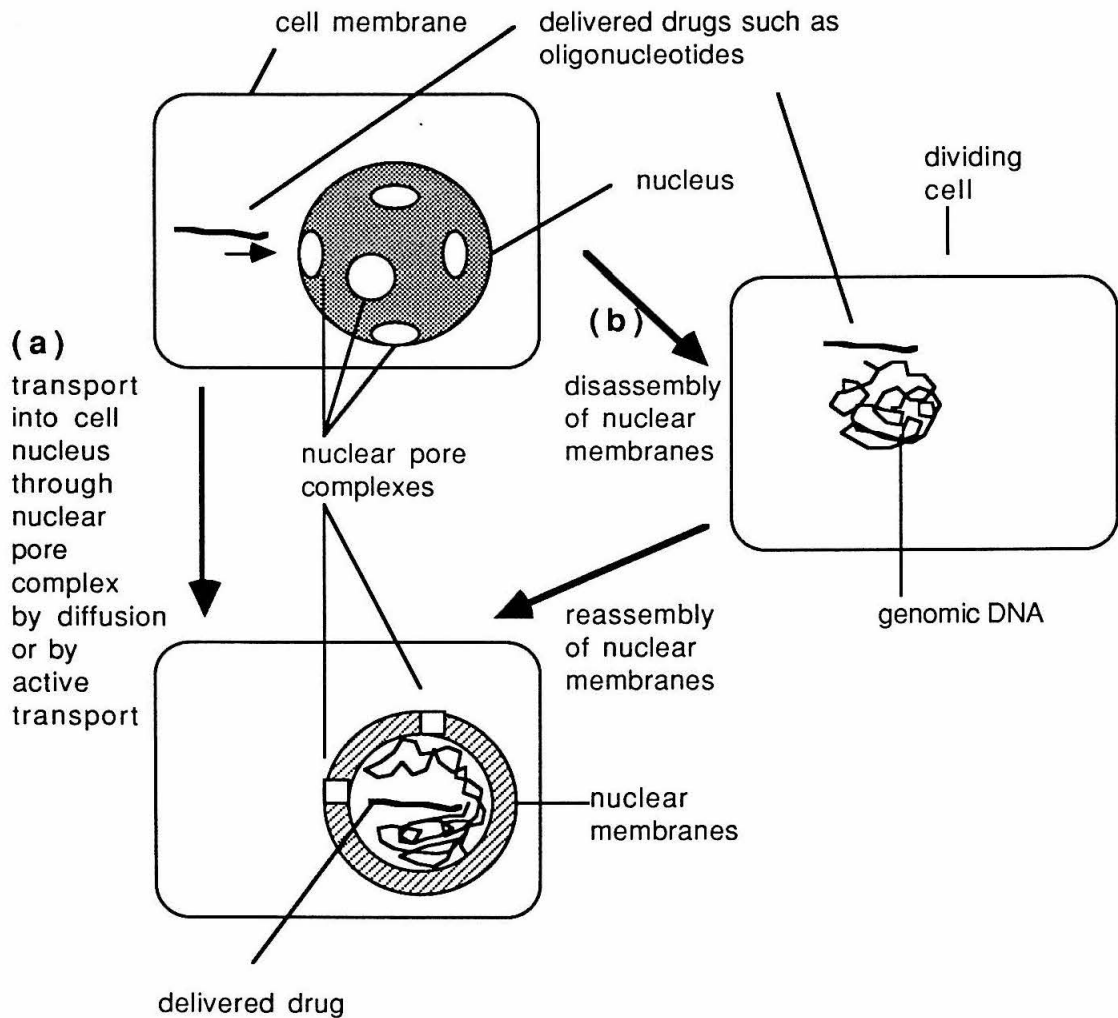
**Fig. 6. Drug delivery via folate receptor-mediated endocytosis**





**Fig. 7. Possible mechanisms of delivery of oligonucleotides into the cell nucleus**

- (a) Direct transport into nucleus through nuclear pore complexes by free diffusion or by active transport
- (b) Cell cycle-dependent delivery into nucleus



**Chapter 2: The roles of folate receptor and an anion carrier  
in the intracellular transport of 5-methyltetrahydrofolate**

**SUMMARY** The roles of the folate receptor and an anion carrier in the uptake of 5-methyltetrahydrofolate (5-MeH<sub>4</sub>folate) were studied in cultured human (KB) cells using radioactive 5-MeH<sub>4</sub>folate. Binding of the 5-MeH<sub>4</sub>folate was inhibited by folic acid, but not by probenecid, an anion carrier inhibitor. The internalization of 5-MeH<sub>4</sub>folate was inhibited by low temperature, folic acid, probenecid and methotrexate. Prolonged incubation of cells in the presence of high concentrations of probenecid appeared to inhibit endocytosis of folate-receptors as well as the anion carrier. The  $V_{\max}$  and  $K_M$  values for the carrier were  $8.65 \pm 0.55$  pmol/min/mg cell protein and  $3.74 \pm 0.54$   $\mu$ M, respectively. The transport of 5-MeH<sub>4</sub>folate was competitively inhibited by folic acid, probenecid and methotrexate. The carrier dissociation constants for folic acid, probenecid and methotrexate were 641  $\mu$ M, 2.23 mM and 13.8  $\mu$ M, respectively. Kinetic analysis suggests that 5-MeH<sub>4</sub>folate at physiological concentration is transported through an anion carrier with the characteristics of the reduced-folate carrier after 5-MeH<sub>4</sub>folate is endocytosed by folate receptors in KB cells. Our data with KB cells suggest that folate receptors and probenecid-sensitive carriers work in tandem to transport 5-MeH<sub>4</sub>folate to the cytoplasm of cells, based upon the assumption that 1 mM probenecid does not interfere with the acidification of the vesicle where the folate receptors are endocytosed.

## INTRODUCTION

**Folate compounds** Folates are a group of heterocyclic compounds based on the *N*-pteridin-6-ylmethyl-*p*-aminobenzoic acid skeleton, often conjugated with one or more L-glutamic acid units (1, Fig. 1). Reduced-folates such as 5-methyltetrahydrofolate (5-MeH<sub>4</sub>folate)<sup>1</sup> and 5-formyltetrahydrofolate serve as carriers of activated one-carbon units in various enzyme-catalyzed reactions such as the biosyntheses of methionine, serine, deoxythymidylic acid and purines (2). Mammals obtain folates from their diets or from microorganisms since they are unable to synthesize a pterine ring. Membrane transport of folate compounds in mammalian cells has been the subject of intensive studies which have provided evidence for the existence of several transport mechanisms for folate (and antifolate) compounds (reviews 3-6, see Table 1).

### Transport systems for folate and methotrexate influx

*High affinity/low capacity transport system (the reduced-folate carrier) in L1210 cells* The reduced-folate carrier (7-11), an anion carrier, has been shown to mediate the uptake of folate compounds such as 5-methyltetrahydrofolate (5-MeH<sub>4</sub>folate) (9), 5-formyltetrahydrofolate (12), folic acid (9,13) and an antifolate compound methotrexate (7-11) by extensive studies with L1210 mouse leukemia cells (7-13) and CCRF-CEM human lymphoblastic cells (14). This system has a greater preference for transport of reduced-folates such as 5-methyltetrahydrofolate than oxidized folate such as folic acid (3). This system is inactivated by carbodiimide-activated methotrexate (15) or *N*-hydroxysuccinimide ester of methotrexate (16) and sulfhydryl modifying reagents such as *p*-chloromercuribenzenesulfonate (pCMBS, refs 17,18) and *N*-ethylmaleimide (18). The uptake of folate compounds by the reduced-folate carrier is competitively inhibited by various anions such as *p*-

[dipropylsulfamoyl]benzoic acid (probenecid, 19, see Fig. 1), phosphate and sulfate (20) as well as folate compounds (4). It has been suggested that the reduced-folate carrier mediates the uptake of folates via an anion-exchange mechanism (10, 21-24). A few of the characteristics of this transmembrane carrier (4) include: (a) high affinity for 5-substituted reduced folates (Michaelis-constant  $K_M$  of 1 - 3  $\mu\text{M}$ ) and low affinity for folic acid ( $K_M$  of 200-400  $\mu\text{M}$ ); (b) a  $V_{\text{max}}$  of 1 - 12 nmol/min/g dry cell; (c) high dependence on temperature, pH and energy; (d) trans-stimulation (10), i.e., stimulation of influx (or efflux) of one folate compound by the presence of a second folate compound inside (or outside) of cells. The use of derivatives of methotrexate to label covalently the carrier responsible for mediating reduced-folate transport in L1210 cells identified a single polypeptide with a molecular weight 43000 Dalton (25-28). The gene coding for this protein has not been isolated yet and the amino acid sequence for this protein is not known either. The reduced-folate carrier-mediated transport system has not been shown definitely to occur in any normal cells (3).

*Low affinity/high capacity transport system in L1210 cells* While the influx of folic acid is mediated in small part by the reduced-folate carrier, its transport is believed to occur predominantly by mechanism(s) which are distinct from this route (29, 30). This conclusion is based upon several observations by Sirotnak et al. (29, 30). First, data showed that the  $V_{\text{max}}$  for initial mediated influx of folic acid was much greater than that shown for initial influx of methotrexate and reduced-folates (29). The initial influx of both L-formyl-tetrahydrofolate and methotrexate was highly saturable (apparent  $K_M=3-4 (\pm 0.6) \mu\text{M}$ ) but exhibited a relatively low apparent  $V_{\text{max}}$  3 ( $\pm 0.4$ ) pmol/min/mg membrane protein. However, initial influx of folic acid exhibited low saturability ( $K_M=409 (\pm 66) \mu\text{M}$ ) and a high  $V_{\text{max}}$  (123 ( $\pm 33$ ) pmol/min/mg membrane protein). Secondly, there

were major discordances between values for influx  $K_M$  and influx  $K_i$  (inhibitor dissociation constant for a carrier) for various folate compounds. For compounds which share a single transport system, values for influx  $K_M$  and influx  $K_i$  for competition experiments should be approximately the same (29). The results show that this was not the case.  $K_i$  values of 5-formyltetrahydro-folate, 5-methyltetrahydrofolate and methotrexate for folic acid uptake were much larger (greater than 1000  $\mu M$ ) than the corresponding  $K_M$  values. On the other hand, 5-formyltetrahydrofolate, 5-methyltetrahydrofolate and methotrexate were very efficient competitive inhibitors for the uptake of radioactive 5-formyltetrahydrofolate whereas folic acid was a poor competitive inhibitor of 5-formyltetrahydrofolate uptake ( $K_i$  values were 1.82 ( $\pm 0.9$ ), 1.25 ( $\pm 0.1$ ), 4.56 ( $\pm 0.6$ ) and 442.0 ( $\pm 72$ )  $\mu M$  for 5-formyltetrahydrofolate, 5-Methyltetrahydrofolate and methotrexate and folic acid, respectively). Thirdly, the uptakes of 5-formyltetrahydrofolate and methotrexate were much more sensitive than that of folic acid to sulfhydryl inhibitors (27). Additionally, the uptake of reduced-folates into the vesicle also showed trans-stimulation by the presence of a folate compounds inside the vesicle. Trans-stimulation was not observed for folic acid uptake. Finally, the time-course for intravesicular accumulation of 5-formyltetrahydrofolate and folic acid by plasma membrane vesicles isolated from wild-type (methotrexate-sensitive) and mutant (methotrexate-resistant) L1210 cells showed additional evidence for the multiplicity of folate entry routes in L1210 cells (29, 30). The initial accumulation of 5-formyltetrahydrofolate was lower in mutant-derived vesicles than in the wild-type. However, initial accumulation of folic acid was the same in mutant and wild-type-derived vesicles. Therefore, it was proposed that folic acid influx in L1210 cells is mediated mainly by a system distinct from the classical reduced-folate carrier

mediating influx of methotrexate and folate compounds (29, 30). This new system is called the low affinity/high capacity transport system (30). The existence of this system is however, controversial and some researchers attribute the existence of this system to a phenomena caused by the impurities in the [ $^3\text{H}$ ]-folic acid used in the experiments (31). This system has not been purified and nothing is known about its nature at molecular level.

*A secondary low capacity system in L1210 cells* Henderson and Strauss (31) examined L1210/R81 cells to determine the mechanism by which methotrexate-resistant cells with a defect in methotrexate transport can achieve folate sufficiency. This cell-line lacked the reduced-folate carrier and the high-affinity folate binding protein. The high affinity-folate binding protein (folate receptor), which is explained below, can mediate the uptake of folate at nanomolar concentration. Their results showed that an alternative transport system is operating in the L1210 variant cell line, which is manifested at low pH and mediates the energy-dependent influx of folate, 5-formyltetrahydrofolate, and methotrexate in the 5-10  $\mu\text{M}$  range. This system binds but does not transport 5-methyltetrahydrofolate. This system was not sensitive to the anion compositions in the transport assay buffer in contrast to the reduced folate carrier. This system was very sensitive to pH whereas the reduced-folate carrier was not. N-hydroxysuccinimide ester of methotrexate or bromosulphophalein, the inhibitors for reduced-folate carrier did not have any effect on this system. In this cell line, the low affinity/high capacity system was not detected. Therefore, Henderson and Strauss (31) attributed the existence of the low affinity/high capacity system claimed by Sirotnak et al. (29, 30) to impurities in [ $^3\text{H}$ ]-folate.

*High affinity folate binding proteins (folate receptors) in KB cells and L1210 cells*

Meanwhile, the membrane-bound folate receptors (32-48) have been shown to mediate the uptake of folate compounds such as 5-methyltetrahydrofolate (33) and methotrexate (34, 35) mainly by the studies with human nasopharyngeal carcinoma (KB) cells. The folate receptor has a greater affinity for folic acid (association constant  $K_a = 1.3 \text{ nM}^{-1}$ , ref. 36) than for reduced-folates ( $K_a = 0.3 \text{ nM}^{-1}$  for 5-methyltetrahydrofolate, ref. 36). The folate receptor is bound to the cell surface through a glycosyl-phosphatidylinositol linker (37-39, Fig. 1). It has been shown that the folate receptor recycles between the cell surface and an as yet undetermined intracellular location and it has therefore been suggested that the folate compounds in KB cells are endocytosed by the folate receptors (34). It has also been shown that the folate receptors are converted to soluble form by metalloprotease(s) and released into culture medium in the presence of high concentration of folates (40-42). The complementary DNA coding for the folate receptor in KB cells has been isolated (43) and the complete amino acid sequence (257 amino acid residues) of the folate receptor is known (44-47). The folate receptor is heavily glycosylated (48) and bound to the cell surface through a glycosyl-phosphatidylinositol linker (37). A role for the reduced-folate carrier, the low affinity/high capacity system, or the secondary low capacity system for the transport of folate compounds has not been investigated in KB cells (3).

Recent studies (6, 49-52) have shown that propagation of the L1210 cells (6, 49-50, 52) or CCRF-CEM cells, a human leukemic cell line (51) in media containing only nanomolar concentrations of folate leads to the gradual expression of a high affinity folate binding protein as well as the reduced-folate carrier, while cells grown in media containing micromolar concentrations of



folate expressed only reduced-folate carrier. It has been shown that this high affinity folate binding protein mediates the uptake of folic acid (36, 38). The folate binding protein in L1210 cells has amino-acid sequence homology to the folate receptor in KB cells and other sources (6), suggesting that it is a folate receptor. Analysis by polyacrylamide gel-electrophoresis has shown that the folate receptor and the reduced-folate carrier in L1210 cells have molecular weights 39 and 43 kDa, respectively (27). It has been suggested that the folate binding protein and the reduced-folate carrier in L1210 cells operate independently to take up folate compounds (52).

*Folate receptor and an anion carrier in MA104 cells* Recent studies (53-58) with cultured monkey kidney cells (MA104) have suggested that the uptake of 5-methyltetrahydrofolate is mediated by both the folate receptor (53, 54) and an anion carrier with characteristics of the reduced-folate carrier (55, see Fig. 2 A). It has been shown that the folate receptor is bound to the extracellular surface of the nonclathrin-coated invaginated regions of the plasma membrane (caveolae, ref. 56) through a glycosylphosphatidyl inositol linker (57). The caveolae can transiently close in MA104 cells to form vesicles (58). It has also been shown that the uptake of 5-methyltetrahydrofolate is mediated by an anion carrier which is impaired by probenecid and has the kinetic parameters ( $K_M$  and  $V_{max}$ ) similar to those of the reduced-folate carrier (55). Therefore it has been suggested that the probenecid-sensitive anion carrier and the membrane-bound folate receptor associated with caveolae work in tandem to transport 5-methyltetrahydrofolate to the cytoplasm as described in Fig. 2 A (5, 54-56). However, in these studies direct evidence that shows the coupling of the two systems has not been presented (3). Therefore, the possibility that the folate receptor and the probenecid sensitive-carrier worked independently to transport 5-

methylnetetrahydrofolate can not be excluded (3, see Fig. 2 B). Moreover, it was not clearly shown whether this probenecid-sensitive anion carrier was exactly the same as the reduced-folate carrier or not (55). According to the studies by Henderson et al. (19), probenecid inhibits the influx and efflux of folate compounds through the reduced-folate carrier. Probenecid also inhibits the transport of sulfate (19). Sulfate is transported via both the reduced-folate-carrier and a general anion carrier (20). One of the primary functions of the general anion carrier is to exchange rapidly intracellular bicarbonate for extracellular chloride (20). Therefore, inhibition of 5-methylnetetrahydrofolate uptake by probenecid does not necessarily mean that the reduced-folate carrier is the only system responsible for the 5-methylnetetrahydrofolate uptake in MA104 cells. It is equally possible that the general anion carrier mediates 5-methylnetetrahydrofolate uptake in MA104 cells. This issue was not clarified in MA104 cells (55). Sulfate inhibits the uptake of methotrexate, but methotrexate hardly inhibits the sulfate transport in L1210 cells (20). If 5-methylnetetrahydrofolate transport occurs by the general anion carrier as sulfate transport does, it should not be inhibited by methotrexate. However, inhibition of 5-methylnetetrahydrofolate by methotrexate has not been reported in those studies (55). Finally, the concentrations of the probenecid in those studies were too high (10 mM) and the effect of this inhibitor on other cellular processes such as endocytosis of folate receptor was not studied (55). Probenecid is known to slightly affect the ATP level, membrane potential and glucose utilization in the cell, suggesting that it is a weak metabolic inhibitor (19).

**Membrane carriers involved in methotrexate efflux** Based upon kinetic analysis Dembo and Sirotiak (59, 60) proposed a model in which the influx and efflux of methotrexate take place via different carriers in L1210 cells. According

to this model, cells have a distinct influx carrier and efflux carrier (60). The efflux carrier is coupled to energy and it carries methotrexate unidirectionally out of the cell at the direct expense of ATP (61). But the influx carrier, the reduced-folate carrier is indirectly coupled to energy. According to them, return of the unloaded influx carrier from the inner to the outer side of the cell membrane could be accelerated by an elevated intracellular concentration of a specific competitive counter ion (perhaps one of the naturally occurring folates or even some kind of simple organic anions). Alternatively, it is hypothesized that accelerated cycling of free carrier could be mediated by a mechanism based on nonspecific differences in the pH or ionic strength of the interior and exterior cellular compartments. Henderson et al. (11) reported that there are at least three routes for methotrexate efflux in cells (Table 2). The major efflux of this drug occurred through the reduced-folate carrier, which can be shown by the reduction in efflux in cells treated with the *N*-hydroxysuccinimide ester of methotrexate. A second route was identified by the sensitivity to bromosulphophthalein and insensitivity to *N*-hydroxysuccinimide ester of methotrexate. A third route was identified by the insensitivity to both reagents. All three efflux routes were inhibited by probenecid (19). However, recent studies by Sirotnak et al. (62) showed that L1210 cells have only two efflux routes; the influx carrier and the bromosulphophthalein-, probenecid-, and verapamil-inhibitable efflux route. The existence of the third efflux route suggested by Henderson et al. (11) was denied by Sirotnak et al. (62) since no evidence was obtained for the third bromosulphophthalein-insensitive, probenecid-inhibitable route for methotrexate efflux in their experiments. The ATP-dependent, bromosulphophthalein-, probenecid-, and verapamil-inhibitable efflux route accounted for 90 % of methotrexate efflux in ATP-replete cells

whereas in ATP depleted cells overall efflux of methotrexate was markedly reduced and appeared to be mediated solely by the methotrexate influx carrier. It has not been clearly understood whether 5-methyltetrahydrofolate uses the same efflux routes as suggested in the above model in L1210, KB or MA104 cells partly because the 5-methyltetrahydrofolate is rapidly metabolized inside the cells.

**Purpose of this study** Various systems in the transport of folate compounds in mammalian cells were briefly reviewed above. Many issues remain to be resolved in these systems. Especially, the inter-relationship between the folate receptor, the probenecid-sensitive anion carrier and the reduced-folate carrier in the intracellular transport of 5-methyltetrahydrofolate and other folate compounds in eukaryotic cells has not been clearly understood (3). In order to determine whether the folate receptor and the probenecid-sensitive anion carrier work in tandem for the uptake of 5-methyltetrahydrofolate as suggested by the studies in MA104 cells (55, see Fig. 17 B), or independently as suggested by others (52, see Fig. 17 A), and to determine the identity of the probenecid-sensitive anion carrier, we have studied the effects of folic acid and probenecid on various steps of 5-methyltetrahydrofolate uptake in KB cells.

We report evidence here for 5-methyltetrahydrofolate uptake by a probenecid-sensitive anion carrier as well as the folate receptor in KB cells. Our data suggest that probenecid at very high concentration (5 mM) inhibits the endocytosis of the folate receptor as well as the anion carrier. Our data also show that the uptake of 5-methyltetrahydrofolate in KB cells is competitively inhibited by probenecid, folic acid and methotrexate, suggesting that the uptake is mediated by an anion carrier with the characteristics of the reduced-folate carrier. Finally, our data show that the occupancy of folate receptor by 5-

methyltetrahydrofolate appears to enhance the transport of the vitamin through the probenecid-sensitive carrier, assuming that probenecid does not interfere with the acidification of the lumen of the endosomes (possibly caveola).

## MATERIALS AND METHODS

### Materials

Human epidermoid carcinoma (KB) cells (passage No. : 364) were obtained from American Type Culture Collection, Rockville, MD. Media constituents were obtained from Gibco Laboratories. Vitamins were purchased from Sigma Chemical Company. Fetal calf serum (FCS) was purchased from HyClone Laboratories, Inc., Logan, Utah. Fungi-Bact solution (penicillin G 10,000 units/ml, streptomycin sulfate 10,000 µg/ml, fungizone 25 µg/ml in normal saline) were obtained from Irvine Scientific, Santa Ana, CA. (6S)-5-methyltetrahydro[3', 5', 7, 9-<sup>3</sup>H]pteroylglutamate ([<sup>3</sup>H]-5-methyltetrahydrofolate) and [3', 5', 7, 9-<sup>3</sup>H]-folic ([<sup>3</sup>H]-folic acid) acid were purchased from Moravsek Biochemicals, Brea, CA. DL-5-methyl-tetrahydrofolate (DL-5-methyltetrahydrofolate, disodium salt), *p*-[dipropylsulfamoyl]benzoic acid (probenecid), bovine serum albumin (BSA, fraction V, Cat. No A-4378) and vitamins were obtained from Sigma Chemical Company. 1-(3-dimethylaminopropyl)-3-ethylcarbodiimide hydrochloride (EDC·HCl) was purchased from Aldrich Chemical Company, Inc., Milwaukee, Wisconsin. Na<sup>125</sup>I was purchased from Amersham Corporation, Arlington Heights, IL. Iodo-beads were purchased from Pierce Chemical Company, Rockford, IL. Centriprep-30 concentrators were purchased from Amicon, Danvers, MA.

**Preparation of cell culture media** (a) *Folate-deficient Dulbecco's modified Eagle's medium (fdDMEM) and folate-deficient Dulbecco's modified Eagle's medium supplemented with 5 % fetal calf serum (fdDMEM, 5% FCS)* : Folate-deficient Dulbecco's modified Eagle's medium (fdDMEM) was required to enhance the expression of folate receptors in KB cells (32, 63). fdDMEM which has the same amounts of the media components as Dulbecco's modified Eagle's medium

(Gibco Laboratories manual) except for folic acid was formulated as follows (see Appendix A); For 1 liter medium, Earle's Balanced salt solution (powder, 1 pkg./L), 40 ml basal medium Eagle supplements (amino acid solution), 21 ml HEPES (1.0 M), 10 ml MEM sodium pyruvate solution (100 mM), 20 ml L-glutamine solution (200 mM), 10  $\mu$ l ferric nitrate solution ( $\text{Fe}(\text{NO}_3)_3 \cdot 9\text{H}_2\text{O}$ , 10 mg/ml), 0.3 ml glycine solution (100 mg/ml), 4.2 ml L-serine solution (10 mg/ml), 2.2 g  $\text{NaHCO}_3$ , 10 ml Fungi-Bact solution and 40 ml vitamin stock solution made in the laboratory (100 mg/ml D-Ca pantothenate, 100 mg/ml choline chloride, 200 mg/ml i-inositol, 100 mg/ml nicotinamide, 100 mg/ml pyridoxal-HCl, 10 mg/ml riboflavin, and 100 mg/ml thiamine-HCl) were mixed. The volume of the solution was adjusted to about 900 ml with deionized water and the pH was adjusted to 7.3 with NaOH solution. For assay medium (fdDMEM), the final volume was adjusted to 1 liter. For cell culture medium (fdDMEM, 5% FCS), the final volume was adjusted to 1 liter after adding 50 ml heat-inactivated fetal calf serum. Since fetal calf serum contains almost 20 nM folate (32), the final folate content in fdDMEM, 5% FCS is estimated to be a maximum of 1 nM.

(b) *Minimum essential medium, 10 % fetal calf serum(MEM, 10 % FCS)* : Minimum essential medium was prepared as described by the vendor and supplemented with 10 % (vol/vol) heat-inactivated fetal calf serum, penicillin (100 units/ml), streptomycin (100  $\mu$ g/ml) and fungizone (0.25  $\mu$ g/ml). This medium contains about 2.3  $\mu$ M folic acid. All media were sterilized by filtering through 0.2  $\mu$ m filter units and kept at 4 °C.

**Cell culture** Cultures of KB cells were initiated as described by the supplier.  $7 \times 10^5$  KB cells were inoculated into 15 ml MEM, 10 % FCS in 75 cm<sup>2</sup> culture flasks and grown as a monolayer at 37 °C in a 5 % CO<sub>2</sub>/95 % air

humidified atmosphere. The supernatant medium with cryopreservative was removed and fresh medium added to the cells after 24 hours culture. Cells were passed into fresh medium every 7 days using 0.25 % trypsin-1mM EDTA solution. 3 days after each passage, the medium was replaced with fresh medium. For 5-methyltetrahydrofolate uptake assays, cells were transferred for two consecutive passages into fdDMEM, 5 % FCS to enhance the expression of folate receptors and the uptake of folates according to modified procedures of Leamon et al. (63); On day 0, about  $5 \times 10^5$  cells were passed into 15 ml fdDMEM, 5% FCS and propagated as described above in 75 cm<sup>2</sup> culture flasks. On day 6, cells were harvested and transferred into 6-well culture trays.  $1.5 \times 10^5$  cells were seeded into each well containing 3 ml fdDMEM, 5 % FCS and cultured for 4 days. The cells were used for uptake assays on day 10.

**Modification of proteins** (a) *Conjugation of DL-5-methyltetrahydrofolate to bovine serum albumin*: DL-5-methyltetrahydrofolate was conjugated to bovine serum albumin (BSA) by the modified procedures of Leamon *et al.* (63). 5-methyltetrahydrofolate solution (0.15 ml of 0.1 M) was prepared by mixing 0.125 ml of 0.127 M 5-methyltetrahydrofolateNa<sub>2</sub> in DMSO and 0.025 ml 1 N HCl. 1-(3-dimethylaminopropyl)-3-ethylcarbodiimide hydrochloride (EDC·HCl) solution (1 ml of 0.3 M in dimethylsulfoxide, DMSO) was added to 5-methyltetrahydrofolate solution and the carboxyl groups of 5-methyltetrahydrofolate were activated for 15 min at room temperature (23 °C). The 5-methyltetrahydrofolate/EDC·HCl solution was added to 3 ml of 10 mg/ml BSA in PBS solution dropwise. After reaction for 5-6 hours, BSA which was covalently conjugated with 5-methyltetrahydrofolates was purified by three consecutive gel filtrations; twice on a Sephadex G-25 gel filtration column (2.5 x 40 cm) and once on a Sephadex G-100-120 column (2.5 x 47 cm). PBS (pH 7.4)



was used as an elution buffer. For the second and third gel filtration, eluted protein fractions were pooled and concentrated by centrifugation at 3,000 rpm for an hour in a GSA rotor (Beckman) using a Centriprep-30 concentration device (Amicon). After the third filtration, eluted protein fractions were collected and kept at -20 ° C.

(b) *Conjugation of folic acid to bovine serum albumin*: Folic acid was conjugated to bovine serum albumin (BSA) by the modified procedures of Leamon *et al.* (63). Folic acid in DMSO (1.25 ml of 0.02M) was added to 1-(3-dimethylaminopropyl)-3-ethylcarbodiimide hydrochloride (EDC·HCl) solution (1.127 ml of 0.3 M in DMSO) and the carboxyl groups of folic acid were activated for 15 min at room temperature (23 °C). The folic acid/EDC·HCl solution was added to BSA in PBS solution (10 ml of 10mg/ml solution) dropwise. The reaction mixture was incubated at room temperature for 4 hours and purified as described above using gel filtration chromatography.

(c) *Characterization of the folate-conjugated BSA*: Protein concentrations were determined using the Bio-Rad protein assay solution with BSA as a standard. The extent of DL-5-methyltetrahydrofolate conjugation to BSA was determined spectrophotometrically by measuring the absorbance of the conjugated protein at 300 nm in 1x PBS (pH 7.4) with DL-5-methyltetrahydrofolate as a standard. 350 nm was used for folic acid. The absorbance of the conjugated protein was subtracted from the absorbance of free BSA at the same concentration.

(d) *Radioiodination of proteins*: BSA and 5-methyltetrahydrofolate-conjugated BSA (mfBSA) were labelled with  $^{125}\text{I}$  using Iodo-beads at room temperature (23°C) for 45 minutes as described by the supplier (see Appendix B). Radioiodinated proteins were purified on Sephadex G-25 gel filtration columns (1.5x35 cm) pre-equilibrated with 50 mM Tris-HCl(pH 7.5).  $\gamma$ -Ray emissions were

measured on a Beckman Biogamma II counter for 20  $\mu$ l aliquots from each 4 ml fractions. Protein concentrations of the radioiodinated proteins were determined using the Bio-Rad protein assay solution with BSA as a standard. Specific radioactivities of the iodinated proteins were determined by liquid scintillation counting using a Beckman LS 6800 scintillation counter.

**Binding and uptake assay** The effects of folic acid and probenecid on the uptake of 5-methyltetrahydrofolate and 5-methyltetrahydrofolate-BSA conjugate were investigated according to modified procedures described by Kamen et al. (64) and Leamon et al. (63). On day 10 of cell growth in low-folate medium, the medium was removed by aspiration and 1 ml fresh fdDMEM was used to wash the cells. To measure the uptake of [ $^3$ H]-5-methyltetrahydrofolate or 5-methyltetrahydrofolate-BSA conjugate, appropriate amounts of [ $^3$ H]-5-methyltetrahydrofolate or 5-methyltetrahydrofolate-BSA in fdDMEM were added to the medium to desired concentrations in 1 ml final volumes. Cells were incubated for various lengths of time at 0 or 37 °C (64). At the end of the incubation, cells were chilled on ice immediately and the supernatants were collected by aspiration. After rinsing cells three times with 1 ml ice-cold Dulbecco's phosphate buffered saline (DPBS), cell-surface bound [ $^3$ H]-5-methyltetrahydrofolate or radioiodinated 5-methyltetrahydrofolate-BSA conjugate was released from the cells by washing rapidly for 30 seconds with 2 ml ice-cold acid saline (0.15 M NaCl, adjusted to pH 3 with glacial acetic acid, twice with 1 ml saline solution where indicated) followed by a rinse with 1 ml cold DPBS. The radiolabelled folate or 5-methyltetrahydrofolate-BSA conjugate in the acid saline was combined with 1 ml cold DPBS wash to represent [ $^3$ H]-5-methyltetrahydrofolate or 5-methyltetrahydrofolate-BSA conjugate released from the cell surface receptors by acid wash (acid-dissociable fractions). The cells

were detached from the culture dish by incubating the cells in 1 ml 0.25 % trypsin-1 mM EDTA for 5 min at 37°C and the flask was rinsed twice with 1 ml DPBS. The trypsin-EDTA cell suspension and DPBS washes were combined and represent [ $^3\text{H}$ ]-5-methyltetrahydrofolates, or 5-methyltetrahydrofolate-BSA conjugates that are internalized by cells (acid-resistant fractions). Alternatively, cells were solubilized in 1 ml of 1 % SDS, 0.1 N NaOH solution and the flask was rinsed twice with 1 ml DPBS. The amount of [ $^3\text{H}$ ]-5-methyltetrahydrofolate was measured by counting in duplicate 0.1 ml aliquots of the incubation media and 1 ml aliquots of acid-dissociable and acid-resistant fractions in scintillation fluid, Safety Solve with a Beckman LS 6800 scintillation counter. The amount of [ $^3\text{H}$ ]-5-methyltetrahydrofolate or 5-methyltetrahydrofolate-BSA conjugate was quantitated using a specific activity value taken from the slope of a standard curve for the radioactivity versus the amount of [ $^3\text{H}$ ]-5-methyltetrahydrofolate or 5-methyltetrahydrofolate-BSA conjugate. The protein content for each of the trypsin-EDTA cell suspensions was determined using 0.1 ml aliquots in duplicate by Peterson's modified Lowry method (65, see Appendix C) with bovine serum albumin as a standard. The amount of trypsin in the suspension, which was determined separately, was subtracted from the protein content of the trypsin-EDTA cell suspension. In order to determine the average mass of a KB cell, cells were counted using a hemocytometer and the protein content was determined as described above.

## RESULTS

**Cooperative binding of 5-methyltetrahydrofolate to the folate receptor in KB cells** We measured the amount of 5-methyltetrahydrofolate associated with the cell or media after incubation of the cells in the presence of varying concentrations of [ $^3\text{H}$ ]-5-methyltetrahydrofolate for 4 hours at 0 °C (Fig. 3 A). The internalization of 5-methyltetrahydrofolate was negligible at 0 °C. Most of the cell-associated vitamin was in the acid-dissociable fraction. This shows that 5-methyltetrahydrofolate can bind to the cell surface but can not be internalized by the cells at 0°C. In order to determine whether the folate receptors bind 5-methyltetrahydrofolate cooperatively or not, the data partly shown in Fig. 3 A were analysed by a Scatchard plot (66). In the analysis, it was assumed that a cell is a macromolecule containing multiple binding sites for 5-methyltetrahydrofolate. The Scatchard plot (Fig. 3 B) showed that the binding of the 5-methyltetrahydrofolate to the cell is positively cooperative. It has been shown that the folate receptor has only one binding site per molecule (36). If the folate receptor exists as a monomer, binding of 5-methyltetrahydrofolate to a receptor would not be affected by the occupancy of a neighboring folate receptor. Therefore, our result suggests that the folate receptors exist as oligomers on the cell surface. Using fluorescent antibodies against folate receptors Rothberg et al. (56) have shown that the receptors are clustered on the cell surface. This result is consistent with our suggestion that the folate receptors exist as oligomers. The average number of binding sites on a KB cell was determined using a graph as shown in Fig. 3 C and D. The approximate number of binding sites per mg cell protein obtained from the extrapolation of graph (Fig. 3 C) was 135 pmol/mg cell protein, which corresponds to  $44 \times 10^6$  sites per cell (using  $5.36 \times 10^{-7}$  mg as an average mass of KB cell). This is slightly smaller than the previously reported

value in KB cells (193 pmol/mg, ref. 32). This difference could be due to the maintenance of cells in different media.

**Inhibition of 5-methyltetrahydrofolate uptake by probenecid, folic acid and low temperature in KB cells** We studied the effects of probenecid and temperature on the uptake of [ $^3\text{H}$ ]-5-methyltetrahydrofolate to define the role of the reduced-folate carrier in KB cells since it has already been shown that the cell surface-bound folate receptors are involved in the transport of [ $^3\text{H}$ ]-5-methyltetrahydrofolate in KB cells (33). Our data show that probenecid inhibits the internalization of [ $^3\text{H}$ ]-5-methyltetrahydrofolate (Fig. 4 A and C, also see Fig. 5 A) but does not influence the binding of the vitamin to the receptors significantly (Fig. 4 A, also see Fig. 5 B). The reason why the acid-dissociable fraction appears to increase as the concentration of probenecid increases in Fig. 4 B is that as probenecid inhibits the uptake of the vitamin more, the concentration of the vitamin in the medium remains higher and more of the folate molecules are bound to cell surface. In order to see if the probenecid-sensitive uptake process is inhibited at low temperature, we measured the acid-resistant fractions and acid-dissociable fractions with or without 5 mM probenecid at 0 °C or 37 °C (Fig. 5 A and B). The results (Fig. 5 A) show that the uptake of 5-methyltetrahydrofolate is inhibited by probenecid significantly at 37 °C and uptake is abolished at 0 °C, which is consistent with the previous results by others (55). Probenecid did not have any further inhibitory effect on the uptake of the vitamin at 0 °C. This indicates that the probenecid-inhibitable uptake process is sensitive to temperature. The data for acid-dissociable fractions of 5-methyltetrahydrofolate at 0 or 37 °C with or without 5 mM probenecid are shown in Fig. 5 B. At 0 °C the acid-dissociable fractions show a concentration dependent increase and saturation over 0.5  $\mu\text{M}$  (Fig. 5 B). The maximum amount

of 5-methyltetrahydrofolate bound was about 70 pmol/mg cell protein, which is approximately a half of 135 pmol/mg cell, the maximum number of binding sites per mg cell obtained from Fig. 3 D. This could be due to the assumption that only the L-isomer of 5-methyltetrahydrofolate is active in binding and internalization. These experimental results suggest that D-isomer can also bind to the folate receptor with almost identical affinity as the L-isomer. However, throughout the calculation in this work, we assumed that only the L-isomer can bind and be internalized by the cells.

Interestingly, at 37 °C the acid-dissociable fractions increase in a concentration-dependent manner below 0.2  $\mu$ M and decreases above 0.2  $\mu$ M and does not change much above 1  $\mu$ M (Fig. 5 B). Above 1  $\mu$ M 5-methyltetrahydrofolate the amount of the acid-dissociable fraction at 37 °C is approximately one-third of that at 0 °C. Probenecid does not have any significant effect on the acid-dissociable fractions at both 0 °C and 37 °C, which is consistent with the results shown in Fig. 4 A. This indicates that the factor that changes the number of 5-methyltetrahydrofolate binding proteins on the cell surface is not probenecid. It has been reported that folate-receptors are down-regulated in the cells grown in media containing high concentrations of 5-methyltetrahydrofolate (67). It has been also shown that the membrane-bound folate receptors are released into the medium by a membrane-associated metalloprotease in the presence of high concentration of folates (42). Therefore we suggest that the decrease in the acid-dissociable fractions over 0.5  $\mu$ M 5-methyltetrahydrofolate at 37 °C (Fig. 5 B) is the result of receptor down-regulation which is sensitive to temperature and the concentration of 5-methyltetrahydrofolate, but not to probenecid. Further studies would be required to verify this interpretation.

In order to define further the role of the probenecid-sensitive carrier and the folate receptors in the uptake of 5-methyltetrahydrofolate at physiological concentrations, we studied the effects of combinations of probenecid and folic acid on the uptake of [ $^3\text{H}$ ]-5-methyltetrahydrofolate by KB cells. Experimental results show that both folic acid and probenecid inhibit the uptake of 5-methyltetrahydrofolate in KB cells (Fig. 6A and B). 100-fold excess of folic acid almost completely abolished the binding of 5-methyltetrahydrofolate to the cell. This shows that folic acid is a very efficient reagent for blocking the binding site of folate receptors on the cell surface. However, small amounts of 5-methyltetrahydrofolate were still taken up by the cells (Fig. 6B) even though almost all the folate receptors were blocked by folic acid (Fig. 6A). This small fraction of uptake could be further inhibited by probenecid (Fig. 6B). These results suggest that KB cells have a separate system which is different from the folate receptor for the uptake of 5-methyltetrahydrofolate. Summarizing the results of the above experiments, KB cells appear to have a probenecid-sensitive system as well as folate receptors for the internalization of 5-methyltetrahydrofolate.

**Folate receptor-dependent uptake of folate-BSA conjugates** In order to determine whether the effect of probenecid on 5-methyltetrahydrofolate uptake was solely due to the inhibition of a putative anion carrier for 5-methyltetrahydrofolate transport, we needed to measure the effect of probenecid on endocytosis of folate receptors. It has been shown that conjugation of folic acid to proteins enhanced the uptake of the proteins by KB cells (63). It has also been shown that folyl polyglutamates can not diffuse out of the cell through the probenecid anion carrier in MA104 cells (55). It has also been shown that a methotrexate derivative which was covalently linked to fluorescein isothiocyanate



via a diaminopentyl spaced linker, was bound to, but was not transported by the reduced-folate carrier of L1210 cells over a period of a few hours (68). Therefore we reasoned that the functional diameter of the carrier would be small and the 5-methyltetrahydrofolate-BSA conjugate would not translocate to the cytoplasm through the probenecid sensitive anion carrier and the uptake of the 5-methyltetrahydrofolate-conjugated BSA would not be sensitive to probenecid. Therefore we measured the effect of probenecid on the uptake of the 5-methyltetrahydrofolate-BSA conjugate in order to determine whether this reagent has any inhibitory effect on the endocytosis of folate receptors.

Before we measured the effect of probenecid on the uptake of 5-methyltetrahydrofolate-BSA, we determined whether the uptake of the vitamin-BSA conjugate was folate receptor-dependent. Our data (Fig. 7 A) showed that covalent conjugation of the DL-5-methyltetrahydrofolate to BSA enhanced the uptake of BSA by KB cells. This result is consistent with the report by Leamon et al. (63). In order to determine whether this enhanced uptake was due to specific interactions between the folate receptors and the conjugated 5-methyltetrahydrofolates, uptake assays were performed in the presence of 0-100  $\mu\text{M}$  DL-5-methyltetrahydrofolate. The average number of 5-methyltetrahydrofolates conjugated to BSA was 10 ( $\pm 1$ ) and the concentration of 5-methyltetrahydrofolate in 12  $\mu\text{g/ml}$  5-methyltetrahydrofolate-conjugated BSA solution corresponded to 1.8 ( $\pm 0.2$ )  $\mu\text{M}$ . Our data (Fig. 7 B) showed that the acid-dissociable fractions, i.e., the binding of the 5-methyltetrahydrofolate-conjugated BSA to the receptors on the cell surface were reduced to background in the presence of excess free 5-methyltetrahydrofolate, indicating that the binding of the 5-methyltetrahydrofolate-conjugated BSA is specific for folate receptors. On the contrary, the acid-resistant fractions of 5-methyltetrahydrofolate-conjugated



BSA were not completely reduced to background even in the presence of more than 50 times excess of 5-methyltetrahydrofolate. This background could be due to uptake by nonspecific interaction. Other data represented in Fig 7C showed that folate-BSA conjugate inhibited the uptake of [ $^3\text{H}$ ]-folic acid more than 98 %. Goldman (9) reported that the uptake of methotrexate in Ehrlich ascites tumor cells was reduced in the presence of human serum albumin. This was attributed to the electrostatic interaction between methotrexate and albumin. Our data in Fig. 7D showed that the inhibition of [ $^3\text{H}$ ]-folic acid uptake by folate-BSA conjugate shown in Fig. 7C was not solely due to albumin. The uptake of [ $^3\text{H}$ ]-5-methyltetrahydrofolate at 90 nM was smaller in the presence of folate-BSA conjugate than in the presence of the same concentration of BSA (Fig. 7D). These results suggest that folate or 5-methyltetrahydrofolate conjugated BSA molecules bind to folate receptors and are endocytosed by KB cells.

**Inhibition of uptake of 5-methyltetrahydrofolate-BSA conjugate by prolonged incubation of KB cells in the presence of high concentrations of probenecid.** The effect of probenecid on the uptake of 5-methyltetrahydrofolate-BSA conjugates is shown in Figs. 8 and 9. In Fig. 8 A, probenecid appears to inhibit the uptake of the 5-methyltetrahydrofolate-BSA conjugate at low concentrations whereas at high concentrations the uptake appears to be slightly stimulated in the presence of probenecid. It is not clear whether this is due to experimental error or to some other effect. One possible reason for this will be discussed below. The inhibition of the uptake of the 5-methyltetrahydrofolate-BSA conjugate by probenecid was more clearly shown in a time-dependent uptake experiment (Fig. 9 A and B). The inhibition of uptake was undetectable during the first 30 min and became pronounced after 2 hours Fig. 9 A. The uptake of 5-methyltetrahydrofolate-BSA conjugate appears slightly more in the

presence of 5 mM probenecid than in the absence of the inhibitor during the first 30 min period in Fig. 9 B. As mentioned above, Goldman (9) reported that the uptake of methotrexate in Ehrlich ascites tumor cells was reduced in the presence of human serum albumin. This was attributed to the electrostatic interaction between methotrexate and albumin. Then, it is possible that 5-methyltetrahydrofolate-BSA conjugates aggregate by charge-charge interactions, i.e., the electrostatic interaction between positively charged groups of 5-methyltetrahydrofolate-BSA conjugate and free carboxyl groups from the conjugated-folates. This would be possible since the conjugated BSA still contains many unmodified lysines as well as other positively charged groups. Then, the concentration of accessible 5-methyltetrahydrofolate in the 5-methyltetrahydrofolate-BSA conjugate solution might be smaller than expected. In the presence of probenecid, however, the accessible concentration of 5-methyltetrahydrofolate in the 5-methyltetrahydrofolate-BSA conjugate solution would be increased since the carboxyl group of probenecid could compete for positive charges with 5-methyltetrahydrofolate. This might be the reason why the uptake of 5-methyltetrahydrofolate-BSA conjugate appears slightly more in the presence of 5 mM probenecid than in the absence of the inhibitor during the first 30 min period in Fig. 9 B. Our data shown in Fig. 7 D support this argument. The uptake of [ $^3$ H]-5-methyltetrahydrofolate in the presence of both BSA and 1 mM probenecid is more than that in the presence of BSA only. This implies that the reduction of the free [ $^3$ H]-5-methyltetrahydrofolate concentration by BSA could be reversed by the addition of 1 mM probenecid. It is expected that probenecid should inhibit the uptake of [ $^3$ H]-5-methyltetrahydrofolate even in the presence of BSA. Then, it is believed that the inhibition of [ $^3$ H]-5-methyltetrahydrofolate uptake by probenecid was masked by a larger increase of

[<sup>3</sup>H]-5-methyltetrahydrofolate uptake due to a large increase of [<sup>3</sup>H]-5-methyltetrahydrofolate concentration in the solution by probenecid. A similar situation could occur at high concentration of 5-methyltetrahydrofolate-BSA conjugate. The degree of aggregation of 5-methyltetrahydrofolate-BSA conjugate should depend on the total concentration of the added conjugate. It is expected that the average size of aggregates of 5-methyltetrahydrofolate-BSA conjugate would increase as the total concentration of 5-methyltetrahydrofolate-BSA conjugate increase. Then, the reversal effect of probenecid would appear greater as the total concentration of 5-methyltetrahydrofolate-BSA conjugate increases. If this is the case, the inhibition of 5-methyltetrahydrofolate-BSA uptake by probenecid could be masked by the increase in uptake due to a large increase of free 5-methyltetrahydrofolate-BSA conjugate in the solution by probenecid. This might be the reason why the uptake of 5-methyltetrahydrofolate-BSA conjugate appears slightly more in the presence of 5 mM probenecid than in the absence of the inhibitor over 10 µg/ml region in Fig. 8 A. Further experiments are required to verify this.

Summarizing the above results, the uptake of 5-methyltetrahydrofolate-BSA conjugate appears to be slightly slowed down by prolonged incubation of cells in the presence of 5 mM probenecid. As mentioned earlier, it has been shown that folyl polyglutamates can not diffuse out of the cell through the probenecid anion carrier in MA104 cells (55) and that methotrexate covalently linked to fluorescein isothiocyanate via diaminopentyl spaced linker, bound to, but was not transported by the reduced-folate carrier of L1210 cells over a few hour period (68). This suggests that the functional diameter of the probenecid-sensitive carrier is not big enough for the translocation of folate-conjugated BSA through this carrier. This suggests that the inhibition of 5-methyltetrahydrofolate-BSA

uptake by probenecid is not due to the blocking of the probenecid-sensitive carrier by probenecid and suggests that probenecid inhibits folate receptor-mediated endocytosis of 5-methyltetrahydrofolate-conjugated BSA in KB cells.

**Effect of short-term incubation of KB cells in varying concentrations of probenecid on the uptake of 5-methyltetrahydrofolate-BSA conjugate by KB cells.** In order to see if the endocytosis of folate receptor is inhibited significantly by concentrations of probenecid lower than 5 mM, we measured the effect of 30 min-incubations at varying concentrations of probenecid on the uptake of 5-methyltetrahydrofolate-BSA conjugate. The results presented in Fig. 10 show that incubation of cells in the presence of up to 1 mM probenecid for 30 min does not significantly change the uptake of 5-methyltetrahydrofolate-BSA conjugate compared to the cells without probenecid treatment.

**Effect of probenecid on the kinetics of 5-methyltetrahydrofolate binding to folate receptor** In order to verify that the decreased uptake of 5-methyltetrahydrofolate-BSA is not due to simple inhibition of the binding of the 5-methyltetrahydrofolate residues to folate receptors, we measured time-dependent binding of 5-methyltetrahydrofolate to cells in the presence and absence of probenecid. The results shown in Fig. 11 suggested that the binding kinetics were not significantly altered by the presence of 1 mM probenecid.

**Time-dependent uptake of 5-methyltetrahydrofolate at micromolar concentrations by KB cells** In order to study the kinetics of 5-methyltetrahydrofolate uptake by the putative probenecid-sensitive anion carrier, time-dependent uptake by KB cells was measured at micromolar concentrations. The initial uptake of 5-methyltetrahydrofolate was very rapid and began to approach steady-state after a few minutes (Fig. 12). This uptake experiment was performed in the presence of 0.5 mM excess folic acid, under

conditions for which almost all the folate receptors should be saturated by folic acid (see Fig. 6 A). These results suggest that KB cells have a transport system for 5-methyltetrahydrofolate which is distinct from the folate receptor. If this alternative system is a transmembrane anion carrier similar to the reduced-folate carrier in L1210 cells, the steady state of uptake could be explained by the rapid increase in the efflux of the 5-methyltetrahydrofolate. Similar experiments were done at 0 °C to make sure that the uptake was temperature-dependent. Scintillation counting of the samples for uptake at 0 °C gave values close to background (data not shown). This showed that the transport of the 5-methyltetrahydrofolate was temperature-dependent. In order to see if the initial uptake of the 5-methyltetrahydrofolate increased linearly during the first few minutes, time-dependent uptake experiments were done at varying concentrations as shown in Fig. 13. Our data showed that the increase in the acid-resistant fraction was almost linear during the first 3 minutes. The effect of excess folic acid on the uptake of 5-methyltetrahydrofolate was also measured as shown in Fig. 14. Excess folic acid with a fixed concentration ratio to 5-methyltetrahydrofolate inhibited the uptake of the 5-methyltetrahydrofolate slightly. A double-reciprocal (Lineweaver Burk) plot showed that the uptake of 5-methyl-tetrahydrofolate by KB cells followed Michaelis-Menten kinetics. The double-reciprocal plots in the presence and absence of folic acid showed that the two curves have very similar slopes. This could be explained if folic acid acts as a competitive inhibitor for the 5-methyltetrahydrofolate carrier as described by the following equations;

$$\frac{1}{V} = \frac{1}{V_{\max}} + \frac{K_M}{V_{\max}} \left(1 + \frac{[I]}{K_i}\right) \frac{1}{[S]} \dots\dots\dots (i)$$

$$\frac{1}{V} = \left(\frac{1}{V_{\max}} + \frac{K_M}{V_{\max}} \frac{1}{K_i} \frac{[I]}{[S]}\right) + \frac{K_M}{V_{\max}} \frac{1}{[S]} \dots (ii)$$

where  $V$ ,  $V_{\max}$ ,  $K_M$ ,  $K_i$ ,  $[I]$  and  $[S]$  are the rate of uptake, maximum rate of uptake, Michaelis constant of 5-methyltetrahydrofolate for the carrier, dissociation constant of the inhibitor to the carrier, concentration of inhibitor, folic acid and concentration of 5-methyltetrahydrofolate, respectively. Equation (i) which is the Michaelis-Menten equation with the competitive inhibitor  $i$  at a concentration  $[I]$ , can be rearranged as equation (ii). Since the ratio  $[I]/[S]$  is fixed, the first term on the right-hand side of equation (ii) becomes a constant. Therefore the slope of curve  $1/V$  against  $1/[S]$  at  $[I]=0$  is equal to that at non-zero  $[I]$ .

**Competitive inhibition of 5-methyltetrahydrofolate uptake by probenecid, folic acid and methotrexate.** In order to characterize further the putative anion carrier for 5-methyltetrahydrofolate in KB cells, the effect of probenecid, folic acid and methotrexate on the transport of 5-methyltetrahydrofolate was studied (Fig. 15). The data presented in Fig. 15 D, E and F showed that the uptake of 5-methyl-tetrahydrofolate in the presence and absence of probenecid, folic acid and methotrexate followed Michaelis-Menten kinetics. The average  $V_{\max}$  and  $K_M$  values of 5-methyltetrahydrofolate for the carrier are  $8.65 (\pm 0.55)$  pmol/min/mg cell protein and  $3.74 (\pm 0.54)$   $\mu\text{M}$ , respectively. Least squares analysis of the lines in the Lineweaver Burk plots showed that the two lines in each figure intercept at points very close to the y-axis, suggesting that the transport of 5-methyltetrahydrofolate was competitively inhibited by folic acid, probenecid and methotrexate (Fig. 15 D, E and F). The

carrier dissociation constants for folic acid, probenecid and methotrexate were 641  $\mu\text{M}$ , 2.23 mM and 13.8  $\mu\text{M}$  respectively. The  $K_M$  and  $K_i$  values showed that the carrier has the highest affinity for 5-methyltetrahydrofolate followed by methotrexate, folic acid and probenecid. The fact that methotrexate was a competitive inhibitor for the uptake of 5-Methyltetrahydrofolate in KB cells has a very important implication. As discussed above, sulfate inhibits the uptake of methotrexate but methotrexate hardly inhibits the sulfate transport in L1210 cells (20). Sulfate was transported by both the general anion carrier and the reduced-folate carrier whereas methotrexate was transported only by the reduced-folate carrier (20). If 5-methyltetrahydrofolate was transported by the general anion carrier as sulfate was, it should not be inhibited significantly by methotrexate. Our data showed that the uptake of 5-methyltetrahydrofolate was indeed substantially inhibited by 30  $\mu\text{M}$  methotrexate (Fig. 15 C and F). This was strong evidence that in KB cells 5-methyltetrahydrofolate was not transported by the general anion carrier, but by a specialized anion carrier with the characteristics of the reduced-folate carrier found in L1210 cells.

**Approximate rate of folate-receptor endocytosis** In the analyses of uptake kinetics by Michaelis-Menten equations, we assumed that the uptake of 5-methyltetrahydrofolate by folate receptor endocytosis was negligible. In order to see if this assumption was valid, we measured the rate of folate receptor endocytosis using the modified procedures of Kamen et al. (54). In this measurement, we assumed that the transport of folic acid via the reduced-folate carrier would be very small since folic acid has a very low affinity for the reduced-folate carrier. The approximate value of the endocytosis rate was obtained by preincubating the cells in the presence of 100 nM [ $^3\text{H}$ ]-folic acid for 4-6 hours at 0 °C to saturate the receptors without any uptake and by incubating



the cells at 37 °C for varying periods of time. Our data showed that [ $^3\text{H}$ ]-folic acid initially bound to the folate receptors moved into the cells as the cells were incubated at 37 °C (Fig. 16 A). It was also clear that a considerable amount of [ $^3\text{H}$ ]-folic acid was released into the incubation medium from the cell surface (Fig. 16 B). Therefore, the rate of [ $^3\text{H}$ ]-folic acid uptake would be only a lower limit for the true endocytosis rate. The uptake of [ $^3\text{H}$ ]-folic acid was almost linear for the first 15 minutes and began to slow down after that (Fig. 16 C and D). The initial rate of [ $^3\text{H}$ ]-folic acid uptake was 0.2 pmol/mg cell/min (Fig. 16 D). The rates of 5-methyltetrahydrofolate uptake at micromolar concentrations was typically more than a few picomoles/min/mg cell protein (Fig. 14 A and Fig. 15 A, B, and C). Therefore, we could assume that the error in the determination of true rate of 5-methyltetrahydrofolate by the reduced-folate carrier would not be significant under our experimental conditions. However, the fraction of uptake via endocytosis would be considerable at very low vitamin concentrations. More accurate kinetic parameters could be obtained by measuring the uptake rate in the presence of excess folic acid to reduce the uptake of 5-methyltetrahydrofolate by endocytosis.

**The interrelationship between the folate receptor and the reduced-folate carrier in intracellular 5-methyltetrahydrofolate uptake** In order to define further the role of the probenecid-sensitive anion carrier and the folate receptors in the uptake of 5-methyltetrahydrofolate at physiological concentrations, we studied the effects of combinations of probenecid and folic acid on the uptake of [ $^3\text{H}$ ]-5-methyltetrahydrofolate by KB cells (see Fig. 17). We reasoned that the transport of 5-methyltetrahydrofolate through the probenecid-sensitive anion carrier would be enhanced by folate receptors if the folate receptor and the probenecid-sensitive carrier work in tandem as suggested by the studies with



MA104 cells (see Fig. 2 A and Fig. 17 B, ref. 55). On the contrary, if folate receptors and the reduced-folate carrier work independently, folate receptors would not enhance the uptake of 5-methyltetrahydrofolate through the probenecid-sensitive anion carrier (see Fig. 2 B and Fig. 17 A).

In order to measure the transport of 5-methyltetrahydrofolate through the probenecid-sensitive anion carrier with, or without the participation of the folate receptor, we needed to inactivate selectively one of the two transport systems without disturbing the other significantly. We showed that probenecid does not interfere with binding of 5-methyltetrahydrofolates to the folate receptors significantly (Fig. 5 B and Fig. 11). We also showed that incubation of KB cells for 30 minutes in the presence of 1 mM probenecid does not interfere with endocytosis of folate receptors significantly (Fig. 10). If we make an additional assumption that probenecid does not significantly interfere with the acidification of the lumen of vesicles where the 5-methyltetrahydrofolate-folate receptor complexes are endocytosed and the 5-methyltetrahydrofolates are released from the receptors at low pH as proposed by others (54, 55), without interfering with folate receptors, we could measure the 5-methyltetrahydrofolate transport into the cell cytoplasm through the probenecid-sensitive anion carrier by taking the differences of [ $^3\text{H}$ ]-5-methyltetrahydrofolate uptake in the presence and absence of 1 mM probenecid (see explanations in Fig. 17). Meanwhile, if folic acid at micromolar concentrations could block the binding of 5-methyltetrahydrofolate at nanomolar concentrations to the receptors, the folate receptor-mediated uptake of 5-methyltetrahydrofolate at physiological concentrations could be inhibited selectively by folic acid without affecting the probenecid-sensitive carrier significantly. As shown in Fig. 6 A, 100-fold excess folic acid blocked the binding of [ $^3\text{H}$ ]-5-methyltetrahydrofolate almost completely. The transport of

the vitamin through the probenecid-sensitive carrier should not be inhibited significantly by folic acid since the  $K_i$  of folic acid for the carrier is very large (641  $\mu\text{M}$ ). This can be shown by a simple calculation for the transport of 5-methyltetrahydrofolate in the absence and presence of folic acid as an inhibitor using the Michaelis-Menten equation as follows;

$$V = \frac{V_{\max}[S]}{K_M(1 + \frac{[I]}{K_i}) + [S]} \dots\dots\dots (\text{iii})$$

where  $V$ ,  $V_{\max}$ ,  $K_M$ ,  $K_i$ ,  $[I]$  and  $[S]$  are the rate of uptake, maximum rate of uptake, Michaelis constant of 5-Methyltetrahydrofolate, dissociation constant of folic acid to the carrier, concentration of folic acid and concentration of 5-Methyltetrahydrofolate, respectively. Our calculations showed that the expected amount of uptake of  $[^3\text{H}]$ -5-methyltetrahydrofolate through the probenecid-sensitive carrier at 50 nM in the absence and presence of 5  $\mu\text{M}$  folic acid would be 0.114 and 0.113 pmol/mg cell/min, respectively. This showed that the inhibition of the carrier by folic acid would not be significant. In the presence of 1 mM probenecid, the inhibition by excess folic acid could be calculated using a Michaelis-Menten equation with two competitive inhibitors shown below;

$$V = \frac{V_{\max}[S]}{K_M(1 + \frac{[I_1]}{K_{i1}} + \frac{[I_2]}{K_{i2}}) + [S]} \dots\dots\dots (\text{iv})$$

where  $[I_1]$ ,  $[I_2]$ ,  $K_{i1}$  and  $K_{i2}$  are the concentration of inhibitor 1, that of inhibitor 2, carrier dissociation constant of inhibitor 1 and that of inhibitor 2, respectively. For example, the transport of 5-methyltetrahydrofolate at 50 nM in the presence of 1 mM probenecid without and with 5  $\mu\text{M}$  folic acid would be 0.0791 and 0.0787 pmol/mg cell/min, respectively. Again the difference was very small. As shown by these calculations, the inhibition of the probenecid-sensitive carrier by

folic acid would not be very significant. Therefore, in the presence of excess folic acid, the [ $^3\text{H}$ ]-5-methyltetrahydrofolate transport into the cell cytoplasm through the probenecid-sensitive anion carrier without the function of folate receptors could be measured by taking the differences of [ $^3\text{H}$ ]-5-methyltetrahydrofolate uptake in the presence and absence of 1 mM probenecid (see explanations in Fig. 17). In summary, these considerations suggest that the lower limits of the amounts of [ $^3\text{H}$ ]-5-methyltetrahydrofolate that are transported through the probenecid-sensitive carrier with and without the participation of the folate receptors could be measured selectively under the experimental conditions discussed above.

The results of such experiments are shown in Fig. 18 A and analysed in Fig. 18 B. The amount of [ $^3\text{H}$ ]-5-methyltetrahydrofolate for (-P)-(+P) in Fig. 18 B, which is the difference between the amount of [ $^3\text{H}$ ]-5-methyltetrahydrofolate uptake in the absence and presence of 1 mM probenecid in Fig. 18 A, corresponds to the lower limit of the [ $^3\text{H}$ ]-5-methyltetrahydrofolate uptake through the probenecid-sensitive carrier into the cytoplasm when the folate receptors are working since there is no excess folic acid and the transport through the carrier is not 100 % inhibited in the presence of 1 mM probenecid (Fig. 3A and C). The amount of [ $^3\text{H}$ ]-5-methyltetrahydrofolate for (100xF)-(100xF,+P) in Fig. 18 B, which is the difference between the amount of [ $^3\text{H}$ ]-5-methyltetrahydrofolate uptake in the absence and presence of 1 mM probenecid (in the presence of 100-fold excess folic acid in both cases) in Fig. 18 A, corresponds to the lower limits of the [ $^3\text{H}$ ]-5-methyltetrahydrofolate uptake through the probenecid-sensitive carrier without the participation of the folate receptors. It is because 100-fold excess folic acid blocks the binding of [ $^3\text{H}$ ]-5-methyltetrahydrofolate to folate receptors and could also reduce the transport of

[<sup>3</sup>H]-5-methyltetrahydrofolate to a certain extent by competitive inhibition. Comparing the the two values, i.e., the amount of [<sup>3</sup>H]-5-methyltetrahydrofolate for (-P)-(+P) and for (100xF)-(100xF, +P), it is suggested that the uptake of [<sup>3</sup>H]-5-methyltetrahydrofolate through the probenecid-sensitive carrier is enhanced by the participation of folate receptors (Enhancement in Fig. 18 B). We believe that this could be strong evidence that the folate receptors and probenecid-sensitive carriers work in tandem to transport 5-methyltetrahydrofolate to the cytoplasm assuming that 1 mM probenecid does not interfere with the acidification of the lumen of the endosomes (Fig. 2 A). However if probenecid interferes with acidification of the membrane vesicles by an as yet unknown mechanism and interferes with the release of 5-methyltetrahydrofolates from the receptors instead of blocking the carriers in the membrane vesicle, it could also inhibit the transport of 5-methyltetrahydrofolate transport into the cell cytoplasm (Figs. 17 C and D). If this is true, our data shown in Fig. 18 are also compatible with the independent model shown in Fig. 2 B. However, an effect of probenecid on the pH of endosomes has not been reported.

## DISCUSSION

Our results from the experiments with folic acid and probenecid inhibition suggest that KB cells have a probenecid-sensitive anion carrier as well as the folate receptor for intracellular 5-methyltetrahydrofolate uptake. The uptake of 5-methyltetrahydrofolate by the probenecid-sensitive carrier was competitively inhibited by folic acid, probenecid and methotrexate. The carrier has a much smaller affinity for folic acid than for 5-methyltetrahydrofolate and methotrexate. These characteristics are similar to those of the reduced-folate carrier in L1210 mouse leukemia cells (4).

Our data show that probenecid can interfere with endocytosis of folate receptors at high concentrations (Fig. 9). We do not know exactly how high concentration of probenecid affects the endocytosis of folate receptors. It has been shown that probenecid has a very broad affinity for anion transport systems (19). Besides the reduced-folate carrier, probenecid inhibits the transport of sulfate (20), phthalate (69), lactate (69), chloride (70), urate (71), citrate (72),  $\alpha$ -ketoglutarate (72) and a leukotriene (73). It has also been shown that probenecid lowers the level of ATP in the cell and also changes membrane potentials (19). If the endocytosis rate is coupled to the concentration of intracellular ATP, the rate of endocytosis might be reduced by reduction of ATP concentrations in the cell due to an as yet unknown action of probenecid.

It is not clear whether probenecid can interfere with intracellular pH regulation. In order to determine the effect of probenecid on the pH of endosomes, we tried to measure the pH of the environment where folate receptors are endocytosed in KB cells using folate-conjugated BSA derivatives which were modified with a few molecules of a pH-sensitive fluorescent probe (DM-Nerf, molecular probe). However, the fluorescence of the conjugates taken

up by KB cells for 24-48 hours was undetectable and we could not measure the pH change due to probenecid (data not shown). In order to test whether probenecid actually interferes with the acidification process, folate-conjugated liposomes containing a pH-sensitive fluorescent probe such as 8-hydroxy-1,3,6-pyrenetrisulfonate (74) would be useful to monitor the change of pH due to probenecid. Recent studies have identified different systems which regulate intracellular pH (ref.75 , Fig. 19). It has been shown that  $\text{Na}^+/\text{H}^+$  antiporter,  $\text{Na}^+$ -dependent  $\text{Cl}^-/\text{HCO}_3^-$  exchanger, ATP-dependent proton pump are responsible for alkalization of the cell cytoplasm whereas  $\text{Na}^+$ -independent  $\text{Cl}^-/\text{HCO}_3^-$  and exchanger and  $\text{Na}^+/\text{HCO}_3^-$  symporter are responsible for acidification. Recently, Madhus et al. (76) reported that probenecid and ethacrynic acid inhibited the intracellular uptake of  $^{36}\text{Cl}^-$  ion by the  $\text{Na}^+$ -independent  $\text{Cl}^-/\text{HCO}_3^-$  exchanger in Vero cells. The intracellular alkalization induced by removal of extracellular chloride in the absence of  $\text{Na}^+$  ion was inhibited by ethacrynic acid. However, the intracellular pH change mediated by  $\text{Na}^+$ -dependent  $\text{Cl}^-/\text{HCO}_3^-$  exchanger in cells given an acid load was not affected by the drugs. Considering the directionality of acidification, it is believed that the  $\text{Na}^+$ -dependent  $\text{Cl}^-/\text{HCO}_3^-$  exchanger is responsible for acidification of endosomes. Therefore, probenecid is not likely to inhibit the acidification of endosomes. Puc  at et al. (77) reported that in rat cardiac cells, probenecid, ethacrynic acid and 4,4'-diisothiocyanatostilbene-2,2'-disulphonic acid (DIDS) inhibited the intracellular acidification which was induced by extracellular ATP in the presence of  $\text{Mg}^{2+}$  ion. It has been proposed that the extracellular ATP activates  $\text{Cl}^-/\text{HCO}_3^-$  exchanger in the presence of  $\text{Mg}^{2+}$  ion (77). It is not known whether the folate receptor-mediated endocytosis is associated with the  $\text{Cl}^-/\text{HCO}_3^-$  exchanger. Furthermore, the assay media did not

contain any ATP molecules in our experiments. Therefore, it is unlikely that probenecid interferes with the acidification of the endosomes associated with the folate receptor-mediated endocytic pathway. Further studies are required to verify this.

Assuming that probenecid did not interfere with the release of the 5-methyltetrahydrofolate from the folate receptors due to the acidification of endosomes containing folate receptor-5-methyltetrahydrofolate complexes (see Figs. 17 B and 18), our data suggested that in KB cells there exists a mechanism by which the occupancy of folate receptors by 5-methyltetrahydrofolate enhances the uptake of 5-methyltetrahydrofolate through the probenecid-sensitive anion carrier at physiological concentrations. The folate receptor is known to recycle between the cell surface and an as yet undetermined intracellular location in KB cells (34, 55). It is attached to the membrane surface through a glycosylphosphatidylinositol linker (37). Therefore, it might be energetically unfavorable for the folate receptor to move across the plasma membrane to deliver the vitamin to the cytoplasm while it recycles between the surface and inside of the cell. This implies that the folate receptor is internalized by endocytosis (34, 54 Fig. 2). It might be also energetically unfavorable for folates with negatively charged carboxyl groups to diffuse into the cytoplasm across the membrane unless they are protonated (Fig 2 B). Antony et al. (78) reported that folates can diffuse into the cell cytoplasm when they are protonated in acidic compartments. However, it is not certain whether this is actually occurring in the cell at physiological concentrations of folates. In order to explain this apparent enhancement of the vitamin transport through the probenecid-sensitive carrier by folate receptors at physiological vitamin concentrations, it could be suggested that the 5-methyltetrahydrofolate molecules are transported to the cytoplasm



through the probenecid-sensitive carriers after the vitamin-folate receptor complexes are endocytosed in a vesicle which may or may not pinch off from the plasma membrane into the cell (cf Fig. 2 A). If the endocytosed 5-methyltetrahydrofolates are released from the receptors inside the small membrane vesicle, this would create a concentrated vitamin solution in a vesicle (cf Fig. 2 A). For example, if the folate receptors release only 25 molecules of 5-methyltetrahydrofolate in a vesicle with the diameter of 100 nm , the final concentration of the vitamin in the vesicle would be 10  $\mu$ M, which is enough to drive the transport of the vitamin into the cytoplasm. This interpretation is analogous to the model of Rothberg et al. (56) in MA104 monkey kidney cells, where the 5-methyltetrahydrofolates are transported through probenecid-sensitive transporters after they are endocytosed and concentrated in the caveolae (Fig. 2 A). In MA104 cells, about 750 receptors form a cluster on the plasma membrane and there are about 800 clusters per cell (56).

There have been several reports about cell lines which have folate receptors and impaired reduced-folate carriers (79-81). Studies of membrane transport of folates or folate analogs in cell lines with folate receptors and impaired reduced-folate carriers have often suggested that the two systems work independently (79, 80, 82). Dixon et al. (79) recently reported that methotrexate accumulation into human breast cancer cells (ZR-75-1) involved a system with characteristics of the reduced-folate carrier, that methotrexate resistant cells (MTR<sup>R</sup> ZR-75-1) which were isolated from the ZR-75-1 cells did not have a carrier for methotrexate transport, and that the two cell lines did not have folate receptors. The two cell lines which did not have folate receptors, could not grow in media containing less than 100 nM folic acid. When they expressed folate receptors in the two human breast cancer cell lines by gene transfection, the two cell lines



were able to grow in media containing only 1 nM folic acid. The accumulation of folic acid, folinic acid, and methotrexate was enhanced in the ZR-75-1 cells and MTR<sup>R</sup> ZR-75-1 cells by expressing folate receptors. The uptake of folates and methotrexate was similar in both cell lines expressing folate receptors. Therefore, they suggested that alterations in the reduced-folate carrier did not affect the folate receptor function much, thereby, the reduced-folate carrier and the folate receptor work independently (79). However, more folate receptors were found in the ZR-75-1 cells than in MTR<sup>R</sup> ZR-75-1 cells after transfection and accurate comparison of folate uptake in the two cell lines was not possible. If the reduced-folate carrier and the folate receptor work completely independently, it might be possible to isolate cell-lines without any reduced-folate carrier but with folate receptors. If the two systems work dependently as suggested by Rothberg et al. (56), it might not be possible to isolate a cell-line with only the folate receptors since in such a cell-line folates would be endocytosed by cells but would never reach the cytoplasm unless simple diffusion of folates across the plasma membrane occurs at a reasonable rate to support cell growth. The MTR<sup>R</sup> ZR-75-1 cells which were reported not to have any functional reduced-folate carrier nor folate receptors could grow in media containing 1  $\mu$ M folic acid. If one of the two systems were abolished completely, the cells could not survive. Therefore, this suggests that the MTR<sup>R</sup> ZR-75-1 cells had residual reduced-folate carrier activity. The CEM/MTX cell line, which was isolated from human CCRF-CEM leukemia cells by culturing them at high concentrations of methotrexate for prolonged periods, was claimed to be "transport defective" (81). However in this cell-line there was still substantial reduced-folate carrier activity (17 % of parental cell line for 1 hour uptake of methotrexate uptake, ref. 81). L1210/R81 cells which have been shown to express the secondary low capacity transport system

by Henderson et al. (31) did not have the reduced-folate carrier nor the folate binding protein. The lack of the reduced-folate carrier was therefore, compensated for by the presence of this novel transport system. Therefore, the effect of absence of the reduced-folate carrier on the survival of this cell line could not be measured. Recently, Matsue et al. (83) reported that expression of folate receptors in PAM 212 cells, a mouse keratinocyte cell line, induced by gene transfection enabled the cells to grow in media containing 1 nM 5-methyltetrahydrofolate, in which untransfected parental PAM 212 cells cannot proliferate. It should be interesting to see if this cell line has the reduced-folate carrier or not. If this cell line does not have any functional reduced-folate carrier, this would be strong evidence for the model in which folate receptors and the reduced-folate carriers work independently.

We do not know whether the folate receptors are associated with caveolae or with other membrane organelles such as clathrin coated pits in KB cells. Leamon et al. (63) reported that folate-conjugated bovine serum albumin and horseradish peroxidase were taken up by KB cells. The former was shown to be intact in the cell by polyacrylamide gel-electrophoresis and the latter also retained its catalytic activity. This indicates that in KB cells the endocytosed folate-conjugated macromolecules were not delivered to the lysosomal compartment where those molecules could be degraded by proteases. This fact favors the caveolae model (5).

We do not know how the vitamin molecules could be released from the receptors in the vesicle if they are endocytosed in KB cells. Kamen et al. (54) reported that in MA104 cells the uptake of the 5-methyltetrahydrofolate was inhibited by monensin, the potassium-sodium ionophore (84, 85). They reasoned that monensin interferes with the establishment of low pH in the caveolae,

thereby inhibiting the dissociation of 5-methyltetrahydrofolate from the receptors, and further the transport of it into cytoplasm (54). A similar mechanism could apply to the KB cells.

Our data (Fig. 3 B) suggest that the folate receptors might be down-regulated in the presence of high concentrations of 5-methyltetrahydrofolate. This indicates that the rate of uptake of 5-methyltetrahydrofolate could be down-regulated by reducing the number of vitamin-receptor complexes that are endocytosed. Further studies are required to understand how the sequential events of 5-methyltetrahydrofolate uptake are triggered and controlled in KB cells and other cells.

We have not studied the efflux of [ $^3\text{H}$ ]-5-methyltetrahydrofolate in KB cells. In order to understand the relationship between the probenecid-sensitive carrier, folate receptor and yet unidentified efflux carriers in KB cells further studies should follow.

## IMPLICATIONS AND FUTURE RESEARCH

**5-Methyltetrahydrofolate uptake mechanism** We studied the roles of the folate receptor and an anion carrier with the characteristics of the reduced-folate carrier in KB cells. We were able to show that KB cells have an anion carrier for 5-methyltetrahydrofolate uptake, which was not known previously. We were also able to provide evidence that probenecid, which was previously considered to inhibit only several anion carriers, inhibits the endocytosis via the folate receptors as well. We examined two current models of 5-methyltetrahydrofolate uptake in cells in detail (Fig. 2). Assuming that probenecid did not interfere with the release of the 5-methyltetrahydrofolate from the folate receptors due to the acidification of endosomes containing folate receptor-5-methyltetrahydrofolate complexes, our data suggested that the 5-methyltetrahydrofolate molecules are transported to the cytoplasm through the probenecid-sensitive carriers after the vitamin-folate receptor complexes are endocytosed in a vesicle (see Figs. 17 B and 18). However, if the assumption is not correct, currently available data from this research and from other studies are compatible with both of the models (see Fig. 17 C and D). Future research should be focused on the effect of probenecid on cellular pH regulation in more detail. Also, other specific inhibitors for the reduced-folate carrier, such as the *N*-hydroxysuccinimide ester of methotrexate could be employed instead of probenecid to avoid some of these complications. The effect of this reagent on the various steps of the 5-methyltetrahydrofolate uptake should be investigated in combination with folic acid. In order to block folate receptors, antibodies against the folate receptors could be used to avoid the possible complications due to the effect of folic acid on the uptake of 5-methyltetrahydrofolate.

**Folate receptor-mediated endocytosis as a potential drug delivery route; an alternative to the clathrin-coated pit endocytic pathway** Folate uptake pathways have been the subject of intensive studies for the past several decades since the discovery was made that methotrexate and other chemotherapeutic agents for leukemia utilize the reduced-folate carrier for cellular entry (3, 4, 5, 6). Development of the resistance of cancer cells to these antifolate chemotherapeutic agents also prompted the search for alternative pathways and led to the discovery of several different transport systems for folate and antifolate compounds in mammalian cells (7, 11, 29, 31, 33, 34, 55). Strategies to design new antifolates depend on the mechanisms folate uptake.

Recently, the folate-receptor endocytosis pathway has been investigated from a different point of view for an alternative drug delivery route into cells by Leamon et al. (63). They showed that folate-conjugated BSA internalized by KB cells was intact using SDS/polyacrylamide gel electrophoresis. They also showed that the DL-5-methyltetrahydrofolate-conjugated horseradish peroxidase retained its enzymatic activity after its uptake by KB cells. These results are consistent with the findings by Rothberg et al. (56) that folate endocytosis (potocytosis, ref. 5) occurs via membrane pits (caveola) which are different from clathrin-coated pits. Molecules that are endocytosed by the clathrin-coated pit endocytic pathway are eventually delivered to lysosomes where the endocytosed molecules are digested by digestive enzymes (86). The findings by Leamon et al. (63) suggests that folate receptor endocytosis is not related to the lysosomal cycle. They have recently shown that folate-conjugated plant toxin (momordin) is taken up by the KB and HeLa cells and inhibits protein synthesis inside the cell (87), suggesting that a folate-conjugated protein can be delivered to cell cytoplasm via folate receptor-mediated endocytic pathway.

Momordin is a single polypeptide plant toxin with a molecular weight of 31 kDa, which inactivates ribosomes, thereby inhibiting protein synthesis (88). In a time-course uptake experiment, Leamon et al. (87) showed that after incubation for 5 hours about 24 % of the cell-associated (cell-surface bound and internalized) folate-momordin conjugates were taken up and that the uptake increased steadily to 32 % in 50 hours. In contrast, protein synthesis was not affected for the first 5 hour incubation. Protein synthesis began to be affected after 5 hours and was fully inhibited after 50 hours. These data suggested that release of toxin conjugate into the cytoplasm does not occur immediately upon entry into the cell by endocytosis, but instead takes several hours before access to the ribosome is achieved. Leamon et al. (87) suggested that folate-conjugated momordin was endocytosed via the folate uptake pathway and translocated into cell cytoplasm by an as yet undefined mechanism. Momordin is a member of a family of ribosome inactivating proteins from plants (89, 90). It exists in the seeds of *Momordica charantia* (bitter pear melon, ref. 88). It inactivates ribosomes in cell-free systems, but has very little effect on intact cells (88). It has been shown that the toxin becomes very cytotoxic if it is conjugated through a disulfide bond to antibodies which are specific to target cells (91-93). Gelonin, a plant toxin similar to momordin also has similar properties (94, 95). It has been suggested that toxins conjugated to antibodies are endocytosed by target cells and the endocytosed immunotoxins are processed such that the toxins can translocate to the cell cytoplasm (96). This implies that the momordin or gelonin has an intrinsic ability to translocate into cell cytoplasm once it is endocytosed, although little is known about the translocation mechanism. It might be possible that folate-conjugated momordins are endocytosed by folate receptor-mediated endocytosis, processed inside the cell and delivered to the cell cytoplasm by a

similar mechanism. In other words, it might be possible that folates in the folate-momordin conjugates serve merely as ligands to folate-receptors on the cell surface but folates might not be directly involved in the translocation of the folate-momordin conjugates into the cell cytoplasm after endocytosis. It is not clear whether proteins such as bovine serum albumin or horseradish peroxidase can translocate into the cell cytoplasm by conjugation to folates (63). It might be possible that these proteins could not cross the membrane and remain in intracellular vesicles whereas momordin translocates to the cell cytoplasm using an as yet undefined cellular protein-translocation mechanism (87). Therefore it remains to be determined whether the method of folate conjugation can be extended to other toxins such as diphtheria toxin fragment A (97-101) in order to deliver them to the cell cytoplasm using the folate-uptake pathway.

**Cellular entry and cytotoxicity of bacterial toxins** Certain bacteria and plants produce proteins that are strongly cytotoxic to mammalian cells (97-101, reviews). Bacterial toxins, such as diphtheria toxin (DT) and *Pseudomonas* exotoxin A (PE), enter mammalian cells and kill them by inhibiting protein synthesis (Fig. 20).

Diphtheria toxin (DT) is secreted as a single polypeptide from *Corynebacterium diphtheriae* that has been lysogenized by a bacteriophage carrying a DT gene (see Fig. 21, ref. 102). X-ray structure analysis shows that diphtheria toxin has three functional domains (103): a catalytic domain at the amino terminus, a receptor domain at the carboxyl terminus and a transmembrane domain which functions in the translocation of the catalytic domain to the cytoplasm of a target cell. Mild trypsinization and reduction of DT *in vitro* generates two fragments, fragment A (amino terminal, about 21 K) and fragment B (carboxyl terminal, about 37 K), as a result of cleavage at residue



190, 192 or 193 between the catalytic domain and transmembrane domain (104, 105). A similar proteolytic cleavage occurs *in vivo* before or soon after the toxin binds to a sensitive cell (106). The catalytic domain and transmembrane domain are covalently linked by a disulfide bond (see Fig. 21). The catalytic domain has a  $\text{NAD}^+$  binding site (103). The toxin is catalytically inactive until it is processed and the  $\text{NAD}^+$  binding pocket is exposed by the cleavage of the catalytic domain from the whole toxin (103). After the receptor domain recognizes its ligand on a target cell, the bound toxin is endocytosed via the clathrin-coated pit (receptor-mediated endocytosis, see Fig. 20., ref. 97, 98). Upon entry into the lysosome, low pH in the lysosome induces a conformational change of the toxin and the hydrophobic transmembrane domain inserts into the membrane of the lysosome (107-109). In the lysosome the catalytic domain is released from the transmembrane domain after cleavage between the catalytic domain and the transmembrane domain by a trypsin-like cellular protease and after reduction of the disulfide bridge which links the two domains (104-106). It has been proposed that the catalytic domain partially unfolds for translocation into cytosol (110). The transmembrane domain permeabilized the cell membrane to sulfate and sucrose in addition to monovalent cations and therefore, the formation of a cation-channel in the cell membrane was implicated (111). It has been shown that the formation of a cation channel is important for the translocation of the catalytic domain across the plasma membrane and that the low pH requirement for the translocation of the catalytic domain (A fragment) is partly determined by the B fragment (transmembrane domain and the receptor domain) (112). However, it is not known in detail how the B fragment assists translocation of the catalytic domain to the cytosol. Inside the cytoplasm, the catalytic domain transfers the ADP-ribose moiety, derived from  $\text{NAD}^+$ , to a modified histidine,



diphthamide of an elongation factor EF-2 (113). ADP-ribosylated EF-2 can no longer support protein synthesis and this leads to cell death (114). A single DT molecule can kill a cell (115). According to Chaudhary et al. (116), the N-terminal sequence of diphtheria toxin, Gly-Ala-Asp-Asp-Val-Val-Asp (GADDVVD, the N-terminus of catalytic domain) is important for the cytotoxicity of the toxin. When the N-terminal sequence was deleted by mutagenesis, the cytotoxicity of the whole toxin molecule was reduced without affecting either cell-binding or ADP ribosylation activity (116).

A mature *Pseudomonas* exotoxin A (PE) is also a single polypeptide which consists of three functional domains (Fig. 21 b, refs 97, 98). In *Pseudomonas* exotoxin A, the order of the functional domains is opposite to that of DT (97, 98, 117, 118). The receptor domain is located at the N-terminal region. The catalytic domain with ADP ribosylation activity is at the carboxyl terminal region. The transmembrane domain is in the middle. A small segment of polypeptide which links the transmembrane domain and the catalytic domain is also a part of the receptor binding domain (118). PE enters a target cell by receptor-mediated endocytosis similar to DT (119, see Fig. 20). It is believed that unlike DT, the PE catalytic domain is translocated into the cytoplasm after the toxin is delivered to trans-Golgi network via coated pits (120). When target cells were treated with Brefeldin A which disrupts the Golgi apparatus of the cell (121), the cytotoxicity of PE was abolished whereas the cytotoxicity of DT was not affected (120). It has been shown that the carboxyl terminal sequence Arg-Glu-Asp-Leu-Lys (REDLK) of PE is required for its cytotoxicity (122). It has been proposed by Chaudhary et al. (122) that the REDLK sequence is involved in the retention of the catalytic domain in the intracellular compartment. When the REDLK sequence was replaced with KDEL, an endoplasmic reticulum retention signal sequence of

cellular proteins, the cytotoxicity of PE was enhanced compared to the wild-type PE with the REDLK carboxyl terminal sequence (123).

**Differential cytotoxicity of liposome-encapsulated gelonin and diphtheria toxin fragment A** It has been shown that liposomes can be used to deliver some toxin molecules into the cytoplasm. McIntosh et al. (125) reported that gelonin encapsulated in liposomes could be delivered to the cytoplasm of cells to inhibit protein synthesis. They showed that gelonin showed cytotoxicity to TLX5 cells (a CBA/Ca mouse T lymphoma), XC cells (Rous sarcoma virus transformed rat fibroblasts) and phytohaemagglutinin-stimulated CBA mouse lymphocytes, when gelonin was encapsulated in phosphatidylserine liposomes, phosphatidylcholine/cholesterol (1:1 molar ratio) liposomes, or phosphatidylcholine/ cholesterol/gangliosides (5 : 5: 1 molar ratio) liposomes. Gelonin and lipid alone or mixed showed no toxicity. However, diphtheria toxin fragment A encapsulated in phosphatidylserine liposomes had no effect on the level of protein synthesis in TLX5 cells or Daudi cells, a human lymphoblastoid B-cell line known to be sensitive to whole diphtheria toxin. Both toxins showed enzymatic activity after encapsulation or radioiodination. The encapsulated toxins were released from the vesicles by incubation with 0.05% Triton-X 100 for 30 min room temperature. Released gelonin retained 90 % of the control and diphtheria toxin fragment A retained 100 % of control (untreated toxin). Lysed liposomes containing buffer had no inhibitory effect on the levels of protein synthesis. Uchida et al. (126) also reported that liposome encapsulated diphtheria toxin fragment A was not cytotoxic. However, when the same toxin was encapsulated in reconstituted Sendai virus vesicles which can fuse with target cell plasma membranes, it exerted cytotoxicity to the cells. If the delivery of liposome contents were a result of fusion with the plasma membrane, both

gelonin and the A chain of diphtheria toxin would be injected into the cytoplasm and would exert their effects equally. Therefore, the experimental results of McIntosh et al. (125) and Uchida et al. (126) suggest that the delivery of liposome contents were not the result of membrane fusion. If the delivery of liposome contents involved the endocytosis of liposomes by the cell, lysis of the liposomes in the endosomes and processing of the toxins in the endosomes for translocation to cytoplasm, the differential effects of liposome encapsulated gelonin and diphtheria toxin fragment A could be explained (125). It might be possible that gelonin was processed in the cell and delivered to the cell cytoplasm whereas diphtheria toxin fragment A was not (125). As discussed in the above section, translocation of diphtheria toxin fragment A requires the cooperation of fragment B. Therefore, it could be explained why the diphtheria toxin fragment A encapsulated in liposomes was not cytotoxic unlike gelonin.

**A test for the possible use of folate conjugation for drug delivery of macromolecules** As stated above, it remains to be determined whether the method of folate conjugation (87) can be extended to any therapeutic molecules such as oligonucleotides in order to deliver them to the cell cytoplasm using the folate-uptake pathway. Since it has been shown that diphtheria toxin fragment A can not translocate to the cell cytoplasm without the cooperation of fragment B, it would be useful to test whether folate conjugation could overcome this barrier. If it turns out that folate conjugated-diphtheria toxin fragment A shows cytotoxicity, this would suggest that there exists a cellular mechanism by which folate-conjugated macromolecules reach the cell cytoplasm. If not, this would suggest that the folate conjugation method could not be generalized for the delivery of macromolecules to the cell cytoplasm. However, even in the case in which folate conjugation can not be generalized for the delivery of

macromolecules, the folate receptor-mediated endocytosis pathway might be still useful as a drug delivery pathway as an alternative to clathrin-coated pit endocytic pathway if folate-conjugated liposomes are used. Folate-conjugated liposomes might be able to fuse with the endosomes after folate receptor-mediated endocytosis and the liposome contents will be delivered to the cell cytoplasm (Fig. 22). This would be more advantageous than endocytosis via clathrin-coated pits for the delivery of drugs since the delivered molecules would not be damaged by the lysosomal enzymes. Additionally, folate receptors are expressed in some normal or cancer cells. Weitman et al. (127) reported limited expression of the folate receptor in a large number of normal human tissues such as choroid plexus, lung, thyroid, and kidney. The liver, intestines, muscle, cerebellum, cerebrum, and spinal cord did not have a detectable amount of folate receptor (127). They also reported that some brain tumors such as anaplastic ependymoma from cerebellum, subependymal giant cell astrocytoma from lateral ventricle, high-grade sarcoma from occipital lobe and juvenile pilocytic astrocytoma from cerebellum overexpress folate receptors (127). Folate receptors have also been found in some ovarian cancer cells (128). Therefore, the folate receptor pathway may be a useful target for liposome-mediated drug delivery as well as for selective immunotherapy or chemotherapy (87, 127).

## REFERENCES

1. Blakley, R. L. (1987) *Eur. J. Biochem.* **251**, 251-253
2. Blakley, R. L. (1969) "The biochemistry of folic acid and related pteridines," in *Frontiers of biology*, Vol. 13 (Neuberger, A. and Tatum, E. L. ed), North-Holland Publishing Company, Amsterdam and London
3. Antony, A. C. (1992) *Blood* **79** (11), 2807-2820
4. Sirotinak, F. M. (1985) *Cancer Res.* **45**, 3992-4000
5. Anderson, R. G. W., Kamen, B. A., Rothberg, K. G. and Lacey, S.W. (1992) *Science* **255**, 410-411
6. Brigle, K. E., Westin, E.H., Houghton, M. T. and Goldman, I. D (1991) *J. Biol. Chem.* **266**, 17243-17249
7. Goldman, I. D., Lichtenstein, N. S. and Oliverio, V. T. (1968) *J. Biol. Chem.* **243**, 5007-5017
8. Goldman, I. D. (1969) *J. Biol. Chem.* **244**, 3779-3785
9. Goldman, I. D. (1971) *Ann N. Y. Acad. Sci.* **186**, 400-422
10. Goldman, I. D. (1971) *Biochim. Biophys. Acta* **233**, 624-634
11. Henderson, G. B. and Zevely, E. M. (1984) *J. Biol. Chem.* **259**, 1526-1531
12. Nahas, A., Nixon, P. F. and Bertino, J. R. (1972) *Cancer Res.* **32**, 1416-1421
13. Henderson, G. B., Suresh, M. R., Vitols, K. S. and Huennekens, F. M. (1986) *Cancer Res.* **46**, 1639-1643
14. Henderson, G. B., Tsuji, J. M. and Kumar, H. P. (1986) *Cancer Res.* **46**, 1633-1638
15. Henderson, G. B., Zevery, E. M. and Huennekens, F. M. (1980) *J. Biol. Chem.* **255**, 4829-4833
16. Henderson, G. B. and Montague-Wilkie, B. (1983) *Biochim. Biophys. Acta* **735**, 123-130

17. Rader, J. I., Neithammer, D. and Huennekens, F. M. (1973) *Biochem. Pharmacology* **23**, 2057-2059
18. Henderson, G. B. and Zevely, E. M. (1981) *Biochim. Biophys. Acta* **640**, 549-556
19. Henderson, G. B. and Zevely, E. M. (1985) *Biochem. Pharmacol.* **34**, 1725-1729
20. Henderson, G. B. and Zevely, E. M. (1982) *Biochemistry International* **4**, 493-502
21. Henderson, G. B. and Zevely, E. M. (1980) *Arch. Biochem. Biophys.* **400**, 149-155
22. Henderson, G. B. and Zevely, E. M. (1981) *Biochem. Biophys. Res. Comm.* **99**, 163-169
23. Henderson, G. B. and Zevely, E. M. (1981) *Biochem. Biophys. Res. Comm.* **104**, 474-482
24. Henderson, G. B. and Zevely, E. M. (1983) *Arch. Biochem. Biophys.* **221**, 438-446
25. Henderson, G. B. and Zevely, E. M. (1984) *J. Biol. Chem.* **259**, 4558-4562
26. Pope, L. E., Fan, J., Chang, C. -M., Minskoff, S. A., Vitols, K. S. and Huennekens, F. M. (1987) *Adv. Enzymme Regul.* **28**, 3-11
27. Fan, J., Vitols, K. S. and Huennekens, F. M. (1992) *Adv. Enzymme Regul.* **32**, 3-15
28. Freishem, J. H., Ratnam, M., McAlinden, K. M., Prasad, K. M. R., Williams, F. E., Westerhoff, G. R., Schnagel, J. H. and Jansen, G. (1992) *Adv. Enzymme Regul.* **32**, 17-31
29. Yang, C. -H., Dembo, M. and Sirotnak, F. M. (1983) *J. Membrane Biol.* **75**, 11-20

30. Sirotnak, F. M., Goutas L. J., Jacobsen, D. M., Mines, L. S., Barrueco, J. R., Gaumont, Y. and Kisliuk, R. L. (1987) *Biochem. Pharmacol.* **36**, 1659-1667
31. Henderson, G. B. and Strauss, B. P. (1990) *Cancer Res.* **50**, 1709-1714
32. McHugh, M. and Cheng, Y.-C. (1979) *J. Biol. Chem.* **254**, 11312-11318
33. Antony, A. C., Kane, M. A., Portillo, R. M., Elwood, P. C. and Kolhouse, J. F. (1985) *J. Biol. Chem.* **260**, 14911-14917
34. Deutsch, J. C., Elwood, P. C., Portillo, R. M., Macey, M. G. and Kolhouse, J. F. (1987) *Arch. Biochem. Biophys.* **274**, 327-337
35. Kane, M. A., Portillo, R. M., Elwood, P. C., Antony, A. C. and Kolhouse, J. F. (1986) *J. Biol. Chem.* **261**, 44-49
36. Elwood, P. C., Kane, M. A., Portillo, R. M. and Kolhouse, J. F. (1986) *J. Biol. Chem.* **261**, 15416-15423
37. Luhrs, C. A. and Slomiany, B. L. (1987) *J. Biol. Chem.* **25**, 21446-21449
38. Verma, R. S., Gullapalli, S. and Antony, A. C. (1992) *J. Biol. Chem.* **267**, 4119-4127
39. Ferguson, M. A. J. (1991) *Current Opinion in Structural Biology* **1**, 522-529
40. Kane, M. A., Elwood, P. C., Portillo, R. M., Antony, A. C. and Kolhouse, J. F. (1986) *J. Biol. Chem.* **261**, 15625-15631
41. Luhrs, C. A., Pitiranggon, P., Costa, M. D., Rothenberg, S. P., Slomiany, B. L., Brink, L., Tous, G. I. and Stein, S. (1987) *Proc. Natl. Acad. Sci. USA* **84**, 6546-6549
42. Elwood, P. C., Deutsch, J. C., and Kolhouse, J. F. (1991) *J. Biol. Chem.* **266**, 2346-2353
43. Sadasivan, E. and Rothenberg, S. P. (1987) *J. Biol. Chem.* **264**, 5806-5811
44. Elwood, P. C. (1987) *J. Biol. Chem.* **264**, 15873-14901

45. Ratnam, M., Marquart, H., Duhring, J. L. and Freisheim, J. H. (1987) *Biochemistry* **28**, 8249-8254
46. Sadasivan, E., Cedeno, M. and Rothenberg, S. P. (1992) *Biochim. Biophys. Acta* **1131**, 91-94
47. Campbell, I. G., Jones, T. A., Foulkes, W. D. and Trowsdale, J. (1991) *Cancer Res.* **51**, 5329-5338
48. Luhrs, C. A. (1991) *Blood* **77**, 1171-1180
49. Henderson, G. B., Tsuji, J. M. and Kumar, H. P. (1988) *J. Membrane Biol.* **101**, 247-258
50. Jansen, G., Kathmann, I., Rademaker, B. C., Braakhuis, B. J. M., Westerhof, G. R., Rijksen, G. and Schornagel, J. H. (1987) *Cancer Res.* **49**, 1959-1963
51. Jansen, G., Westerhof, G. R., Kathmann, I., Rademaker, B. C., Rijksen, G. and Schornagel, J. H. (1987) *Cancer Res.* **49**, 2455-2459
52. Westerhof, G. R., Jansen, G., van Emmerik, N., Kathmann, I., Rijksen, G., Jackman, A. L. and Schornagel, J. H. (1991) *Cancer Res.* **51**, 5507-5513
53. Kamen, B. A. and Capdevila, A. (1986) *Proc. Natl. Acad. Sci. USA* **83**, 5983-5987
54. Kamen, B. A., Wang, M. -T., Streckfuss, A. J. Peryea, X. and Anderson, R. G.W. (1988) *J. Biol. Chem.* **263**, 13602-13609
55. Kamen, B. A., Smith, A. K. and Anderson, R. G. W. (1991) *J. Clin. Invest.* **87**, 1442-1449
56. Rothberg, K. G., Ying, Y. -S., Kolhouse, J. F., Kamen, B. A. and Anderson, R. G. W. (1990) *J. Cell. Biol.* **110**, 637-649
57. Lacey, S. W., Sanders, J. M., Rothberg, K. G., Anderson, R. G.W. and Kamen, B. A. (1987) *J. Clin. Invest.* **84**, 715-720



58. Rothberg, K. G., Heuster, J. E., Donzell, W. C., Ying, Y.-S., Glenney, J. R. and Anderson, R. G. W. (1987) *Cell* **68**, 673-682
59. Dembo, M. and Sirotnak, F. M. (1976) *Biochim. Biophys. Acta* **448**, 505-516
60. Dembo, M., Sirotnak, F. M. and Moccio, D. M. (1984) *J. Membrane Biol.* **78**, 9-17
61. Schlemmer, S. R. and Sirotnak, F. M. (1985) *J. Biol. Chem.* **267**, 14746-14752
62. Sirotnak, F. M. and O'Leary, D. F. (1991) *Cancer Res.* **51**, 1412-1417
63. Leamon, C. P. and Low, P. S. (1991) *Proc. Natl. Acad. Sci. USA* **88**, 5572-5576
64. Kamen, B. A., Johnson, C. A., Wang, M.-T. and Anderson, R. G. W. (1987) *J. Clin. Invest.* **84**, 1379-1386
65. Peterson, G. L. (1977) *Analytical Biochemistry* **83**, 346-356
66. Cantor, C. R. and Schimmel, P. R. in *Bioophysical Chemistry Vol. III* (W. H. Freeman and Company, San Francisco) pp. 849-886
67. Kane, M. A., Elwood, P. C., Portillo, R. M., Najfeld, V., Finley, A., Waxman, S., and Kolhouse, J. F. (1988) *J. Clin. Invest.* **81**, 1398-1406
68. Henderson, G. B., Russell, A. and Whiteley, J. M. (1980) *Arch. Biochem. Biophys.* **202**, 29-34
69. Henderson, G. B. and Zevely, E. M. (1986) *J. Membrane Biol.* **87**, 99-106
70. Motaïs, R. and Cousin, J. L. (1976) *Biochim. Biophys. Acta* **419**, 309-313
71. Knight, T. F., Senekjian, H. O., Sansom, S. and Weinman, E. J. (1979) *Am. J. Physiol.* **236**, F526-F529
72. Pakarinen, A. and Runeberg, L. (1969) *Biochem. Pharmacol.* **18**, 2439-2452
73. Lam, B. K., Xu, K., Atkins, M. B. and Austen, K. F. (1992) *Proc. Natl. Acad. Sci. USA* **87**, 11598-11602
74. Kano, K. and Fendler, J. H. (1978) *Biochim. Biophys. Acta* **509**, 287-299
75. Boron, W. F. (1986) *Ann. Rev. Physiol.* **48**, 377-388

76. Madshus, I. H. and Olsnes, S. (1987) *J. Biol. Chem.* **262**, 7486-7491
77. Pucéat, M., Clément, O. and Vassort, G. (1991) *J. Physiol.* **444**, 241-256
78. Antony, A. C., Kane, M. A., Krishnan, S. R., Kincade, R. S., and Verma, R. S. (1987) *Biochem. J.* **260**, 401-411
79. Dixon, K. H., Mulligan, T., Chung, K. -N., Elwood, P. C. and Cowan, K. H. (1992) *J. Biol. Chem.* **267**, 24140-24147
80. Hill, B. T., Bailey, B. D., Whie, J. C. and Goldman, I. D. (1979) *Cancer Res.* **39**, 2440-2446
81. Rosowsky, A., Lazarus, H., Yuan, G. C., Beltz, W. R., Mangini, L., Abelson, H. T., Modest, E. J. (1979) *Biochem. Pharmacol.* **29**, 648-652
82. Jansen, G., Schornagel, J. H., Westerhof, Rijkse, G., Newell, D. R. and Jackman, A. L. (1990) *Cancer Res.* **50**, 7544-7548
83. Matsue, H., Rothenberg, K. G., Takashima, A., Kamen, B. A., Anderson, R. G. W. and Lacey, A. W. (1992) *Proc. Natl. Acad. Sci. USA* **87**, 6006-6009
84. Ledger, P. W. and Tanzer, M. L. (1984) *TIBS* **9**, 313-314
85. Basu, S. K., Goldstein, J. L., Anderson, R. G. W. and Brown, M. S. (1981) *Cell* **24**, 493-502
86. Alberts, B., Bray, D., Lewis, J., Raff, R., Roberts, K. and Watson, J. D. (1983) in *Molecular Biology of the cell* (Garland Publishing, Inc., New York & London) pp. 367-376
87. Leamon, C. and Low, P. S. (1992) *J. Biol. Chem.* **267**, 24966-24971
88. Barbieri, L., Zamboni, M., Lorenzoni, E., Montanaro, L., Sperti, S. and Stirpe, F. (1980) *Biochem. J.* **186**, 443-452.
89. Lord, J. M., Hartley, M. R. & Roberts, L. M. (1991) *seminars in Cell Biology* **2**, 15-22
90. Stirpe, F. & Barbieri, L. (1986) *FEBS letters* **195**, 1-8

91. Stirpe, F., Wawrzynczak, E. J., Brown, A. N., Knyba, R. E., Watson, G. J., Barbieri, L. & Thorpe, P. E. (1988) *Br. J. Cancer* **58**, 558-561
92. Dinota, A., Barbieri, L., Gobbi, M., Tazzari, P. L., Rizzi, S., Bontadini, A., Bolognesi, A., Tura, S. & Stirpe, F. (1989) *Br. J. Cancer* **60**, 315-319
93. Cumber, A. L., Henry, R. V., Parnell, G. D. Wawrzynczak, E. J. (1990) *J. Immunological Methods* **135**, 15-24
94. Stirpe, F., Olsnes, S. and Pihl, A. (1980) *J. Biol. Chem.* **255**, 6947-6953
95. Wawrzynczak, E. J., Cumber, A. J., Henry, R. V., May, J., Newell, D. R., Parnell, G. D., Worrell, N. R. & Forrester, J. A. (1990) *Cancer Res.* **50**, 7519-7526.
96. Vitetta, E. S. & Thorpe, P. E. (1991) *seminars in Cell Biology* **2**, 47-58.
97. Roberts, L.M. and Lord, J. M. (1992) *Current Opinion in Biotechnology* **3**, 422-429
98. Li, J. (1992) *Current Opinion in Structural Biology* **2**, 545-556
99. Madshus, I. H. and Stenmark, H. *Current Topics in Microbiology and Immunology* **175**, 1-26
100. Wilson, B. A. and Collier, J. (1992) *Current Topics in Microbiology and Immunology* **175**, 27-41
101. Fong, W. P., Wong, R. N. S., Go, T. T. M., and Yeung, H. W. (1991) *Life Science* **49**, 1859-1869
102. Greenfield, L., Bjorn, M. J., Horn, G., Fong, D., Buck, G. A., Collier, J. and Kaplan, D. (1983) *Proc. Natl. Acad. Sci. USA* **80**, 6853-6857
103. Choe, S., Bennett, M. J., Fujii, G., Curmi, P. M. J., Kantardjieff, K. A., Collier, R. J. and Eisenberg, D. (1992) *Nature* **357**, 216-222

104. Moskaug, J. O., Sletten, K., Sandvig, K. and Olsnes, S. (1989) *J. Biol. Chem.* **264**, 15709-15713
105. Collier, R. J. and Kandel, J. (1971) *J. Biol. Chem.* **246**, 1496-1503
106. Sandvig, K. and Olsnes, S. (1981) *J. Biol. Chem.* **256**, 9068-9076
107. Papini, E., Schiavo, G., Tomasi, M., Colombatti, M., Rappuoli, R. and Montecucco, C. (1987) *Eur. J. Biochem.* **169**, 637-644
108. Moskaug, J. O., Stenmark, H. and Olsnes, S. (1991) *J. Biol. Chem.* **266**, 2652-2659
109. McGill, S., Stenmark, H., Sandvig, K. and Olsnes, S. (1989) *EMBO J.* **8**, 2843-2848
110. Jian, J. X., Abrams, F. S. and London, E. (1991) *Biochemistry* **30**, 3857-3864
111. Stenmark, H., McGill, S., Olsnes, S. and Sandvig, K. (1989) *EMBO J.* **8**, 2849-2853
112. Falnes, P. O., Madshus, I. H., Sandvig, K., and Olsnes, S. (1992) *J. Biol. Chem.* **267**, 12284-12290
113. Van Ness, B. G., Howard, J. B. and Bodley, J. W. (1980) *J. Biol. Chem.* **255**, 10710-10716
114. Honjo, T., Nishizuka, Y., Hayaishi, O. and Kato, I. (1968) *J. Biol. Chem.* **243**, 3533-3535
115. Yamaizumi, M., Mekada, E., Uchida, T. and Okada, Y. (1978) *Cell* **15**, 245-250
116. Chaudhary, V. K., FitzGerald, D. and Pastan, I. (1991) *Biochem. Biophys. Res. Comm.* **180**, 545-551
117. Gray, G. L, Smith, D. H., Baldrige, J. S., Harkins, R. N., Vasil, M. L., Chen, E. Y. and Heynecker, H. (1984) *Proc. Natl. Acad. Sci. USA* **81**, 2645-2649

118. Allured, V. S., Collier, R. J., Carrol, S. F. and McKay, D. B. (1986) *Proc. Natl. Acad. Sci. USA* **83**, 1320-1324
119. Ogata, M., Chaudhary, V. K., Pastan, I., FitzGerald, D. J. (1990) *J. Biol. Chem.* **265**, 20678-20685
120. Yoshida, T., Chen, C., Zhang, M. and Wu, H. C. (1991) *Exp. Cell. Res.* **192**, 389-395
121. Pelham, H. R. B. (1991) *Cell* **57**, 449-451
122. Chaudhary, V. K., Jinno, Y., FitzGerald, D. and Pastan, I. (1990) *Proc. Natl. Acad. Sci. USA* **87**, 308-312
123. Seetharam, S., Chaudhary, V. K., FitzGerald, D. and Pastan, I. (1991) *J. Biol. Chem.* **266**, 17376-17381
124. Pastan, I. and FitzGerald (1991) *Science* **254**, 1173-1177
125. McIntosh, D. P. and Heath, T. D. (1982) *Biochim. Biophys. Acta* **690**, 224-230
126. Uchida, T., Kim, Jaeman., Yamaizumi, M., Miyake, Y. and Okada, Y. (1979) *J. Cell Biol.* **80**, 10-20
127. Weitman, S. D., Lark, R. H., Coney, L. R., Fort, D. W., Frasca, V., Zurawski, Jr., V. R. and Kamen, B. A. (1992) *Cancer Res.* **52**, 3396-3401
128. Coney, L. R., Tomassetti, A., Carayannopoulos, L., Frasca, V., Kamen, B. A., Colnaghi, M. I. and Zurawski, Jr., V. R. (1991) *Cancer Res.* **51**, 6125-6132
129. Madshus, I. H. (1988) *Biochem. J.* **250**, 1-8

## ACKNOWLEDGMENTS

This work was supported by a grant from Vestar Inc., San Dimas, CA, 91773. We thank Dr. Barton A. Kamen and Christopher P. Leamon for their advice and Dr. Wilton E. Vannier for helpful discussions.

## FOOTNOTES

<sup>1</sup> The abbreviations used are: 5-MeH<sub>4</sub>folate, 5-methyltetrahydrofolate; [<sup>3</sup>H]-5-MeH<sub>4</sub>folate, (6S)-5-methyltetrahydro[3', 5', 7, 9-<sup>3</sup>H]pteroylglutamate; [<sup>3</sup>H]-folic acid, [3', 5', 7, 9-<sup>3</sup>H]pteroylglutamate; probenecid, *p*-[dipropyl-sulfamoyl]benzoic acid; MEM, minimum essential medium; fdDMEM, folate-deficient Dulbecco's modified Eagle's medium; FCS, fetal calf serum; HEPES, 4-(2-hydroxyethyl)-1-piperazineethanesulfonate; DPBS, Dulbecco's phosphate buffered saline; EDTA, ethylenediaminetetraacetate.

**Table. 1. Transport systems for folate and antifolate uptake**

Abbreviations: NHS-MTX, *N*-hydroxysuccinimide ester of methotrexate; *p*CMBS, *p*-chloromercuribenzenesulfonate; DIDS, 4,4'-diisothiocyanato-2,2'-disulfonic acid stilbene; SITS, 4-acetamido-4'-isothiocyanato stilbene-2,2'-disulfonic acid; NEM, *N*-ethylmaleimide; BSP, bromosulfophthalein, L1210, mouse leukemia cells; L1210/R81, subcellline of L1210 cells; ZR-75-1, human breast cancer cells; MA104, monkey kidney cells; CCRF-CEM, human leukemic cells

**Table. 1. Transport systems for folate and antifolate uptake**

Systems	1.	2.	3.	4.
	High affinity/ low capacity system (the reduced- folate carrier)	Low affinity/ high capacity system	A secondary low capacity system	High affinity folate binding proteins (folate receptors)
Cell lines with transport systems	L1210 CCRF-CEM ZR-75-1 MA104 (?)	L1210	L1210/R81	<b>KB*</b> MA104 L1210 CCRF-CEM
Substrates in the order of affinity to the transport systems from top to bottom	1. 5-MeH <sub>4</sub> folate 2. 5-formylH <sub>4</sub> - folate 3. methotrexate 4. folic acid	1. folic acid	1. folic acid 2. 5-formyltetra- hydrofolate 3. methotrexate	1. folic acid 2. 5-MeH <sub>4</sub> folate 3. methotrexate
Inhibitors	probenecid carbodiimide- activated folates NHS-MTX pCMBS DIDS SITS NEM BSP phosphate sulfate	less susceptible to pCMBS DIDS SITS	insensitive to NHS-MTX and BSP	folic acid NHS-MTX monensin (MA104) nigericin(MA104)
Sensitivity to pH	insensitive	very sensitive	unknown	low affinity at low pH
Molecular weight	43 kD in L1210 cells	unknown	unknown	39 KD in L1210 cells
Gene	unknown	unknown	unknown	cloned
Transport mechanism	anion exchange- (trans- stimulation by folates)	unknown	unknown	endocytosis
References				

\* Used in this study; ?, unclear



**Table 2. Membrane carriers involved in methotrexate efflux in L1210 cells**

Abbreviations: see Table 1.

---

Efflux routes	Route 1	Route 2	Route 3
	the reduced-folate carrier(influx carrier)	BSP-sensitive route	NHS-MTX-, BSP-insensitive route
Henderson et al. (ref. 19) in L1210 cells	NHS-MTX probenecid	BSP probenecid	insensitive to both BSP and NHS-MTX
Sirotnak et al. (62) in L1210 cells	NHS-MTX probenecid	BSP probenecid verapamil	not found

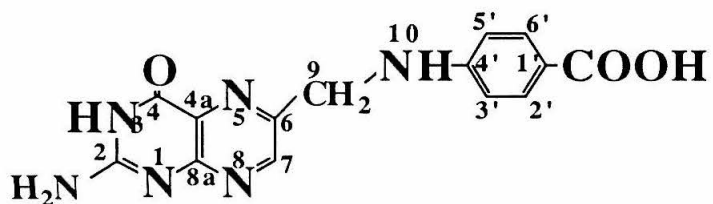
---

**Fig. 1. Structures of pteronic acid, folate derivatives, probenecid and a glycosylphosphatidylinositol linker**

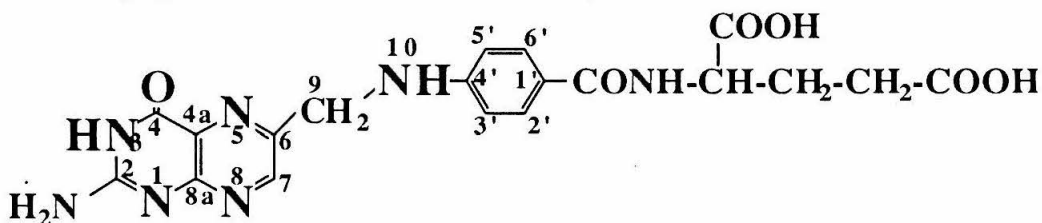
(A) pteronic acid (B) folic acid (C) 7,8-dihydrofolic acid (D) (6S)-5,6,7,8-tetrahydrofolic acid (L-isomer) (E) (6S)-5-methyltetrahydrofolic acid (F) methotrexate (G) pteroylpolyglutamate (H) probenecid (I) glycosyl phosphatidylinositol (GPI) linker

Fig. 1

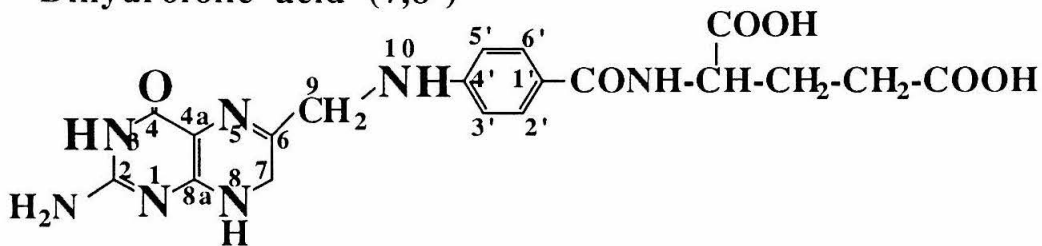
## A. Pterotic acid



## B. Pteroylglutamic acid (folic acid)



## C. Dihydrofolic acid (7,8-)



## D. (6S)-5,6,7,8-tetrahydrofolic acid (L-isomer)

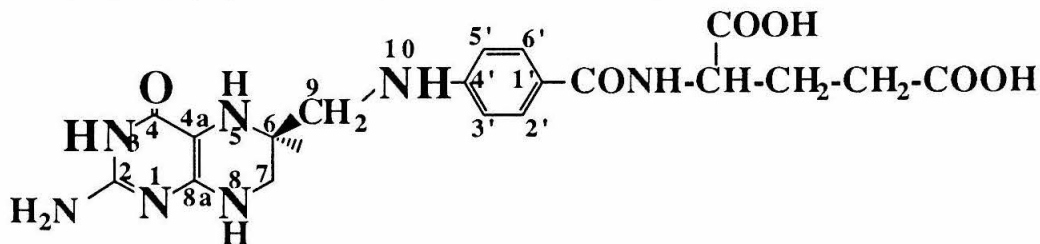
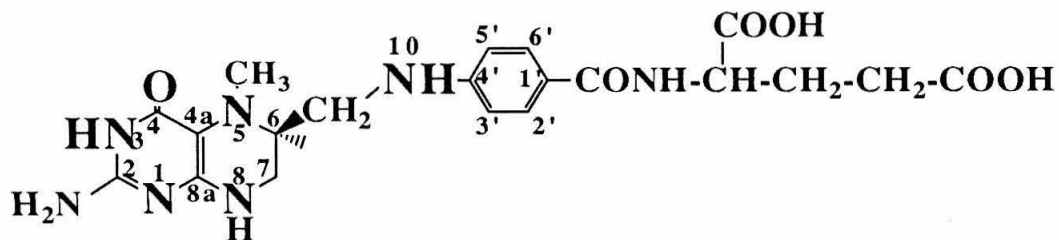
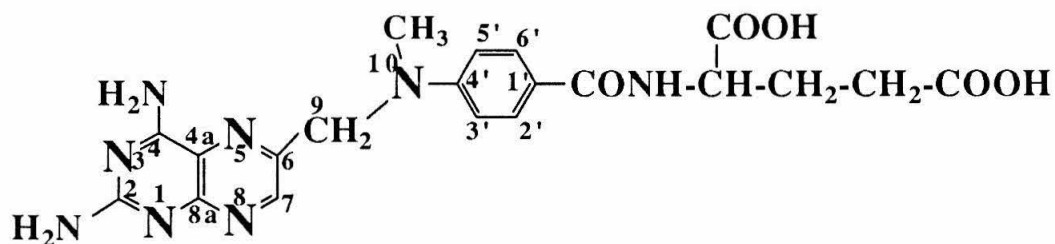


Fig. 1

## E. (6S)-5-methyltetrahydrofolic acid (L-isomer)

F. Methotrexate; 4-amino-*N*<sup>10</sup>-methylpteroylglutamic acid

## G. Polyglutamates

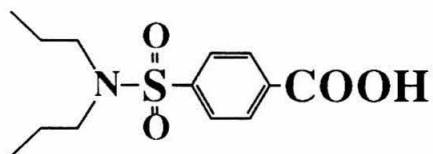
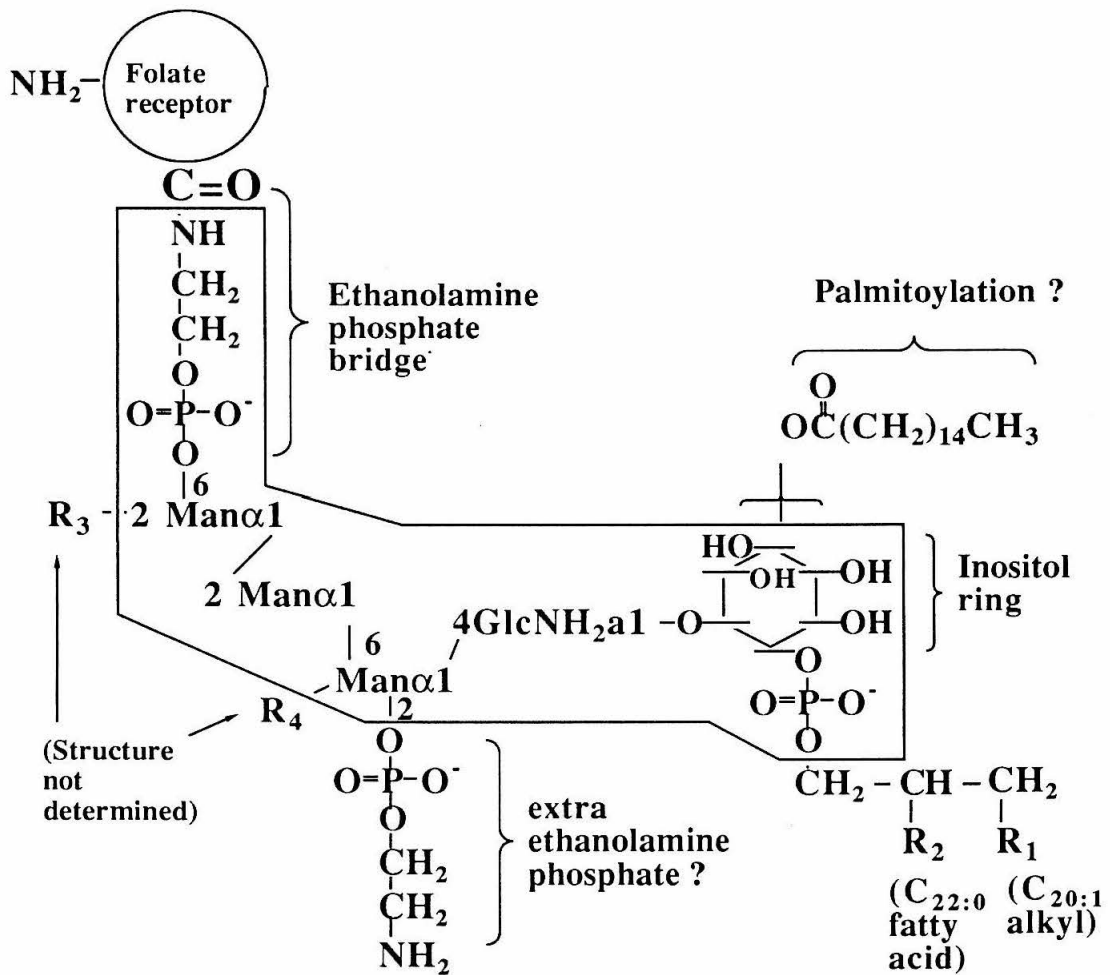
H. Probenecid; *p*-(dipropylsulphamoyl)-benzoic acid

Fig. 1

## G. GPI-linker



$\text{Man}\alpha$ ;  $\alpha$ -mannose

$\text{GlcNH}_2$ ; *N*-acetylgalactosamine

?; unknown

box; conserved structure  
in other GPI linkers

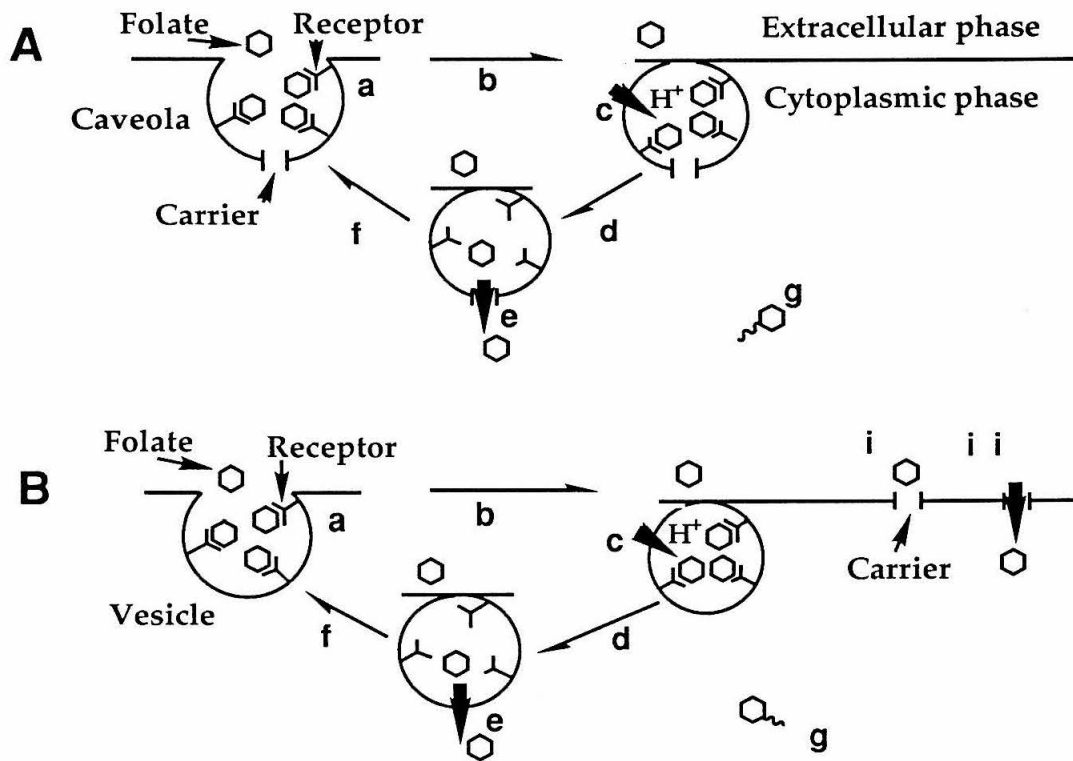
This was adapted from Ferguson, M. A. J., reference 39.

**Fig. 2. Models for folate uptake**

(A) A model for folate uptake in which folate receptors and anion carriers work in tandem to transport folates into a cell. Folates bind to the folate receptors bound to the cell membrane (b), and a proton gradient is generated (c) that causes the folate to dissociate from the receptor (d). Folates move across the membrane by an anion carrier due to the high folate concentration generated in the caveola (e). The caveola reopens to initiate another round of folate uptake (f) and the transported folates are polyglutamated in the cytoplasm to retain the vitamins within the cell (g). This figure was adapted from R. G. W. Anderson et al. (5).

(B) An alternative model for folate uptake in which folate receptors and carriers work independently to transport folates into a cell. Folates bind to membrane-bound receptors (a) and the vitamin-receptor complexes are endocytosed (b). A proton gradient is generated (c) and folates dissociate from the receptors (d). Folates move across the membrane by simple diffusion (ref. 74) or by an unknown mechanism (e) and the vesicle which could be the caveola or not recycles to the cell surface (f). Independently, anion carriers transport folates into cytoplasm (i and ii). The folates are polyglutamated in the cytoplasm (g).

Fig. 2. Models for folate uptake



**Fig. 3. Binding of 5-MeH<sub>4</sub>folate to KB cells**

**(A) Concentration dependent binding of 5-MeH<sub>4</sub>folate to folate receptors** KB cells were incubated in the presence of [<sup>3</sup>H]-5-MeH<sub>4</sub>folate at the indicated concentrations for 4 hours at 0 °C in duplicate. Acid-resistant (AR) and acid-dissociable (AD) fractions were measured as described in MATERIALS AND METHODS.

**(B) Scatchard plot**

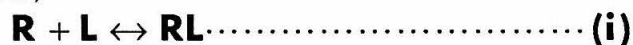
KB cells were incubated in the presence of [<sup>3</sup>H]-5-MeH<sub>4</sub>folate at the indicated concentrations for 4 hours at 0 °C in duplicate. Acid-dissociable (AD) fractions, concentrations of free 5-MeH<sub>4</sub>folate in the incubation media and the mass of the cells per each flask were measured as described in the MATERIALS AND METHODS section. The parameter *V* is defined as the moles of 5-MeH<sub>4</sub>folate bound per mole of a cell, which was calculated using acid-dissociable fractions and the amount of cells. The mass of  $5.36 \times 10^{-7}$  mg per cell, which was measured as described in the MATERIALS AND METHODS section, was used to calculate the molar concentration of cells in this plot. [*L*] in the unit of nM is the free concentration of the 5-MeH<sub>4</sub>folate in the incubation media. The intercept on the *V*-axis is the number of binding sites per cell (approximately  $40 \times 10^6$  sites/cell). The absolute value of the slope of a line connecting the intercepts of the curve with the *V*/[*L*]- and [*L*]- axis corresponds to the association constant of 5-MeH<sub>4</sub>folate for the folate receptor.

**(C) and (D) 1/[*L*] vs. [*m*]/[AD] plot**

The equilibrium (association) constant between free 5-MeH<sub>4</sub>folate, free receptor and receptor-vitamin complex can be expressed in terms of acid-dissociable



fraction ([AD]), free vitamin concentration ([L]) and the concentration of cells([m]) as follows;

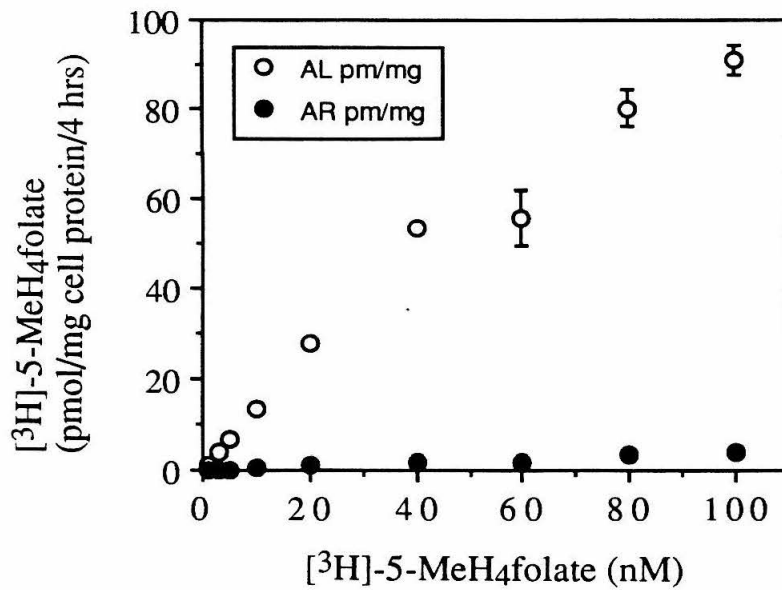


$$\mathbf{K_a = \frac{[RL]}{[R][L]} = \frac{[AD]}{(k[m] - [AD])[L]} \dots (\mathbf{ii})}$$

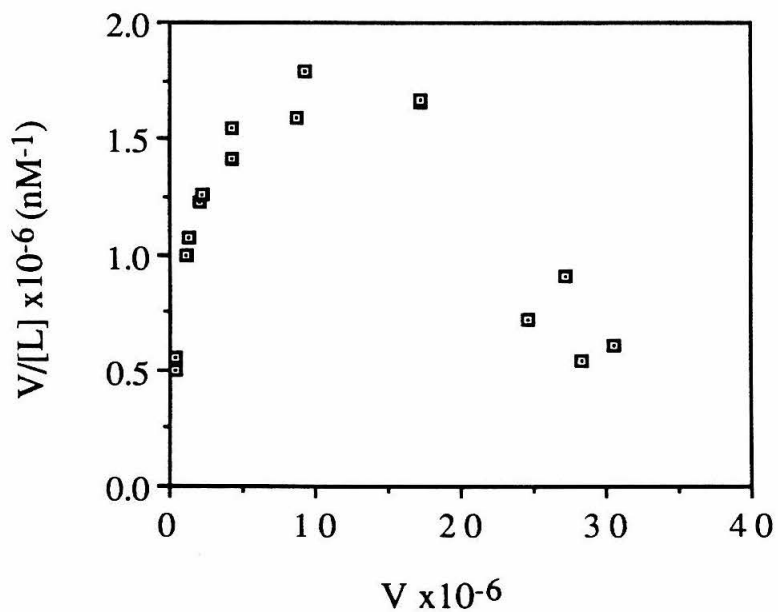
$$\frac{\mathbf{1}}{\mathbf{[L]}} = \mathbf{kK_a \frac{[m]}{[AD]} - K_a} \dots\dots\dots (\mathbf{iii})$$

where R, L, RL,  $K_a$  represent folate receptor, 5-MeH<sub>4</sub>folate, folate receptor-vitamin complex and the association constant for the equilibrium reaction. Now [RL]=[AD] and [R]=[R]<sub>total</sub>-[RL]. If we define a constant k such that [R]<sub>total</sub>=k[m], we can express the association constant in terms of [AD], [L], [m] and k (equation (ii)). Rearranging the equation (ii) yields equation (iii). The intercept of the curve on [m]/[AD] axis corresponds to 1/k and that of on the 1/[L] axis corresponds to - $K_a$ . Plot (D) shows the expanded region around the origin of the graph (C). Calculated k and  $K_a$  were 0.135 pmol/μg cell and 0.05 nM<sup>-1</sup>.

**Fig. 3. (A) Concentration dependent binding of 5-MeH<sub>4</sub>folate to folate receptors**



**Fig. 3 (B) Scatchard plot**



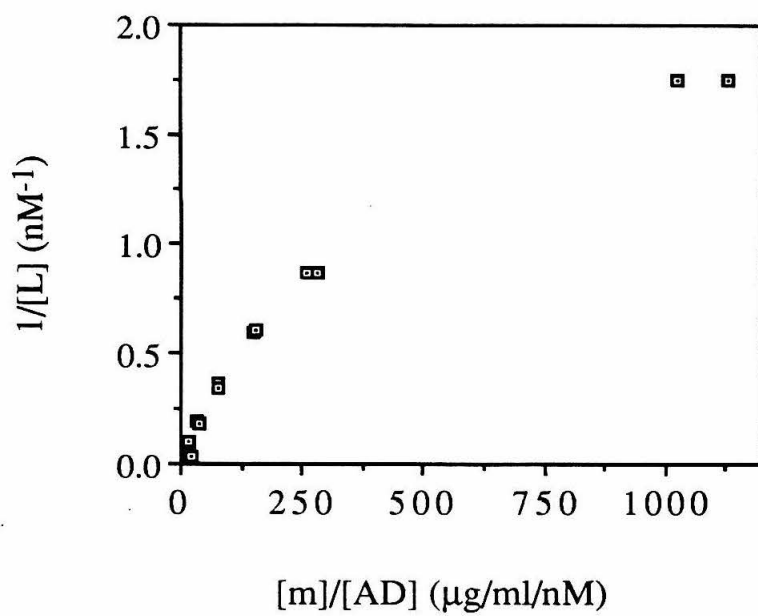
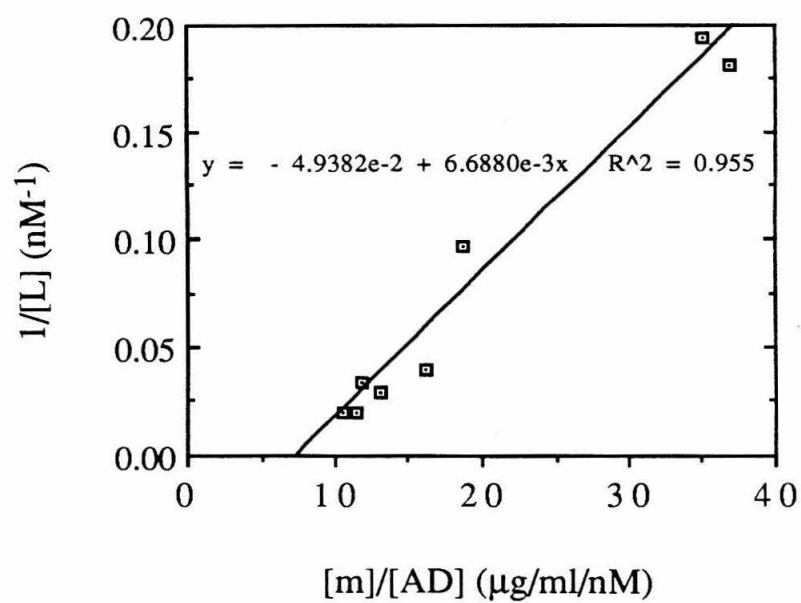
**Fig. 3 (C)  $1/[L]$  vs.  $[m]/[AD]$  plot**

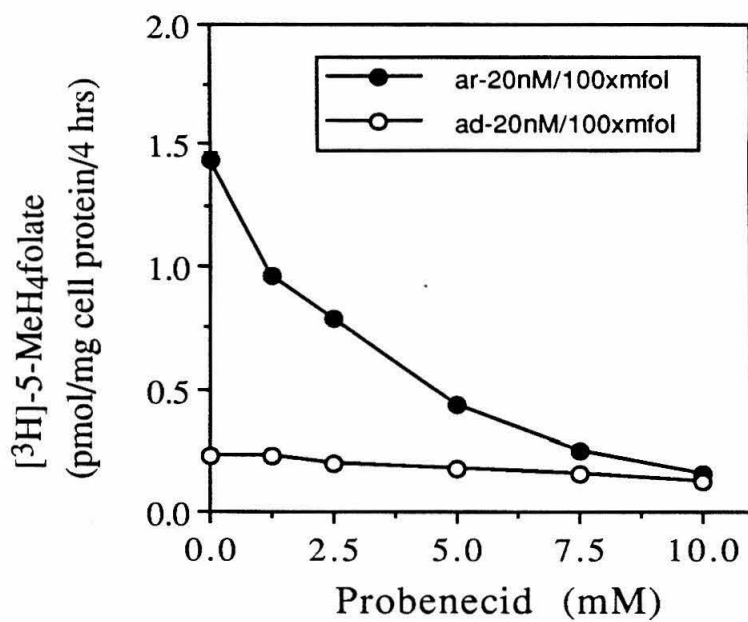
Fig. 3 (D) Extrapolation of fig. 3 C



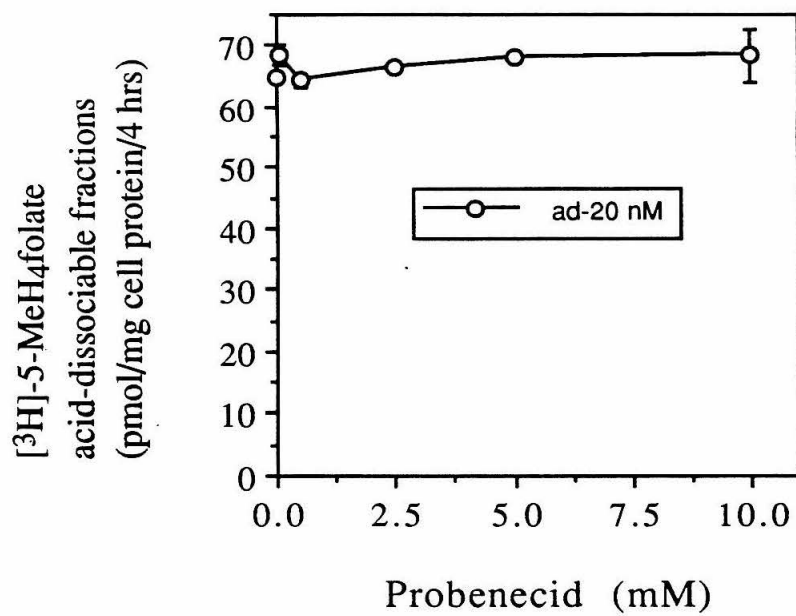
**Fig. 4. Effect of probenecid on the uptake of [ $^3\text{H}$ ]-5-MeH<sub>4</sub>folate**

KB cells were incubated for 30 min at 37 °C in 0.5 ml fdDMEM containing varying concentrations of probenecid in duplicate. [ $^3\text{H}$ ]-5-methyl-tetrahydrofolate ([ $^3\text{H}$ ]-5-MeH<sub>4</sub>folate) with (A) or without (B and C) 100-fold excess nonradioactive DL-5-MeH<sub>4</sub>folate (100x mfol.) was added to the cells to a final concentration of 20 nM in a final 1 ml volume and cells were further incubated for 4 hours at 37 °C in the presence of probenecid at the final concentrations as indicated. Acid-resistant (ar, filled circle) and acid-dissociable(ad, open circle) fractions of [ $^3\text{H}$ ]-5-MeH<sub>4</sub>folate were measured as described in MATERIALS and METHODS. Acid-resistant (AR) fractions represent the amounts of the [ $^3\text{H}$ ]-5-MeH<sub>4</sub>folate internalized by cells and acid-dissociable (AD) fractions represent the amount of the vitamin bound to the cell surface.

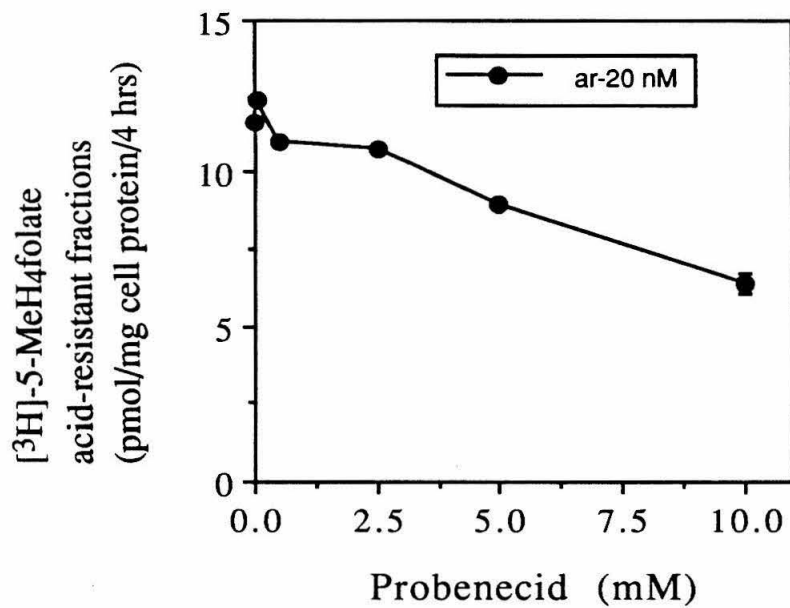
**Fig. 4 (A)** Effect of probenecid on the uptake of [ $^3\text{H}$ ]-5-methyltetrahydrofolate in the presence of 100 fold excess DL-5-methyltetrahydrofolate



**Fig. 4 (B)** Effect of probenecid on the binding of [ $^3\text{H}$ ]-5-methyltetrahydrofolate to KB cells



**Fig. 4 (C)** Effect of probenecid on the uptake of [ $^3\text{H}$ ]-5-methyltetrahydrofolate in the absence of 100 fold excess DL-5-methyltetrahydrofolate





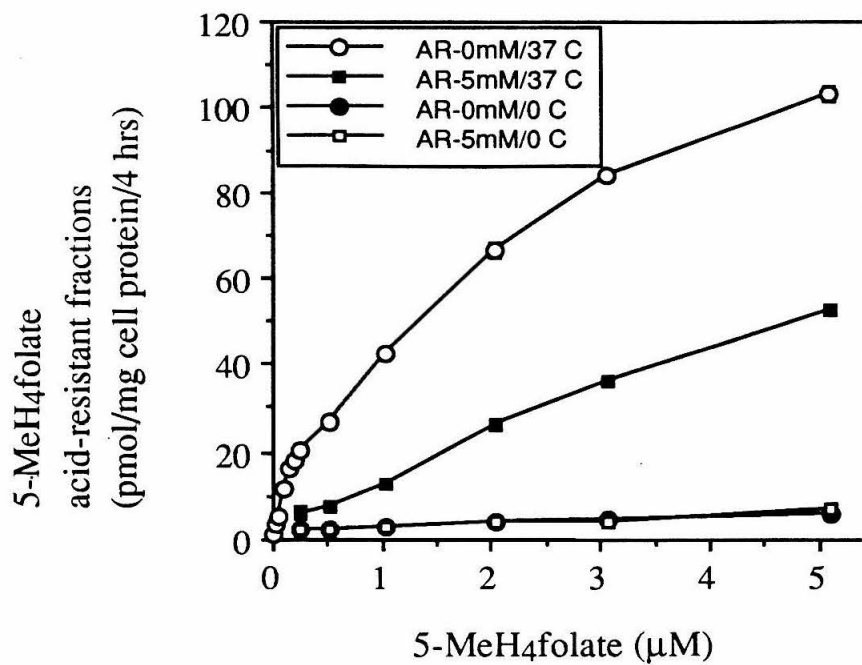
**Fig. 5. Effect of temperature and probenecid on the uptake of 5-MeH<sub>4</sub>folate**

KB cells were incubated in the presence or absence of 10 mM probenecid in 0.5 ml fdDMEM for 30 min at 37 °C. At the end of the incubation appropriate volumes of 20 µM DL-5-MeH<sub>4</sub>folate solution containing 200 nM [<sup>3</sup>H]-5-MeH<sub>4</sub>folate were added to the cells to a final volume of 1 ml at the indicated concentrations and temperatures. Cells were further incubated at the indicated temperatures for 4 hours. Total amounts of 5-MeH<sub>4</sub>folate associated per mg cell protein were calculated assuming that only the L-isomer can bind and translocate into cell. Only the concentration of L-isomer is shown in the plot.

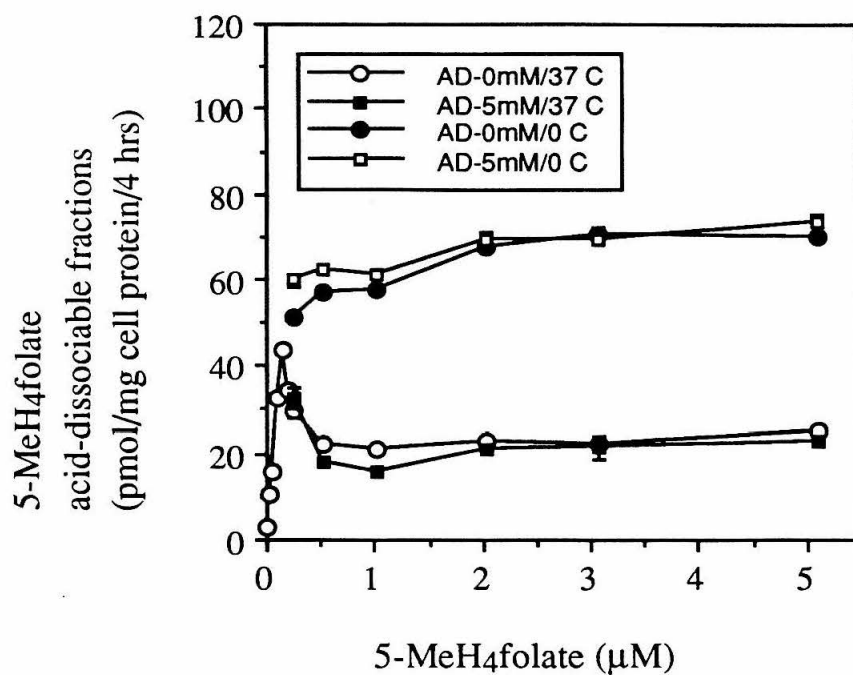
**A.** Acid-resistant fractions; open circle - at 37 °C without probenecid; filled square - at 37 °C with 5 mM probenecid; filled circle - at 0 °C without probenecid; open square - at 0 °C with 5 mM probenecid.

**B.** Acid-dissociable fractions; The same legends were used as in (A).

**Fig. 5 (A) Effect of temperature and probenecid on the uptake of 5-MeH<sub>4</sub>folate by KB cells**



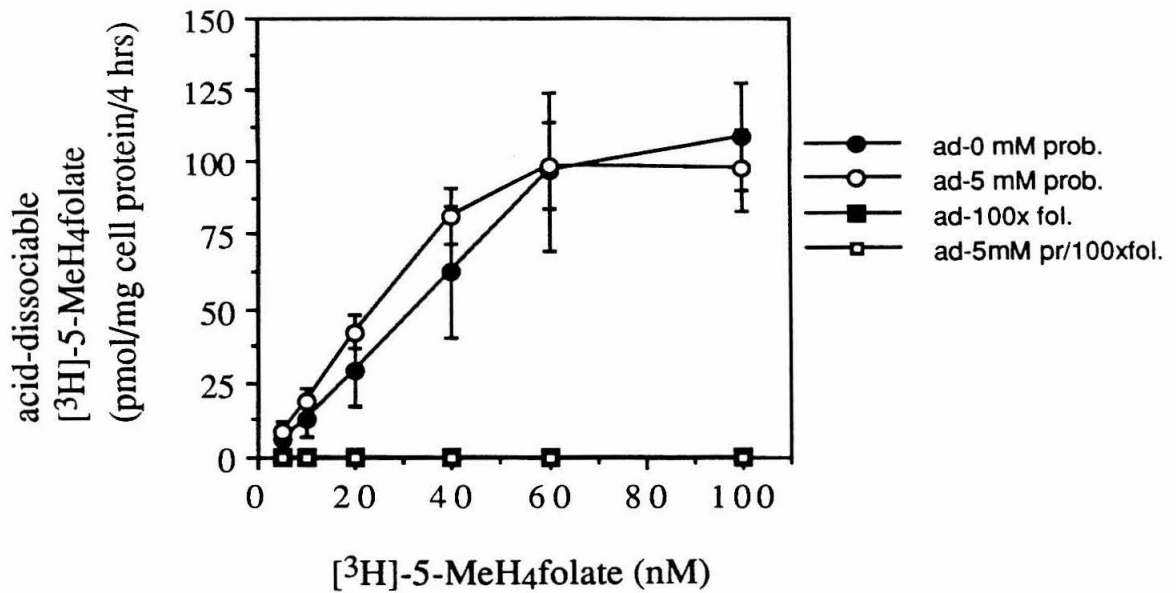
**Fig. 5 (B)** Effect of temperature and probenecid on the binding of 5-MeH<sub>4</sub>folate to KB cells



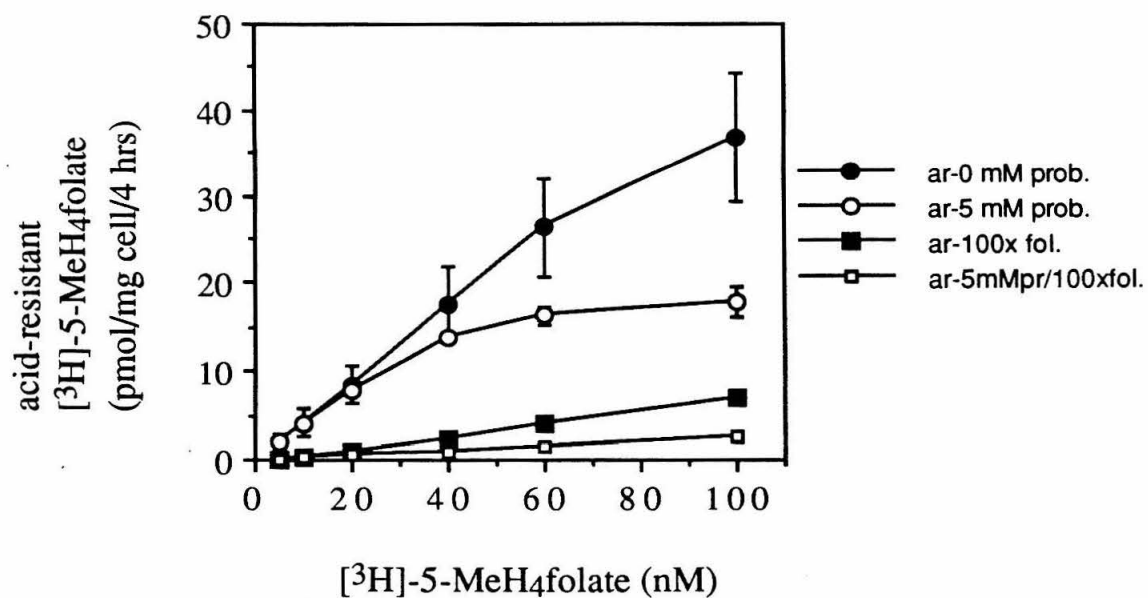
**Fig. 6. Effects of folic acid and probenecid on the uptake of physiological concentrations of [ $^3\text{H}$ ]-5-MeH $_4$ folate**

KB cells were incubated in 0.5 ml fdDMEM containing either 0 or 10 mM probenecid for 30 min at 37 °C. At the end of the incubation, 200 nM [ $^3\text{H}$ ]-5-MeH $_4$ folate solution with or without 100-fold excess folic acid was added to the cells to the indicated concentrations in a final volume of 1 ml. Cells were further incubated for 4 hours at 37 °C. Acid-dissociable and acid-resistant fractions were determined as described in MATERIALS and METHODS. Acid-dissociable and acid-resistant fractions are shown in **A.** and **B.**, respectively using the following symbols; filled circle - without probenecid and folic acid; open circle - with 5 mM probenecid; filled square - with 100x folic acid; open square - with 5 mM probenecid and 100x folic acid. Curves 1, 2, and 4 represent the mean values of two separate experiments and curve 3 represents the result of one experiment. Each experiment was performed using duplicate samples.

**Fig. 6 (A)** Effects of folic acid and probenecid on the binding of physiological concentrations of [ $^3$ H]-5-MeH<sub>4</sub>folate to KB cells



**Fig. 6 (B)** Effects of folic acid and probenecid on the uptake of physiological concentrations of [ $^3$ H]-5-MeH $_4$ folate by KB cells



**Fig. 7 Endocytosis of folate-BSA conjugates by folate receptors**

**(A) Uptake of [ $^{125}$ I]-BSA and [ $^{125}$ I]-DL-5-MeH<sub>4</sub>folate-conjugated BSA ([ $^{125}$ I]-mfBSA)** KB cells were preincubated in 0.6 ml fdDMEM for 30 min. BSA in fdDMEM (0.3 ml, 16.7 mg/ml BSA) was added to cells prior to the addition of [ $^{125}$ I]-BSA or [ $^{125}$ I]-5-MeH<sub>4</sub>folate-BSA (average 10 ( $\pm$  1) DL-5-MeH<sub>4</sub>folates per BSA) in order to reduce the nonspecific binding of the modified BSA molecules to cells and culture flasks. [ $^{125}$ I]-BSA or [ $^{125}$ I]-5-MeH<sub>4</sub>folate-BSA in 50 mM Tris-HCl (pH7.5) were added to cells at various concentrations. The final volume of the media was adjusted to 1 ml with 50 mM Tris-HCl (pH 7.5). Cells were further incubated for 4 hours at 37 °C. Acid-dissociable fractions of [ $^{125}$ I]-BSA(open square) and [ $^{125}$ I]-mfBSA(filled square) and acid-resistant fractions of [ $^{125}$ I]-BSA(open circle) and [ $^{125}$ I]-mfBSA(filled circle) were determined as described in the MATERIALS AND METHODS section. The reported values are the averages of duplicate samples.

**(B) Effect of free DL-5-MeH<sub>4</sub>folate on the uptake of [ $^{125}$ I]-mfBSA** KB cells were incubated with 12  $\mu$ g/ml [ $^{125}$ I]-5-MeH<sub>4</sub>folate-BSA in the presence of varying concentrations of DL-5-MeH<sub>4</sub>folate in 1 ml media for 4-hours at 37 °C. Free BSA (5 mg/ml) was present in the media. Acid-dissociable (filled square) and acid-resistant (filled circle) fractions were measured as described in the MATERIAL AND METHODS section. The reported values are the averages of duplicate samples.

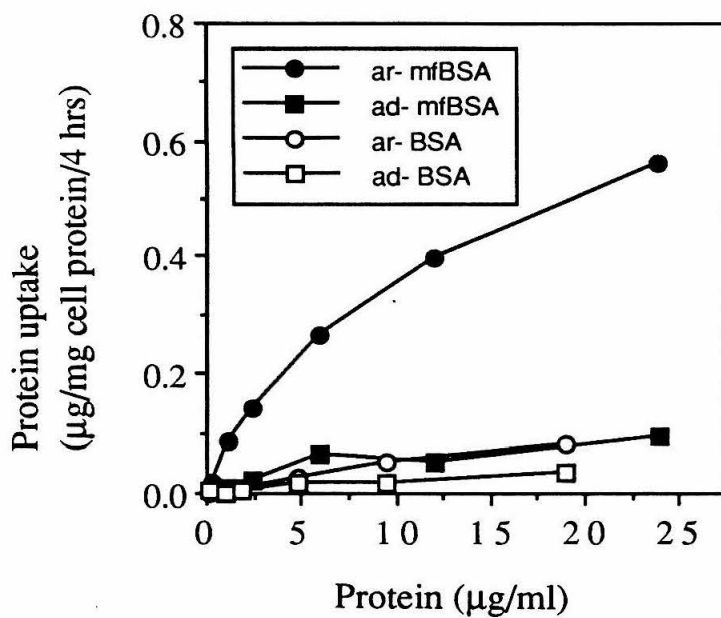
**(C) Effect of folate-BSA conjugate on the uptake of [ $^3$ H]-folic acid by KB cells** KB cells were pre-incubated with folate-BSA conjugate (5.2  $\pm$ 0.3 folate per BSA) in 0.5 ml fdDMEM at 0 °C for 15 min. [ $^3$ H]-folic acid in a volume of 0.5 ml fdDMEM was added to the cells to a final concentration of 50 nM and cells were

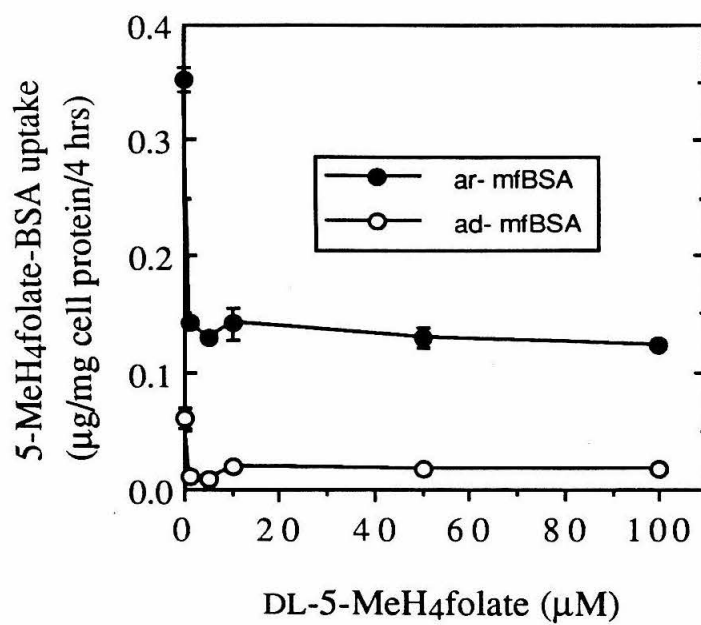
further incubated for 30 min on ice. Flasks containing the cells were moved to a water bath at 37 °C and warmed for 10 min and transferred to an incubator at 37 °C and incubated for another 30 min. After the incubation, media was removed. The cells were rinsed three times with 1 ml DPBS. Cells were washed twice with 1 ml acid-saline solution (0.15 N NaCl, pH 3) for 30 seconds each time. Cells were rinsed with 1 ml DPBS. Cells were dissolved in 1 ml of 1 % SDS, 0.1 N NaOH solution. Flask was rinsed twice with 1 ml DPBS solution. Solubilized cells in total 3 ml volumes were used to determine the acid-resistant fractions as described in the MATERIALS AND METHODS section. Final concentrations of fol-BSA after addition of [<sup>3</sup>H]-folic acid are shown in the graph. The reported values are averages of duplicate samples.

**(D) Effect of probenecid, BSA and folate-conjugated BSA on the uptake of [<sup>3</sup>H]-5-MeH<sub>4</sub>folate by KB cells** KB cells were incubated for 30 min at 37 °C in fdDMEM containing 90 nM [<sup>3</sup>H]-5-MeH<sub>4</sub>folate in the presence or absence of 1 mM probenecid (P), BSA (BSA, 0.75 mg protein/ml), or folate-conjugated BSA (fol-BSA, 0.75 mg protein/ml). Acid-resistant fractions were determined as described in MATERIALS AND METHODS. Averages of five different experiments are reported (error bars, 95 % confidence limit).

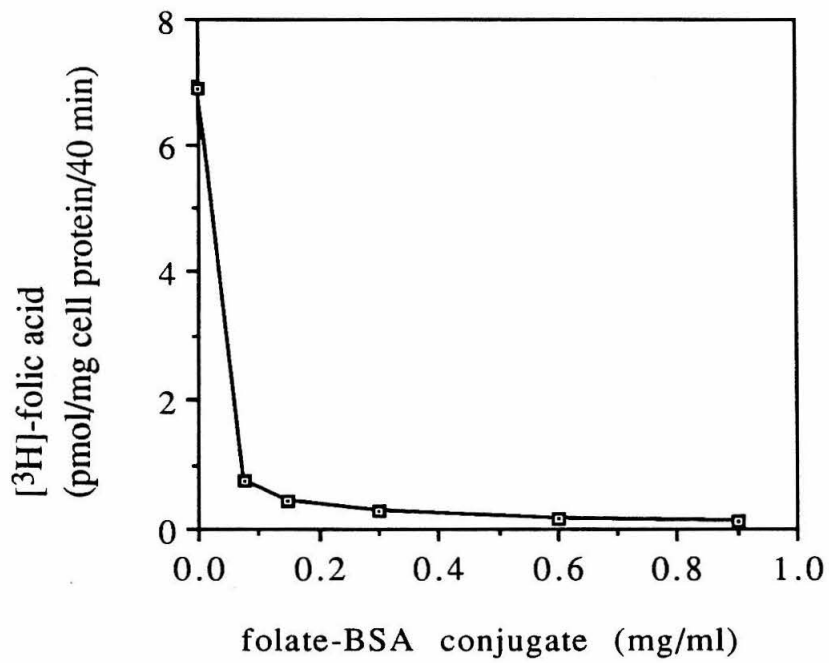


**Fig. 7 (A)** Uptake of [ $^{125}$ I]-BSA and [ $^{125}$ I]-DL-5-MeH<sub>4</sub>folate-conjugated BSA ([ $^{125}$ I]-mfBSA)

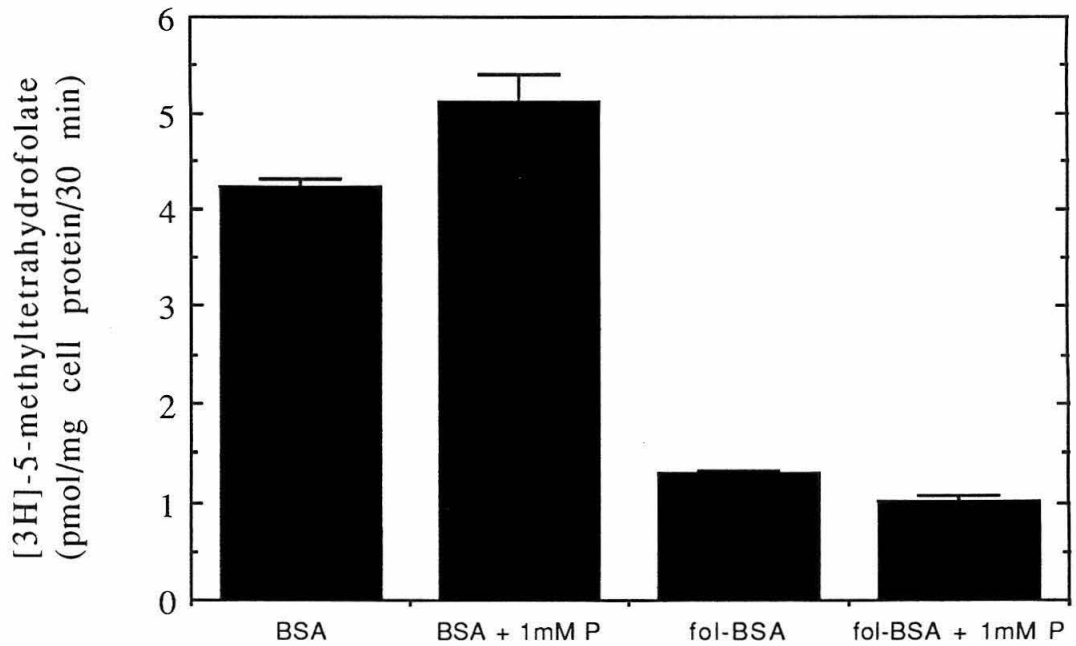


**Fig. 7 (B)** Effect of free DL-5-MeH<sub>4</sub>folate on the uptake of [<sup>125</sup>I]-mfBSA

**Fig. 7 (C)** Effect of folate-BSA conjugate on the uptake of [ $^3\text{H}$ ]-folic acid by KB cells



**Fig. 7 (D)** Effect of probenecid, BSA and folate-conjugated BSA on the uptake of [ $^3\text{H}$ ]-5-MeH $_4$ folate by KB cells



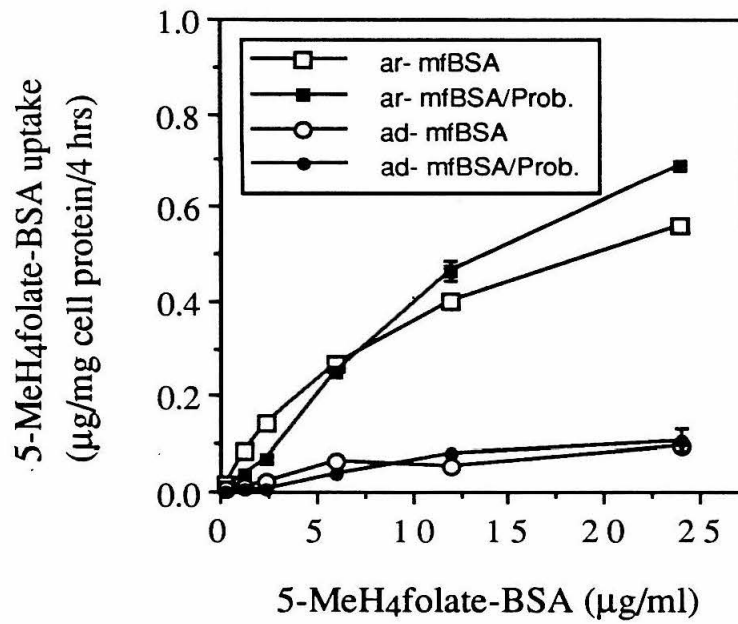
**Fig. 8 (A) Effect of probenecid on the uptake of [ $^{125}$ I]-5-MeH<sub>4</sub>folate-BSA by KB cells**

KB cells were preincubated in 0.5 ml fdDMEM containing 10 mM probenecid for 30 min at 37 °C. BSA solution (0.3 ml, 16.7 mg/ml in fdDMEM) and 0.05 ml 50 mM Tris·HCl were added to cells prior to the addition of [ $^{125}$ I]-5-MeH<sub>4</sub>folate-BSA (5-MeH<sub>4</sub>folate/BSA ratio =  $10 \pm 1$  for this preparation) to a final concentration of 12 µg/ml. Cells were further incubated for 4 hours at 37 °C. At the end of the incubation cells were chilled on ice and acid-dissociable fractions in the presence (filled circle) and absence (open circle) of probenecid and acid-resistant fractions in the presence (filled square) and absence (open square) of probenecid were determined from the samples prepared in duplicate as described in MATERIALS AND METHODS.

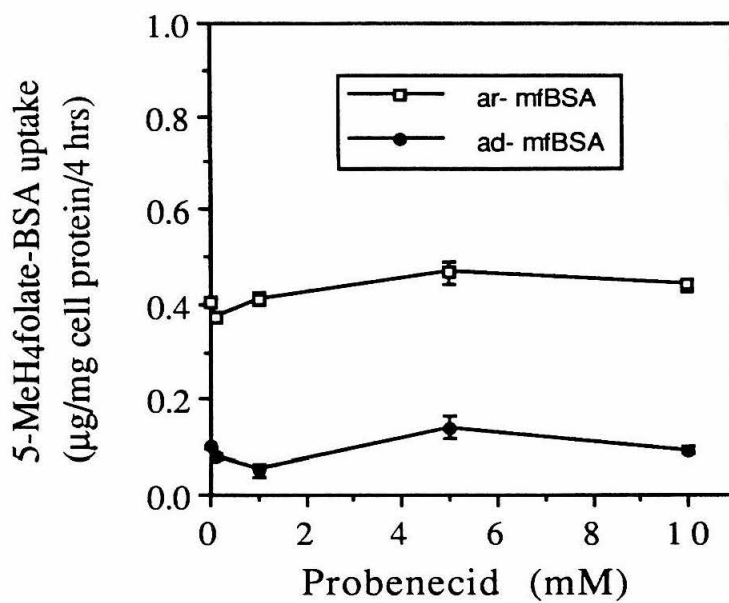
**Fig. 8 (B) Effect of varying concentrations of probenecid on the uptake of [ $^{125}$ I]-5-MeH<sub>4</sub>folate-BSA conjugate by KB cells**

KB cells were incubated for 30 minutes at 37 °C in 0.5 ml fdDMEM containing probenecid at the indicated concentrations. After this, 0.1 ml fdDMEM, 0.3 ml BSA solution in fdDMEM (16.7 mg/ml) and 0.05 ml 50 mM Tris-HCl (pH 7.5) were added to the cells. Finally, [ $^{125}$ I]-5-MeH<sub>4</sub>folate-BSA (5-MeH<sub>4</sub>folate/BSA ratio =  $10 \pm 1$  for this preparation) was added to the cells to a final concentration of 12 µg/ml in 1 ml total volume and further incubated for 4 hours at 37 °C. After addition of radioiodinated protein, the concentrations of probenecid were reduced to a half of the initial values. Acid-dissociable (filled circle) and acid-resistant (open square) fractions were determined from the samples prepared in duplicate as described in MATERIALS AND METHODS.

**Fig. 8 (A)** Effect of probenecid on the uptake of [ $^{125}$ I]-5-MeH<sub>4</sub>folate-BSA by KB cells



**Fig. 8 (B)** Effect of varying concentrations of probenecid on the uptake of [ $^{125}$ I]-5-MeH<sub>4</sub>folate-BSA conjugate by KB cells

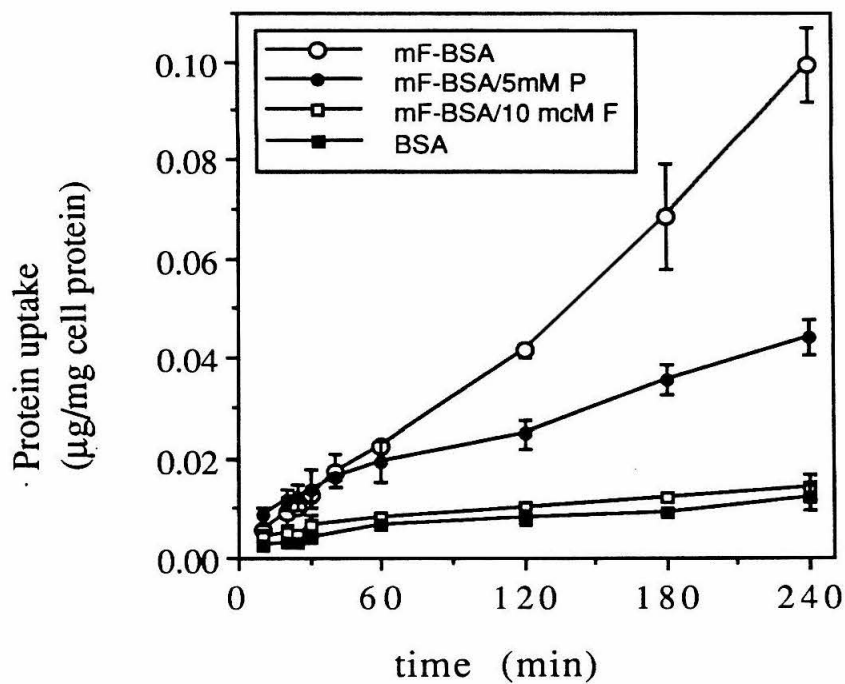


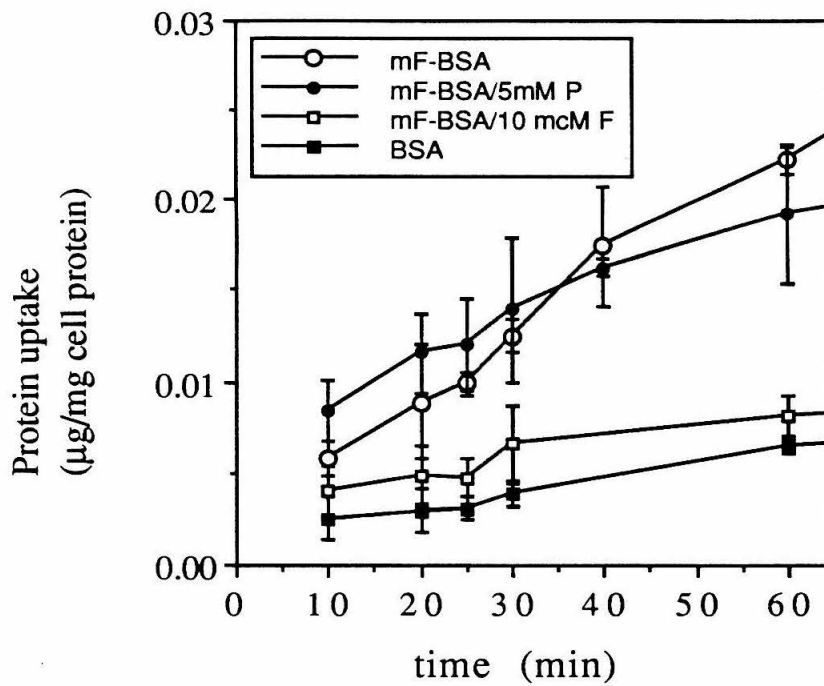
**Fig. 9** Time-dependent uptake of 5  $\mu\text{g/ml}$  5-MeH<sub>4</sub>folate-BSA conjugate and BSA by KB cells at 37 °C

**(A)** KB cells were incubated with 5  $\mu\text{g/ml}$  radioiodinated 5-MeH<sub>4</sub>folate-BSA (5-MeH<sub>4</sub>folate/BSA ratio = 11.7 for this preparation) in the presence of excess 5 mg/ml BSA. Some experiments were performed in the presence of 5 mM probenecid or 10  $\mu\text{M}$  folic acid. As a control, KB cells were incubated with radioiodinated BSA (5  $\mu\text{g/ml}$ ) in the presence of 5 mg/ml BSA. Incubation periods were 10, 20, 25, 30, 45, 60, 120, 180, and 240 minutes. Acid-resistant fractions of radioiodinated fractions were determined as described in MATERIALS AND METHODS. The experimental values are the averages of three different samples. **(B)** Fig. 9 B represents the expanded region of 0-60 min period in Fig 9 A.



**Fig. 9 (A)** Time-dependent uptake of 5  $\mu\text{g/ml}$  5-MeH<sub>4</sub>folate-BSA conjugate and BSA by KB cells at 37 °C

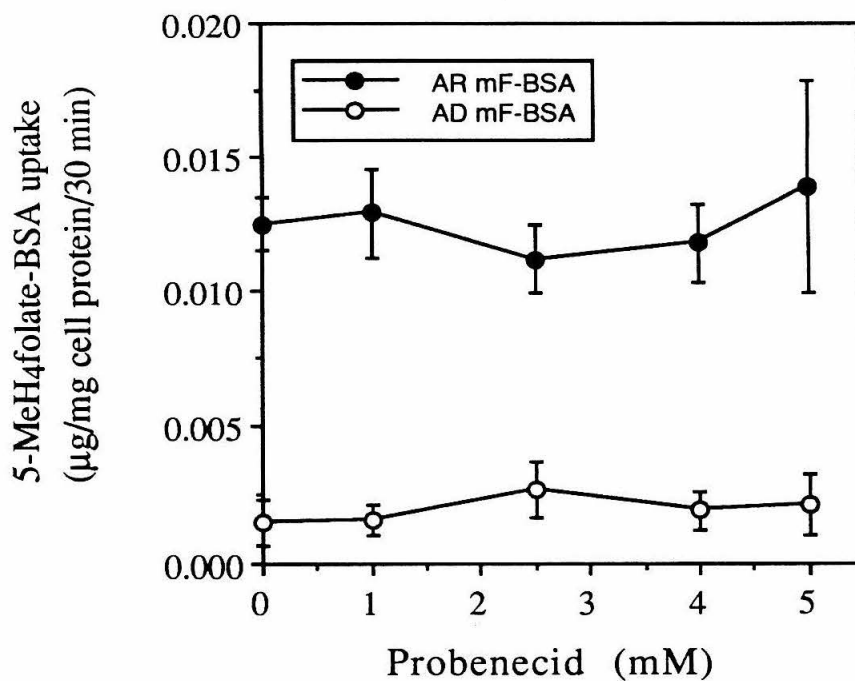


**Fig. 9 (B)** Expanded region of 0-60 min period in Fig 9 (A)

**Fig. 10. Effect of short-term incubation of KB cells in varying concentrations of probenecid on the uptake of 5-MeH<sub>4</sub>folate-BSA conjugate by KB cells**

KB cells were incubated in the presence of 5 µg/ml radioiodinated 5-MeH<sub>4</sub>folate-BSA conjugate (folate/BSA ratio = 11.7) for 30 min at 37 °C. Acid-resistant (AR) and acid-dissociable (AD) fractions were measured as described in MATERIALS AND METHODS. The experimental values are the averages of three different samples.

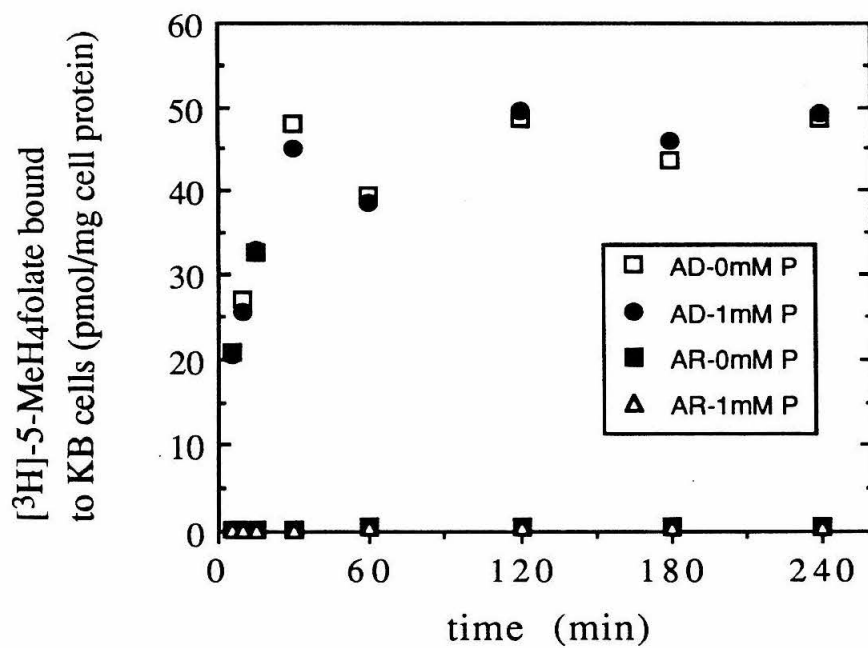
**Fig. 10** Effect of short-term incubation of KB cells in varying concentrations of probenecid on the uptake of 5-MeH<sub>4</sub>folate-BSA conjugate by KB cells



**Fig. 11. Effect of probenecid on the time-dependent binding of 5-MeH<sub>4</sub>folate to folate receptors**

KB cells were chilled on ice. [<sup>3</sup>H]-5-MeH<sub>4</sub>folate was added to cells to a final concentration of 20 nM in the presence or absence of 1 mM probenecid. Cells were incubated at 0 °C for 5, 10, 15, 30, 60, 120, 180 and 240 minutes. Acid-dissociable fractions in the presence (AD-1mM P) or absence (AD-0mM P) of probenecid and acid-resistant fractions in the presence (AR-1mM P) or absence (AR-0mM P) of probenecid were determined as described in MATERIALS AND METHODS. Reported values are from single experiments for each time point. The amount of the cells per well of flask used in each experiment varied between 0.26 and 0.41 mg/ml and the concentration of 10 nM 5-Methyltetrahydrofolate is not enough to saturate the folate receptors.

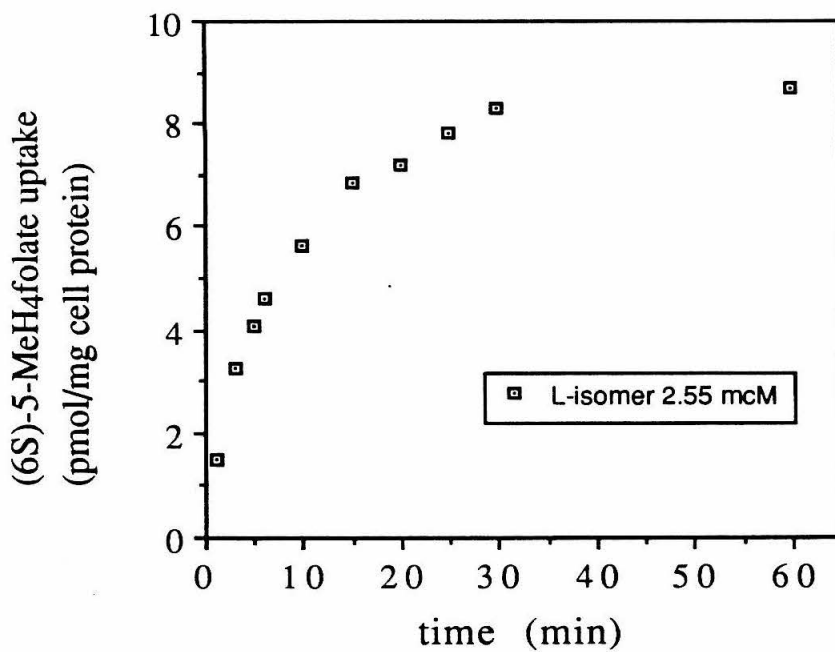
**Fig. 11** Effect of probenecid on the time-dependent binding of 5-MeH<sub>4</sub>folate to folate receptors



**Fig. 12. Time-dependent uptake of 5-MeH<sub>4</sub>folate in the presence of 0.5 mM folic acid**

KB cells were incubated with 50 nM [<sup>3</sup>H]-5-MeH<sub>4</sub>folate in the presence of 5 μM DL-5-MeH<sub>4</sub>folate for 1, 3, 5, 6, 10, 15, 20, 25, 30 and 60 minutes at 37 °C. The amount of L-5-MeH<sub>4</sub>folate was measured as described in MATERIALS AND METHODS. The initial concentration of L-isomer of 5-MeH<sub>4</sub>folate was 2.55 μM. The experimental values were obtained from a single experiment for each time point.

**Fig. 12.** Time-dependent uptake of 5-MeH<sub>4</sub>folate in the presence of 0.5 mM folic acid.

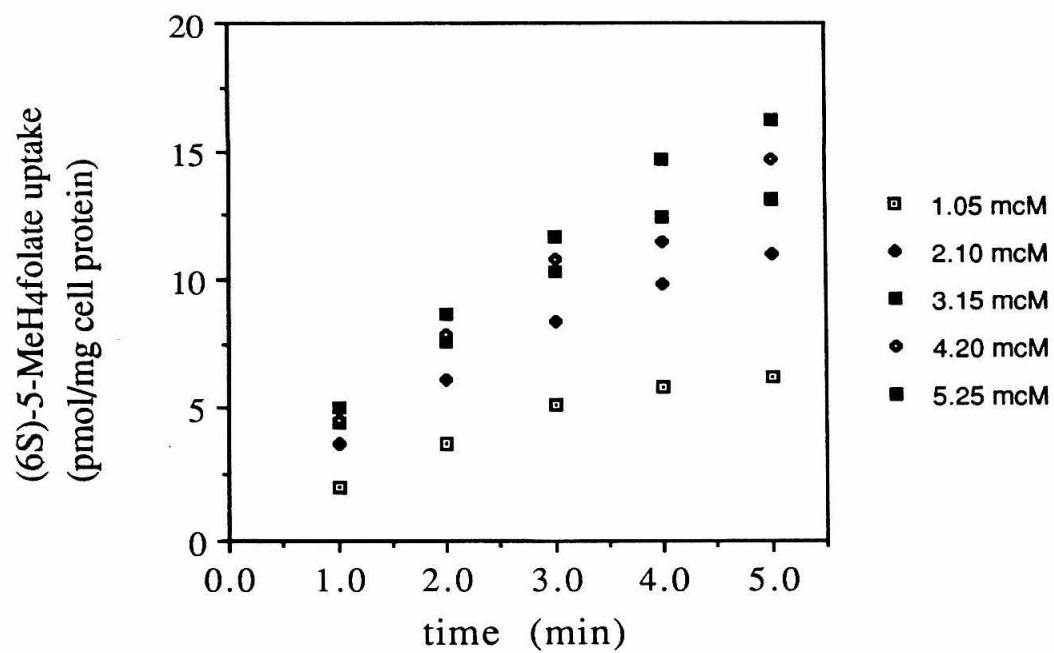




**Fig. 13. Initial rates of 5-MeH<sub>4</sub>folate uptake at varying concentrations of 5-MeH<sub>4</sub>folate**

A stock solution containing 0.5  $\mu\text{M}$  [<sup>3</sup>H]-5-MeH<sub>4</sub>folate (L-isomer), 20  $\mu\text{M}$  DL-5-MeH<sub>4</sub>folate, and 1 mM folic acid was prepared and this stock solution was diluted (to final concentrations of 2, 4, 6, 8, 10  $\mu\text{M}$  of DL-5-MeH<sub>4</sub>folate). To KB cells 1 ml of the diluted solutions were added and incubated for the indicated times at 37 °C in a water bath. Acid-resistant fractions were determined as described in MATERIALS AND METHODS. Only the amount of L-form of the 5-MeH<sub>4</sub>folate was reported at the indicated concentrations (L-isomer) from a single experiment.

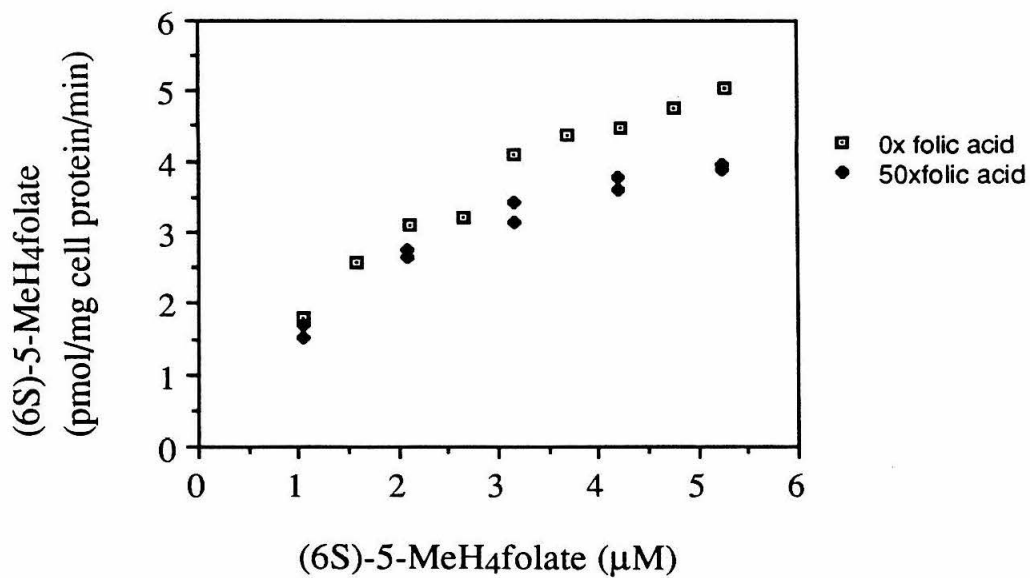
**Fig. 13.** Initial rates of 5-MeH<sub>4</sub>folate uptake at varying concentrations of 5-MeH<sub>4</sub>folate

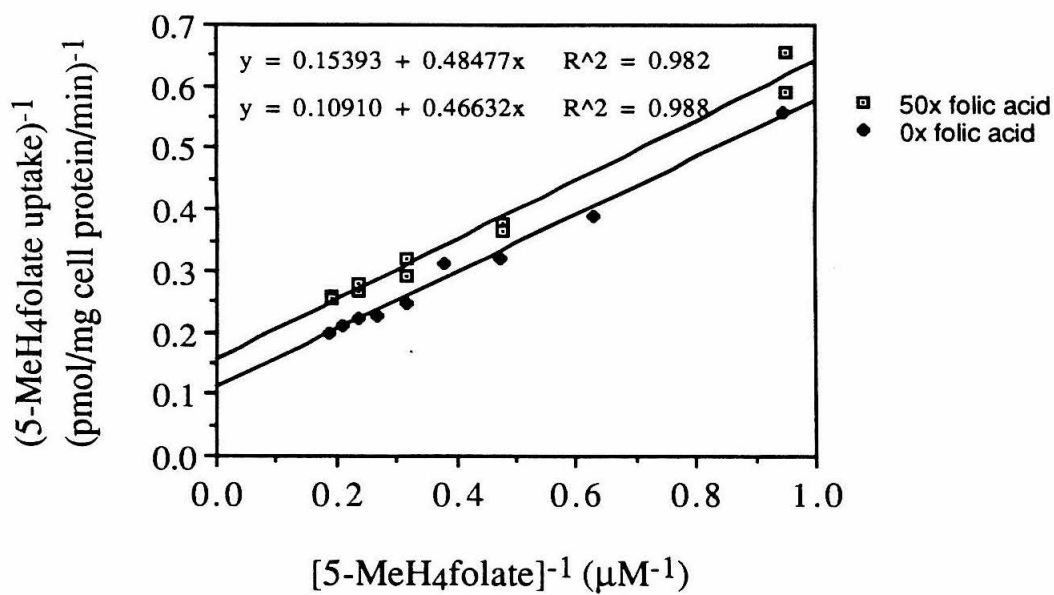


**Fig. 14. Effect of folic acid on the uptake of 5-MeH<sub>4</sub>folate at a fixed concentration ratio.**

Stock solutions containing 0.5  $\mu$ M [<sup>3</sup>H]-5-MeH<sub>4</sub>folate (L-isomer), 20  $\mu$ M DL-5-MeH<sub>4</sub>folate with or without 1 mM folic acid were prepared and these stock solutions were diluted to appropriate concentrations. To KB cells 1 ml of the diluted solutions were added and incubated for 3 minutes at 37 °C in a water bath. Acid-resistant fractions were determined as described in MATERIALS AND METHODS. Only the amounts of L-form of the 5-MeH<sub>4</sub>folate were reported at the indicated concentrations (L-isomer) from a single experiment. (A) Uptake of 5-MeH<sub>4</sub>folate in the absence (0xfolic acid) and presence (50xfolic acid) (B) Lineweaver-Burk plot of Fig. 14 A

**Fig. 14 (A)** Effect of folic acid on the uptake of 5-MeH<sub>4</sub>folate at a fixed concentration ratio.

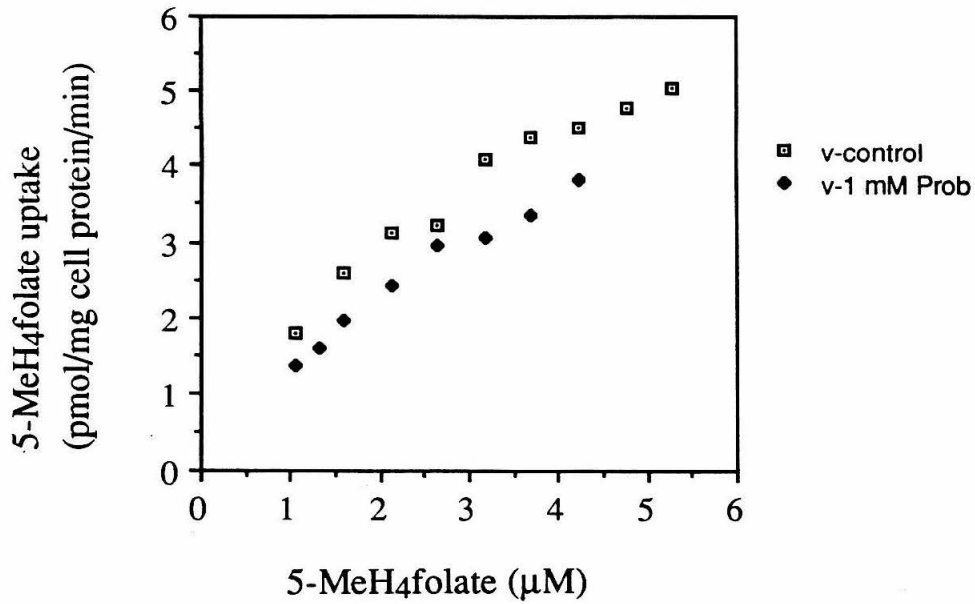


**Fig. 14 (B) Lineweaver-Burk plot of Fig. 14 A**

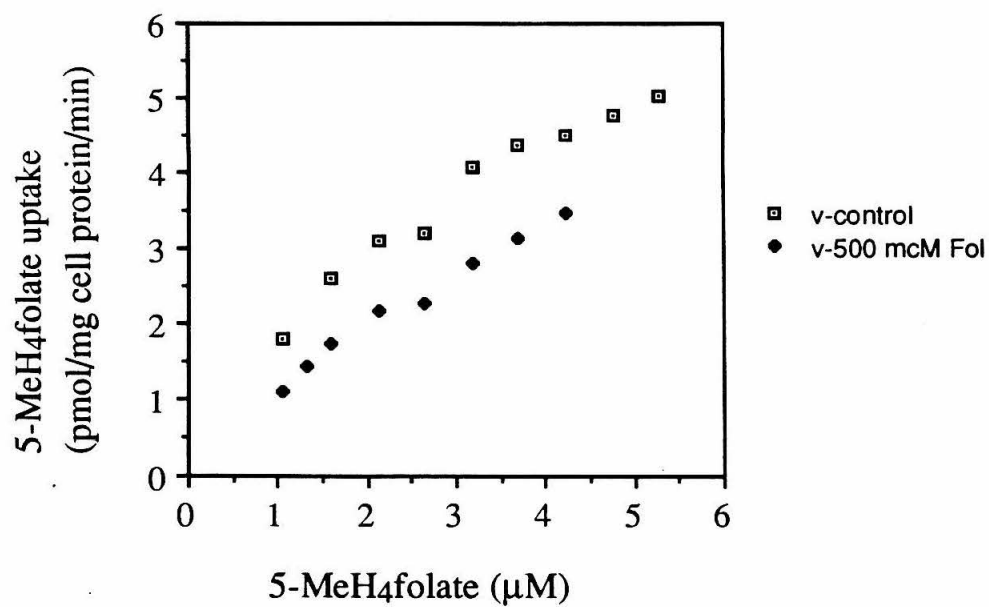
**Fig. 15. Competitive inhibition of 5-MeH<sub>4</sub>folate uptake by probenecid, folic acid and methotrexate.**

KB cells were incubated for 3 minutes at varying concentrations of D,L-5-MeH<sub>4</sub>folate in the presence of trace amount of [<sup>3</sup>H]-5-MeH<sub>4</sub>folate at 37 °C. Appropriate volumes of solution containing 0.5 µM [<sup>3</sup>H]-5-MeH<sub>4</sub>folate (L-isomer) and 20 µM DL-5-MeH<sub>4</sub>folate were used to give the final concentration of total L-5-MeH<sub>4</sub>folate at the indicated concentrations in 1 ml. Similar experiments were also performed in the presence of 1 mM probenecid, 500 µM folic acid or 30 µM methotrexate. Acid-resistant fractions were determined as described in MATERIALS AND METHODS. The uptake of 5-MeH<sub>4</sub>folate in the presence of 1 mM probenecid (A), 500 µM folic acid (B), or 30 µM methotrexate (C) is compared with control experiment without any inhibitor. Fig. 15 D, E and F show the Lineweaver-Burk plots of A, B and C, respectively.

**Fig. 15 (A)** Uptake of 5-methyltetrahydrofolate by KB cells in the presence or absence of 1 mM prpbenecid

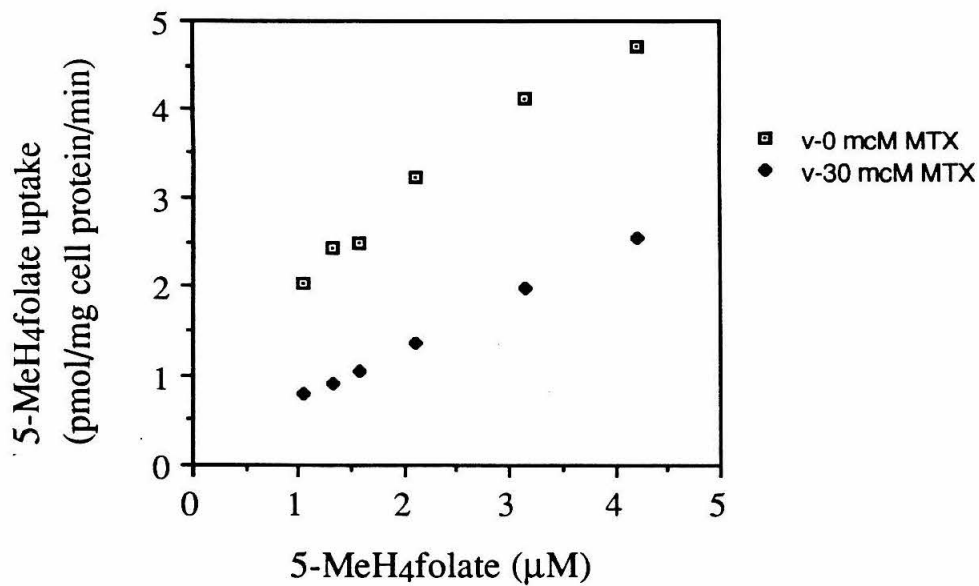


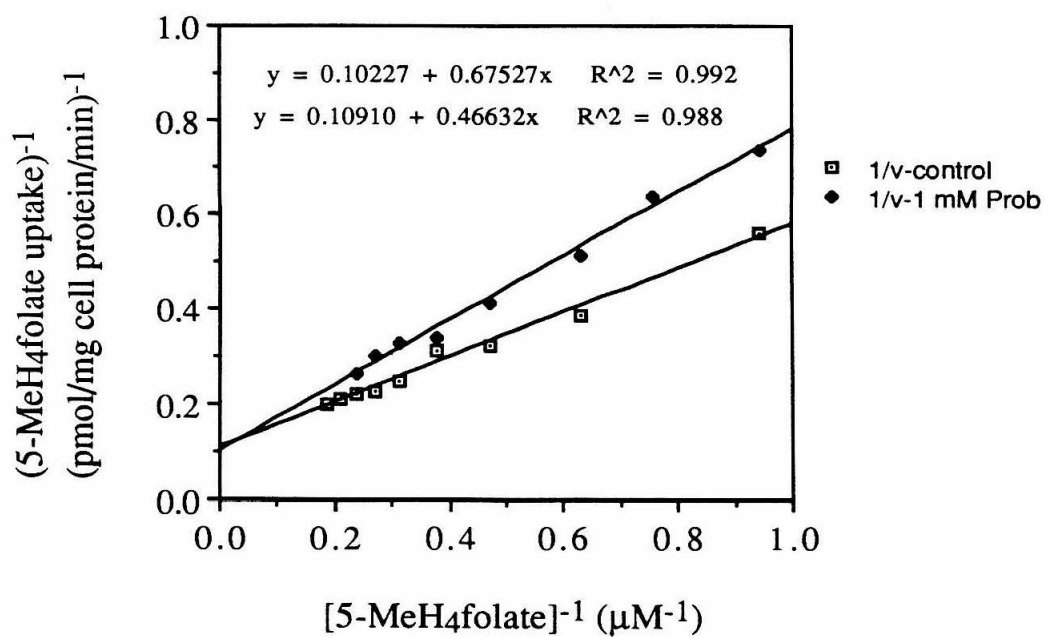
**Fig. 15 (B) Uptake of 5-methyltetrahydrofolate by KB cells in the presence or absence of 500  $\mu$ M folic acid**

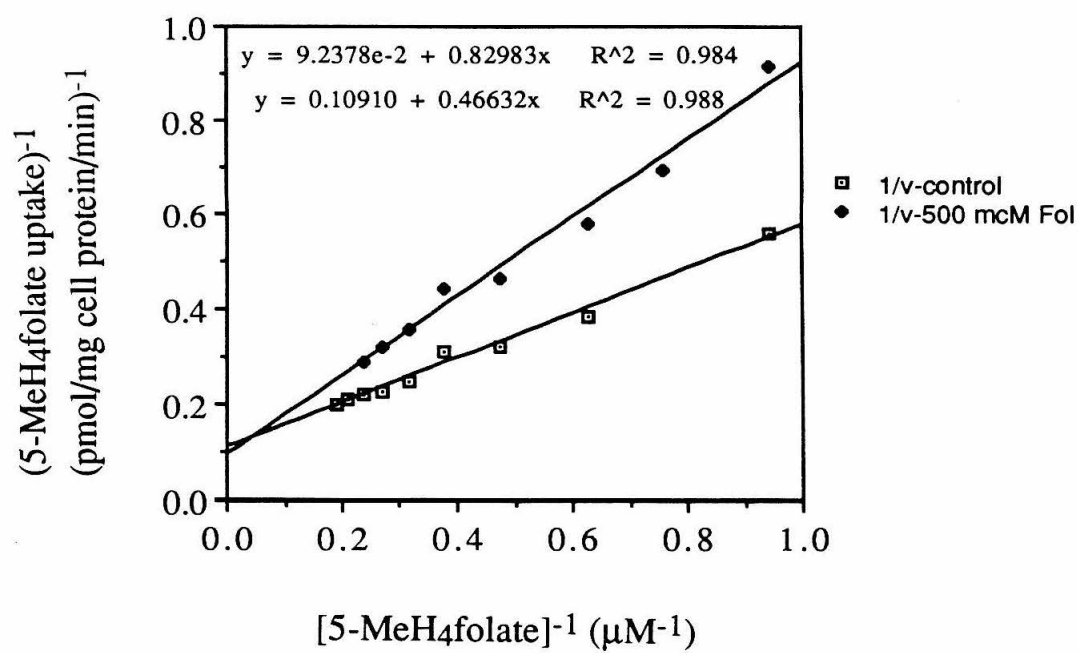


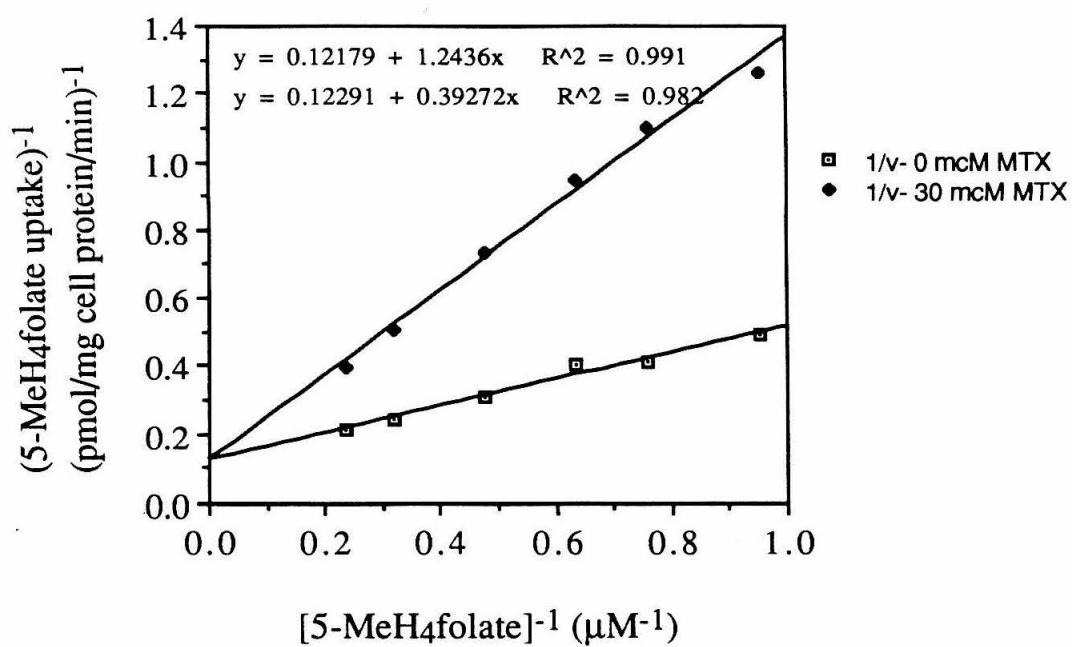


**Fig. 15 (C) Uptake of 5-methyltetrahydrofolate by KB cells in the presence or absence of 30  $\mu$ M methotrexate**



**Fig. 15 (D) Lineweaver-Burk plot of Fig. 15 (A)**

**Fig. 15 (E) Lineweaver-Burk plot of Fig. 15 (B)**

**Fig. 15 (F) Lineweaver-Burk plot of Fig. 15 (C)**

**Fig. 16** The rate of uptake of [ $^3\text{H}$ ]-folic acid by KB cells

KB cells were chilled on ice for 30 minutes. Ice-cold [ $^3\text{H}$ ]-folic acid (1 ml of 100 nM in fdDMEM) was added to the cells and further incubated on ice for 4-6 hours to saturate the folate receptors. After incubation on ice, the media was removed and unbound folic acid was washed off by rinsing the cells three times with 1 ml DPBS briefly. After this, the flask was placed in the water bath warmed to 37 °C. At the same time, 1 ml fdDMEM (at 37 °C) was added to the cells and the media was shaken gently. The culture flasks containing cells were placed in a water bath at 37 °C for 1-15 min incubations. For prolonged incubations, cells were initially warmed up for 2 min in the water bath and moved into a cell culture incubator at 37 °C. The amount of radioactive folic acid in the media, acid-dissociable fractions and acid-resistant fractions were determined as described in MATERIALS AND METHODS. **(A)** % Change of acid-resistant and acid-dissociable fractions as a function of time. **(B)** % Change of [ $^3\text{H}$ ]-folic acid in the media as a function of time. **(C)** Acid-resistant fractions as a function of time. **(D)** Rate of endocytosis for the initial 15 min. This is the expanded region of graph (A) for 1-15 min period.

Fig. 16 (A) % Change of acid-resistant and acid-dissociable fractions as a function of time

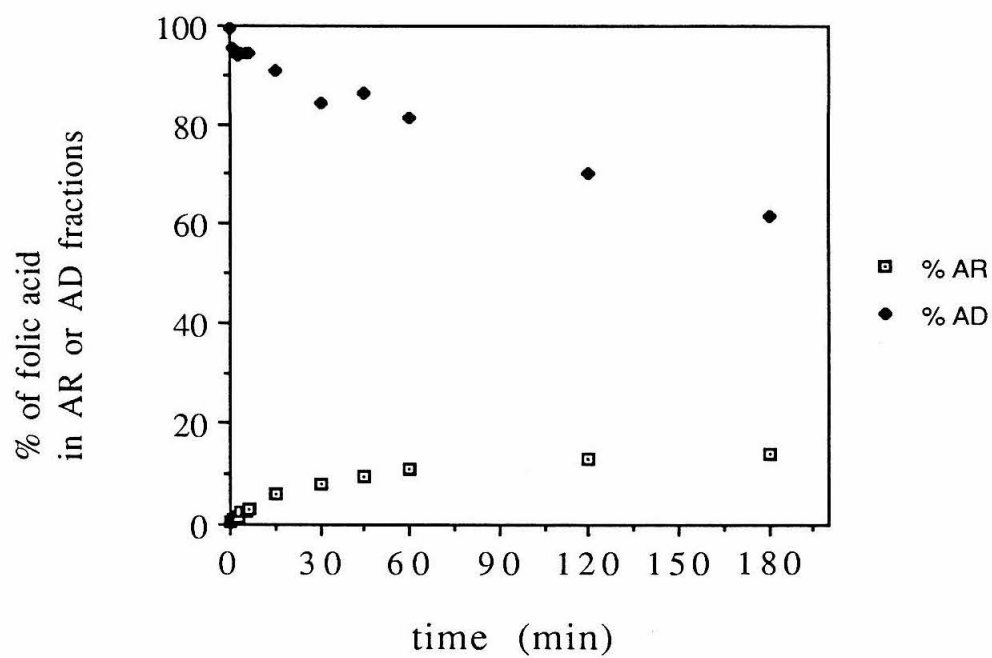
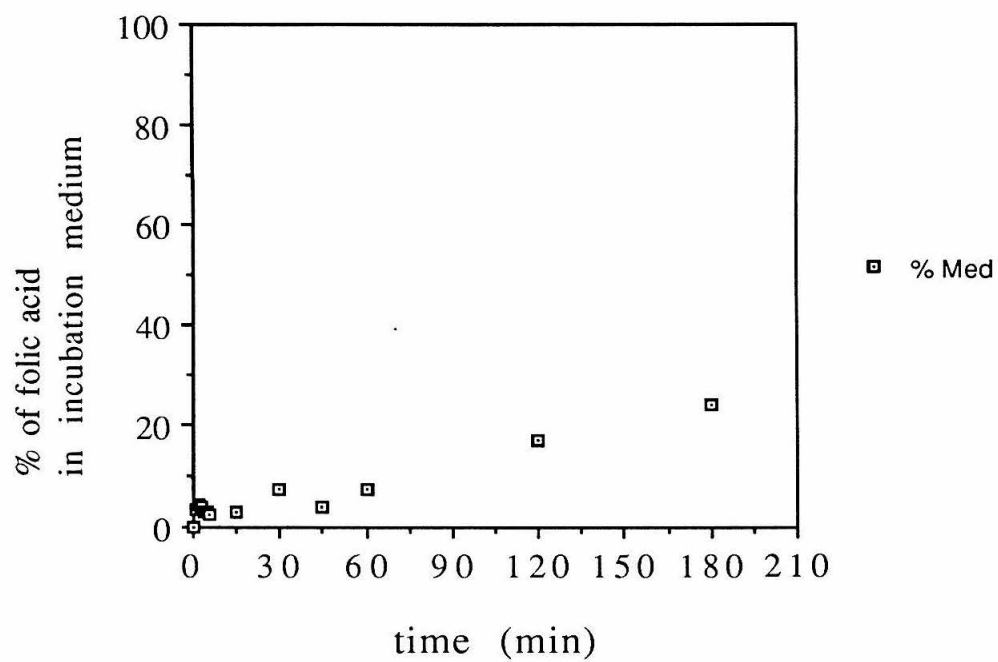
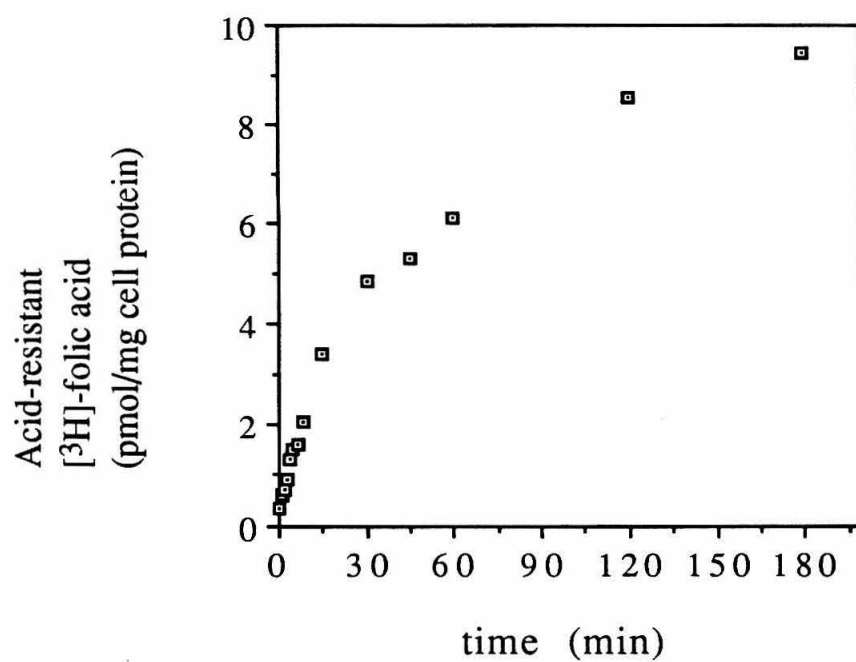


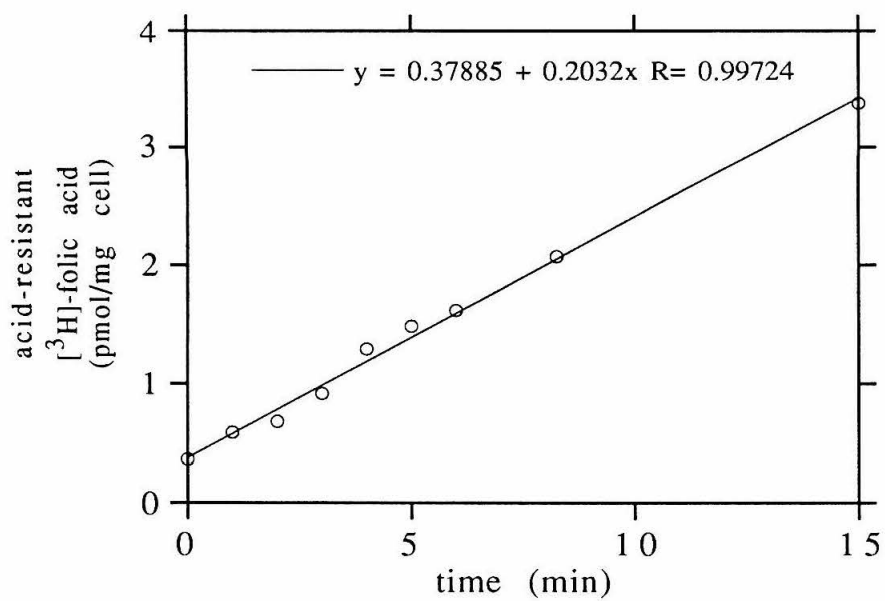
Fig. 16 (B) % Change of [ $^3\text{H}$ ]-folic acid in the media as a function of time



**Fig. 16 (C)** Uptake of [ $^3\text{H}$ ]-folic acid by KB cells as a function of time





**Fig. 16 (D) Rate of endocytosis for the initial 15 min**

**Fig. 17. Experimental scheme to define the interrelationship between the folate receptor and a probenecid-sensitive anion carrier in the transport of  $[^3\text{H}]\text{-5-MeH}_4\text{folate}$**

Figures (a), (b), (c), and (d) in Figs. 17 (A), (B), (C), and (D) show the schematic representation of  $[^3\text{H}]\text{-5-MeH}_4\text{folate}$  uptake via folate receptor-dependent and folate receptor-independent pathway under various conditions: (a), without folic acid and probenecid; (b), with 1 mM probenecid; (c), with 100 fold excess folic acid; (d), with 100 fold folic acid and 1 mM probenecid. The arrows associated with a circle (the caveola), represent  $[^3\text{H}]\text{-5-MeH}_4\text{folate}$  uptake via folate receptors and the probenecid-sensitive carrier. The arrows associated with isolated carrier represent the  $[^3\text{H}]\text{-5-MeH}_4\text{folate}$  uptake without the participation of the folate receptor, i.e., uptake through the probenecid-sensitive carrier when the carrier is exposed to culture media. The length of the arrows represent the amount of  $[^3\text{H}]\text{-5-MeH}_4\text{folate}$  uptake in an arbitrary unit. E represents the amount of  $[^3\text{H}]\text{-5-MeH}_4\text{folate}$  in the endocytic vesicle when the vesicle is closed. R represents the amount of  $[^3\text{H}]\text{-5-MeH}_4\text{folate}$  transported to the cytoplasm via folate receptors (and the anion carrier if the folate receptor and probenecid-sensitive carrier work in tandem). T represents the amount of  $[^3\text{H}]\text{-5-MeH}_4\text{folate}$  transported to the cytoplasm only through the anion carrier without the help of folate receptors. Subscripts for E, R, T represent the conditions for the  $[^3\text{H}]\text{-5-MeH}_4\text{folate}$  uptake. Experimentally measured values for uptake, the acid-resistant fraction (AR) is the sum of E, R, and T. Therefore, we have the following equations for acid-resistant fractions measured under four different conditions;

$$\text{AR(a)} = \text{E(a)} + \text{R(a)} + \text{T(a)} \quad \text{-----} \quad \text{(i)}$$

$$AR(b) = E(b) + R(b) + T(b) \quad \text{-----} \quad (ii)$$

$$AR(c) = E(c) + R(c) + T(c) \quad \text{-----} \quad (iii)$$

$$AR(d) = E(d) + R(d) + T(d) \quad \text{-----} \quad (iv)$$

Here, we could assume that the  $E(a) \approx E(b)$  since probenecid does not affect endocytosis of folate receptors at low concentration and for short periods of incubation time (see Fig. 10). We also assume that  $E(c) \approx E(d) \approx 0$  since the binding of 5-MeH<sub>4</sub>folate to folate receptor is almost completely blocked by excess folic acid (see Fig. 6). Then, we obtain the following equations by taking the differences between (i) and (ii) and between (iii) and (iv).

$$AR(a) - AR(b) = R(a) - R(b) + T(a) - T(b) \quad \text{-----} \quad (v)$$

$$AR(c) - AR(d) = R(c) - R(d) + T(c) - T(d) \quad \text{-----} \quad (vi)$$

By taking the difference between (v) and (vi) we obtain equation (vii) as follows;

$$\begin{aligned} &\{AR(a) - AR(b)\} - \{AR(c) - AR(d)\} \\ &= \{R(a) - R(b)\} - \{R(c) - R(d)\} + \{T(a) - T(b)\} - \{T(c) - T(d)\} \quad \text{-----} \quad (vii) \end{aligned}$$

which can be rearranged as follows;

$$\begin{aligned} &\{AR(a) - AR(b)\} - \{AR(c) - AR(d)\} \\ &= \{R(a) - R(b)\} - \{R(c) - R(d)\} + \{T(a) - T(c)\} - \{T(b) - T(d)\} \quad \text{-----} \quad (viii) \end{aligned}$$

This equation can be further simplified as follows if we assume that  $R(c)=R(d)\approx 0$  since folate receptors are almost completely blocked by folic acid and assume that  $T(a) \approx T(c)$  and  $T(b) \approx T(d)$  since folic acid has a very small affinity for the carrier and would not inhibit the transport of 5-MeH<sub>4</sub>folate significantly;

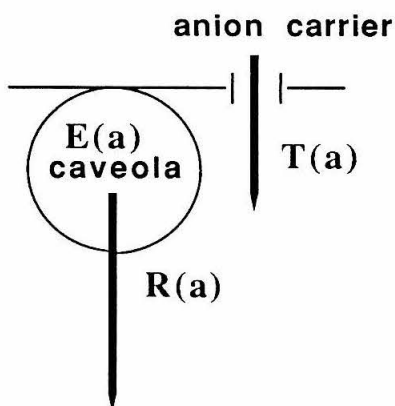
$$\begin{aligned} &\{AR(a) - AR(b)\} - \{AR(c) - AR(d)\} \\ &\approx \{R(a) - R(b)\} \quad \text{-----} \quad (ix) \end{aligned}$$

If probenecid interferes with the translocation of [<sup>3</sup>H]-5-MeH<sub>4</sub>folate from the endosome to the cytoplasm,  $R(a) > R(b)$  and if not,  $R(a) = R(b)$ . Therefore if  $\{AR(a) - AR(b)\} - \{AR(c) - AR(d)\} = 0$ , probenecid does not interfere with the

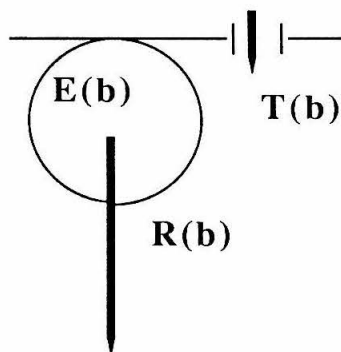
translocation of  $[^3\text{H}]\text{-5-MeH}_4\text{folate}$  from the endosome to the cytoplasm, thereby proving that folate receptor and the anion carrier work independently (see **Fig. 17 A**). If  $\{\text{AR(a)} - \text{AR(b)}\} - \{\text{AR(c)} - \text{AR(d)}\} > 0$ , probenecid interferes with the translocation of  $[^3\text{H}]\text{-5-MeH}_4\text{folate}$  from the endosome to the cytoplasm, suggesting that folate receptor and the anion carrier work in a dependent manner unless probenecid interferes with the acidification of the endosome and inhibits the release of  $[^3\text{H}]\text{-5-MeH}_4\text{folate}$  from the folate receptors into the endosome (see **Fig. 17 B**). If probenecid interferes with the acidification of the lumen of the endosome,  $\{\text{AR(a)} - \text{AR(b)}\} - \{\text{AR(c)} - \text{AR(d)}\} > 0$  whether the folate receptor and the anion carrier work independently (**Fig. 17 C**) or not (**Fig. 17 D**)

Fig. 17 (A). If the folate receptor and the probenecid-sensitive anion carrier work independently and if probenecid does not interfere with the acidification of the lumen of caveola,  $\{AR(a) - AR(b)\} - \{AR(c) - AR(d)\} \approx 0$ .

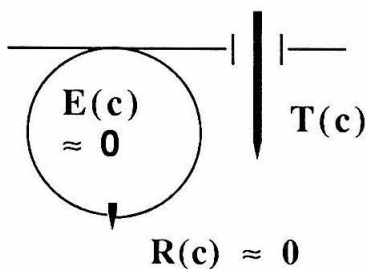
(a). Control



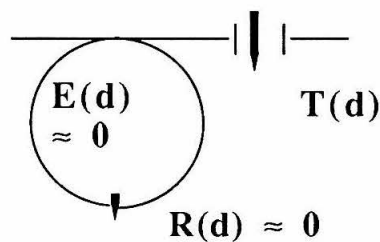
(b). With 1 mM probenecid



(c). With 100x excess folic acid



(d). With 1 mM probenecid and 100x excess folic acid



AR; acid-resistant fraction of  $[^3\text{H}]\text{-5-MeH}_4\text{folate}$

E;  $[^3\text{H}]\text{-5-MeH}_4\text{folate}$  in the caveola

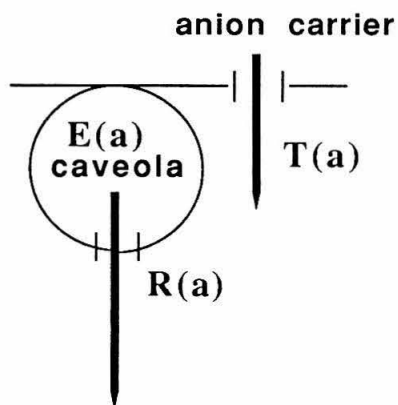
R;  $[^3\text{H}]\text{-5-MeH}_4\text{folate}$  transported to the cytoplasm  
by folate receptor

T;  $[^3\text{H}]\text{-5-MeH}_4\text{folate}$  transported to the cytoplasm  
by the probenecid-sensitive anion carrier

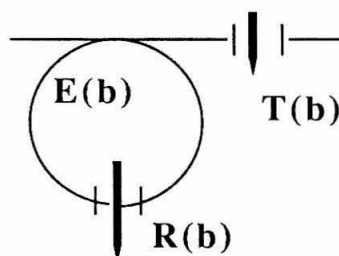
Bold arrows; transport of  $[^3\text{H}]\text{-5-MeH}_4\text{folate}$ . The length of the arrows represents the amount of  $[^3\text{H}]\text{-5-MeH}_4\text{folate}$  transport in an arbitrary unit.

Fig. 17 (B). If the folate receptor and the probenecid-sensitive anion carrier work in tandem and if probenecid does not interfere with the acidification of the lumen of caveola,  $\{AR(a) - AR(b)\} - \{AR(c) - AR(d)\} > 0$ .

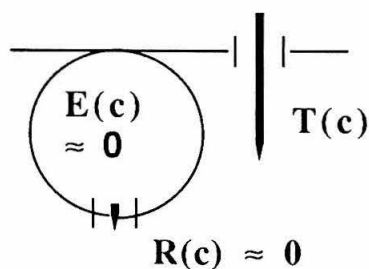
(a). Control



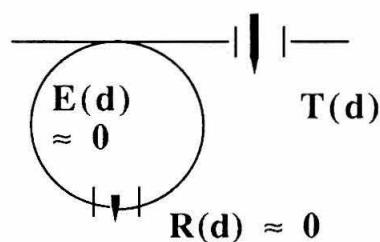
(b). With 1 mM probenecid



(c). With 100x excess folic acid



(d). With 1 mM probenecid and 100x excess folic acid



AR; acid-resistant fraction of  $[^3\text{H}]\text{-5-MeH}_4\text{folate}$

E;  $[^3\text{H}]\text{-5-MeH}_4\text{folate}$  in the caveola

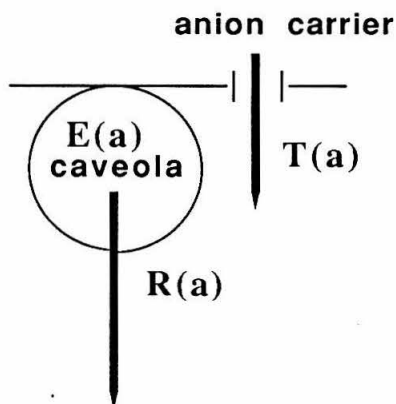
R;  $[^3\text{H}]\text{-5-MeH}_4\text{folate}$  transported to the cytoplasm  
by folate receptor

T;  $[^3\text{H}]\text{-5-MeH}_4\text{folate}$  transported to the cytoplasm  
by the probenecid-sensitive anion carrier

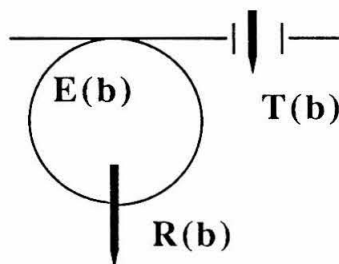
Bold arrows; transport of  $[^3\text{H}]\text{-5-MeH}_4\text{folate}$ . The length of the arrows represents the amount of  $[^3\text{H}]\text{-5-MeH}_4\text{folate}$  transport in an arbitrary unit.

Fig. 17 (C). If the folate receptor and the probenecid-sensitive anion carrier work independently and if probenecid interferes with the acidification of the lumen of caveola,  $\{AR(a) - AR(b)\} - \{AR(c) - AR(d)\} > 0$ .

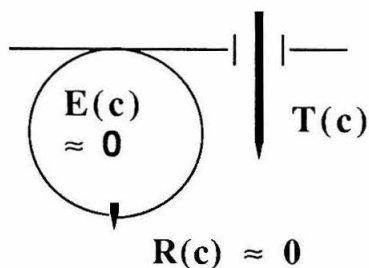
(a). Control



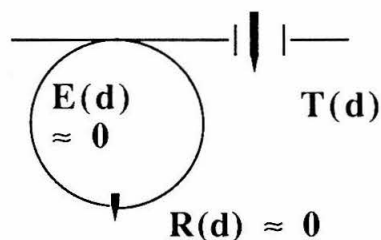
(b). With 1 mM probenecid



(c). With 100x excess folic acid



(d). With 1 mM probenecid and 100x excess folic acid



AR; acid-resistant fraction of  $[^3H]$ -5-MeH<sub>4</sub>folate

E;  $[^3H]$ -5-MeH<sub>4</sub>folate in the caveola

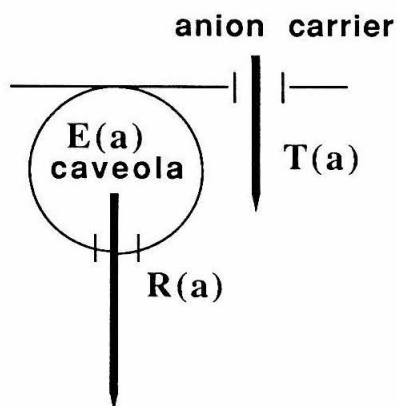
R;  $[^3H]$ -5-MeH<sub>4</sub>folate transported to the cytoplasm  
by folate receptor

T;  $[^3H]$ -5-MeH<sub>4</sub>folate transported to the cytoplasm  
by the probenecid-sensitive anion carrier

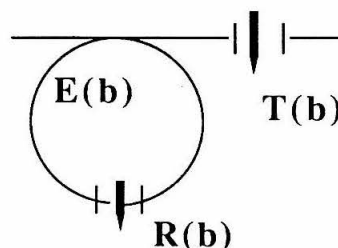
Bold arrows; transport of  $[^3H]$ -5-MeH<sub>4</sub>folate. The length of the arrows represents the amount of  $[^3H]$ -5-MeH<sub>4</sub>folate transport in an arbitrary unit.

Fig. 17 (D). If the folate receptor and the probenecid-sensitive anion carrier work in tandem and if probenecid interferes with the acidification of the lumen of caveola,  $\{AR(a) - AR(b)\} - \{AR(c) - AR(d)\} > 0$ .

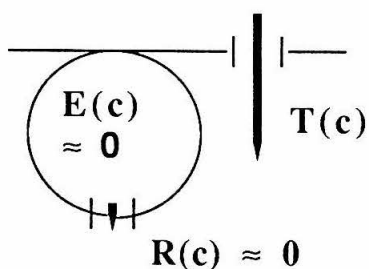
(a). Control



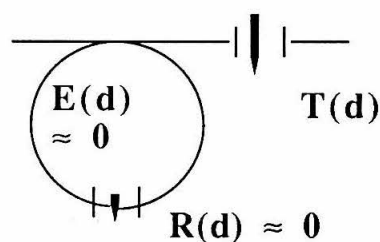
(b). With 1 mM probenecid



(c). With 100x excess folic acid



(d). With 1 mM probenecid and 100x excess folic acid



AR; acid-resistant fraction of  $[^3H]$ -5-MeH<sub>4</sub>folate

E;  $[^3H]$ -5-MeH<sub>4</sub>folate in the caveola

R;  $[^3H]$ -5-MeH<sub>4</sub>folate transported to the cytoplasm  
by folate receptor

T;  $[^3H]$ -5-MeH<sub>4</sub>folate transported to the cytoplasm  
by the probenecid-sensitive anion carrier

Bold arrows; transport of  $[^3H]$ -5-MeH<sub>4</sub>folate. The length of the arrows represents the amount of  $[^3H]$ -5-MeH<sub>4</sub>folate transport in an arbitrary unit.



**Fig. 18. Effect of probenecid and folic acid on uptake of 5-MeH<sub>4</sub>folate at 50 nM.**

**(A)** KB cells were incubated in 1ml fdDMEM containing 50 nM [<sup>3</sup>H]-5-MeH<sub>4</sub>folate at 37 °C for 30 minutes in the absence (-Prob(0mM)) or presence (+Prob(1mM)) of 1 mM probenecid, or in the presence of 5 µM folic acid with (100xFol, +Prob.) or without (100xFol(5 mcM)) 1 mM probenecid. Identical experiments were done at 0 °C for control. Uptake of [<sup>3</sup>H]-5-MeH<sub>4</sub>folate by KB cells was determined as described in MATERIALS AND METHODS. For each set, distributions of the acid-resistant fraction of [<sup>3</sup>H]-5-MeH<sub>4</sub>folate were obtained by averaging nine samples at 37 °C and three samples at 0°C. Acid-resistant fractions at 0 °C experiments were subtracted from those at 37 °C. Error bars represent 95 % confidence limit.

**(B)** (-P)-(+P) represents the difference between acid-resistant fractions (without 100x folic acid) in the absence and presence of 1 mM probenecid. (100xF)-(100x,+P) represents the difference between acid-resistant fractions in the absence and presence of 1 mM probenecid with 100x folic acid. Enhancement represents the difference between (-P)-(+P) and (100xF)-(100xF,+P).

Fig. 18 (A)

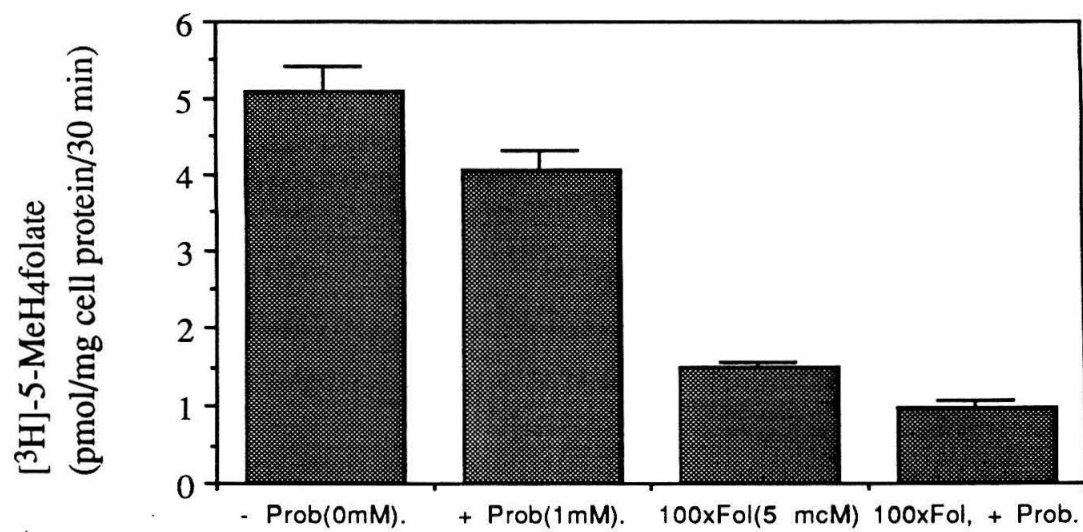
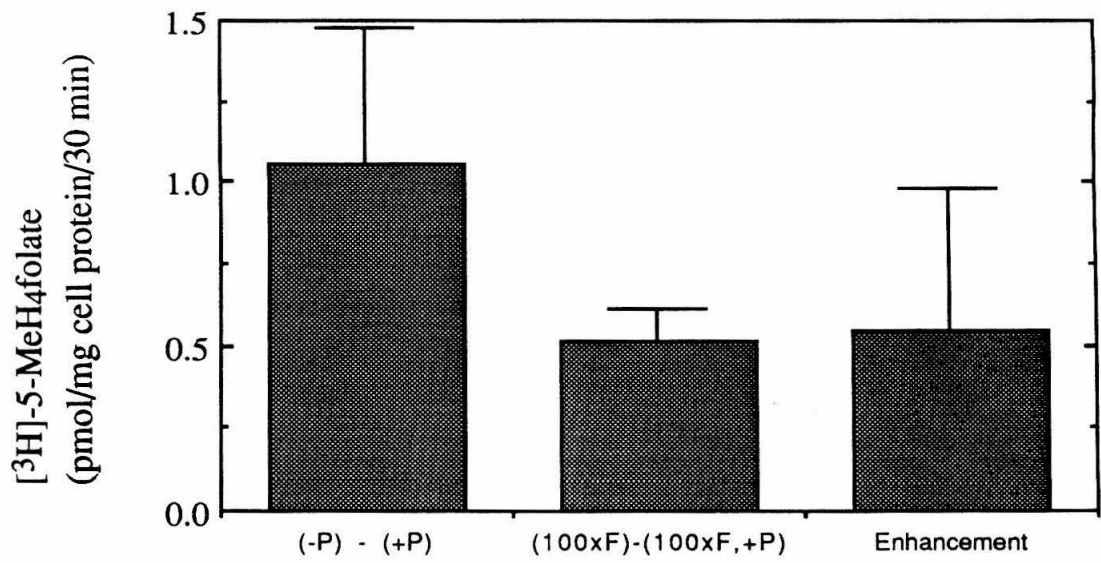


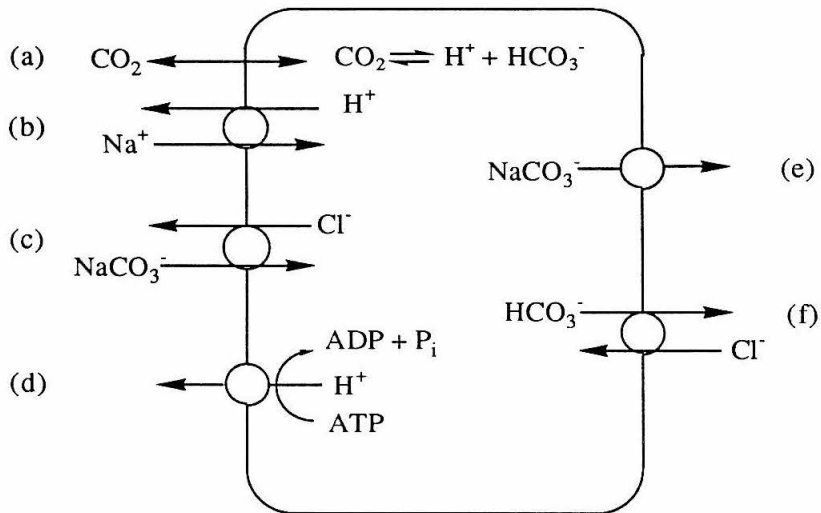
Fig. 18 (B)



**Fig. 19. Transport systems regulating intracellular pH**

- (a)  $\text{CO}_2$  gas can diffuse in and out of the cell across the plasma membrane. It is dissolved in water and in equilibrium with proton and carbonate ion.
- (b)  $\text{Na}^+/\text{H}^+$  antiporter; A transporter normally exchanges extracellular  $\text{Na}^+$  for intracellular  $\text{H}^+$  in a 1:1 stoichiometry. It does not require  $\text{HCO}_3^-$  or  $\text{Cl}^-$ . It exists in a variety of vertebrate cells.
- (c)  $\text{Na}^+$ -dependent  $\text{Cl}^-/\text{HCO}_3^-$  exchanger; A transporter, or family of transporters, that exchanges extracellular  $\text{Na}^+$  and  $\text{HCO}_3^-$  (or a similar species) for intracellular  $\text{Cl}^-$  and  $\text{H}^+$ . It is found in several invertebrate cells and in certain cultured mammalian cells.
- (d) Proton pumps; ATP-driven  $\text{H}^+$  pumps play a central role in acid secretion by certain epithelia.
- (e)  $\text{Na}^+/\text{HCO}_3^-$  cotransporter; A transporter which mediates net efflux of  $\text{HCO}_3^-$  and  $\text{Na}^+$ , giving rise to transcellular transport of  $\text{HCO}_3^-$  in various organisms.
- (f)  $\text{Na}^+$ -independent  $\text{Cl}^-/\text{HCO}_3^-$  exchanger; A transporter, or a family of transporters, which exchanges anions on opposite sides of the cell membrane in a stoichiometry of 1:1, and is inhibited or blocked by disulfonic stilbene derivatives. Probenecid was also found to block this transporter in Vero cells (ref. 76). Efflux of one molecule of carbonate generates one proton in the cell.

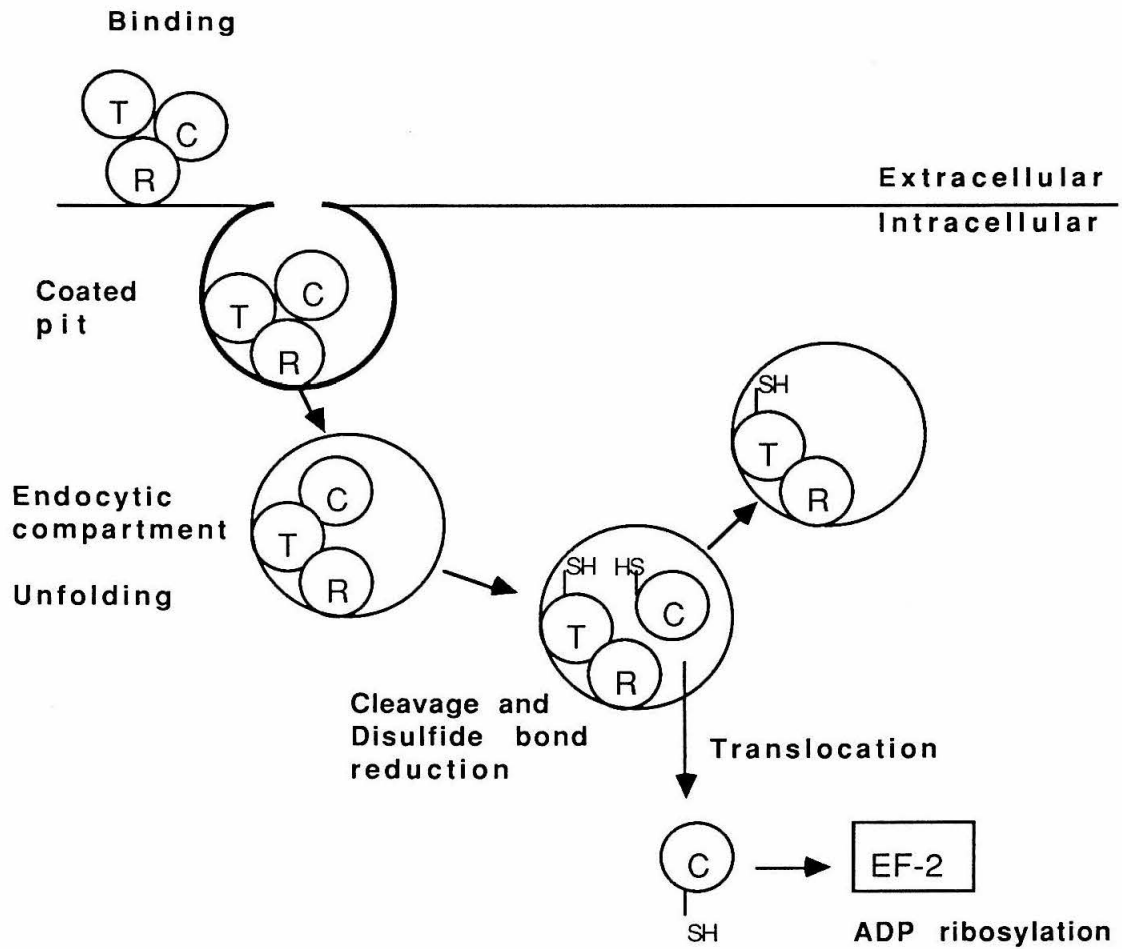
All of the above transporters do not exist in one cell.

**Fig. 19. Transport systems regulating intracellular pH**Adapted from Madshus, I. H. (*Biochem. J.* (1988) 250, 1-8)

**Fig. 20. Schematic diagram of Diphtheria toxin and *Pseudomonas* exotoxin action**

Receptor domain R of toxin (diphtheria toxin, DT or *Pseudomonas* exotoxin A, PE) binds to a cell surface receptor and is endocytosed via the coated pits. The low pH of the endosome and possibly other factors cause the toxin to unfold. Toxin is then proteolytically cleaved between translocation domain T and catalytic domain C. Cleavage is followed by reduction of the disulfide bond and the release of catalytic domain that translocates to the cytosol. In case of diphtheria toxin N-terminal 21 KDa catalytic domain is released from the transmembrane domain T. In case of *Pseudomonas* exotoxin A, C-terminal 37 kDa is released. DT 21 KDa fragment translocates into cytoplasm from the lysosome, whereas PE 37 KDa travels to the Golgi apparatus and translocates into cytosol. In the cytosol DT Catalytic domain of each toxin adds an ADP ribosyl moiety to elongation factor-2 (EF-2). ADP ribosylated EF-2 can no longer support protein synthesis, leading to cell death. This was adapted from Pastan et al. (124).

Fig. 20. Schematic diagram of Diphtheria toxin and *Pseudomonas* exotoxin action

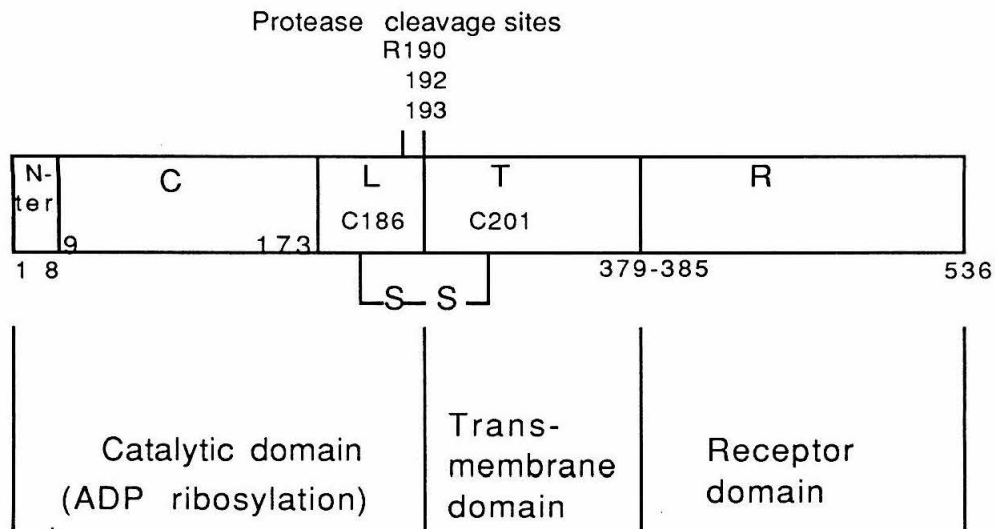


**Fig. 21.** Schematic representation of the subunit composition of diphtheria toxin and *Pseudomonas* exotoxin A



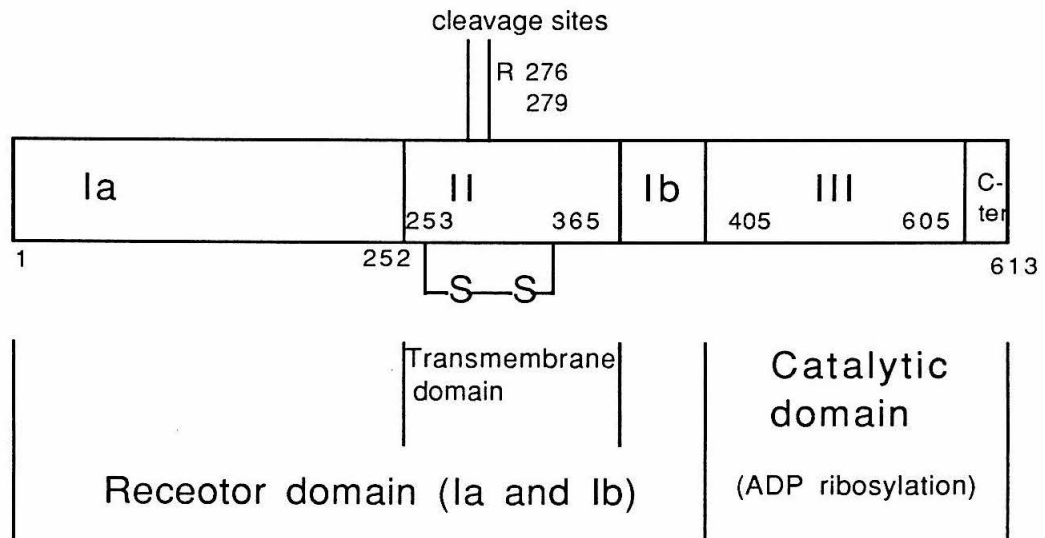
Fig. 21

## (a) Diphtheria toxin



\* N-ter: N-terminal GADDVVD- sequence; L: linker seq. 174-194  
T: transmembrane domain; R: receptor domain ; C: catalytic domain

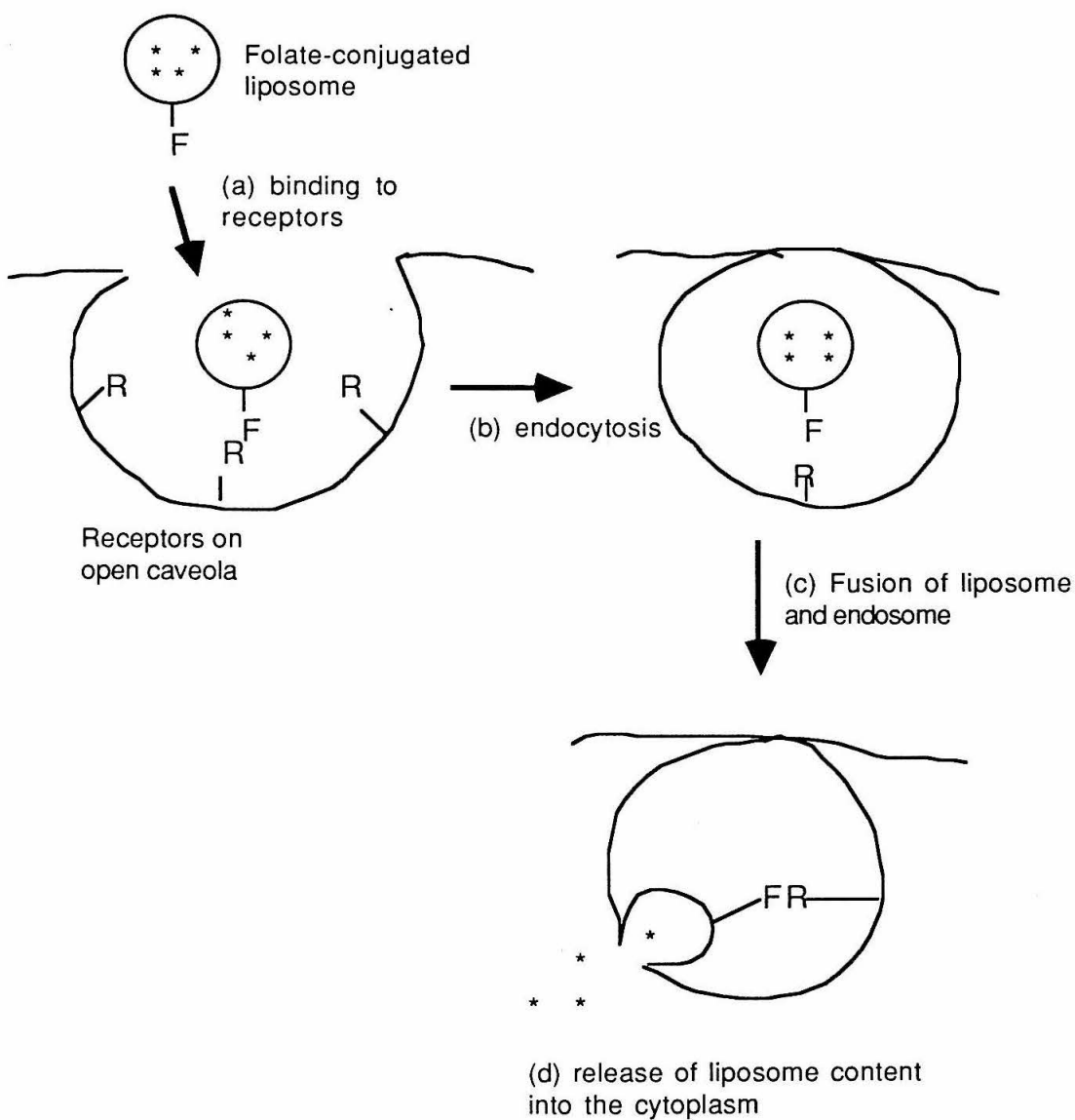
## (b) Pseudomonas exotoxin A



\* C-ter: C-terminal signal sequence --REDLK

**Fig. 22. Schematic diagram of drug delivery using folate receptor-mediated endocytosis of folate-conjugated liposomes** Folate-conjugated liposome containing drug binds to the folate receptors associated with caveola (a). The liposome is endocytosed by cells (b) and fuses with the caveola (c) and the liposome contents are released into the cell cytoplasm (d).

**Fig. 22. Schematic diagram of drug delivery using folate receptor-mediated endocytosis of folate-conjugated liposomes**



**Chapter 3: Transport kinetics of oligonucleotides into  
reconstituted cellular nuclei  
and  
the effect of a nuclear localization signal peptide  
on the transport**

**SUMMARY** Oligodeoxynucleotides designed to hybridize to specific mRNA sequences (antisense oligonucleotides) or double stranded DNA sequences have been used to inhibit the synthesis of a number of cellular and viral proteins (Crooke, S. T. (1993) *FASEB J.* 7, 533-539; Carter, G. and Lemoine, N. R. (1993) *Br. J. Cancer* 67, 869-876; Stein, C. A. and cohen, J. S. (1988) *Cancer Res.* 48, 2659-2668). However, the distribution of the delivered oligonucleotides in the cell, i.e., in the cytoplasm or in the nucleus has not been clearly defined. We studied the kinetics of oligonucleotide transport into the cell nucleus using reconstituted cell nuclei as a model system. We present evidences here that oligonucleotides can freely diffuse into reconstituted nuclei. Our results are consistent with the reports by Leonetti et al. (*Proc. Natl. Acad. Sci. USA*, Vol. 88, pp. 2702-2706, April 1991), which were published while we were carrying out this research independently. We also investigated whether a synthetic nuclear localization signal (NLS) peptide of SV40 T antigen could be used for the nuclear targeting of oligonucleotides. We synthesized a nuclear localization signal peptide-conjugated oligonucleotide to see if a nuclear localization signal peptide can enhance the uptake of oligonucleotides into reconstituted nuclei of *Xenopus*. Uptake of the NLS peptide-conjugated oligonucleotide was comparable to the control oligonucleotide at similar concentrations, suggesting that the NLS signal peptide does not significantly enhance the nuclear accumulation of oligonucleotides. This result is probably due to the small size of the oligonucleotide.

## INTRODUCTION

**Methods for delivery of oligonucleotides into cells** Oligodeoxynucleotides designed to hybridize to specific mRNA sequences (antisense oligonucleotides) or double stranded DNA sequences have been used to inhibit the synthesis of a number of cellular and viral proteins and therefore show promise as therapeutic agents to block the synthesis of specific proteins (reviews, 1). It is believed that potential mechanisms of action of the oligonucleotides include inhibition of RNA synthesis and RNA processing in the cellular nucleus, degradation of mRNA by RNase H and translational arrest by inhibiting the interaction between ribosome and the mRNA in the cytoplasm (Fig. 1 A, ref. 1a). In order for the oligonucleotides to exert their effects on cellular activity, they must be delivered into the cellular cytoplasm and into the cellular nucleus. However, the efficiency of uptake of oligonucleotides by various cellular mechanisms may be too low (2). In order to circumvent this problem, different methods have been developed (1). Modifications of the backbone, base or sugar ring of the oligonucleotides (review 1), covalent conjugation of oligonucleotides to polylysine (3), cholesterol (4) or phospholipid (5), encapsulation of oligonucleotides in liposomes (6), and complex formation with positively charged liposomes (DOTMA liposomes, ref. 7) all enhanced cellular uptake of oligonucleotides. All of these methods enhance the delivery of oligonucleotides into the cytoplasm. However, the oligonucleotides are to exert their inhibitory effects in the cell nucleus, they must also enter the nucleus. In principle, oligonucleotides could enter the cell nucleus through the same entry routes as nuclear proteins or when nuclear membranes disassemble during mitosis.

**Transport of proteins into cell nucleus** Studies have shown that the translocation of proteins and RNAs between the nucleus and the cytoplasm of

eukaryotic cells occurs through the nuclear pore complex (reviews 8-14, Fig. 1 B). Cell physiology experiments carried out with a number of different cells indicate that the pore complex has the properties of a molecular sieve containing an aqueous channel with a functional diameter of about 100 Å (9, 10). Accordingly, small molecules or particles such as potassium ions, aminobutyric acid, sucrose, and inulin can passively diffuse across the pore complex into the nucleus (8). Many nuclear proteins are too large to be accommodated by the apparent diameter of the pore. Most nuclear proteins with molecular weights greater than 20 kD, as well as some small nuclear proteins, are transported into the nucleus through nuclear pores by a process that requires the recognition of a peptide signal sequence (13, 14). Various studies have shown that the nuclear proteins have one or two short nuclear localization signal (NLS) peptides (13) and these signal peptides are recognized by the nuclear localization signal binding proteins in the cell cytoplasm or by the nuclear pore complex for nuclear transport (11, 14, Fig. 1 C). Nuclear protein import, which requires ATP hydrolysis and is temperature-dependent (15), involves at least two steps (16-18): binding of the signal sequence at the recognition site, possibly to nuclear pore-associated fibrils (19, 20), followed by slower, energy-dependent translocation through nuclear pores (16-18).

**Nuclear localization sequences in nuclear proteins** Dingwall et al. (21) found that when the carboxy terminal third of nucleoplasmin (125 kD), a *Xenopus* nuclear protein, was removed by protease digestion, the amino terminal core was unable to enter the nucleus. The separated carboxy tail of nucleoplasmin, in contrast, quickly entered the nucleus. It has since been shown that complexing nucleoplasmin to large nonnuclear molecules such as immunoglobulin, IgG (22), an algal protein, phycoerythrin (23), or even to large

gold particles (24) confers rapid entry into the nucleus. Feldherr (24) injected nucleoplasmin-coated gold particles into *Xenopus* oocytes, and observed that particles up to 200 Å in diameter enter the nucleus through the central channel of the pore, whereas particles coated with proteins lacking signal sequences remain in the cytoplasm. Nuclear localization signals have been analyzed for a number of proteins in viruses, yeast, *Xenopus* and mammals (13). The signal sequences frequently contain short regions of basic amino acids containing proline residues, but not all are of this type (13).

The most extensively studied localization signal peptide is that of the large T antigen of SV 40 (simian virus 40). The 94 kD T antigen polypeptide becomes highly concentrated in the nucleus following synthesis in the cytoplasm. The T antigen localization signal peptide comprises a stretch of 7 amino acids surrounding the 128th amino acid residue in the T antigen polypeptide with the sequence <sup>126</sup>pro-lys-<sup>128</sup>lys-lys-arg-lys-<sup>132</sup>val (25). T antigen transport is abolished when this region is deleted, or when certain amino acid substitutions are induced (25). The lysine residue 128 is particularly critical ; when this amino acid is changed to asparagine, as found in a naturally occurring variant of the T antigen (26), or to threonine (25), the resulting protein remains in the cytoplasm. When cells express chimeric genes consisting of the sequence of the wild-type SV 40 T antigen localization signal peptide coupled to the amino terminus of the gene for β-galactosidase (116 kD) or pyruvate kinase (58 kD), the resultant chimeric proteins accumulate at high levels in the nucleus (27). In contrast, the proteins remain in the cytoplasm when the signal sequence is modified at lysine 128 or with no added signal sequence. Most strikingly, when synthetic peptides containing the wild-type localization sequence are chemically coupled to nonnuclear proteins (~ 10 peptides per protein) such as ovalbumin (43 kD;



diameter 54 Å, ref. 28), bovine serum albumin (67 kD, diameter 70 Å, ref. 28, 29), immunoglobulin G (150 kD, 35x35x140 Å, ref. 28, 29) or ferritin (465 kD; diameter 94 Å, ref. 28), the resulting conjugates accumulate rapidly in the nucleus. The rate of transport is influenced by the number of peptides per cytoplasmic protein and to some extent by the size of the protein (28). The presence of excess free signal peptide reduces nuclear transport of peptide-protein conjugates (29), suggesting the possible saturation of a receptor protein within the pore.

**Purpose of this study** Even though many methods have been developed to target nucleic acids into cells, it has not been clearly shown that the delivered oligonucleotides could reach the cell nucleus until recently (30). It is possible for the short oligonucleotides to diffuse into the cellular nucleus through the nuclear pore complexes (8). Alternatively, the oligonucleotides could interact with genomic DNA when the nuclear membranes disassemble during cellular division (31). Therefore, we studied the kinetics of oligonucleotide transport into the cell nucleus using reconstituted nuclei (32) as an *in vitro* model system to answer this question. We also investigated whether a synthetic nuclear localization signal peptide of SV40 T antigen could be used for nuclear targeting of oligonucleotides. We synthesized a nuclear localization signal peptide-conjugated oligonucleotide in order to determine whether the nuclear localization signal peptide could enhance the uptake of oligonucleotides into the reconstituted nuclei of *Xenopus*. Our results were consistent with the reports by Leonetti et al. (30), which was published while we were doing this research independently.

## MATERIALS AND METHODS

### Materials

*N*- $\epsilon$ -Fmoc-*N*- $\alpha$ -Boc-L-lysine was purchased from Bachem, Inc., Torrance, CA. Amino link 2 (Fig. 2) was purchased from Applied Biosystems. Maleimidobenzoyl succinimide (MBS) was purchased from Pierce Chemical Company. Sephadex G-25 (fine) and fluorescein isothiocyanate (FITC) were purchased from the Sigma Chemical Company. Tetramethylrhodamine-6-isothiocyanate (TRITC) was purchased from Molecular Probes, Inc. *Xenopus laevis* eggs and sperm nuclei were the gifts of professor William Dunphy in the Division of Biology at the California Institute of Technology.

**Synthesis of an oligonucleotide containing an aminohexyl linker** A 20-mer oligonucleotide with the sequence of CGACCGATGC-CCTTGAGAGC (5'-3', 1721th-1740th nucleotide sequence of a plasmid, *sisCAT*) was synthesized using phosphoramidite chemistry (33, 34) in the laboratory of Dr. Suzanna Horvath at California Institute of Technology. Amino link 2 (see Fig. 2, Applied Biosystems) was coupled to the 5'-end and an aminohexyl containing oligonucleotide was prepared.

### Solid-phase synthesis of nuclear localization signal peptides

(a) *Synthesis of a nuclear localization signal peptide (peptide1);* A synthetic nuclear localization signal peptide (Pro-Lys-Lys-Lys-Arg-Lys-Val-Glu-Asp-Tyr-Cys, peptide 1) was prepared using tBOC chemistry (35) in the laboratory of Dr. Suzanna Horvath at the California Institute of Technology.

(b) *Synthesis of fluorescein labeled nuclear localization signal peptide (F-peptide2);* The fluorescein isothiocyanate (FITC)-conjugated peptide (FITC-Lys-Pro-Lys-Lys-Lys-Arg-Lys-Val-Glu-Asp-Tyr-Cys, F-peptide 2, see Fig. 3.) was prepared using the modified procedures of Halleck et al. (36). A peptide, Lys-Pro-Lys-Lys-

Lys-Arg-Lys-Val-Glu-Asp-Tyr-Cys was synthesized on resin by a solid-phase synthesis using 2-chlorobenzyloxycarbonyl protection of the  $\epsilon$ -amino groups of internal lysines and 9-fluorenylmethyloxycarbonyl (Fmoc) protection of the  $\epsilon$ -amino group of the N-terminal lysine in the laboratory of Dr. Suzanna Horvath at the California Institute of Technology. After synthesis of the peptide, the Fmoc group was removed by washing the resin with 50 % (vol/vol) piperidine in dichloromethane manually. The deprotected  $\epsilon$ -amine group of the N-terminal lysine was labeled with fluorescein by treating the resin (about 200 mg) consecutively with fluorescein isothiocyanate (FITC, 50-60 mg) three times for several hours. Peptides were deprotected and released from the resin using hydrofluoric acid. Fluorescein isothiocyanate-conjugated peptides (F-peptide 2) were purified by reverse-phase HPLC and the molecular weights of the peptides were verified by mass spectrometry.

**Conjugation of peptides to bovine serum albumin** The synthetic nuclear localization signal peptides (peptide 1 and F-peptide 2) were coupled to bovine serum albumin (BSA) using a bifunctional cross-linking reagent, maleimidobenzoyl succinimide (MBS) according to the modified procedures of Lanford et al.(28, Fig. 4). The maleimidobenzoyl succinimide (MBS) solution (5 mg in 0.5 ml DMF) was added to the bovine serum albumin (BSA) solution (10 mg in 2 ml phosphate buffered saline, pH 7.4) dropwise and allowed to react for 1 hour at room temperature. Bovine serum albumin which had been modified with maleimidobenzoyl succinimide (MBS) was purified by gel-filtration chromatography using a Sephadex G-25 column (1.5x20 cm ) with 0.1 M sodium phosphate solution (pH 6.0) as the elution buffer. Fractions containing the modified BSA were collected and concentrated by centrifugation at 3,000 rpm for 15 minutes in a GSA rotor (Beckman) using a Centriprep-30 concentration device

(Amicon). 5 mg of signal peptide (peptide 1) was dissolved in 1 ml volume of 0.1 M sodium phosphate buffer (pH 6.0) and was immediately added to the MBS-modified BSA solution dropwise and the reaction mixture incubated at room temperature for 1 hour. The peptide-conjugated BSA was purified by gel-filtration chromatography using 0.1 M  $\text{NH}_4\text{HCO}_3$  as the elution buffer on a Sephadex G-25 column (1.5x20 cm). Fractions of eluted solution containing peptide-conjugated BSA were collected, washed twice by centrifugation with 15 ml 0.1 M  $\text{NH}_4\text{HCO}_3$  solution in Centriprep-10 concentrator and lyophilized. Peptide-BSA conjugates were analysed by amino acid analysis to determine the average number of peptide ligands per BSA molecule.

Similarly, FITC-labeled nuclear localization signal peptide (F-peptide 2, 0.7 mg/0.5 ml DMF) was conjugated to BSA (about 10 mg in 1 ml 0.1 M sodium phosphate buffer, pH 6.0) after modification with MBS. The number of conjugated peptides per BSA molecule was determined by measuring the absorbance of the fluorescein groups in the peptide-BSA conjugate at 494 nm using the FITC-labeled peptide as a standard. The protein concentration was determined using the Bio-Rad protein assay method with BSA as a standard.

**Conjugation of oligonucleotide to FITC-labeled peptide (F-peptide2)**  
FITC-conjugated peptides containing a cysteine residue were coupled to oligonucleotides containing an aminohexyl group using maleimidobenzoyl succinimide (Fig. 4). Oligonucleotides containing an aminohexyl group (55  $\mu\text{l}$  of 0.545 mM in 0.1 M sodium borate solution, pH 7.0) were mixed with MBS solution (110  $\mu\text{l}$  of 10 mg/ml *N,N*-dimethylformamide solution). The reaction was carried out for 45 minutes at room temperature. At the end of the reaction, 335  $\mu\text{l}$  of 0.1 M sodium borate solution was added to the reaction mixture followed by 1 ml cold ethanol and the mixture then incubated on dry ice-chilled

ethanol for 10 min to precipitate DNA. Precipitated oligonucleotides were pelleted by centrifugation at 12,000 g for 10 min at 4 °C. The oligonucleotide pellet was dissolved in 100 µl Tris-EDTA solution (TE, 10 mM Tris, 1 mM EDTA, pH 8.0) and the solution was centrifuged once more for 5 min to remove insoluble material. The supernatant solution containing modified oligonucleotides was collected after centrifugation. To this solution, a 9.1 µl volume of 3 M sodium acetate solution (pH 5.2) was added followed by two volumes of cold ethanol and incubation as described above for ethanol precipitation. Oligonucleotide precipitates were collected again by centrifugation. An additional ethanol precipitation and centrifugation was performed to further purify the oligonucleotides. The oligonucleotide pellet was lyophilized overnight and was dissolved in 50 µl TE buffer to a final concentration of 0.22 mM. The concentration of the oligonucleotide solution was determined by the measurement of absorbance at 260 nm and the use of the molar extinction coefficient of  $2 \times 10^5 \text{ M}^{-1} \text{ cm}^{-1}$  for the 20-mer oligonucleotide. The FITC-labeled peptide (F-peptide 2) was dissolved in 250 µl of 50 mM Tris (pH 7.4) to a final concentration of 1.4 mM. The oligonucleotides modified with maleimidobenzoyl succinimide were added to the FITC-peptide solution and the reaction mixture was incubated for 3 hours at room temperature. This coupling reaction resulted in a yellow viscous material. This was dissolved in the TE buffer and purified by seven consecutive ethanol precipitations. In order to verify the conjugation of FITC-labeled peptide (F-peptide 2) and the oligonucleotide, a larger scale synthesis was performed and the products were analysed by polyacrylamide-gel electrophoresis (37).

**Labeling of peptide1, BSA and peptide1-conjugated BSA with fluorescein isothiocyanate (FITC) or tetramethylrhodamine isothiocyanate (TRITC) (see**

**Fig. 5)** 5-10 mg/ml protein solutions were prepared in deionized water. 0.2-2.0 mg/ml FITC solution was prepared in 0.2 M sodium carbonate buffer (pH 9.5). The reaction was started by mixing the two solutions and the reaction allowed to continue for 2 hours at room temperature. FITC-labeled proteins were purified by Sephadex G-25 gel filtration chromatography using 0.2 M sodium carbonate buffer. Protein concentrations were determined using the Bio-Rad protein assay solution. The number of fluorescein groups per protein molecule was determined by measuring the absorbance of fluorescein at 494 nm using the FITC-labeled peptide 2 as a standard. Protein concentrations were determined using Bio-Rad protein assay solution. Peptide1-conjugated BSA was labeled with TRITC, similarly. The number of TRITC per protein molecule was not determined.

**Labeling of oligonucleotide with FITC or TRITC (see Fig. 5 and 6)** A volume of 40  $\mu$ l of the oligonucleotide solution (0.70 mM in 0.2 M sodium carbonate buffer (pH 9.5)) was added to 120  $\mu$ l FITC solution (12.8 mM in the same buffer). The reaction mixture was incubated at room temperature for 2 hours. The FITC-labeled oligonucleotide was purified by two consecutive ethanol precipitations, desalted using SEP-PAK C18 cartridges (Millipore) and lyophilized.

Similarly, oligonucleotide samples were labeled with TRITC in the 0.2 M sodium bicarbonate buffer. 10  $\mu$ l of oligonucleotide solution (1.76 mM) was added to 90 ml of TRITC solution (1.44 mM) and allowed to react for 3 hours. TRITC-labeled DNA was purified by 5 repeated ethanol precipitations followed by desalting using SEP-PAK C18 cartridges (Millipore). Approximate concentrations of the oligonucleotide solutions were determined by measuring the absorbance of diluted oligonucleotide solutions at 260 nm.

**Reconstitution of nuclei using *Xenopus laevis* egg extracts** Transport competent nuclear membranes were reconstituted using *Xenopus* egg extracts and *Xenopus* sperm nuclei as described in the Appendix. D (references 32, 38)

**Nuclear transport of proteins and oligonucleotides** Appropriate concentrations of fluorescently labeled proteins or oligonucleotides were added to reconstituted nuclei (28, 29). After incubation for appropriate periods of time and temperatures, aliquots of the assay solution were mixed with Hoechst 33258 dye in a fixation buffer to stain sperm DNA (see Appendix. D) and the fluorescence of the sperm DNA or added compounds were observed with a fluorescence microscope (Zeiss Axioplan).



## RESULTS

**Synthesis of peptides, BSA-peptide conjugates, oligonucleotide-peptide conjugate and fluorescent labeling of peptide 1, BSA, BSA-peptide conjugate and oligonucleotides** The approximate chemical formulae and concentrations of the compounds used in the transport experiments are summarized in Table 1. A typical mass spectrum of FITC-labeled peptide (F-peptide 2) is shown in Fig. 7. The major peak at 1912 (m/e) indicates that we obtained a peptide which was labeled with FITC as desired. Conjugation reactions of peptides to BSA resulted in BSA-conjugates with 10-20 peptides per molecule of BSA. Conjugation of fluorescein-labeled peptide (F-peptide 2) to DNA was demonstrated by polyacrylamide-gel electrophoresis.

**Reconstitution of the functional nuclear envelope and transport of the nuclear localization signal peptide-conjugated BSA into reconstituted nuclei** Time-dependent morphological changes of *Xenopus* sperm DNA and nuclear membranes are shown in Fig. 9. Initially, sperm chromatin showed compact and elongated structures and the nuclear membranes were not visible. In about 10-20 min, the sperm chromatin became decondensed and in 30-40 min the nuclear membranes became clearly visible. This stage corresponds to interphase in the cell cycle (31, 32). In order to see if the reconstituted nuclei were active in nuclear protein transport, we added FITC-labeled nuclear localization signal peptide-conjugated BSA [F-(B-P1)] to reconstituted nuclei and nuclear fluorescence was observed as indicated in Fig. 10 A. At time zero, FITC-labeled nuclear localization signal peptide-conjugated BSA molecules [F-(B-P1)] had not accumulated in the nuclei. In about 30 min of incubation at room temperature the concentration of the protein in the nuclei became clear. After 60 min the fluorescence of the nuclei became more intense, suggesting that the FITC-labeled



nuclear localization signal peptide-conjugated BSA molecules were transported into the nuclei and concentrated. On the contrary, FITC-labeled BSA molecules (F-BSA) did not accumulate in the nuclei (Fig. 10 B). These results confirmed the previous observation that the nuclear localization signal peptides of SV 40 T antigen confer the translocation of large molecules to which the peptides are conjugated (28, 29). However, the synthetic nuclear localization signal peptides labeled with fluorescein isothiocyanate (F-peptide 1) did not accumulate in the nuclei (Fig. 10 B). Lobl et al. (39) have reported that synthetic nuclear localization signal peptides of SV 40 which were labeled with a small fluorescent probe (monobromobimane) also did not accumulate in cell nucleus. Our results are consistent with their finding. The signal peptide can probably diffuse in and out of the nuclei freely via the nuclear pore complex since the size of the peptide is small. Interestingly, reconstituted nuclei with apparent nuclear membranes were not always active at protein import as shown in Fig. 10 A (60 min at room temperature). We counted the number of reconstituted nuclei with membranes and the number of transport competent nuclei simultaneously using different light filters with a fluorescence microscope. Typically about 50 percent of the reconstituted nuclei were active in protein import and the percentage varied slightly from experiment to experiment.

**Accumulation of oligonucleotides in the reconstituted nuclei by free diffusion** Transport experiments with FITC-labeled oligonucleotides showed that oligonucleotides could be associated with the reconstituted nuclei even though the oligonucleotides did not have a signal peptide (Fig. 11). This fluorescence was not due to Hoechst 33258 dye since the fluorescence of the Hoechst dye was not detectable through the light filter used for fluorescein (Fig. 10 B). Similar results were obtained from the experiments carried out with

tetramethylrhodamine isothiocyanate-labeled oligonucleotide (R-DNA, Fig. 12). The fluorescence of the nuclei became more intense as the incubation time increased (see 120 min incubation in Fig. 12). In order to determine whether the time-dependent nuclear accumulation of oligonucleotides was related to the activity of protein uptake by the reconstituted nuclei, we carried out an uptake experiment (fig. 13) with both fluorescein labeled BSA-peptide 1 conjugates [F-(B-P1)] and TRITC-labeled oligonucleotides (R-DNA). The association of oligonucleotide with transport-competent nuclei was clearly shown after 90 and 120 min incubation. The rhodamine fluorescence was not due to fluorescein since the fluorescence of fluorescein labeled BSA-peptide 1 conjugates [F-(B-P1)] through the light filter for rhodamine emission was undetectable (third row of Fig. 13). The association of the oligonucleotides with the nuclei was also shown in the presence of unlabeled BSA-peptide 1 conjugate (fourth row of Fig. 13). These data suggest that the association of oligonucleotides with the reconstituted nuclei is related to active protein uptake by the nuclei. It might be possible that transport-competent nuclei could actively accumulate proteins to which the oligonucleotides bind after diffusion into the nuclei via the nuclear pore complex. If the oligonucleotides could not diffuse into the nuclei, they could bind to the nuclear proteins in the incubation media and later are transported into the reconstituted nuclei along with the proteins. In order to define further the mechanism of nuclear association of oligonucleotides, we carried out a time-differential dual label experiment (Fig. 14). Reconstituted nuclei were incubated with fluorescein-labeled BSA-peptide 1 conjugate [F-(B-P1)] for 60 min in order to discern transport-competent nuclei. At the end of incubation, the reconstituted nuclei were chilled on ice for 20 min to stop the transport process. After this, the medium containing reconstituted nuclei was divided into two

fractions. One was incubated on ice for 5 min and the other was incubated at room temperature for 5 min. At the end of this incubation, TRITC-labeled oligonucleotides (R-DNA) or tetramethylrhodamine labeled BSA-peptide 1 conjugate (R-(B-P1)) were added to each fraction and the fluorescence associated with the nuclei was observed. Our data showed that the association of oligonucleotides with transport-competent nuclei occurred immediately at both room temperature and 0 °C (pictures in the 1st and 2nd row in Fig. 14). The rhodamine fluorescence was not due to the background fluorescence of fluorescein (Pictures in the 3rd row of Fig. 14). The rhodamine fluorescence of tetramethylrhodamine labeled BSA-peptide 1 conjugate [R-(B-P2)] was not observed immediately after addition to the nuclei which had accumulated fluorescein-labeled BSA-peptide 1 conjugate [F-(B-P1)] (pictures in the 4th row of Fig. 14). However, the rhodamine fluorescence of tetramethylrhodamine labeled BSA-peptide 1 conjugate [R-(B-P2)] was detectable after further incubation for 90 min. It was not clear whether BSA-peptide 1 conjugates accumulated in the reconstituted nuclei enhanced the accumulation of the oligonucleotides slightly. However, it was clear that the nuclear accumulation of the oligonucleotides was not entirely due to BSA-peptide 1 conjugates since the association of oligonucleotides with nucleotides was observed in experiments performed without BSA-peptide 1 conjugates (Figs. 11 and 12). These results showed that small oligonucleotides freely diffused into the reconstituted nuclei and stayed inside the nuclei whereas large proteins were only slowly transported to the nuclei via a process requiring a nuclear localization signal peptide.

**Effect of the nuclear localization signal peptide on the nuclear accumulation of oligonucleotides** As shown in Fig. 15, the nuclear localization signal peptide did not change the nuclear accumulation of oligonucleotides

significantly. At similar concentrations of oligonucleotide, the accumulation of oligonucleotides (F-DNA) was comparable to that of fluorescein labeled peptide (peptide 2)-conjugated oligonucleotide [(F-P2)-DNA]. The activity of the FITC-labeled nuclear localization signal peptide (peptide 2) was compared to that of FITC peptide 1 in Fig. 16. According to our observations, for similar sized nuclei, the fluorescence intensity of nuclei which were incubated with fluorescein-labeled BSA-peptide 1 conjugate [F-(B-P1)] for 30 min was comparable to that of nuclei which were incubated in the presence of BSA conjugated to FITC-peptide 2 [(F-P2)-B]. The number of fluoresceins on one molecule of BSA-peptide 1 conjugate [F-(B-P1)] was about 5 (see Table 1) whereas that for BSA conjugated to FITC-peptide 2 [(F-P2)-B] was about 10. Therefore, two nuclei with similar size and similar fluorescence intensity accumulated the two protein conjugates, i.e., BSA-peptide 1 conjugate [F-(B-P1)] and BSA conjugated to FITC-peptide 2 [(F-P2)-B] with a concentration ratio of 2:1. In other words, the concentration of BSA-peptide 1 conjugate (F-(B-P1)) in a nucleus after 30 min incubation was twice as high as the concentration of BSA conjugated to FITC-peptide 2 [(F-P2)-B] in a nucleus with similar size. Therefore, the ratio of rate of accumulation of BSA-peptide 1 conjugate [F-(B-P1)] to that of BSA conjugated to FITC-peptide 2 [(F-P2)-B] in nuclei of comparable size was approximately  $(2/30)/(1/160) \approx 10$  assuming that the uptake of the proteins into the nuclei linearly increased during the measurement. Considering the fact that the initial concentration of BSA-peptide 1 conjugate [F-(B-P1)] was about one half of the concentration of BSA conjugated to FITC-peptide 2 [(F-P2)-B], the ratio of rate of accumulation of BSA-peptide 1 conjugate [F-(B-P1)] to that of BSA conjugated to FITC-peptide 2 [(F-P2)-B] was approximately 20. The number of signal peptides per BSA-peptide 1 conjugate [F-(B-P1)] was about 14 and the number of signal peptides per BSA

conjugated to FITC-peptide 2 [(F-P2)-B] was about 10. Taking all these results into consideration, it can be concluded that the nuclear localization activity of FITC-labeled peptide 2 was significantly reduced compared to peptide 1 (approximately  $(1/20) \times (14/10) \approx 1/14$  assuming that the rate of uptake of BSA is directly proportional to the number of conjugated signal peptides). The bulky fluorescein appears to interfere with the binding of the signal peptide to its receptor. However, the activity was not completely abolished. This residual activity of fluorescein labeled nuclear localization signal peptide (F-peptide 2) was still able to confer the translocation of large BSA molecules into the nuclei. However, the accumulation of oligonucleotide was not affected much by the conjugation of the signal peptide (F-peptide 2). This could be partly due to the small size of the oligonucleotide-peptide conjugates. If the oligonucleotide-peptide conjugate is considered as an elongated rod, its diameter may be much smaller than the functional diameter of the pore of the nuclear pore complex.

**Summary of results** Our experimental data were summarized in Table. 2. Our experimental data confirmed the previous observation that large protein molecules require nuclear localization signal peptides for nuclear transport whereas small molecules freely diffuse into the nuclei.

## DISCUSSION

Our experimental data suggested that oligonucleotides can freely diffuse into the reconstituted nuclei through the nuclear pore complex and that the oligonucleotides can accumulate in the nuclei by binding to presently unknown nuclear factors. These binding sites could be any DNA binding proteins in the nuclei. This interpretation is consistent with the findings by Leonetti et al. (30). They microinjected antisense oligonucleotides (15-mers) conjugated with fluorescein isothiocyanate or tetramethylrhodamine isothiocyanate into the cytoplasm of rat embryo fibroblast cells (REF-52). They observed that the fluorescently tagged oligonucleotides were translocated and concentrated in the nuclei within one minute after microinjection. Using photoaffinity labeling and polyacryl amide gel-electrophoresis, they also showed that primarily four nuclear proteins with molecular weights ranging from 36 kD to 50 kD were cross-linked to photosensitive radioactively labeled oligonucleotides (bromouridine containing oligonucleotide).

We do not know the distribution of the oligonucleotides in the nucleus in detail in our system. We used reconstituted nuclei for transport experiments and we do not know clearly whether in these nuclei intranuclear organelles such as nucleoli were reconstituted faithfully. We usually observed that the oligonucleotides were distributed evenly in the reconstituted nuclei. Since the nucleolus does not have a membrane (40), the targeting of oligonucleotides to the nucleolus might be possible. Then, blocking of RNA processing in the nucleolus as well as in the transcription of genes from genomic DNA might be possible using ther oligonucleotides, which would result in inhibition of cellular activity (41).

Our data showed that nuclear localization by the signal peptide does not enhance the accumulation of oligonucleotides in the nuclei significantly. This could be due to the reduced activity of the signal peptide or due to the small size of the conjugate. Further studies will be necessary to resolve this question unequivocally. Originally, we intended to use the signal peptide to target oligonucleotides to cell nuclei. Our results suggest that this might not be necessary since oligonucleotides alone can diffuse into and accumulate in the nuclei. In summary, oligonucleotides could exert their therapeutic activity both in the cytoplasm and in the cellular nucleus once delivered into the cell cytoplasm by the methods mentioned above (3-7) since oligonucleotides can freely diffuse into the nucleus through nuclear pore complexes.



## IMPLICATIONS AND FUTURE RESEARCH

In this study we showed that short oligonucleotides can freely diffuse into the nuclei reconstituted from *Xenopus* egg extracts and *Xenopus* sperm nuclei. It has been reported that the diameter of the nuclear pore complex varies slightly from species to species. By determining the size of proteins, dextrans, or gold particles that can enter the nucleus when injected into the cytoplasm, the apparent pore diameter has been estimated to be 90 Å for *Xenopus* oocytes and *Drosophila* salivary gland nuclei, 100-110-Å for hepatocytes and hepatoma cells and 120 Å for amoebae (9). Judging from the diameters of the nuclear pores from these organisms, it is likely that small oligonucleotides freely diffuse into the nuclei of other types of cells as well as the *Xenopus* reconstituted nuclei.

We used oligonucleotides with only 20 nucleotides. It would be interesting to determine the limit of size of DNAs that can diffuse into nuclei. It would be interesting to determine whether large DNA molecules such as bacterial plasmids can diffuse into the cell nuclei. If it turns out that large bacterial plasmids can not diffuse into cell nuclei freely, it would imply that plasmid DNA molecules gain access to genomic DNA in a cell cycle-dependent manner. It is possible that large exogenous DNA molecules are enclosed in cell nuclei when the nuclear membranes disassemble and reassemble during cell division (31).

Recently, Kaneda et al. (42) reported that when the plasmid DNA and nuclear protein of rat cells were encapsulated in vesicle complexes (DNA-loaded phospholipid vesicles with gangliosides were fused with Sendai virus and the resulting fusion products were fused with red blood cell ghosts.), and cointroduced into nondividing cells in rat liver by injection into the portal vein of adult rats, the plasmid DNA was carried into the liver cell nuclei efficiently by the nuclear protein. Wienhues et al. (43) reported that reconstituted DNA with



the major core protein VII of adenovirus type 2 or protamine from salmon sperm was rapidly transported into the cell nuclei. These examples showed that large DNA molecules can be carried into cell nuclei using the mechanism of nuclear protein import. Although short oligonucleotides did not require any signal peptide for nuclear accumulation, large DNA molecules or other therapeutic molecules could be targeted into cell nucleus using nuclear localization signal peptides in combination with appropriate methods for intracellular administration as described in the Introduction section.

## ACKNOWLEDGMENTS

This research was supported by the grants from Monsanto Co., Inc., Army Research Office, Caltech Chemistry Consortium and Vestar, Inc. We thank Prof. William Dunphy and Dr. Akiko Kumagai for thier help in reconstitution of the cell nuclei. We thank Drs. John Evans and Karen Shannon for their help in peptide modification on solid-support. We also thank Dr. Wilton Vannier for his helpful discussions.

## REFERENCES

1. (a) Crooke, S. T. (1993) *FASEB J.* **7**, 533-539 (b) Carter, G. and Lemoine, N. R. (1993) *Br. J. Cancer* **67**, 869-876 (c) Stein, C. A. and Cohen, J. S. (1988) *Cancer Res.* **48**, 2659-2668
2. Loke, S. L., Stein, C. A., Zhang, X. H., Mori, K., Nakanishi, M., Subasinghe, C., Cohen, J. S. and Neckers, L. M. (1989) *Proc. Natl. Acad. Sci. USA* **86**, 3474-3478
3. Lemaitre, M., Bayard, B. and Lebleu, B. (1987) *Proc. Natl. Acad. Sci. USA* **84**, 648-652
4. Letsinger, R. L., Zhang, G., Sun, D. K., Ikeuchi, T. and Sarin, P. S. (1989) *Proc. Natl. Acad. Sci. USA* **86**, 6553-6556
5. Shea, R. G., Masters, J. C. and Bischofberger, N. (1990) *Nuc. Acid. Res.* **18**, 3777-3783
6. Hug, P. and Sleight, R. G. (1991) *Biochim. Biophys. Acta* **1097**, 1-17
7. Bennet, C. F., Chiang, M. -Y., Chan, H., Shoemaker, C. J. E. and Mirabelli, C. K. (1992) *Molecular Pharmacology* **41**, 1023-1033
8. Dingwall, C. and Laskey, R. A. (1986) *Ann. Rev. Cell Biol.* **2**, 367-390
9. Newport, J. W. and Forbes, D. J. (1987) *Ann. Rev. Biochem.* **56**, 535-565
10. Gerace, L. and Burke, B. (1988) *Ann. Rev. Cell Biol.* **4**, 335-374
11. Nigg, E. A., Baeuerle, P. A. and Lührmann, R. (1991) *Cell* **66**, 15-22
12. Silver, P. A. (1991) *Cell* **64**, 489-497
13. Garcia-Bustos, J., Heitman, J. and Hall, M. N. (1991) *Biochim. Biophys. Acta* **1071**, 83-101
14. Stochaj, U. and Silver, P. (1992) *Eur. J. Cell Biol.* **59**, 1-11
15. Newmeyer, D. D., Lucocq, J. M., Bürglin, T. R. and De Robertis, E. M. (1986) *EMBO J.* **5**, 501-510

16. Newmyer, D. D. and Forbes, D. J. (1988) *Cell* **52**, 641-653
17. Richardson, W. D., Mills, A. D., Dilworth, S. M., Laskey, R. A. and Dingwall, C. (1988) *Cell* **52**, 655-664
18. Akey, C. W. and Goldfarb, D. S. (1989) *J. Cell Biol.* **109**, 971-982
19. Li, R. and Thomas, J. O. (1989) *J. Cell Biol.* **109**, 2623-2632
20. Adam, S. A., Lobl, T. J., Mitchell, M. A. and Gerace, L. (1989) *Nature* **337**, 276-279
21. Dingwall, C., Sharnick, S. V. and Laskey, R. A. (1982) *Cell* **30**, 449-458
22. Sugawa, H., Imamoto, N., Wataya-Kaneda, M., Uchida, T. (1985) *Exp. Cell Res.* **159**, 419-429
23. Peters, R., Lang, I., Scholz, M., Scholz, B. and Kayne, F. (1986) *Biochem. Soc. Trans. London.* **14**, 821-822
24. Bonner, W. M. (1975) *J. Cell Biol.* **64**, 431-437
25. Kalderon, D., Richardson, D. A., Markham, A. F. and Smith, A. E. (1984) *Nature* **311**, 33-38
26. Lanford, R. E. and Butel, J. S. (1984) *Cell* **37**, 801-813
27. Kalderon, D., Roberts, B. L., Richardson, W. D. and Smith, A. E. (1984) *Cell* **39**, 499-509
28. Lanford, R. E., Kanda, P. and Kennedy, R. C. (1986) *Cell* **46**, 575-582
29. Goldfarb, D. S., Gariépy, J., Schoolnik, G. and Kornberg, R. (1986) *Nature* **322**, 641-644
30. Leonetti, J. P., Mechti, N., Degols, G., Gagnor, C. and Lebleu, B. (1991) *Proc. Natl. Acad. Sci. USA* **88**, 2702-2706
31. Alberts, B., Bray, D., Lewis, J., Raff, M., Roberts, K. and Watson, J. D. (1983) *Molecular Biology of the Cell* (Garland Publishing, Inc., New York & London) pp. 611-671

32. Murray, A. W., Solomon, M. J. and Kirschner, M. W. (1989) *Nature* **339**, 280-286
33. Serge, L. B. and Iyer, R. P. (1992) *Tetrahedron* **48**, 2223-2311
34. Gait, M. J. (1984) *Oligonucleotide Synthesis; A Practical Approach* (IRL press, Oxford, Washington DC)
35. Merrifield, B. (1986) *Science* **232**, 341-347
36. Halleck, M. S. and Rechsteiner, M. (1990) *Proc. Natl. Acad. Sci. USA* **87**, 7551-7554
37. Maniatis, T., Fritsch, E. F. and Sambrook, J. (1982) *Molecular Cloning: A Laboratory Manual* (Cold Spring Harbor Laboratory) pp. 184-185
38. Gourdon, J. B. (1976) *J. Embryol. exp. Morph.* **36**, 523-540
39. Lobl, T. J., Mitchell, M. A. and Maggiora, L. L. (1990) *Biopolymers* **29**, 197-203
40. Alberts, B., Bray, D., Lewis, J., Raff, M., Roberts, K. and Watson, J. D. (1983) *Molecular Biology of the Cell* (Garland Publishing, Inc., New York & London) pp 424-427
41. Orson, F. M., Thomas, D. W., McShan, W. M., Kessler, D.J. and Hogan, M. E. (1991) *Nuc. Acid. Res.* **19**, 3435-3441
42. Kaneda, Y., Iwai, K. and Uchida, T. (1989) *Science* **243**, 375-378.
43. Wienhues, U., Hosokawa, K., Höveler, A., Sigman, B. and Doerfeler, W. (1987) *DNA* **6**, 87-89.

**Table 1. Summary of chemical formulae and concentrations of stock solutions used in the experiments**

Sample stock	Concentration $\mu\text{g}/\mu\text{l}$	$\mu\text{M}$	Chemical formula	Rel. Ab at 494 nm
1x B-P1	1.93	29.1	$(\text{P1})_{13.8}\text{BSA}$	-
1x F-P1	$0.269 \pm 0.005$	192.90	$\text{F}_{0.23}\text{P1}$	2.25
1x F-BSA	$0.427 \pm 0.013$	6.44	$\text{F}_{3.4}\text{BSA}$	1.13
0.1x F-(B-P1)	$0.318 \pm 0.006$	3.73	$\text{F}_{5.3}(\text{P1})_{13.8}\text{BSA}$	1.00
0.1x R-(B-P1)	$0.202 \pm 0.006$	2.37	$\text{R}_x(\text{P1})_{13.8}\text{BSA}$	-
1x (F-P2)-B	$0.710 \pm 0.001$	8.43	$(\text{F-P2})_{9.5}\text{BSA}$	4.06
1x F-DNA	3.96	594	$\text{F}_{0.42}\text{DNA}$	12.92
1x R-DNA	1.67	248	$\text{R}_x\text{DNA}$	-
1x (F-P2)DNA	2.62	312	$(\text{F-P2})_1\text{DNA}$	-

Abbreviations:

B; BSA

F; fluorescein isothiocyanate (FITC)

R; tetramethylrhodamine isothiocyanate (TRITC)

P1; peptide with the sequence of PKKKRKVEDYC(N to C terminal)

P2; peptide with the sequence of KPKKRKVEDYC(N to C terminal)

F-P2; P2 labeled with fluorescein at the  $\epsilon$ -amine of the N-terminal lysine

B-P1; Bovine serum albumin labeled with P1

(F-P2)-B; Bovine serum albumin labeled with F-P2

DNA; DNA with an aminohexyl linker at 5'-end

F- or R-DNA; DNA labeled with FITC or TRITC

x; unknown

**Table. 2. Summary of transport assay**

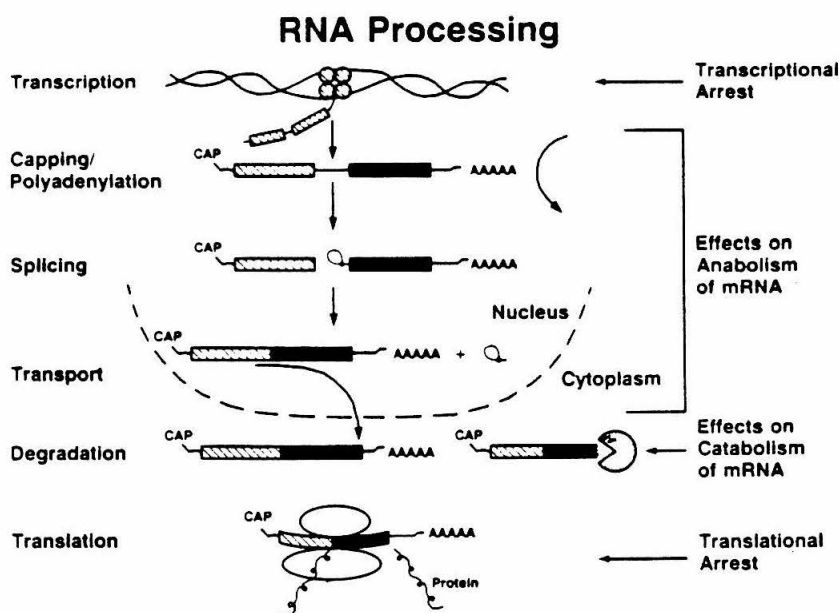
Sample	Transport at		Mechanism of nuclear accumulation
	25 °C	0 °C	
Peptide1	-	-	
BSA	-	-	
BSA-Peptide1	+	-	active transport
(F-P2)-BSA	+	-	active transport
DNA	+	+	free diffusion and binding
(F-P2)-DNA	+	+	probably free diffusion

\* Reconstituted nuclei active for BSA-Peptide1 conjugate were always positive for DNA accumulation. Nuclei inactive for BSA-Peptide 1 conjugate were either positive or negative for DNA accumulation. +, observed; -, not observed

**Fig. 1. (A) Schematic diagram of potential sites of antisense oligonucleotide action**

RNA processing and the potential actions of oligonucleotides are shown.

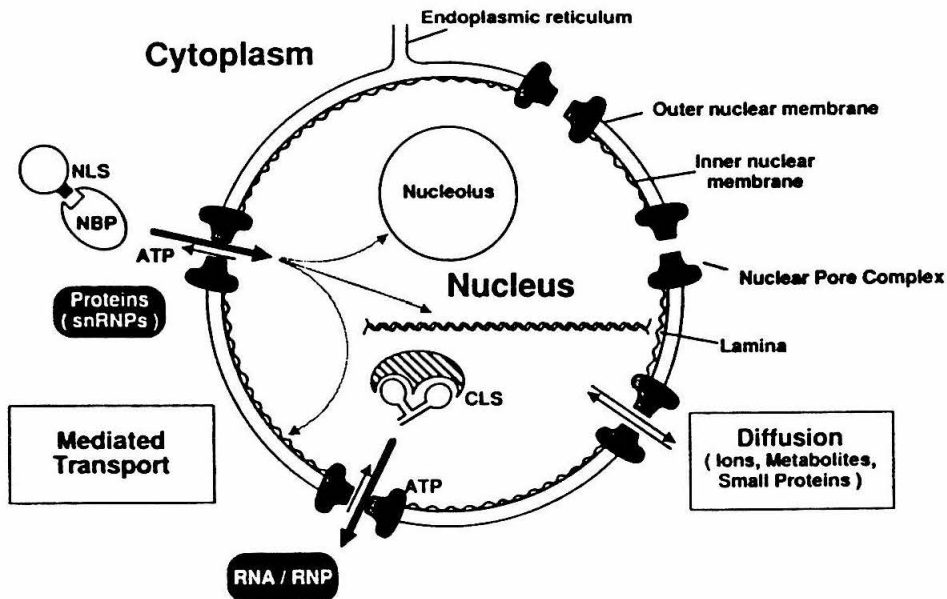
Adapted from Crooke, S. T. (*Faseb J.* 7, 533-539, 1993)





**Fig. 1. (B) Nuclear import and export**

NLS, nuclear localization signal peptide; NBP, NLS-binding protein; CLS, cytoplasmic localization signal; RNP, ribonuclear proteins; snRNP, small nuclear RNP. This was adapted from Nigg et al. (*Cell* 66, 15-22, 1991).



**Fig. 1. (C) Models for protein import into the nucleus**

NLS, nuclear localization signal peptide; NPC, nuclear pore complex. Adapted from Stochaj, U. et al. (*Eur. J. Cell Biol.* 59, 1-11, 1992)

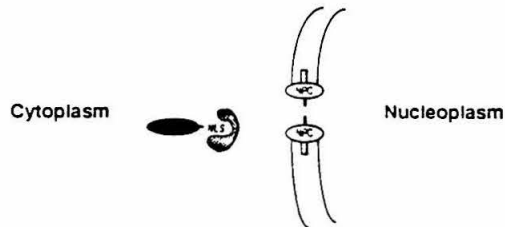
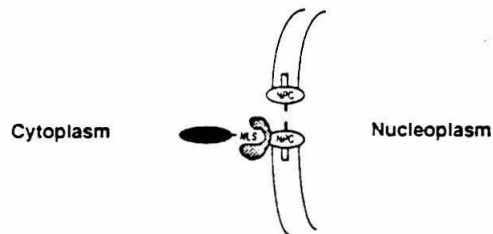
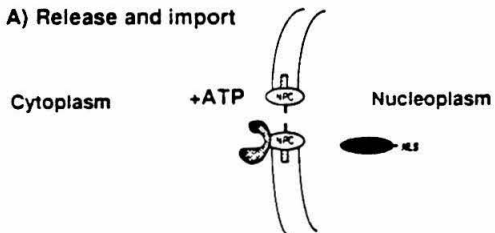
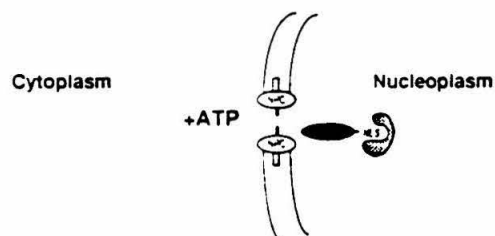
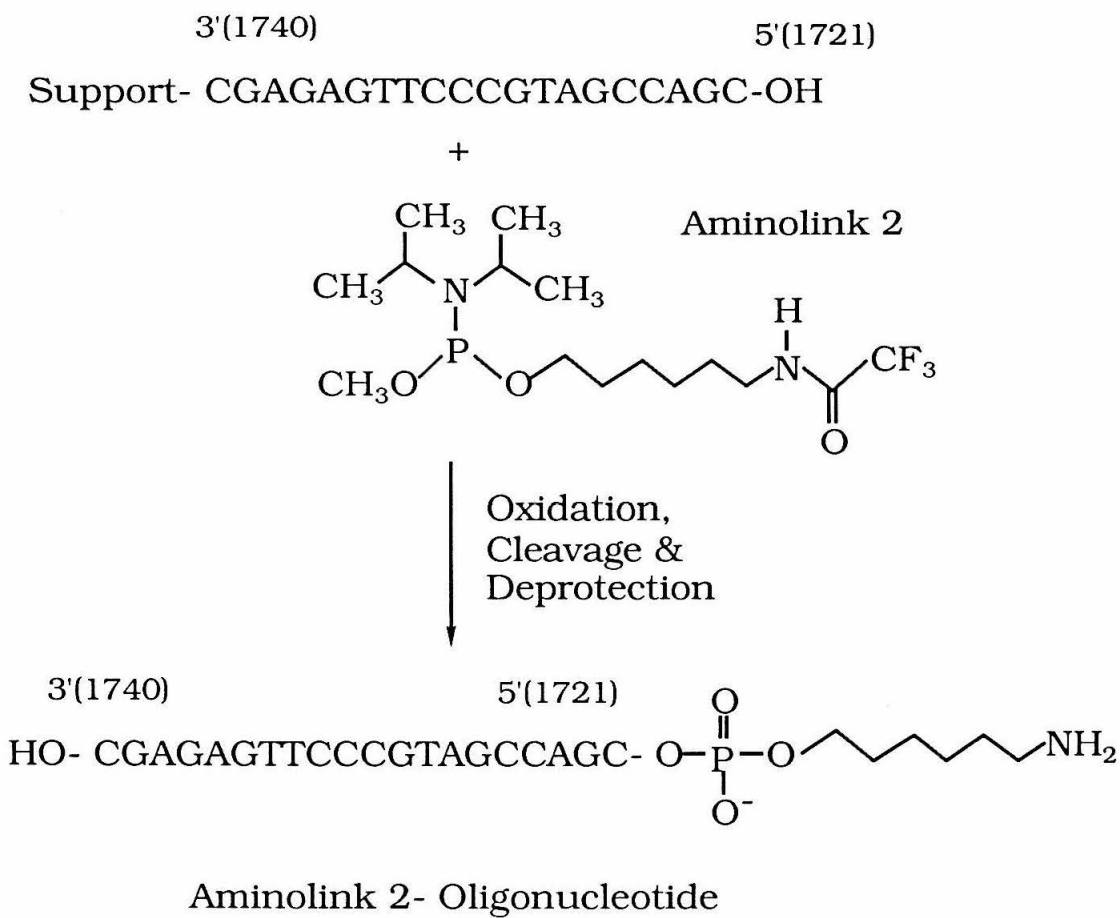
**1) Binding of nuclear proteins to NLS-receptors****2) Association with the nuclear pore complex****3) Translocation across the nuclear envelope****A) Release and import****B) Co-import of protein and receptor**

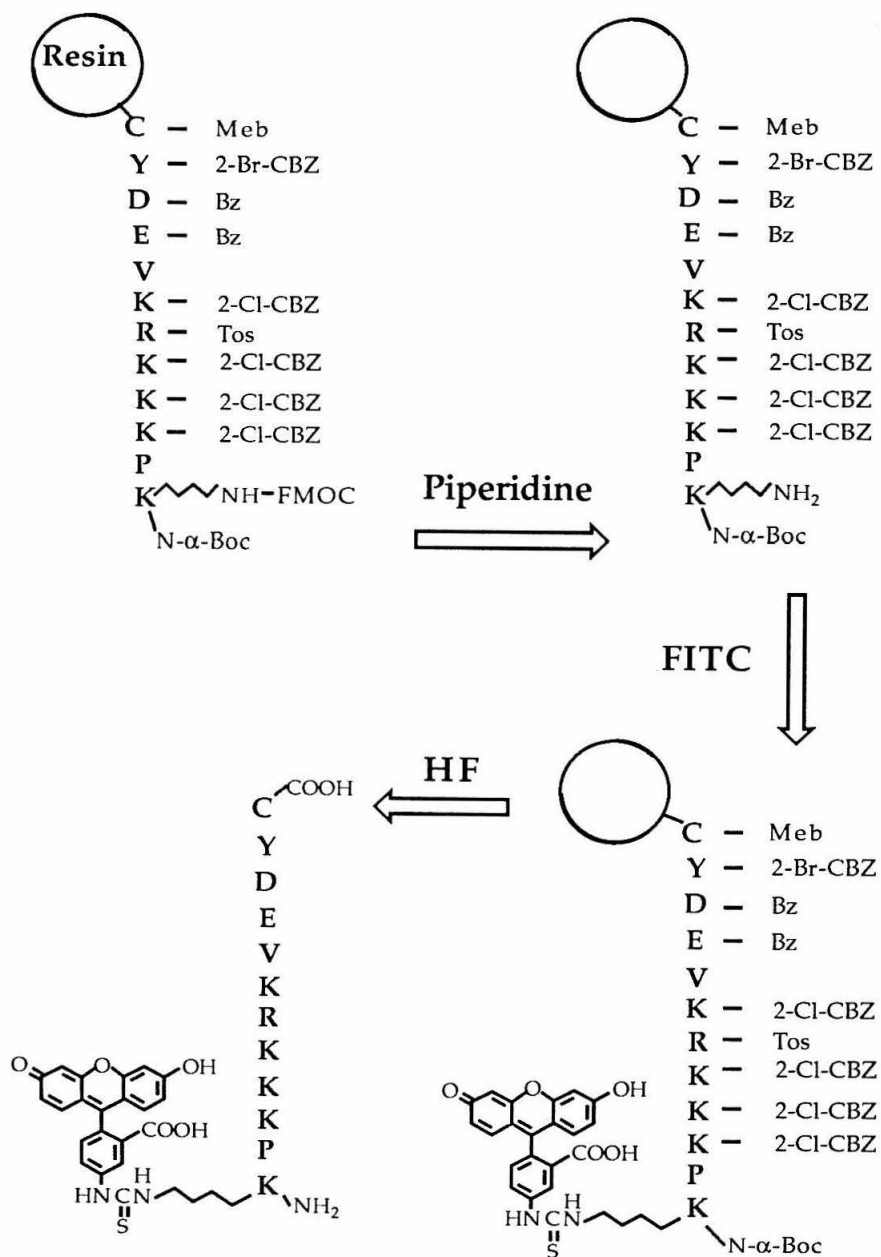
Fig. 2. Synthesis of aminohexyl containing oligonucleotide



**Fig. 3. Schematic diagram of the synthesis of FITC-labeled peptides**

Peptides were synthesized on solid-support. The protecting groups for the side chains are shown in abbreviations: Meb, *S*-4-methylbenzyl; 2-Br-CBZ, 2-bromobenzyloxycarbonyl; Bz, benzoyl; 2-Cl-CBZ, 2-chloro benzyloxycarbonyl; Tos, *p*-tolunesulfonyl; Fmoc, 9-fluorenylmethyloxycarbonyl; Boc, *t*-butyloxycarbonyl.

Fig. 3



**Fig. 4. Conjugation of nuclear localization signal peptide to BSA or oligonucleotide using a bifunctional cross-linking reagent, MBS**

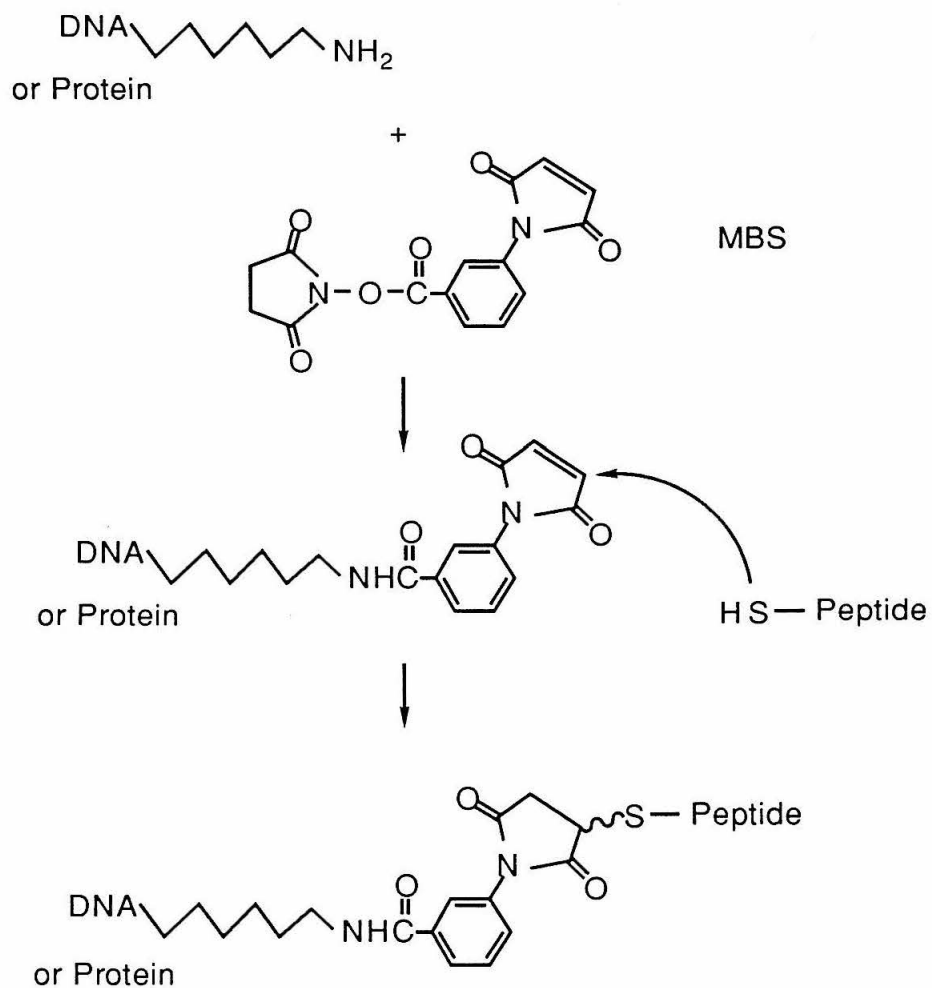


Fig. 5. Coupling of FITC to amine group

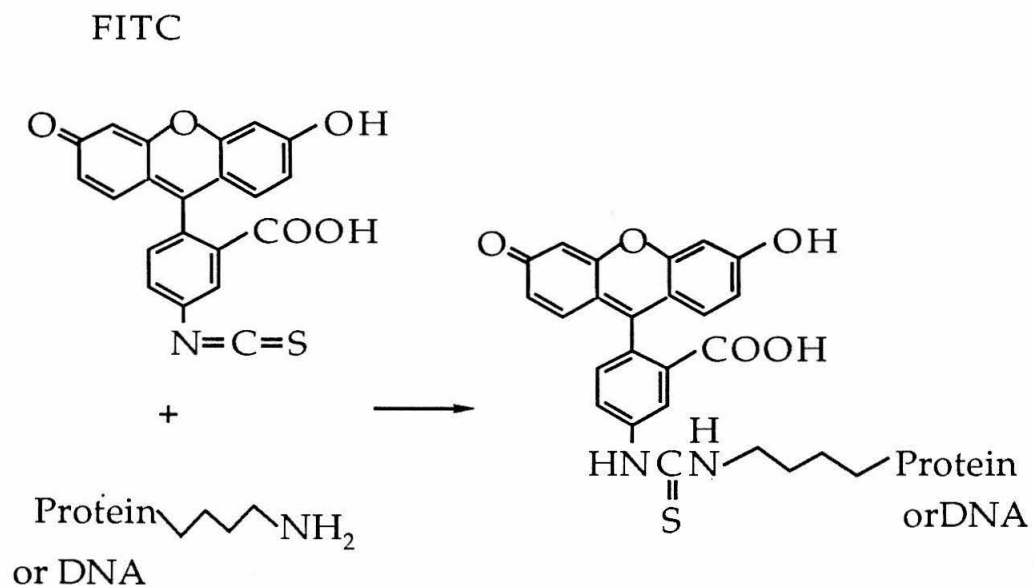
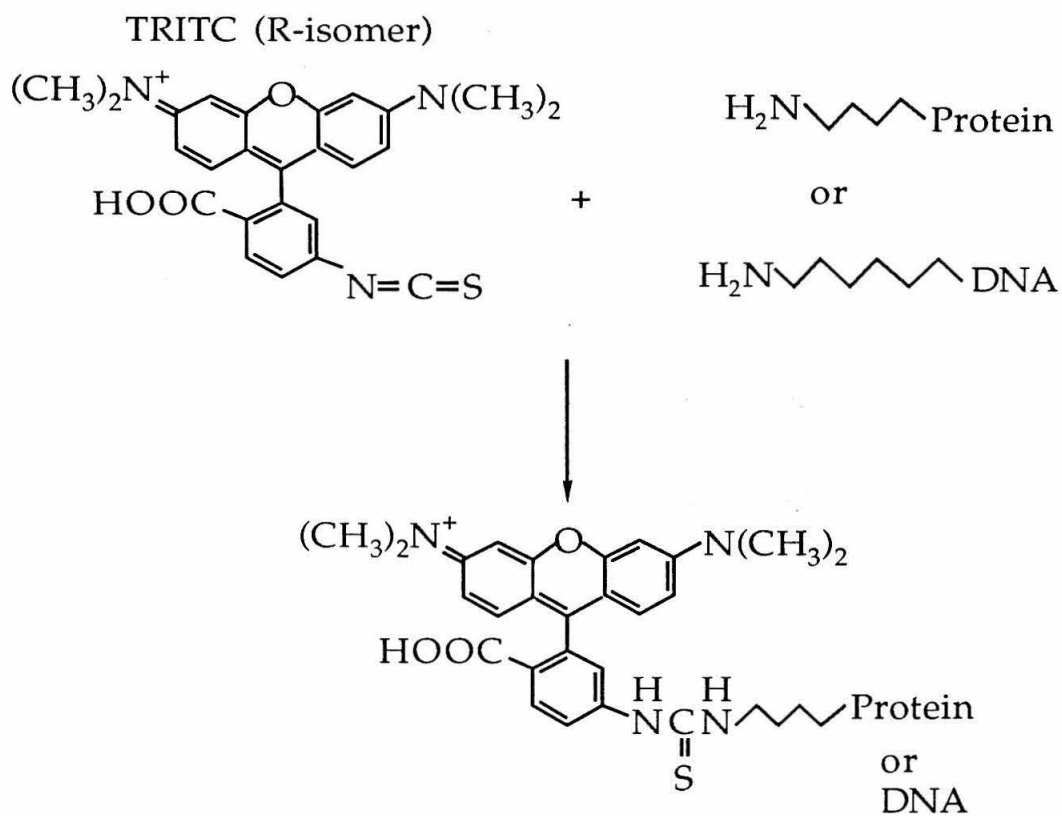


Fig. 6. Coupling of TRITC to amine group

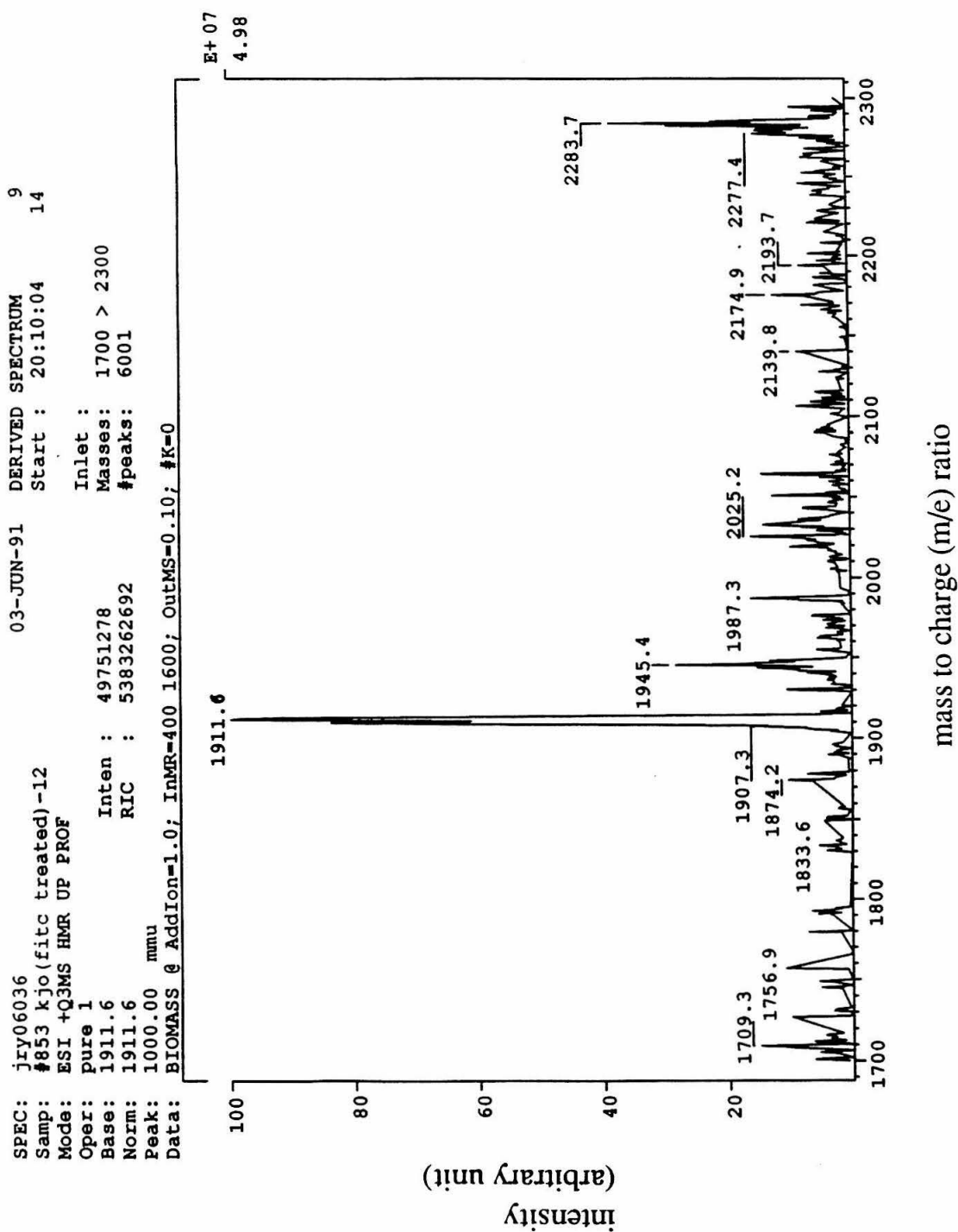




**Fig. 7** Mass spectrum of FITC-labeled peptide 2



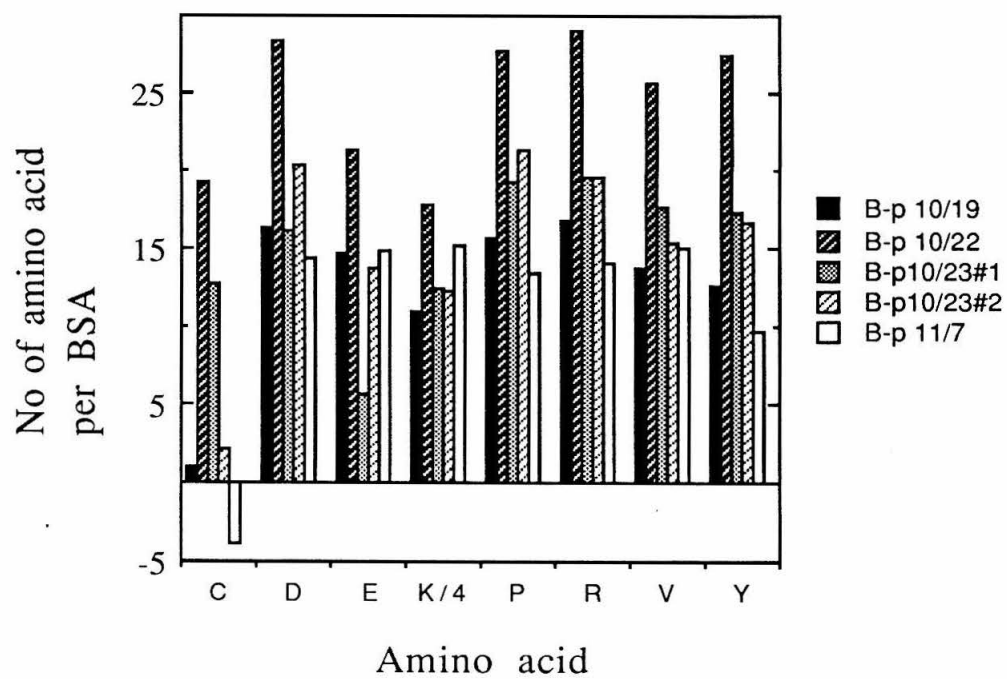
Fig. 7 Mass spectrum of FITC-labeled peptide 2

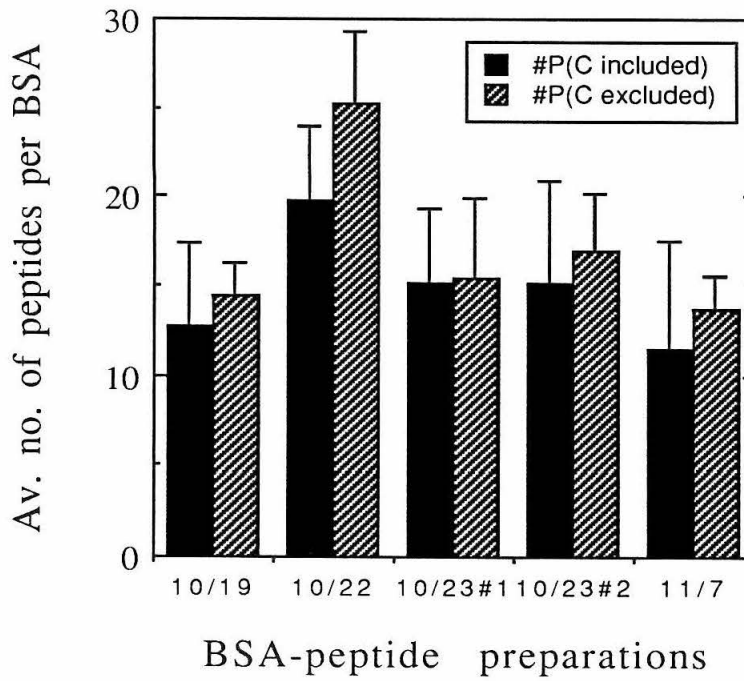


**Fig. 8. Amino acid analysis of peptide 1-conjugated BSA**

(A) Five different preparations of BSA-peptide 1 conjugates were analysed by amino acid analysis. The amino acid composition of BSA from amino acid analysis was used as standard. The differences between the number of amino acids of BSA-peptide 1 conjugates and that of control BSA were shown for the amino acids occurring in peptide 1. The number of lysines was divided by four to calculate the number of peptides which were conjugated to BSA (B) The average number of peptide 1 per BSA was calculated by averaging the number of amino acids for each preparation with or without cysteine residue. Error bars represent 95 % confidence limit.

Fig. 8 (A) Amino acid analysis

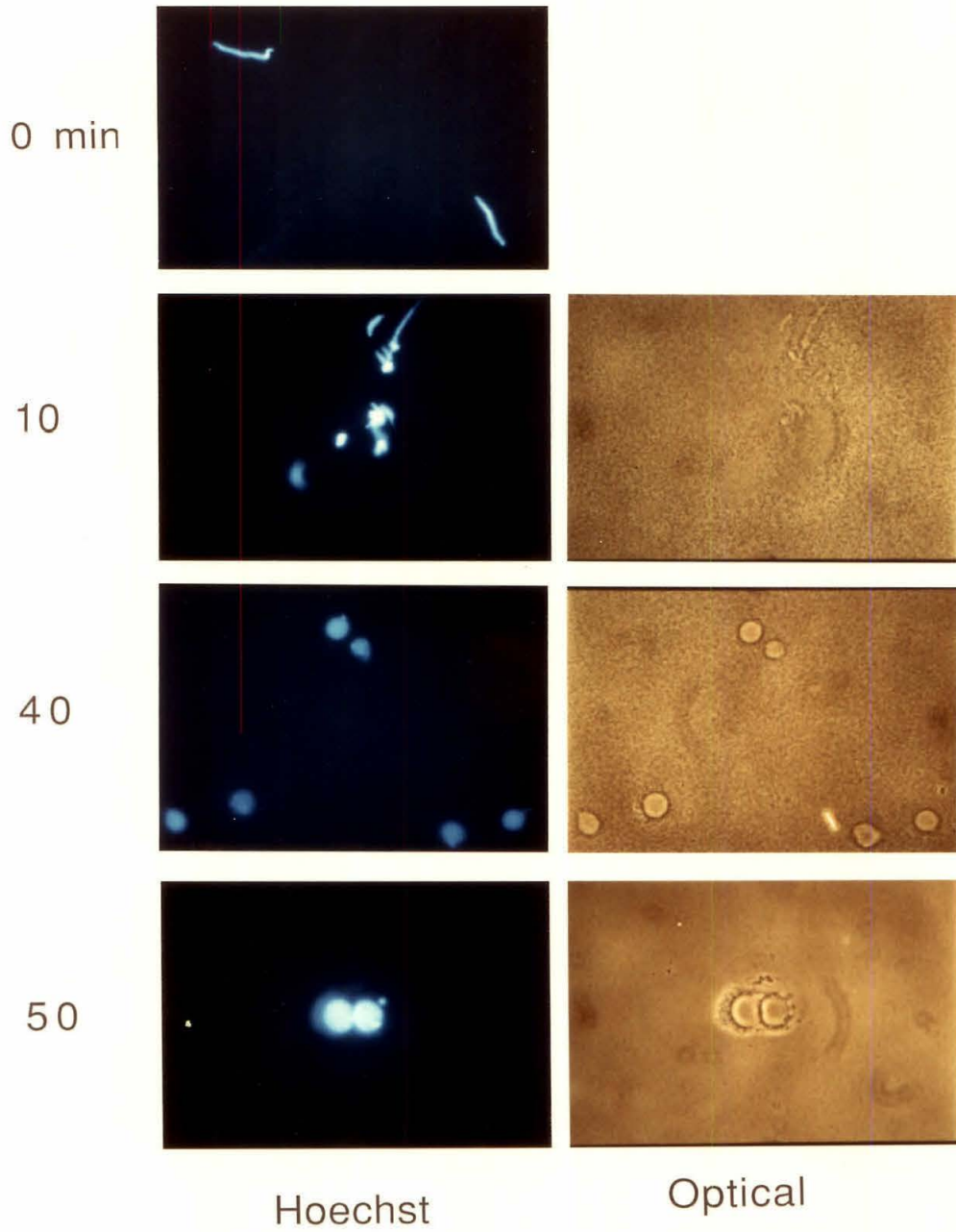


**Fig. 8 (B)** Average number of peptides per BSA

**Fig. 9. Reconstitution of nuclear membranes**

Nuclear membranes were reconstituted using *Xenopus* egg extracts and sperm DNA as described in the Appendix. D. Each pair of images consists of a fluorescent image of the DNA-binding dye, Hoechst 33258, on the left (Hoechst) and a phase contrast image on the right (Optical).

## Reconstitution of nuclei



**Fig. 10 Transport assay with FITC-labeled peptide 1, BSA and peptide1-conjugated BSA**

To 20  $\mu$ l of reconstituted nuclei, 2  $\mu$ l of the following FITC labeled proteins were added. The assay mixture was incubated at the indicated temperatures and observed at the indicated times as shown below using different light filters;

Sample	Temperature	Final concentration	
		$\mu$ g/ $\mu$ l	$\mu$ M
0.1x F-(BSA-Pep1)	0 °C	0.029	0.339
1x F-BSA	0 °C	0.039	0.585
1x F-peptide1	0 °C	0.024	17.5
0.1x F-(BSA-Pep1)	25 °C	0.029	0.339
1x F-BSA	25 °C	0.039	0.585
1x F-peptide1	25 °C	0.024	17.5

Fig. 10 A shows the results of the experiments with F-(BSA-peptide1) and Fig 10 B shows the results of the experiments with F-BSA and F-peptide1. Each pair of images consists of a fluorescent image of the DNA-binding dye, Hoechst 33258, on the left (Hoechst) and a fluorescent image of fluorescein on the right (Fluorescein).



Fig. 10 A

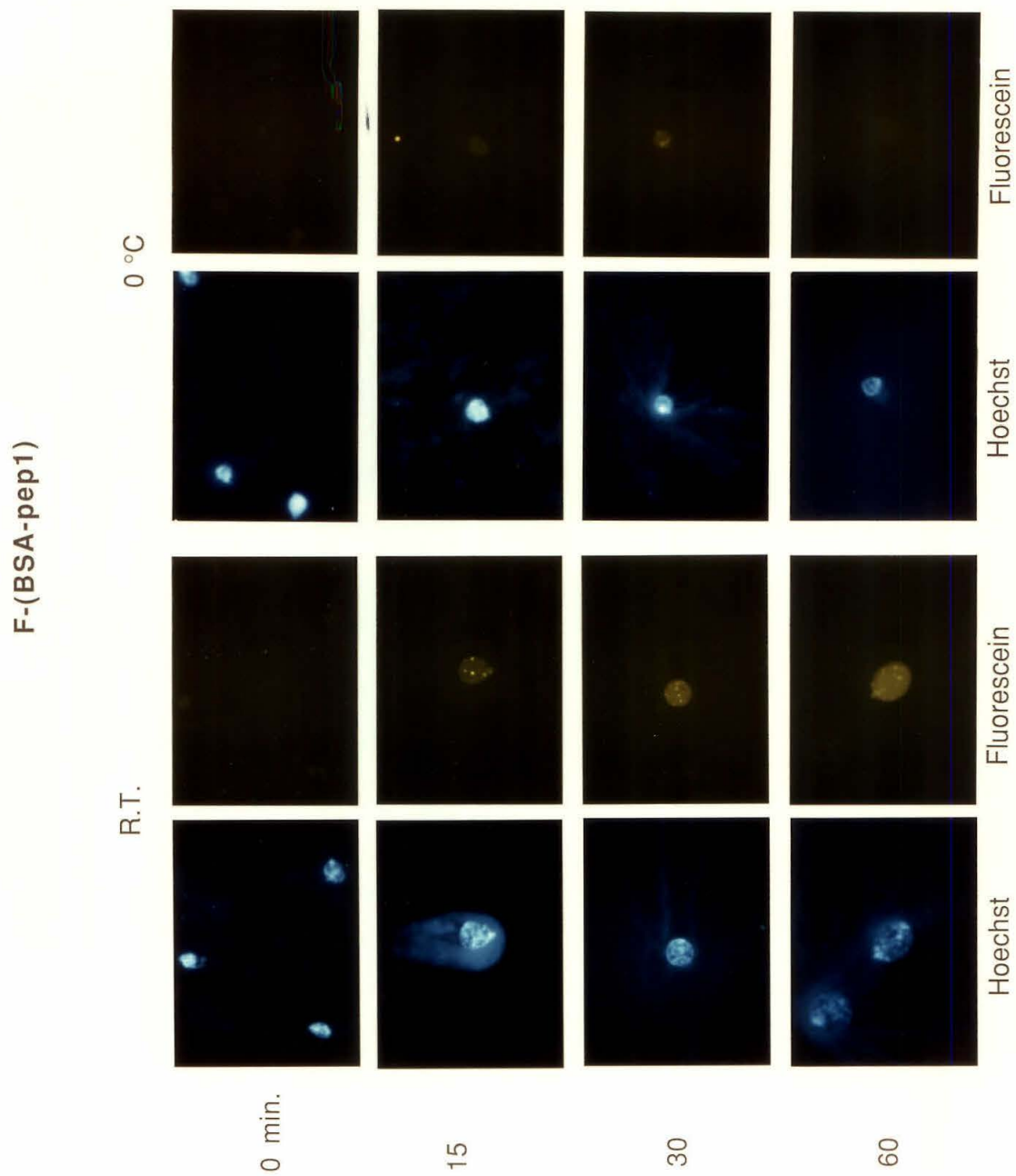
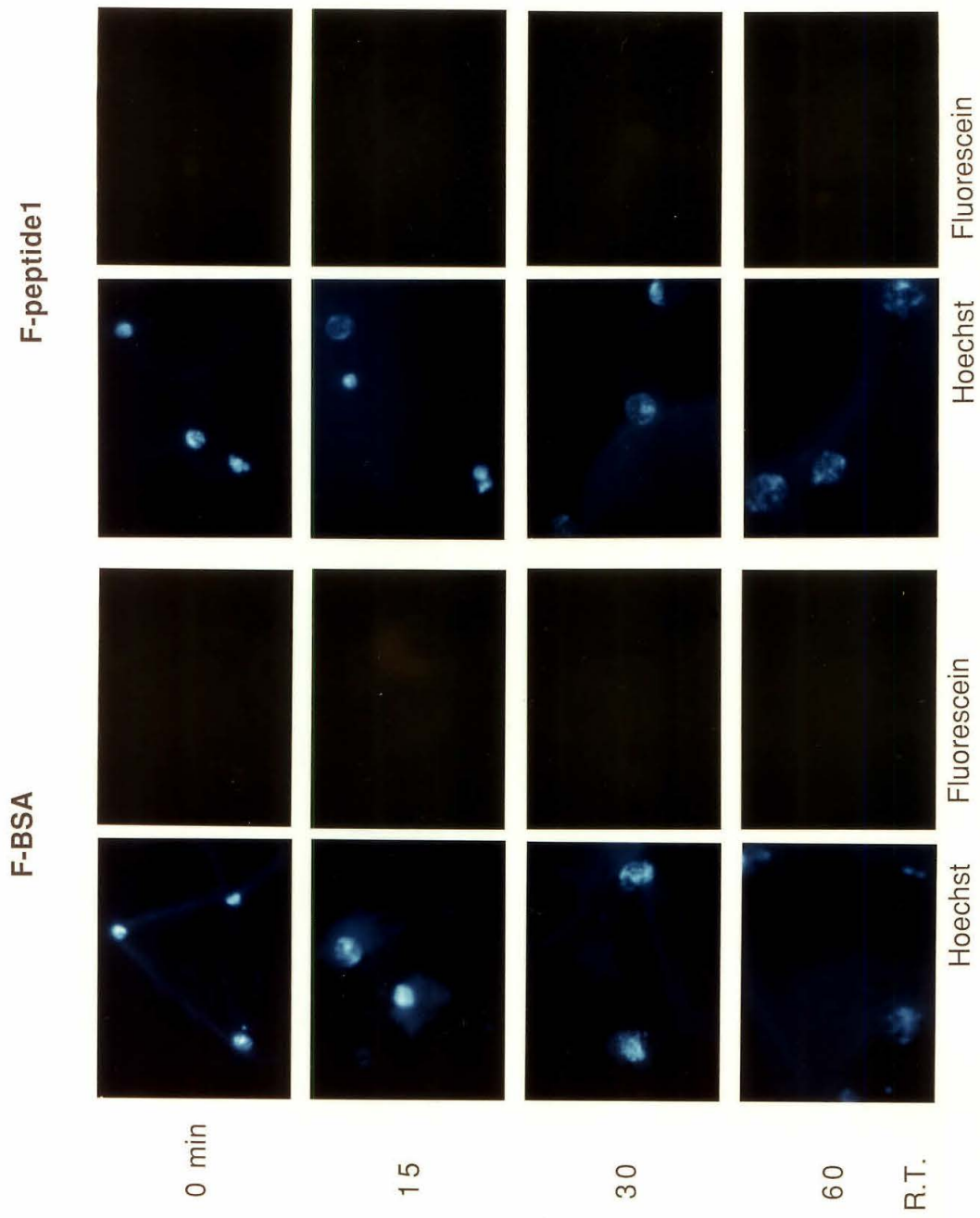


Fig. 10 B



### Fig. 11 Accumulation of FITC-labeled oligonucleotides in reconstituted nuclei

To 20  $\mu$ l of reconstituted nuclei, 2  $\mu$ l volumes of the following FITC labeled DNA were added and incubated at the indicated temperatures as shown below. In the experiments performed with 1x F-DNA, samples were observed at 0, 15, 30, and 60 min after the FITC-labeled oligonucleotide additions (Fig. 11 A). In the experiments performed with F-DNA diluted ten times (0.1x F-DNA), samples were observed at 0, 60 and 120 min after the FITC-labeled oligonucleotide addition using different filters under a fluorescence microscope (Fig. 11 B). Each pair of images consists of a fluorescent image of the DNA-binding dye, Hoechst 33258, on the left (Hoechst) and a fluorescent image of fluorescein on the right (Fluorescein).

Sample	Temperature	Final concentration	
		$\mu\text{g}/\mu\text{l}$	$\mu\text{M}$
1x F-DNA	0 °C	0.36	54.0
1x F-DNA	25 °C	0.36	54.0
0.1x F-DNA	0 °C	0.036	5.4
0.1x F-DNA	25 °C	0.036	5.4

Fig. 11 A

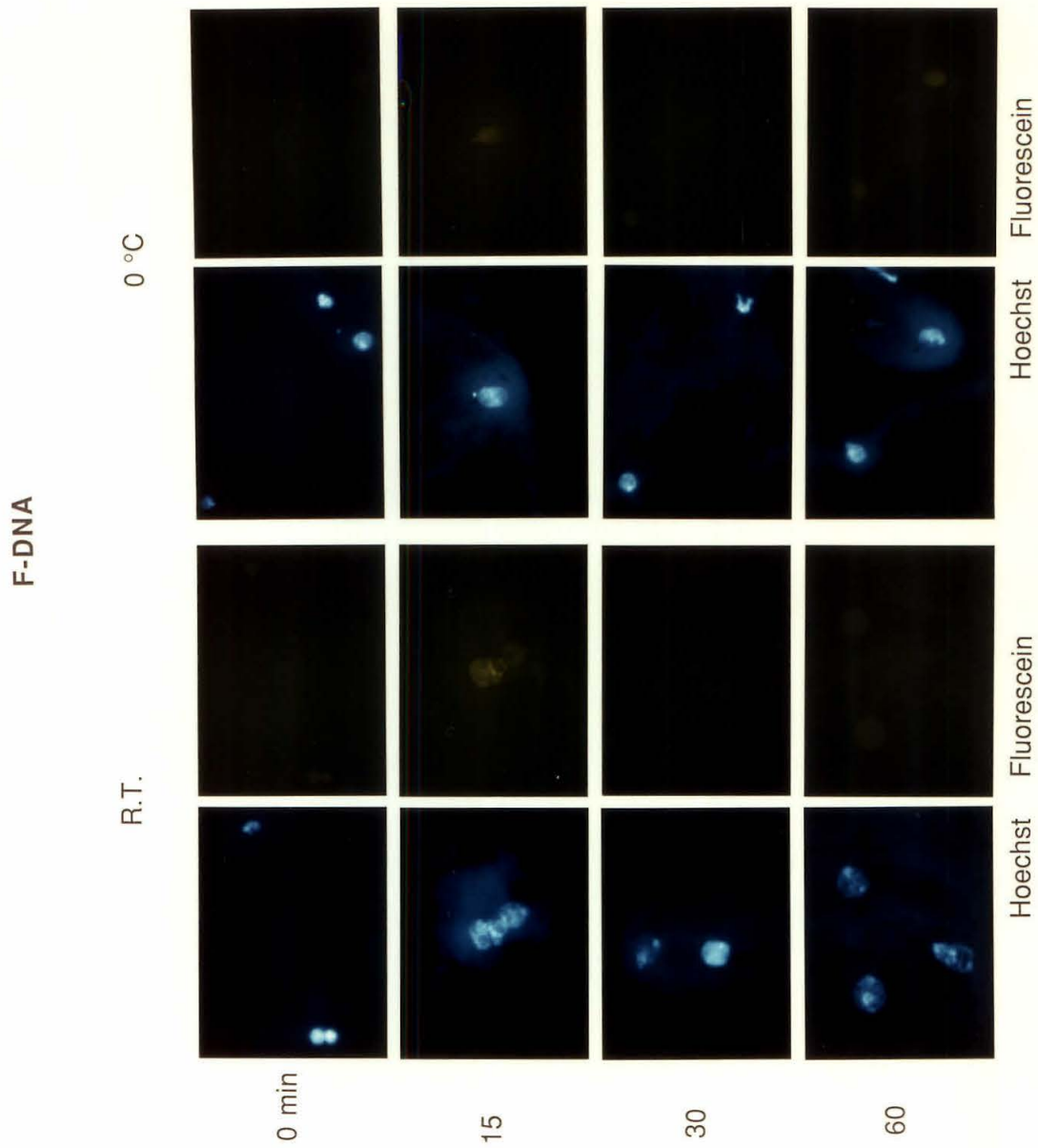
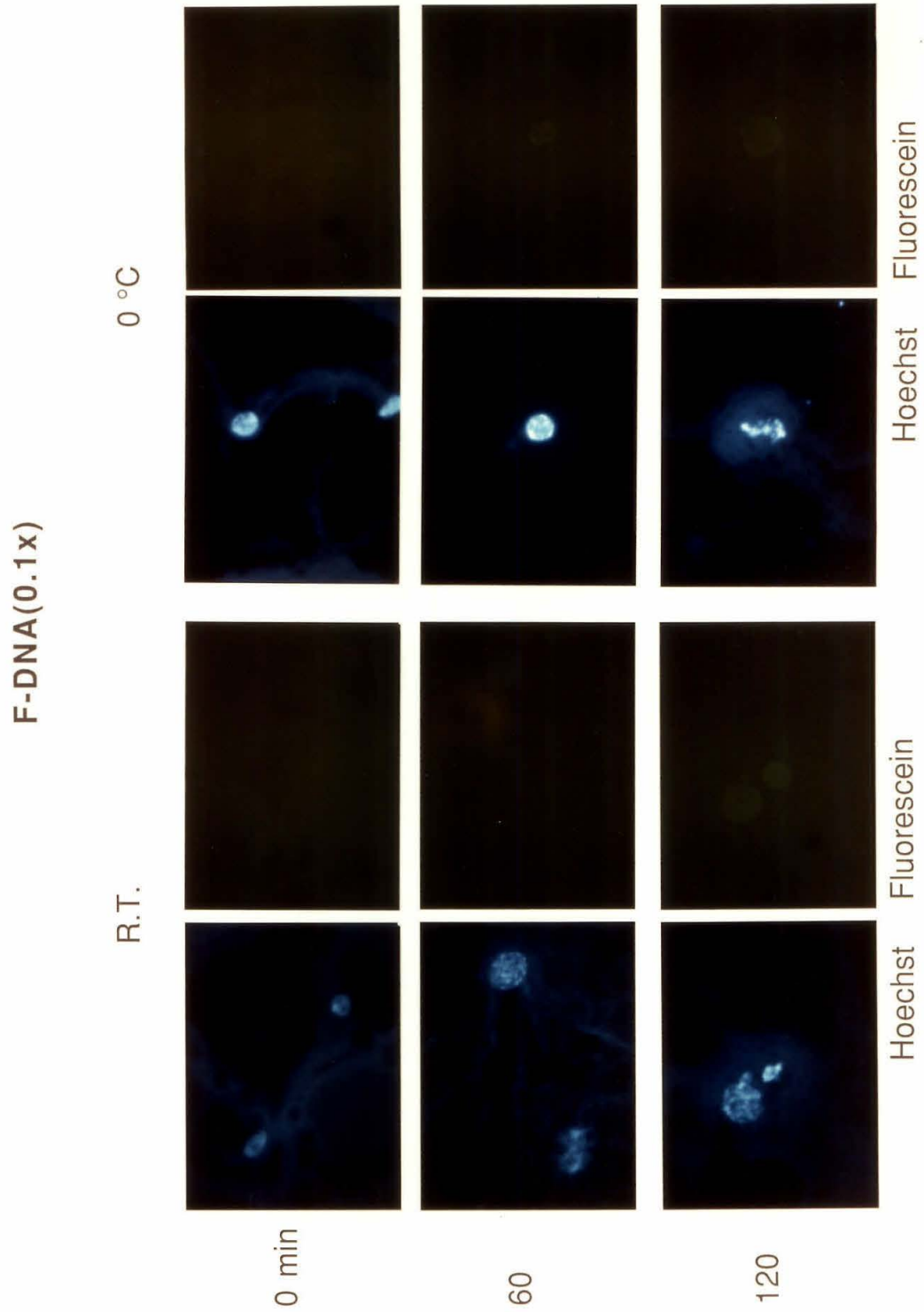


Fig. 11 B



**Fig. 12. Accumulation of TRITC-labeled oligonucleotides in the reconstituted nuclei**

To 20  $\mu\text{l}$  of reconstituted nuclei, 2  $\mu\text{l}$  volumes of the following TRITC (tetramethylrhodamine isothiocyanate)-labeled DNA were added at room temperature. Observations were made at the indicated times using different filters under a fluorescence microscope. Each pair of images consists of a fluorescent image of the DNA-binding dye, Hoechst 33258, on the left (Hoechst) and a fluorescent image of tetramethylrhodamine on the right (Rhodamine).

Sample	Temperature	Final concentration		Observation
		$\mu\text{g}/\mu\text{l}$	$\mu\text{M}$	
0.2x R-DNA	25 °C	0.030	4.51	0, 30, and 90 min.

# Rh-DNA

Added at 30 min to a  
final conc.= 4.5  $\mu$ M at R.T.

Hoechst

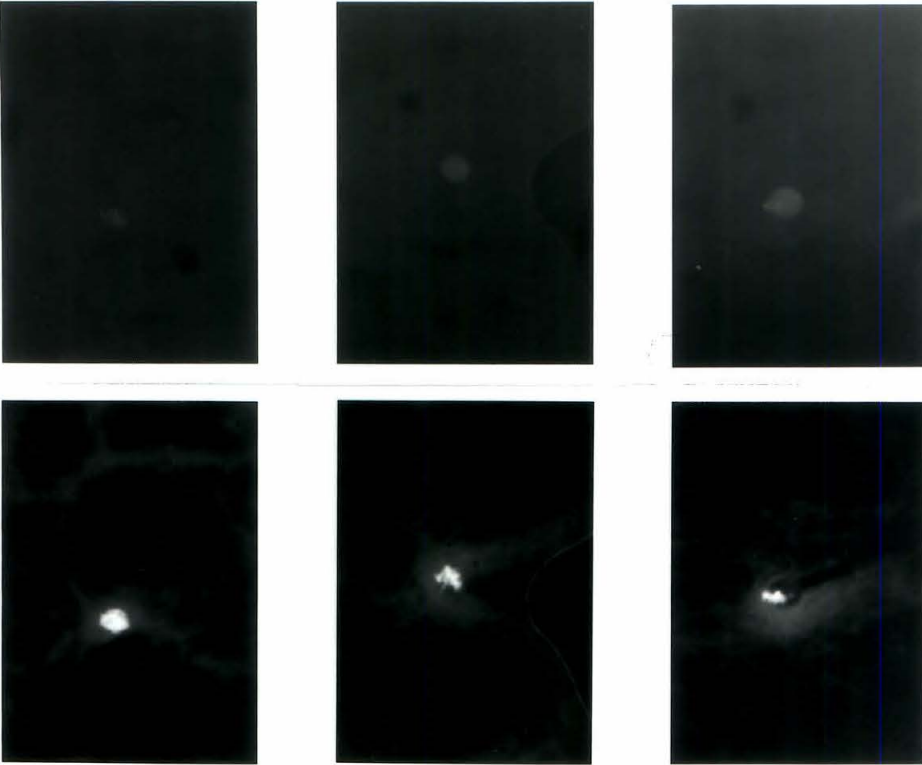
Rhodamine

Time(min.)

30 ( 0 )

60 (30)

120 (90)





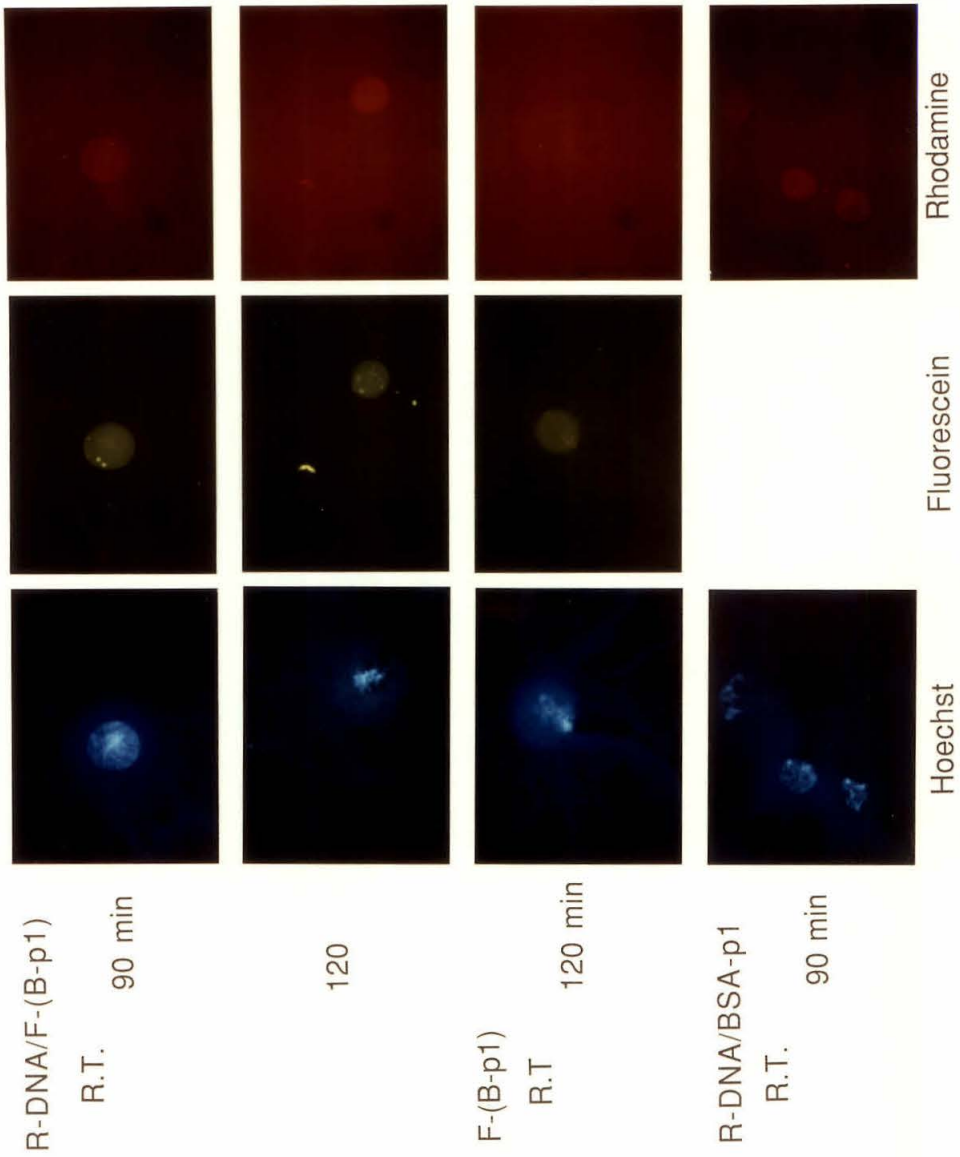
**Fig. 13. Simultaneous uptake of FITC labeled BSA-signal peptide conjugates and TRITC-labeled oligonucleotide**

The following combinations of protein and oligonucleotide were added to reconstituted nuclei at room temperature to the final concentrations as shown below. Each row of images consists of a fluorescent image of the DNA-binding dye, Hoechst 33258, on the left (Hoechst) and fluorescent images of fluorescein in the middle (Fluorescein) and that of tetramethylrhodamine on the right (Rhodamine).

Sample	Final concentration		Observation
	$\mu\text{g}/\mu\text{l}$	$\mu\text{M}$	
0.1x F-(BSA-P1)/0.1x R-DNA	0.027/0.014	0.311/2.067	90, 120 min.
0.1x F-(BSA-P1)/-	0.027/-	0.311/-	90 min.
0.5x (B-P1)/0.1x R-DNA	0.080/0.014	1.210/2.067	90 min.

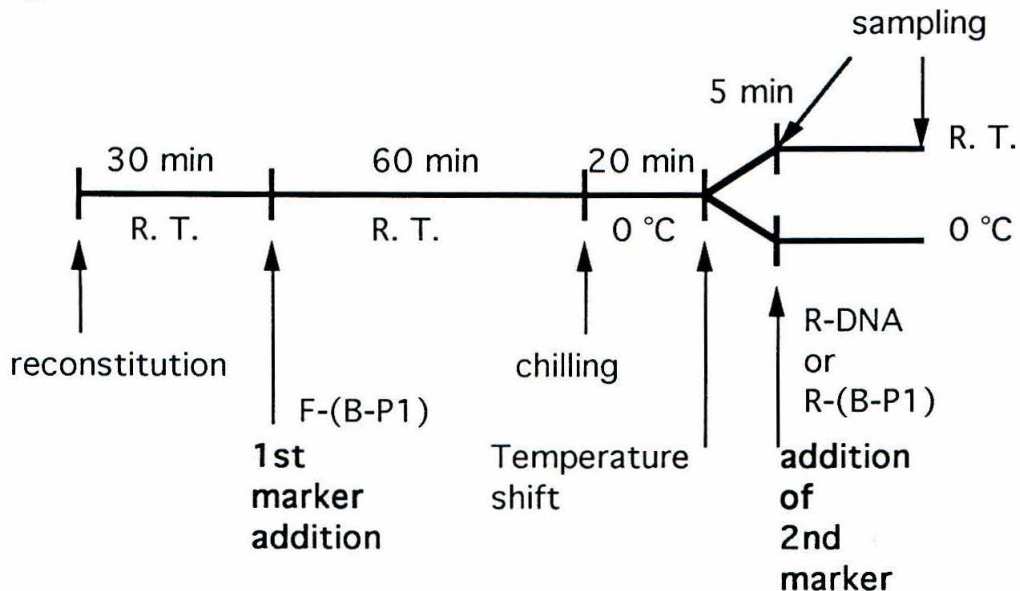


## Dual Label Experiment







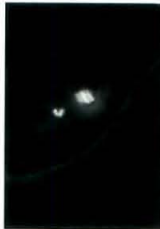





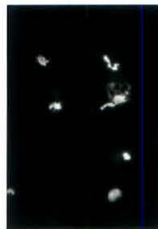




**Fig. 14. Time-differential Dual label Experiment**

Reconstituted nuclei were incubated with fluorescein-labeled BSA-peptide 1 conjugate (F-(B-P1), 0.339  $\mu\text{M}$ ) for 60 min in order to identify transport-competent nuclei. At the end of incubation, the reconstituted nuclei were chilled on ice for 20 min to stop the transport process. After this, the medium containing the reconstituted nuclei was divided into two fractions. One was incubated on ice for 5 min and the other was incubated at room temperature for 5 min. At the end of this incubation, TRITC-labeled oligonucleotides (R-DNA, to a final 4.5  $\mu\text{M}$ ) or TRITC-labeled BSA-peptide 1 conjugates (R-(B-P1), to a final 0.22  $\mu\text{M}$ ) were added to each fraction and the fluorescence associated with the nuclei was observed at the indicated times using different filters under a fluorescence microscope. Each row of images consists of a fluorescent image of the DNA-binding dye, Hoechst 33258, on the left (Hoechst) and fluorescent images of fluorescein in the middle (Fluorescein) and that of tetramethylrhodamine on the right (Rhodamine).



# Time-Differential Dual Label Exp.

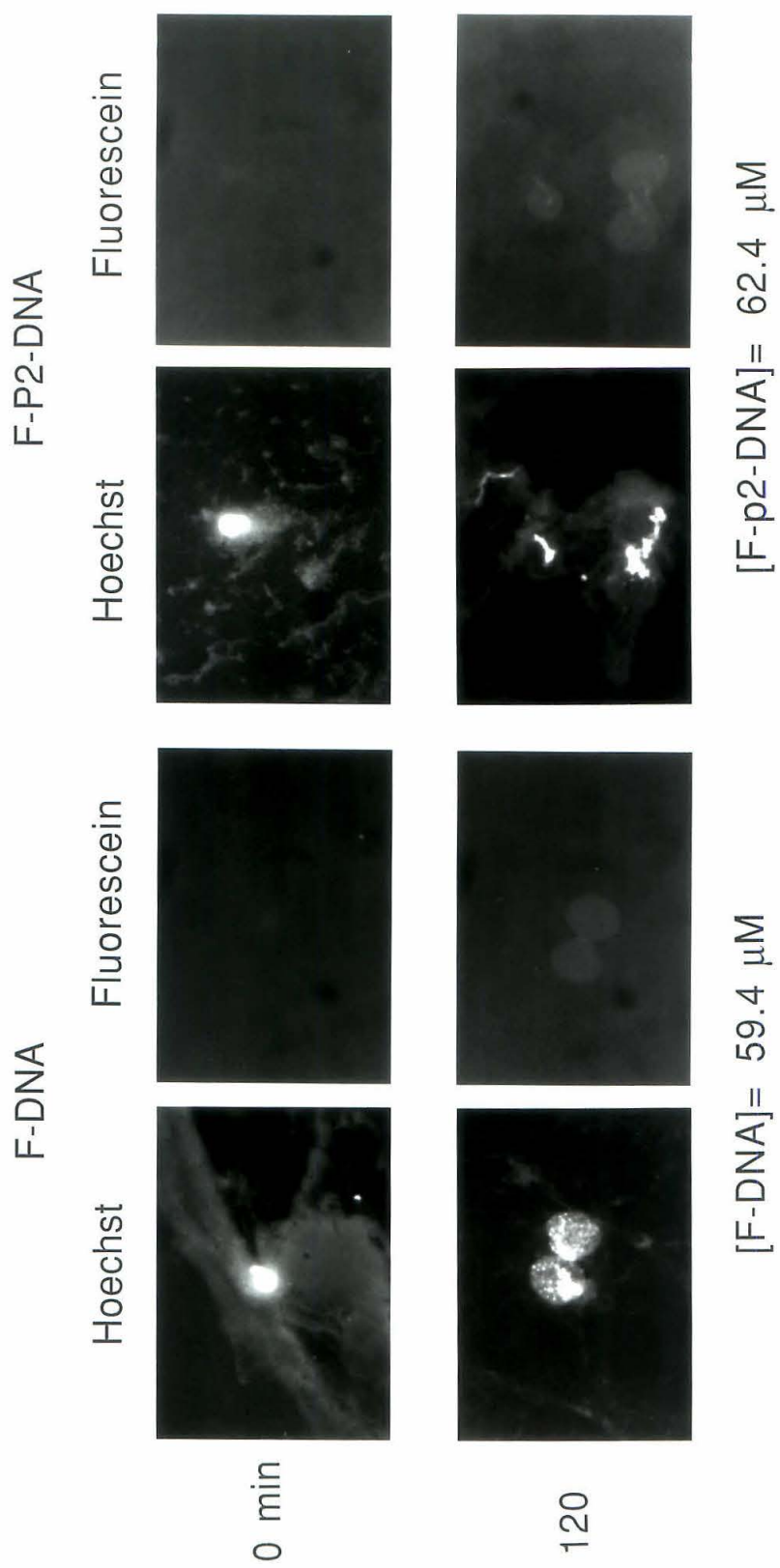
Sample	Incubation		Hoechst	Fluorescein	Rhodamine
	Time(min)	Temp.			
F-(B-P1)/ Rh-DNA	60/0	R.T./R.T.			
F-(B-P1)/ Rh-DNA	60/0	R.T./0			
F-(B-P1)/ -	60/-	R.T./-			
F-(B-P1)/ Rh-(B-P1)	60/0	R.T/0			
F-(B-P1)/ Rh-(B-P1)	150/90	R.T./R.T.			

**Fig. 15. Effect of nuclear localization signal peptide on the nuclear accumulation of oligonucleotides**

The following FITC labeled samples were added to reconstituted nuclei to the following concentrations, incubated at room temperature, and observed under microscope at the indicated times using different filters.

Sample	Temperature	Final concentration		Observation
		$\mu\text{g}/\mu\text{l}$	$\mu\text{M}$	
0.1 $\times$ F-DNA	25 °C	0.036	5.40	0 and 120 min.
0.2 $\times$ (F-P2)-DNA	25 °C	0.048	5.67	0 and 120 min.

# Effect of FITC-pep2 on DNA transport at R.T.



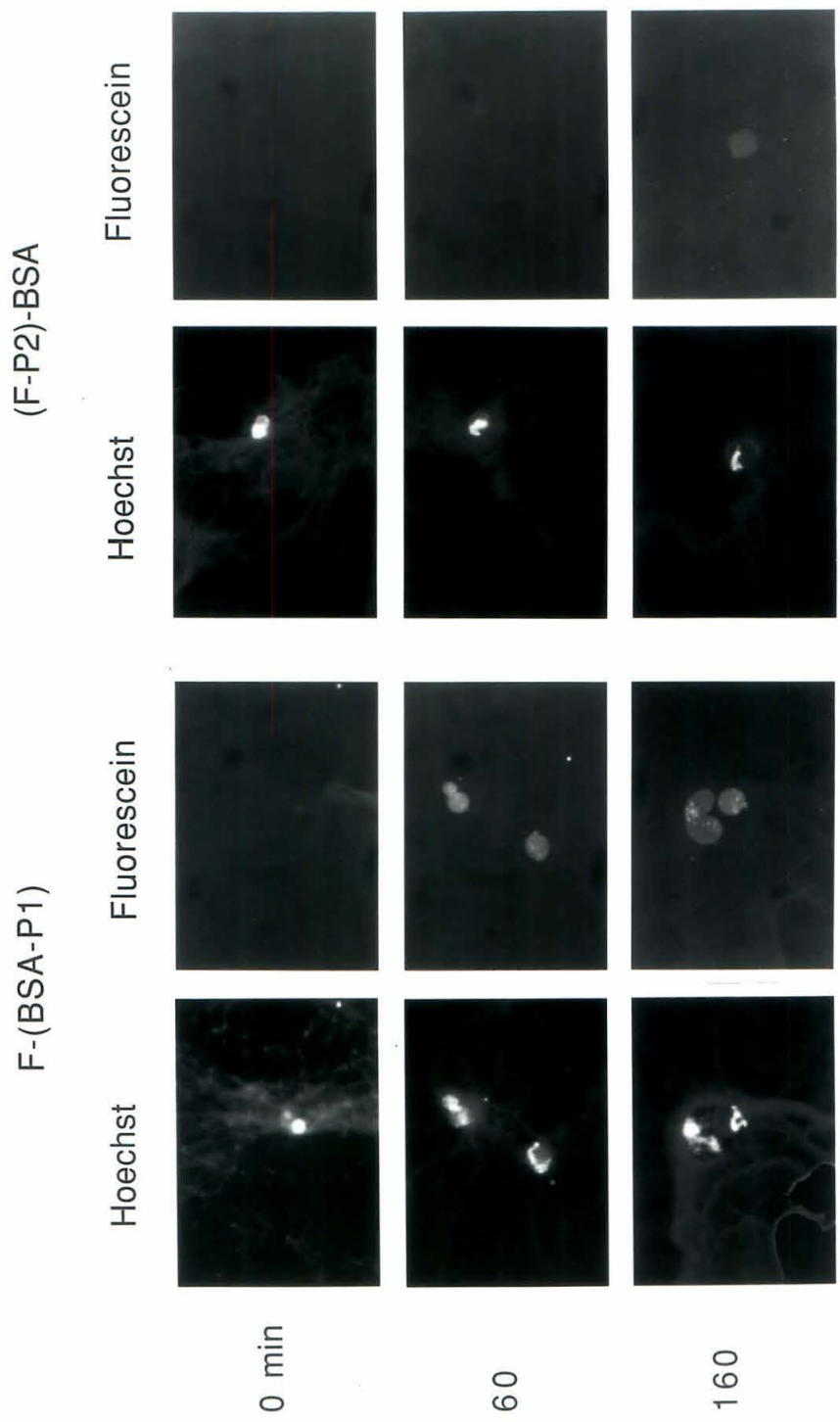
**Fig. 16. Nuclear localization activity of peptide 1 and FITC-labeled peptide 2**

To 20  $\mu\text{l}$  of reconstituted nuclei, 2  $\mu\text{l}$  volumes of the following FITC labeled proteins were added, incubated at room temperature, and observed under microscope at the indicated times. Each pair of images consists of a fluorescent image of the DNA-binding dye, Hoechst 33258, on the left (Hoechst) and a fluorescent image of fluorescein on the right (Fluorescein).

Sample	Temperature	Final concentration		Observation
		$\mu\text{g}/\mu\text{l}$	$\mu\text{M}$	
0.1 $\times$ F-(B-P1)	25 $^{\circ}\text{C}$	0.029	0.339	0, 60, and 160 min.
0.1 $\times$ (F-P2)-B	25 $^{\circ}\text{C}$	0.065	0.766	0, 60, and 160 min.

# Activity of peptide1 and FITC-peptide 2

The fluorescence of nuclei incubated with F-(B-P1) for 30 min was comparable to that with (F-p2)-B for 160 min. [ F-(B-P1) ] = 0.34 microM, [ (F-P2)-B ] = 0.77 microM.



## Appendices



## Appendix. A. Cell culture media

### 1. Formulation of folate-deficient Dulbecco's\*<sup>1-3</sup> Modified Eagle Media (fdDMEM)

Inorganic salts	mg/L
CaCl <sub>2</sub> (anhyd.)	200.00
Fe(NO <sub>3</sub> ) <sub>3</sub> ·9H <sub>2</sub> O	0.10
KCl	400.00
MgSO <sub>4</sub> (anhyd.)	97.67
NaCl	6400.00
NaH <sub>2</sub> PO <sub>4</sub> ·H <sub>2</sub> O	125.00
Other component	
D-glucose	1000.00
Phenol red	15.00
HEPES	5958.00
Sodium pyruvate	110.00
Amino acids	
L-Argine·HCl	84.00
L-Cystine·2HCl	62.57
L-Glutamine	584.00
Glycine	30.00
L-Histidine HCl·H <sub>2</sub> O	42.00
L-Isoleucine	105.00
L-Leucine	105.00
L-Lysine·HCl	146.00
L-Methionine	30.00
L-Phenylalanine	66.00
L-Serine	42.00
L-Threonine	95.00
L-Tryptophan	16.00
L-Tyrosine (disodium salt)	103.79
L-Valine	94.00

*-Continued*

Vitamins	mg/L
D-Ca pantothenate	4.00
Choline chloride	4.00
Folic acid	0.00
i-Inositol	7.20
Nicotinamide	4.00
Pyridoxal·HCl	4.00
Riboflavin	0.40
Thiamine·HCl	4.00

- \*1. Dulbecco, R., Freeman, G. (1959) *Virology* **8**, 396.
2. Smith, J. D., Freeman, G., Vogt, M and Dulbecco, R. (1960)*Virology* **12**, 185.
3. *Tissue culture Standards Committee, In Vitro* **6:2**, 93

## 2. A recipe for folate-deficient DMEM

1. Vitamin stock solution containing the following components at the indicated concentration is made in deionized water and 40 ml is used for 1 liter fdDMEM. Stock solution is kept at -20 °C.

D-Ca pantothenate	100.00 mg/L
Choline chloride	100.00 mg/L
i-Inositol	200.00 mg/L
Nicotinamide	100.00 mg/L
Pyridoxal-HCl	100.00 mg/L
Riboflavin	10.00 mg/L
Thiamine-HCl	100.00 mg/L

2. The following parts (Cat. No) from Gibco Lab. are mixed for 1 liter medium as follows;

Earle's balanced salt solution (450-1100)	1.0 package/L
Basal medium Eagle supplements	
(100x amino acid solution, 320-1051AG)	40.00 ml/L
1 M HEPES buffer solution (380-5630AG)	21.00 ml/L
100 mM MEM sodium pyruvate solution	
(320-1360AG)	10.00 ml/L
200 mM L-glutamine solution	
(100x, 320-5030AG)	20.00 ml/L

3. The following stock solutions are made and the indicated volume is used for 1 liter medium as follows;

Component	Stock solution	Volume/L
Fe(NO <sub>3</sub> ) <sub>3</sub> ·9H <sub>2</sub> O	10.00 mg/ml	10.00 µl/L
Glycine	10.00 mg/ml	3.00 ml/L
L-Serine	10.00 mg/ml	4.20 ml/L

4. 2.2 g NaHCO<sub>3</sub> is added to the mixture for 1 liter medium.
5. Fungi-Bact solution (penicillin G 10,000 units/ml, streptomycin sulfate 10,000 mg/ml, fungizone 25 mg/ml in normal saline, Irvine Scientific, Santa Ana, CA. Cat No. 9350) 10 ml is used for 1 liter medium.
6. Deionized water is added to the mixture to a final volume of 900 ml and pH is adjusted to 7.3 using 1 N NaOH solution.
7. For cell culture medium (fdDMEM, 5% FCS), 50 ml fetal calf serum (Hyclone Laboratories, Inc., Cat. No. A-1111-L, heat-inactivated at 65 °C

- for 30 min.) is added to the above 900 ml solution and final volume is adjusted to 1 liter. For folate uptake assay medium (fdDMEM), fetal calf serum is not added and final volume is adjusted to 1 liter.
8. Media are filtered using two CN 0.2  $\mu\text{m}$  Nalgene disposable filterwares (500 ml size) and kept at 4 °C.

## Appendix. B. Procedures for radioiodination

### Radioiodination using Iodo-beads (Pierce Chemical Company, Cat. 28666)\*\*

1. 10 particles of Iodo-beads (Pierce Chemical Company, Cat. 28666) are washed in 50 mM Tris buffer (pH7.5) in a petridish and dried on Whatman #1 filter paper.
2. 200  $\mu$ l of 50 mM Tris buffer (pH7.5) is added to 10  $\mu$ l(1mCi) Na<sup>125</sup>I (Amersham).
3. 100  $\mu$ l diluted Na<sup>125</sup>I solution is added to each Eppendorf tubes containing 5 iodo-beads and left for 5 min. at room temperature.
4. 100  $\mu$ l 50 mM Tris buffer (pH7.5) is added to 100  $\mu$ l diluted Na<sup>125</sup>I solution containing iodo-beads.
5. To each tube containing iodo-beads, about 2 mg of protein in 50 mM Tris buffer (pH7.5) (protein oncentration  $\approx$  10 mg/ml) is added and left for 1 hour for iodination.
6. Reacted protein solution is transferred to clean Eppendorf tubes by pippetting to stop reaction
7. <sup>125</sup>I-labeled protein is separated from unreacted <sup>125</sup>I using gel-filtration chromatography. Sephadex G-25 (Sigma) column (1.5x35 cm) is made and reaction mixture is loaded on the column and eluted using 50 mM Tris buffer (pH7.5).
8. Eluted fractions are collected and 10  $\mu$ L aliquots from each fraction are analysed for radioactivity using a g-counter or a scintillation counter.
9. Radioactive fractions containing iodinated protein are identified and protein concentrations are determined using an appropriate protein assay. Radioiodinated proteins are kept frozen at -20 °C.

\*\* Markwell, M. A. K. (1982) *Anal. Biochem.* **125**, 427-432

## Appendix. C. Peterson's modified Lowry assay

### 1. Stock solutions for Peterson's modified Lowry protein assay\*\*\*

- A: 20 %  $\text{Na}_2\text{CO}_3$  solution (20 g  $\text{Na}_2\text{CO}_3$  in 100 ml water solution, filtered using CN 0.2  $\mu\text{m}$  Nalgene disposable filterware and kept at 4 °C.)
- B: 0.4 %  $\text{CuSO}_4 \cdot 5\text{H}_2\text{O}$  (0.4 g in 100 ml water solution)
- C: 0.8 %  $\text{Na}_2$  tartarate- $2\text{H}_2\text{O}$  (0.4 g in 100 ml water solution)
- D: 10 % sodium dodecyl sulfate (100g in 1 liter solution)
- E: 0.8 N NaOH
- F: 0.4 N Folin-Ciocalteu's phenol reagent (diluted from 2 N stock solution, Sigma, Cat. F-9252)

### 2. Procedures for protein determination

1. Bovine serum albumin standard solutions and unknown protein samples (concentration range 0-250  $\mu\text{g}/\text{ml}$ ) are prepared in 1 ml water in 13x100 ml test tubes in duplicate.
2. The following 'assay solution' is made by mixing the stock solutions as follows and warmed to 37 °C to prevent precipitation;
  - 1 volume of A
  - 0.5 volume of B
  - 0.5 volume of C
  - 2 volumes of D
  - 2 volumes of E
  - 2 volumes of water
3. To 1 ml protein samples, 1 ml 'assay' solution is added and mixed thoroughly by vortexing. The mixture is incubated at room temperature for 15 minutes.
4. To the mixture made in 3., 0.5 ml of 0.4 N Folin-Ciocalteu's phenol reagent is added and mixed thoroughly by vortexing. The reaction mixture is incubated at room temperature for 45 minutes.
5. Absorbance is measured at 540, 660, or 750 nm using a UV-Visible spectrophotometer.
6. Protein concentrations are calculated using BSA as standards.

\*\*\* Peterson, G. L. (1977) *Analytical Biochemistry* 83, 346-356

# Appendix. D. Reconstitution of cellular nuclei using *Xenopus* egg extracts and sperm nuclei\*\*\*\*

## (1) Solutions and buffers

solution	concentration	
KCl	2.5 M	
MgCl <sub>2</sub>	0.5 M	
CaCl <sub>2</sub>	1.0 M	
NaOH	10.0 N	
KOH	10.0 N	
Na-EGTA (K-EGTA)	0.2 M	7.608 g EGTA (M.W. 380.4) in about 60 ml H <sub>2</sub> O, titrated to pH 8.0 with 10 N NaOH (or KOH). Water is added to a final 100 ml volume.
CLP	10.0 mg/ml	5 mg each of the Chymostatin, Leupeptin, Pepstatin A (Sigma) are dissolved in 0.5 ml DMSO and kept at -20 °C.
CB	10.0 mg/ml	5.0 mg/ml cytochalasin B (from Sigma) in 0.5 ml DMSO. Kept at -20 °C.

<b>Cysteine</b>	2%	L-Cysteine 4 g is dissolved in 200 ml distilled water and 10 M NaOH is added to pH 7.8 at room temperature. It is important to prepare it just before use. It loses its dejelling activity in several hours by air oxidation
<b>Cycloheximide</b>	10 mg/ml	Cycloheximide is prepared in distilled H <sub>2</sub> O and kept at -20 °C.

**10x MMR buffer**

<b>component</b>	<b>conc.</b>	<b>preparation</b>
NaCl	1000.00 mM	29.225 g
KCl	20.0 mM	4.0 ml 2.5 M KCl
MgCl <sub>2</sub>	10.0 mM	10.0 ml 0.5 M MgCl <sub>2</sub>
CaCl <sub>2</sub>	20.0 mM	10.0 ml 1.0 M CaCl <sub>2</sub>
Na-EGTA	1.0 mM	2.5 ml 0.2 M Na-EGTA, pH 8.0
Tris (base)	50.0 mM	3.03 g

Add distilled water to 400 ml volume to the above mixture and titrate with concentrated HCl to pH 7.8. Add distilled water to a final volume of 500 ml. Keep it at 4 °C.

**1x MMR buffer (500 ml per each experiment)**

<b>component</b>	<b>conc.</b>	<b>preparation</b>
NaCl	100.00 mM	2.9225 g
KCl	2.0 mM	0.4 ml 2.5 M KCl
MgCl <sub>2</sub>	1.0 mM	1.0 ml 0.5 M MgCl <sub>2</sub>
CaCl <sub>2</sub>	2.0 mM	1.0 ml 1.0 M CaCl <sub>2</sub>
Na-EGTA	0.1 mM	0.25 ml 0.2 M Na-EGTA, pH 8.0
Tris (base)	5.0 mM	0.303 g

Add distilled water to 400 ml to the above mixture and titrate with concentrated HCl to pH 7.8. Add distilled water to a final volume of 500 ml.

Alternatively 10x MMR is diluted to 1x MMR.



**10x XB (Extract buffer) (1 liter)**

component	conc.	preparation
KCl	1000.0 mM	74.6 g
CaCl <sub>2</sub>	1.0 mM	1.0 ml 1.0 M CaCl <sub>2</sub>
MgCl <sub>2</sub>	10.0 mM	10.0 ml 0.5 M MgCl <sub>2</sub>
HEPES (not salt)	100.0 mM	23.8 g
Sucrose (342.3)	500.0 mM	171.15 g

Add distilled water to a volume of 800 ml to the above mixture and titrate with 10 M KOH to pH 7.7. Add distilled water to a final volume of 1,000 ml. Keep it at 4 °C.

**1x XB (Extract buffer) (1 liter)**

Add 100 ml 10x XB to 900 ml distilled water. Titrate with 10 M KOH to pH 7.7.

**1x XB' (1x XB supplemented with 5 mM K-EGTA and 1 mM MgCl<sub>2</sub>, 1 liter)****preparation**

100 ml	10x XB
2.0 ml	0.5 M MgCl <sub>2</sub>
25.0 ml	0.2 M K-EGTA, pH 8.0

Add distilled water to 1 liter and titrate with 10 M KOH to pH 7.7.

**1x XB' +CLP+CB (XB' with protease inhibitors and cytochalasin B)****preparation**

1.0 ml	1x XB'
4.4 µl	10 mg/ml CLP in DMSO
13.2 µl	10 mg/ml CB in DMSO

**20x Energy mix****preparation**

750 $\mu$ l	0.2 M creatine phosphate (sigma, pH 7-8 when prepared)
200 $\mu$ l	0.1 M ATP( $\text{Na}_2\text{ATP}$ , Boeringer Mannheim, titrated to pH 7.0 with 10 M KOH using pH paper (color pHast <sup>R</sup> indicator strips)
10 $\mu$ l	K-EGTA, pH 7.7
20 $\mu$ l	0.5 M $\text{MgCl}_2$
20 $\mu$ l	distilled $\text{H}_2\text{O}$

**Hoechst dye mixture****preparation**

2.0 $\mu$ l	10 mg/ml Hoechst 33258 (Sigma) in $\text{H}_2\text{O}$
100 $\mu$ l	37 % formaldehyde
1.0 ml	buffer A/sucrose (80.0 mM KCl, 5.0 mM K-EGTA, 15.0 mM piperazine- <i>N,N'</i> -bis[2-ethanesulfonic acid], pH7.2, 15.0 mM NaCl, 7.0 mM $\text{MgCl}_2$ and 200.00 mM sucrose)

**(2) Preparation of Xenopus sperm DNA**

1. Inject 0.1 ml of gonadotropin to a male frog. After incubate for an hour , take out the testis and put it in 50 ml 1x MMR supplemented with 0.25 ml HCG (1,000units/ml, Sigma). Incubate it overnight at 18 °C.
2. Take off the blood vessels from the surface of the testis.
3. Cut the testis into small pieces in 2 ml buffer A/sucrose.
4. Mush the pieces of testis in a small beaker.
5. Put all the pieces into 4 Eppendorf tubes (1.5 ml).
6. Spin the tubes for 30 seconds at setting 4 on the IEC clinical centrifuge.
7. Trnsfer the supernatant into 4 Eppendorf tubes (1.5 ml).
8. Spin the tubes for 1 min at setting 7 on the IEC clinical centrifuge.
9. Remove the supernatant and wipe the wall of the tubes.
10. Add 100  $\mu$ l of lysolecitin solution (Sigma, 0.1 % in buffer A/sucrose) to each tube. Suspend the pellet by pipetting.
11. Incubate the sperm in the above solution for 10 min at room temperature to lyse the sperm membranes.

12. Check the lysis of the membrane by staining the sperm DNA with Hoechst dye mixture (stained if lysed).
13. Spin the sperm DNA at setting 5 for 10 seconds on the IEC clinical centrifuge.
14. Add 0.3 ml of 3 % BSA in buffer A/sucrose to each tube and mix thoroughly.
15. Spin for 3 min at setting 5 on the IEC clinical centrifuge.
16. Add 0.5 ml 3 % BSA solution and resuspend the pellet.
17. Spin for 3 min at setting 5 on the IEC clinical centrifuge.
18. Add 0.5 ml 3 % BSA solution and resuspend the pellet.
19. Spin for 3 min at setting 5 on the IEC clinical centrifuge.
20. Resuspend the pellet in 0.3 ml of buffer A/sucrose and count the number of sperms per  $\mu\text{l}$ . Dilute the sperm solution to a final concentration of  $10^5$  ea/ $\mu\text{l}$ . Aliquots are kept at  $-80^\circ\text{C}$ .

### **(3) Frog priming and inducing ovulation**

1. **Priming frogs;** Frogs are maintained in charcoal filtered water. Prime the frogs by injecting 100 units of Pregnant Mare Serum Gonadotropin (PMSG, Calbiochem) on day 1. Frogs are kept at  $18^\circ\text{C}$  in 5 liter water containing 25 g NaCl after priming. When handling frogs, wear plastic gloves which were washed inside and out with water to remove powder.
2. **Inducing ovulation;** Prepare human chorionic gonadotropin solution (HCG, Sigma) by adding 10 ml distilled and sterilized water to 10, 000 units of lyophilized HCG. Add 25 g NaCl to 5 liters of distilled water in which the frogs will lay eggs. Using 3 cc sterile syringe and 21G1 needle, take out HCG solution. Using 23G1 needle, inject 0.8 ml HCG solution per each primed frog into the dorsal lymph sac (under the skin of thigh) between day 3 and 14. Inject hormone at 4-8 PM to 2-3 frogs and the frogs will usually finish laying eggs before noon the next day. Put the frogs in the saline solution separately.

### **(4) Preparation of cytotstatic factor (CSF) arrested extracts**

1. Transfer the frog eggs from one frog to a 200 ml glass beaker. Wash the eggs with 100-200 ml 1x MMR at room temperature.
2. Dejelly the eggs using freshly made 2 % cysteine, pH7.8 solution. First, add 100 ml cysteine solution to the eggs and gently swirl the eggs with a

- glass pipette. Add second 100 ml cysteine solution and swirl gently until the gelly wrapping the eggs are dissolved and the eggs are packed on the bottom of the beaker. Decant the supernatant solution.
3. Wash the eggs with about 100 ml 1xMMR twice at room temperature. Care must be taken not to break the eggs. Do not decant all the buffer since the surface tension could break the eggs.
  4. Wash the eggs 4 times with about 100 ml 1xXB' buffer (1xXB, 5 mM K-EGTA, 1 mM  $MgCl_2$ ).
  5. Transfer the eggs (about 1 ml) to ultracentrifuge tubes (11x34 mm, 7/16x13/8 inch., Beckman) placed in a rack for 1.5 ml Eppendorf tubes. Use a glass pipette of which the sharp portion is broken and covered with a rubber bulb. Use the wide mouth of the pipette in order not to damage the eggs when transferring the eggs to centrifuge tubes.
  6. Add 0.5 ml XB'+CLP+CB to each tube containing eggs. Cover the tube with a piece of parafilm and invert the tube a few times gently so that the buffer smears between the eggs.
  7. Pack the eggs on a clinical centrifuge (International Equipment company) as follows; Centrifuge the eggs for 15, 60 and 30 seconds at speed controls of 3, 5 and 7, respectively. Remove excess buffer.
  8. Crush the eggs by spinning the eggs at 12,000 rpm for 10 min at 16 °C on a TLS-55 swing bucket rotor in Beckman TL-100 ultracentrifuge.
  9. After centrifugation, the eggs are crushed into three fractions; from top to the bottom, yellow yolk, cytoplasmic fraction and membrane debris. Recover the cytoplasmic (middle) fraction with 21G1 needle and 3 cc syringe by puncturing the ultracentrifuge tube and transfer it to an Eppendorf tube placed on ice.
  10. Transfer the egg extracts to 0.5 ml long and skinny centrifuge tubes (Beckman) using a glass pipette and spin them for 2 min at 4 °C using a Beckman minifuge.
  11. After centrifugation, cut the skinny tube with a razor blade to remove the yolk on top of the extracts and transfer the extracts to pre-weighed Eppendorf centrifuge tube. Measure the weight of the extracts quickly and place the extracts on ice. The weight is used to calculate the approximate volume of the extracts.
  12. Add 1/19th volume of 20x Energy mix to the egg extracts on ice.

13. Add 1/100th volume of cycloheximide (10 mg/ml stock in H<sub>2</sub>O) to the egg extracts on ice to stop the protein synthesis in the extracts.
14. Add *Xenopus* sperm nuclei to a final concentration of 500 ea./ $\mu$ l extract.
15. Add 100 mM CaCl<sub>2</sub> to a final concentration of 0.4 mM and mix well gently in order to activate the cycling of the extracts at room temperature. If the extracts are activated, nuclear membranes are formed around the sperm nuclei in 5-10 min, which can be visualized under a phase contrast microscope (Zeiss Axioplan microscope) at a 400x magnification.
16. After 10-20 minutes of activation, add 2  $\mu$ l of proteins or DNA with proper fluorescent labels to 20  $\mu$ l of the activated extracts at room temperature and incubate for appropriate periods.

\*\*\*\*

1. Murray, A. W., Solomon, M. J. and Kirschner, M. W. (1989) *Nature* 339, 280-286
2. Gourdon, J. B. (1976) *J. Embryol. exp. Morph.* 36, 523-540